Catarina Leal Seabra

Lipid-based Nanostrategies to fight *Helicobacter pylori* gastric infection

Tese de Candidatura ao grau de Doutor em Ciências Biomédicas submetida ao Instituto de Ciências Biomédicas Abel Salazar da Universidade do Porto.

Orientadora:

Doutora Maria Cristina Teixeira Lopes da Costa Pinto Lopes Martins

Categoria – Investigador Auxiliar/Professor Auxiliar

Afiliação – i3S- Instituto de Investigação e Inovação em Saúde, INEB- Instituto de Engenharia Biomédica, ICBAS- Instituto de Ciências Biomédicas Abel Salazar da Universidade do Porto.

Coorientadores:

Doutor Celso Albuquerque Reis

Categoria – Investigador Coordenador/Professor Auxiliar

Afiliação – i3S- Instituto de Investigação e Inovação em Saúde, INEB- Instituto de Engenharia Biomédica, ICBAS- Instituto de Ciências Biomédicas Abel Salazar da Universidade do Porto, FMUP- Faculdade de Medicina da Universidade do Porto.

Doutora Inês de Castro Gonçalves Almada Lobo

Categoria – Investigador Auxiliar

Afiliação – i3S- Instituto de Investigação e Inovação em Saúde, INEB- Instituto de Engenharia Biomédica.

This work presented in this thesis was developed at

BioEngineered Surfaces Group
i3S- Instituto de Engenharia Biomédica
Universidade do Porto, Porto, Portugal
Rua Alfredo Allen, 208
4200-135 Porto, Portugal
www.i3s.up.pt|www.ineb.up.pt

and

Biomodels, Bioanalytics and Biophysic Group
mB^2: Molecular Biophysics and Biotechnology Unite
UCIBIO-REQUIMTE, Laboratório de Química Aplicada
Faculdade de Farmácia
Universidade do Porto, Portugal
Rua de Jorge Viterbo de Ferreira, 228
4050-313 Porto, Portugal

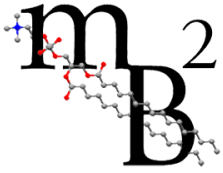

FINANCIAL SUPPORT

Catarina Leal Seabra was supported by a national PhD grant SFRH/BD/89001/ 2012 from Fundação para a Ciência e Tecnologia (FCT).

This work was financed by FEDER- Fundo Europeu de Desenvolvimento Regional funds through the COMPETE 2020- Operational Programme for Competitiveness and Internationalization (POCI), Portugal 2020. FCT/MCTES through the projects: POCI-01-0145-FEDER-007274; PYLORIBINDERS (PTDC/CTM-BIO/ 4043/2014); PYLORICIDAL (PTDC/CTM-BPC/121149/2010) and NORTE-01-0145-FEDER-000012.

ACKNOWLEDGMENT

"Para saborear o cume das montanhas é preciso passar pelos vales.
E quando descemos aos vales são as memórias das montanhas que nos dão forças para
lutar para subi-las de novo"
(Margaret F. Powers)

Esta tese não representa apenas o fruto de extensas horas de trabalho, dedicação e perseverança, mas o culminar de um objetivo de vida a que me propus e que não seria possível sem a ajuda de um número considerável de pessoas. A todos os que percorreram comigo este percurso, por vezes com obstáculos, o meu muitíssimo obrigada.

À minha orientadora, Doutora Cristina Martins, pela disponibilidade para guiar e acompanhar no meu percurso científico durante estes últimos 4 anos. A sua paciência, compreensão e contribuição foram decisivas para a evolução do trabalho aqui apresentado. Obrigada pelo apoio imprescindível na superação dos mais diversos obstáculos e pelos sábios conselhos. Nos momentos mais difíceis (como a mudança de instalações) sempre arranjou uma solução e recursos, para que o nosso trabalho não ficasse estagnado. Obrigada por ter confiado em mim!

À minha co-orientadora, Doutora Inês Gonçalves agradeço o apoio constante, as sugestões pertinentes e estímulo para querer fazer sempre mais e melhor.

Ao meu co-orientador, Doutor Celso Reis, agradeço todo o suporte científico e sugestões de melhoria.

O meu agradecimento muito especial aos meus colegas e amigos do BioEngineered Surfaces, tanto passados como atuais, que foram fundamentais nesta caminhada, proporcionando um bom ambiente no laboratório e momentos de descontração. Obrigada pela proximidade, pelas discussões científicas, pelos jantares de grupo, muitas vezes adiados, mas que se realizavam sempre, pelas ajudas em todas as dúvidas e articulação de recursos e equipamentos. Um

especial agradecimento à Cláudia Monteiro, companheira de secretária e de caminhadas, pela calma, serenidade e apoio; à Maura Cimino, a nossa italiana mais portuguesa, pela boa disposição, sorriso rasgado, gargalhadas, cumplicidade, partilha de secretária, por vezes um quanto desarrumada e caótica, mas sempre com tudo muito controlado; à Paula Parreira, companheira "pylorenta", sempre disponível para me ajudar e apoiar, contigo dei os primeiros passos com a *Helicobacter*, és uma parceira e amiga; à Patrícia Henriques, minha eterna "Bambi", chegaste uma menina, cresceste imenso, mas sempre companheira de biotério, muitas conversas, gargalhadas e cantorias; à Vanessa Graça, que apesar de não estares agora no grupo, fizeste percurso comigo, partilhamos muitas vezes câmara, equipamentos, muita coordenação de reagentes e placas que tivemos de fazer para que nenhuma ficasse parada nas suas experiências.

Obrigada aos meus colegas e amigos INEBianos, por todos os pequenos grandes momentos e pormenores do dia-a-dia, por toda a ajuda, desde recursos, apresentações ou partilha de protocolos e experiências, até a um simples login num computador ou uma gargalhada ao almoço. Quero agradecer em especial às minhas companheiras de laboratório *Starfish* (no antigo edifício do INEB): Estrela, Ana Luísa, Daniela Vasconcelos, Catarina Pereira, Graciosa, que muitas vezes me viram de rastos, desanimada, mas que me deram sempre força e coragem para seguir em frente. Obrigada pelas partilhas científicas e não científicas, que me ajudaram de certa forma a integrar e a perceber o funcionamento do INEB.

A todos os técnicos do INEB, em especial Manuela Brás, Maria Lázaro e Ricardo Vidal que me deram imenso apoio na execução das minhas experiências, ajudaram a ser autónoma na utilização dos equipamentos e confiaram sempre em mim para usar equipamentos fora de horas. Obrigada pelo vosso profissionalismo e generosidade quando vos pedia socorro à última da hora.

Obrigada às minhas parceiras de "Caminhada pós-almoço": Daniela Sousa, Daniela Rocha, Cláudia Monteiro e Marta Laranjeira, por todos os abraços e desabafos, pelas caminhadas revigorantes, verdadeiras lufadas de ar fresco, e por me ajudarem a perceber que existe algo além das paredes do i3s.

Sem esquecer o grupo criado não pela ciência, mas pela partilha de espaço no i3s, agradeço com carinho ao grupo do Bruno Sarmento, em especial à Maria João, Francisca e Rute, pela companhia até tarde no laboratório e por me fazerem sentir que nunca estava verdadeiramente sozinha.

Às minhas "orientadoras emprestadas" de coração, Professora Salette Reis e Doutora Cláudia Nunes, não só pela vossa hábil e perspicaz orientação, imprescindível à evolução deste trabalho, mas pela confiança em mim depositada, por me terem recebido de braços abertos no

vosso grupo. Obrigada pelo vosso apoio na superação dos mais diversos obstáculos, pelos sábios conselhos e sobretudo pela amizade que sempre me aqueceu o coração. Professora Salette, apesar de ter delegado grande parte da "orientação" à Doutora Cláudia, sempre esteve disponível para ouvir, tirar dúvidas e acima de tudo, aconselhar, com uma palavra amiga sobre o que deve ser valorizado na vida, mantendo o foco e serenidade para que tudo flua. De maneira muito especial, quero agradecer à Doutora Cláudia Nunes, por me teres ensinado e acompanhado inteiramente na produção das nanopartículas, por teres sempre uma mente aberta, ouvindo e partilhando ideias e sugestões de melhorias do sistema. Sempre pude contar contigo para discutir os resultados, novos protocolos e planear o trabalho futuro. Para além disso, tornaste-te uma boa amiga, sempre bem-disposta, partilhando alegrias e tristezas, ouvindo as minhas lamentações e desânimos com o trabalho, mas sempre acreditando em mim.

Deixo também aqui um especial agradecimento a todas as pessoas do meu grupo do coração, da Professora Salette, "Mike group" que sempre me receberam muito bem e me proporcionaram um ambiente agradável, descontraído, cheio de boa disposição, experiências gastronómicas e um porto seguro. À Virgínia, Daniela Priscila, Joana, Catarina, Rita, Nini, José e Miguel, um especial obrigado pelas gargalhadas e "travessura" partilhadas, abraços e amizade!

Aos meus pais e irmã agradeço todas as lições valiosas e dedicação que tiveram comigo durante toda a minha vida. Obrigada pela vossa tolerância, compreensão e carinho. Nem sempre foi possível atender às vossas necessidades e exigências, mas à vossa maneira fui tendo o vosso apoio e carinho.

Obrigada às minhas amigas de sempre e para sempre, Liliana Maia, Sónia Pinho, Tânia Brito, Joana Figueiredo, Helena Felgueiras, por todos minutinhos em que houve tempo para partilha da vida, por todas a conversas ao skype, whatsapp, telefone, pelo ombro amigo e colo mimado e por todos os momentos em que me enchem o coração. Em especial à grande amiga Liliana, que apesar de ter estado longe, e de ter que estudar para o exame de especialidade sempre me compreendeu, sempre esteve presente, sempre nos motivamos uma à outra, ajudamo-nos uma à outra a acreditar que somos capazes por mais difícil que seja o caminho, que apesar de haver pessoas que acreditavam que iriamos "cair", sempre estivemos a fazer caminho juntas. Há muitos anos que caminhamos juntas nesta vida cheia de batalhas e superações. À Sónia, Tânia e Joana, as minhas "manas emprestadas" que sempre pude contar nos momentos de desespero, nos momentos de triunfo, nos momentos de colinho e de lágrimas. À Helena, colega de curso, ex-colega de grupo Bioengeneered Surfaces, verdadeira amiga, com a tua simplicidade foste um raio de sol e de boa disposição que entrou no grupo. Não foi possível ficares connosco, mas sempre estiveste disponível para me ouvir, compreender e dar-me

força. A tua capacidade de trabalho é fascinante e uma inspiração. Sempre estiveste disponível para me ajudar, independentemente o dia da semana ou hora. Mesmo agora longe, estás sempre presente, disponível, companheira e amiga.

Por último, um especial agradecimento ao André, o meu André, por felizmente teres surgido no início desta jornada, por me ouvires e apoiares todos os dias, mesmo quando estavas em baixo. Sempre foste o meu porto seguro, incentivando e encorajando. Obrigada pela tua partilha diária, por entenderes o que é e como tem de ser, por ainda assim me alertares quando ultrapasso os limites do razoável e excedo as horas de trabalho. Obrigado por me teres sempre acompanhado nas minhas experiências de mais de 24h, em que eu dormia no sofá do INEB e tu me trazias o jantar e me fazias companhia pela noite dentro. Obrigada pela confiança, incentivo, alento, compreensão, companheirismo e constante partilha. Sem todo o teu amor e calma teria sido ainda mais difícil erguer a cabeça e seguir em frente. Obrigada por todos os ensinamentos, pelos sonhos que temos concretizado juntos e por tudo aquilo que ainda planeamos viver…

“Que você seja um grande empreendedor,

Quando empreender, não tenha medo de falhar,

Quando falhar, não tenha receio de chorar,

Quando chorar, repense a sua vida, mas não recue,

Dê sempre uma nova oportunidade a si mesmo.”

(Augusto Cury)

PUBLICATIONS

Ao abrigo do disposto do nº 2, alínea a) do artigo 31º do Decreto-Lei nº 115/2013 de 7 de Agosto, fazem parte integrante desta tese de doutoramento os seguinte trabalhos já publicados ou submetidos para publicação.

- **SEABRA C.L**, Nunes C., Gomez-Lazaro, M., Correia M., Machado J.C, Gonçalves I.C, Reis C.A, Reis S., Martins M.C.L. (2017) Docosahexaenoic acid loaded lipid nanoparticles with bactericidal activity against *Helicobacter pylori, International Journal of Pharmaceutics, 519:128-137. doi:* http://dx.doi.org/10.1016/j.ijpharm.2017.01.014.

- **SEABRA C.L**, Nunes C., Brás, M., Gomez-Lazaro, M., Gonçalves I.C, Reis C.A, Reis S., Martins M.C.L. (2017) Specific bactericidal non-loaded lipid nanoparticles against *Helicobacter pylori. Submitted.*

- **SEABRA C.L**, Nunes C., Reis S; Martins M.C.L (2016) Specific bactericidal activity of unloaded-nanostructured lipid carriers against *Helicobacter pylori*, PPP: 20161000042469(0198) 2016/06/28-PAT.

ABSTRACT

More than half of the world population is infected with *Helicobacter pylori* (*H. pylori*), a Gram-negative, spiral-shaped bacterium that, after persistent colonization of gastric mucosa, is responsible for the development of several gastric diseases, including gastric adenocarcinoma. Although different treatment regimens have been applied, the eradication is still unsuccessful in approximately 20% of the patients, mainly due to bacteria resistance to available antibiotics.

Docosahexaenoic acid (DHA) is an omega-3 polyunsaturated fatty acid with bactericidal activity against *H. pylori*, inhibiting their growth *in vitro* and decreasing their gastric colonization in 50% of infected mice. The low DHA efficacy *in vivo* could be explained by its high susceptibility to oxidation or by its degradation in the gastric environment. For this reason, the main goal of this work was the development of an antibiotic-free engineered system for the treatment of *H. pylori* gastric infection. DHA was encapsulated into lipid nanoparticles, namely nanostructured lipid carriers (NLC), to protect DHA against the gastric environment and improve its efficacy against *H. pylori.* This system was developed for oral administration and NLC should be able to penetrate through the gastric mucosa and to reach *H. pylori* at infection site.

NLC were synthesized by hot homogenization and ultrasonication using a blend of lipids: a solid lipid (Precirol®ATO5) and a liquid lipid (Miglyol®812), and a surfactant (Tween®60). Homogenous and spherical NLC were successfully optimized and produced with the size of 211 ± 8 nm for unloaded-NLC and 302 ± 14 nm for DHA-loaded NLC. Both NLC have a negative surface charge (-28 ±3 mV). A good entrapment efficiency was obtained (66 ± 7%), with DHA incorporated in the matrix of NLC decreasing NLC crystallinity. NLC were stable in simulated gastric fluid, but were able to release DHA in bacteria medium over 3h (40%). Bactericidal enhancement of DHA activity was proved with DHA nanoencapsulation, since DHA-loaded NLC, even at low DHA concentration (10 µM) are bactericidal against *H. pylori* in opposite to free DHA which was only bactericidal at concentrations higher than 100 µM. Unexpectedly, unloaded-NLC were also bactericidal against *H. pylori* in all concentrations tested. Nevertheless, DHA-loaded NLC (2.5% v/v [containing 50 µM of DHA]) had a faster bactericidal activity (30 min) than unloaded- NLC (> 9h).

NLC mechanism of action towards *H. pylori* was explored using bioimaging and biochemical studies, which demonstrated that NLC were able to adhere to *H. pylori*, cross their outer and inner membrane, promoting an increase of periplasmic space and, subsequently, disruption of bacterial membrane, leakage of cytoplasmic content and bacteria death. Moreover, all observed *H. pylori* were in bacillary shape which is also an indicator of the fast bactericidal effect of NLC, meaning that bacteria did not have time to change their morphology from bacillary to a coccoid shape. Furthermore, the NLC developed are not cytotoxic to human gastric adenocarcinoma cells at bactericidal concentrations (up to 2.5% v/v).

In vivo studies suggested a reduction of *H. pylori* colonization in 82.5% and 92.6% for unloaded and DHA-loaded NLC treatment, respectively. This reduced infection was verified without causing gastric or hepatic toxicity. However, 1/3 of untreated infected mice did not present infection after 14 days of treatment, which indicates the need for further assays.

To evaluate if the unexpected bactericidal effect of unloaded-NLC was selective to *H. pylori*, these NLC were tested against other bacteria. Unloaded-NLC at bactericidal concentrations for *H. pylori*, did not affect the other bacteria tested, namely *Lactobacillus casei* and *Escherichia coli,* from gut microbiota.

These promising findings suggest that NLC should be envisaged an antibiotic-free alternative *H. pylori* infection treatment.

RESUMO

Mais de metade da população mundial está infetada pela bactéria *Helicobacter pylori* (*H. pylori*), uma bactéria Gram-negativa com forma de espiral, que após persistente colonização da mucosa gástrica é responsável pelo desenvolvimento de várias doenças gástricas, nomeadamente o adenocarcinoma gástrico. Embora tenham sido aplicados diferentes regimes de tratamento, a erradicação desta bactéria é ainda ineficaz em aproximadamente 20% dos pacientes, principalmente devido à resistência bacteriana aos antibióticos disponíveis.

O ácido docosahexaenóico (*docosahexaenoic acid*, DHA) é um ómega-3, ácido gordo polinsaturado, com anti-bacteriana contra *H. pylori,* inibindo o seu crescimento *in vitro* e diminuindo cerca de 50% a sua colonização na mucosa gástrica. A reduzida eficácia do DHA *in vivo* poderá ser explicada pela elevada suscetibilidade do DHA oxidar ou pela sua degradação em ambiente gástrico. Por essa razão, o principal objetivo deste trabalho foi o desenvolvimento de um sistema livre do uso de antibióticos para o tratamento da infeção gástrica por *H. pylori*. O DHA foi encapsulado em nanopartículas lipídicas, nomeadamente *nanostructurated lipid carriers* (NLC), para proteger o DHA contra o ambiente gástrico e melhorar a sua eficácia contra a *H. pylori.* Este sistema foi desenvolvido para a administração oral, e as NLC deverão ser capazes de penetrar através da mucosa gástrica e alcançar *H. pylori* no local de infeção.

As NLC foram sintetizadas por homogeneização a quente e ultra-sonicação, usando uma mistura de lípidos: um lípido sólido (Precirol®ATO5) e um lípido líquido (Miglyol®812),e um surfactante (Tween®60).

Foram otimizadas NLC homogéneas e esféricas, e produziram-se NLC com tamanho de 211 ± 8 nm para *unloaded-NLC* e 302 ± 14 nm para *DHA-loaded NLC,* estas NLC possuem uma superfície carregada negativamente (-28 ±3 mV). Após a produção obteve-se uma boa eficiência de encapsulação (66 ± 7%), verificando-se que o DHA foi incorporado na matriz lipídica da NLC, o que resultou numa diminuição da sua cristalinidade.

Estas NLC são estáveis em fluido gástrico, mas também permitem a libertação do DHA em meio de bactéria após 3h (40%). Provou-se que a nanoencapsulação melhorou a atividade bactericida do DHA, uma vez que *DHA-loaded NLC* apresentou efeito bactericida com as

concentrações mais baixas de DHA (10 μM), contrariamente ao DHA-livre que só revelou um efeito bactericida com concentrações maiores do que 100 μM. Inesperadamente, *unloaded-NLC* também revelaram uma atividade bactericida contra *H. pylori*, em todas as concentrações testadas. Além do mais, *DHA-loaded NLC* (2.5% v/v [50 μM of DHA]) manifestou uma atividade bactericida mais rápida (30 min) do que *unloaded- NLC* (> 9h).

O mecanismo de ação das NLC contra *H. pylori* foi explorado utilizando bioimagem e estudos bioquímicos que demonstraram que as NLC são capazes de aderir à membrana de *H. pylori,* atravessar a sua membrana externa e interna, promovendo um aumento do espaço periplásmatico e subsequentemente a rutura da membrana da bactéria, libertando o seu conteúdo citoplasmático e promovendo a morte da bactéria. Além disso, observou-se que todas as bactérias exibiam uma morfologia bacilar, que é um indicador do rápido efeito bactericida das NLC, o que significa que as bactérias não tiveram tempo para alterar a sua morfologia de forma bacilar para forma coccoide. Adicionalmente, verificou-se que as NLC desenvolvidas não são citotóxicas para as células de adenocarcinoma gástrico humano, nas concentrações bactericidas (até 2.5% v/v).

Estudos *in vivo* sugeriram uma redução de 82.5% e 92.6% da colonização de *H. pylori* quando tratadas, respetivamente com *unloaded* e *DHA-loaded NLC*. Verificou-se que esta redução da infeção não causou toxicidade gástrica ou hepática. Contudo, 1/3 dos ratinhos infetados não tratados não manifestaram infeção após 14 dias de tratamento, o que indica a necessidade da repetição destes ensaios.

Para avaliar se o inesperado efeito bactericida das *unloaded-NLC* foi seletivo para *H. pylori*, estas NLC foram testadas contra outras bactérias, demonstrando que estas *unloaded-NLC* não têm efeito contra as bactérias testadas, nomeadamente *Lactobacillus casei* e *Escherichia coli*, bactérias do macrobiota intestinal.

Estas promissoras descobertas propõem que as NLC devem ser consideradas como um tratamento da infeção de *H. pylori* sem recurso a antibióticos.

List of Abbreviations

3D	Three-dimensional
AFM	Atomic force microscopy
ALA	Alpha-linolenic acid
AMP	Antimicrobial peptide
ARA	Arachidonic acid
ATP	Adenosine triphosphate
BAbA	Blood-antigen binding protein A
BB	Brucella broth
CagA	Cytotoxin-associated gene A
CCD	Charge coupled device
CFU	Colony forming unit
CLSI	Clinical & Laboratory Standards Institute
COX-2	Cyclooxygenase 2
DCP	Dicetylphosphate
DHA	Docosahexaenoic acid
DLS	Dynamic light scattering
DMSO	Dimethyl sulfoxide
DPA	Docosapentaenoic acid
DPPC	1,2-dipalmitoyl-sn-glycero-3-phosphocholine

DSC	Differential scanning calorimetry
DSPC	1,2-distearoyl-sn-glycero-3-phosphocholine
E. coli	Escherichia coli
EE	Entrapment efficiency
ELS	Electrophoretic light scattering
EPA	Eicosapentaenoic acid
Epi-1	Epinecidin-1
EUCAST	European Society of Clinical Microbiology and Infectious Diseases
FBS	Fetal bovine serum
FDA	Food drug administration
FWHH	Full width at half height
GLA	Gamma-linolenic acid
GRAS	Generally recognized as safe
H. pylori	*Helicobacter pylori*
HpsC	Heat shock proteins complex
IARC	International agency for research on cancer
IL-8	Interleukine-8
ISO	International Organization for Standardization
L. casei	*Lactobacillus casei*
***L.* strains**	*Lactobacillus* strains
LA	Linoleic acid
LDH	Lactate dehydrogenase
LipoLLA	Liposomal linolenic acid
LipoOA	Liposomal oleic acid
LipoSA	Liposomal steric acid
LPS	Lipopolysaccharide
MALT	Mucosa-associated lymphoid tissue

MBC	Minimal bactericidal concentration
MHB	Müller-Hinton broth
MIC	Minimal inhibitory concentration
MRAS	Methicillin-resistant *Staphylococcus aureus*
MRS	Mann-Rogosa and Shape
MTT	3-(4,5-Dimethylthiazol-2-yl)-2,5-Diphenyltetrazolium Bromide
NAP	Neutrophil-activating protein
NLC	Nanostructured lipid carriers
NP	Nanoparticle
NSAID	Nonsteroidal anti-inflammatory drug
OA	Oleic acid
OAK	Oligo-acyl-lysyl
OD	Optical density
PAA	Poly(acrylic acid)
PAH	Poly(allylamine hydrochloride)
PBS	Phosphate buffer saline
PC	Phosphatidylcholine
PDI	Polydispersion index
PEG	Polyethylene glycol
PEGDSPE	1,2-distearoylsn-glycero-3-phosphoethanolamine-N-(polyethylene glycol-2000)
PHEPC	Partially hydrogenated egg phosphatidylcholine
PPI	Proton-pump inhibitor
PUFA	Polyunsaturated fatty acid
RI	Recrystallization index
ROIs	Reactive oxygen intermediates
RT	Room temperature

S. aureus	*Staphylococcus aureus*
S. epidermidis	*Staphylococcus epidermidis*
SA	Stearylamine
SAbA	Sialic acid-binding adhesin
SD	Standard deviation
SEM	Scanning electron microscopy
SLN	Solid lipid nanoparticles
TEM	Transmission electron microscopy
TP4	Tilapia Piscidin 4
TSA	Tryptic soy agar
TSB	Tryptic soy broth
UreB	Urease B
UV/Vis	Ultra-violet/visible
VacA	Vacuolating cytotoxin A

TABLE OF CONTENTS

CHAPTER I

AIMS AND THESIS ORGANIZATION

1.1 - Motivation and aims

Helicobacter pylori (*H. pylori*) is a Gram-negative and spiral-shaped bacterium that colonizes the stomach of half of the world population [1,2]. Persistent infection with this bacterium has been associated with several gastric diseases including gastritis, peptic ulcers, and gastric adenocarcinoma. It is estimated that approximately 78% of global gastric cancers are attributed to *H. pylori* infection [1,3,4], being this bacterium classified as a type I carcinogen for humans by the International Agency for Research on Cancer (IARC). Therefore, *H. pylori* infection eradication is a promising strategy for gastric cancer prevention [1,3-5]. Although infection has been decreasing worldwide, as a consequence of changes in dietary habits and improvement of socioeconomic conditions, in Portugal, *H. pylori* infection still remains in high values (80%) [6-8]. Recommended treatment is based on the combination of at least two antibiotics and a proton pump inhibitor [5,9]. However, this therapy fails in about 20% of the patients, which could be related to several reasons, but principally, with poor patient compliance to therapy and with the increased number of *H. pylori* strains resistant to conventional antibiotics [9,10]. Strategies to overcome these issues, such as the development of an *H. pylori* vaccine, have been attempted. However, progress has been very slow and no alternative treatments are available.

Natural compounds such as polyunsaturated fatty acids (PUFA) have been suggested as alternatives or as co-adjuvants of available antibiotic therapies. Docosahexaenoic acid (DHA) was able to inhibit *H. pylori* growth *in vitro* in a dose-dependent way and to decrease gastric colonization *in vivo.* Additionally, it was able to attenuate the host inflammatory response [11,12]. Nevertheless, DHA efficiency in the eradication of *H. pylori* from mice gastric mucosa

was significantly lower than the conventional antibiotherapy, failing in 50% of mice [11]. The failure of the orally administered DHA could be related to its poor solubility in water, low penetration through the mucus layer, low residence time in the stomach, and low stability *in vivo.* The low stability *in vivo* may result from oxidation, carboxylic protonation, esterification and lipid-protein complexation in the gastric environment [13,14].

Taking the above-mentioned facts into consideration, the major goal of this thesis was the development of an antibiotic-free strategy for the treatment of *H. pylori* gastric infection. The developed strategy was based on the encapsulation of DHA using lipid nanoparticles, namely nanostructured lipid carriers (NLC), aiming to improve DHA stability and efficacy against *H. pylori*. The proposed system was designed for oral administration, and should be able to penetrate through the gastric mucus layer, reach the surface of gastric epithelial cells and release DHA in a concentration capable of treating *H. pylori* infection *in situ.* As such, encapsulation would overcome problems associated with degradation and oxidation of DHA in gastric environment. NLC are employed in this study since lipids are known to promote oral absorption of compounds, while also showing good physical stability, controlled release and biocompatibility features. The proposed formulations provide an opportunity to exploit antibiotic-free therapies using NLC, either loaded or unloaded, attending that they are safe and well-tolerated both by the gastric mucosa and by other bacteria from gut microbiota.

1.2 - Structure

This thesis is organized in 8 chapters.

Chapter I includes the work motivation, the general objectives and a description of the thesis organization and structure.

An overview of the main features and virulence factors of *Helicobacter pylori,* their relationship with gastric cancer, the current treatments and the new strategies that have been investigated for bacterium eradication are presented in chapter II. This chapter also provides a description of polyunsaturated fatty acids (PUFA), namely its general features, health benefits and its activity against *H. pylori* and other microorganisms. Lipid nanoparticles are also reviewed, with a brief description of solid lipid nanoparticles, nanostructured lipid carriers (NLC) and liposomes, as well as the molecules and methods that can be used for their production. Chapter III comprises a brief introduction to the methodology behind the characterization techniques used to validate the developed nanoparticles.

The production of lipid nanoparticles, namely solid lipid nanoparticles (SLN) and nanostructured lipid carriers (NLC) was optimized as described in appendix 1 and 2. Firstly, SLN were optimized using different lipids, surfactants and parameters of production. Cetyl palmitate, Precirol®ATO5 and Tween®60 were identified as the most promising compounds for lipid nanoparticles production. However, due to the lack of reproducibility after DHA loading into

SLN, a second generation of lipid nanoparticles was pursued. NLC were then optimized using the same solid lipids (cetyl palmitate and Precirol®ATO5). However, Precirol®ATO5 was selected due to its FDA approval for oral administration. As such, the studies described in the following chapters of this thesis used Precirol®ATO5 as solid lipid for NLC production.

The optimization of DHA loading into NLC is described in Chapter IV. The goal of this work was to evaluate if DHA encapsulation was able to improve DHA activity towards *H. pylori* and human gastric cells (cytotoxicity) *in vitro.*

Due to the unexpected bactericidal activity of unloaded-NLC observed in chapter IV, the goal of chapter V was to clarify the NLC selectivity towards *H. pylori* and to understand their mode of action. To assess selectivity, other bacteria with different features, namely morphological (rod *vs* spherical) and structural (Gram-positive *vs* Gram negative), were exposed to unloaded-NLC. This approach also aimed to evaluate if unloaded-NLC were safe to gut microbiota, namely gastrointestinal *Lactobacillus* and *Escherichia coli.*

In chapter VI, additional characterization was performed, evaluating the physical state of the lipid core in the produced NLC and correlating with the DHA loading and DHA release profile. Due to the fast and high affinity of NLC to adhere to *H. pylori* membrane observed in previous chapters, permeability assays were performed for an additional understanding of how NLC may disrupt the bacterial membrane. Attending to the *in vitro* efficiency of NLC, the *in vivo* therapeutic potential of DHA-loaded and unloaded lipid nanoparticles was evaluated. The *in vivo* trial used an infected mice model that was treated with NLC in a non-cytotoxic concentration to a human gastric cell line. The toxicity profile was also evaluated through histological analysis of mouse stomach and liver.

Results described in chapters IV to VI are integrated and discussed in chapter VII, highlighting the major findings of this thesis. Future perspectives regarding the contribution of the present study for development of new alternatives to the conventional *H. pylori* infection treatment are also discussed.

As mentioned before, appendixes 1 and 2 include the optimization of lipid nanoparticles production, while appendix 3 comprises a national patent submitted during the PhD and appendix 4 contains a review that has been published (co-author).

References

1. Correa P (2013) Gastric Cancer: Overview. Gastroenterology Clinics of North America 42: 211-217.

2. Wroblewski LE, Peek RM, Wilson KT (2010) Helicobacter pylori and Gastric Cancer: Factors That Modulate Disease Risk. Clinical Microbiology Reviews 23: 713-739.

3. IARC (2014) *Helicobacter pylori* Eradication as a Strategy for Preventing Gastric Cancer.; Group I*Hp*W, editor. Lyon, France: International Agency for Research on Cancer.

4. de Martel C, Forman D, Plummer M (2013) Gastric Cancer: Epidemiology and Risk Factors. Gastroenterology Clinics of North America 42: 219-240.

5. Malfertheiner P, Megraud F, O'Morain CA, Gisbert JP, Kuipers EJ, et al. (2016) Management of *Helicobacter pylori* infection—the Maastricht V/Florence Consensus Report. Gut.

6. Papoila AL, Riebler A, Amaral-Turkman A, São-João R, Ribeiro C, et al. (2014) Stomach cancer incidence in Southern Portugal 1998–2006: A spatio-temporal analysis. Biometrical Journal 56: 403-415.

7. Bastos J, Peleteiro B, Barros R, Alves L, Severo M, et al. (2013) Sociodemographic Determinants of Prevalence and Incidence of *Helicobacter pylori Infection* in Portuguese Adults. Helicobacter 18: 413-422.

8. Morais S, Ferro A, Bastos A, Castro C, Lunet N, et al. (2016) Trends in gastric cancer mortality and in the prevalence of *Helicobacter pylori* infection in Portugal. European Journal of Cancer Prevention 25: 275-281.

9. Malfertheiner P, Megraud F, O'Morain CA, Atherton J, Axon ATR, et al. (2012) Management of *Helicobacter pylori* infection—the Maastricht IV/ Florence Consensus Report. Gut 61: 646-664.

10. Gonçalves IC, Henriques PC, Seabra CL, Martins MCL (2014) The potential utility of chitosan micro/nanoparticles in the treatment of gastric infection. Expert Review of Anti-infective Therapy 12: 981-992.

11. Correia M, Michel V, Matos AA, Carvalho P, Oliveira MJ, et al. (2012) Docosahexaenoic acid inhibits *Helicobacter pylori* growth in vitro and mice gastric mucosa colonization. PLoS One 7: e35072.

12. Correia M, Michel V, Osorio H, El Ghachi M, Bonis M, et al. (2013) Crosstalk between *Helicobacter pylori* and gastric epithelial cells is impaired by docosahexaenoic acid. PLoS One 8: e60657.

13. Desbois AP, Smith VJ (2010) Antibacterial free fatty acids: activities, mechanisms of action and biotechnological potential. Appl Microbiol Biotechnol 85: 1629-1642.

14. Dyall SC (2011) Methodological issues and inconsistencies in the field of omega-3 fatty acids research. Prostaglandins, Leukotrienes and Essential Fatty Acids (PLEFA) 85: 281-285.

CHAPTER II

GENERAL INTRODUCTION

2.1- *Helicobacter pylori*

Infection with *H. pylori* is very prevalent, being present in at least 50% of adults worldwide. Infection is typically acquired in early infancy remaining present for life if not treated [1,2]. This bacterium inhabits in the stomach and is responsible for several gastrointestinal diseases, including gastritis, peptic ulcer, duodenal ulcer and gastric adenocarcinoma [3-6].

2.1.1- Morphology and structure

H. pylori is a microaerophilic, Gram-negative, spiral-shaped bacterium with 2.5-4.0 μm long and 0.5-1.0 μm wide, four to six unipolar flagella (Figure 1), that persistently inhabits the human stomach [7]. Each flagellum is ~ 30 μm long and approximately 2.5 nm thick. Flagella display a characteristic terminal bulb, which is an extension of the flagellar sheath that exhibits the typical bilayer structure of a membrane [8].

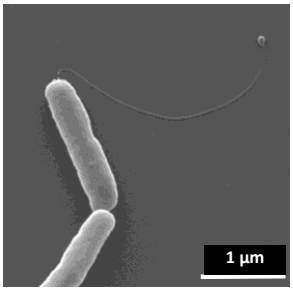

Figure 1-Scanning electron micrograph of *H. pylori.* Adapted from Seabra *et al* [144]

H. pylori has a hydrophilic and negative surface charge *in vitro.* The typical cell wall of this bacterium consists of outer and inner membranes separated by the periplasm of approximately 30 nm thickness. The outer membrane composition is unique in its protein content and lipopolysaccharide structure. The dense cytoplasm contains nucleoid material and ribosomes. *H. pylori* peptidoglycan revealed a unique muropeptide composition, less complex structurally than that observed in other Gram-negative bacteria [9-12].

H. pylori has an unusual fatty acid membrane profile, with the most abundant being the myristic acid (31 to 45%) and the 19-carbon cyclopropane fatty acid (20 to 24%). The *H. pylori* total lipid content (by weight) is 6% neutral lipids, 20.6% glycolipids and 73.4% phospholipids, and cholesterol glucosides that are very rare in animals [12].

A key component of the outer membrane of *H. pylori* is the lipopolysaccharide (LPS), which consists of a lipid A, a core oligosaccharide, and an O-specific chain. The surface exposed O-specific chain of *H. pylori* LPS mimics Lewis blood group antigens in structure. Molecular mimicry between *H. pylori* LPS and the host, based on Lewis antigens, may contribute to pathogenesis, since the expression of Lewis antigens on their surface may help to camouflage the bacteria and thus, allowing *H. pylori* survival [8,10,12].

A large number of proteins such as porins and adhesins are present in the outer membrane of *H. pylori* and are involved in the bacteria adhesion, colonization, and the immune response. Some outer membrane proteins perform transport functions essential for bacterial metabolism while maintaining the selective permeability of the outer membrane to substances like antibiotics [12].

The presence urease, a cytoplasmic protein that can be also found on *H. pylori* surface, allows *H. pylori* to survive and colonize the gastroenteric tract since urease is able to hydrolyze urea into ammonia and carbon dioxide, elevating the acidic gastric pH to neutral pH. However, urea is toxic to the bacterium at neutral pH since an unfavorable alkaline environment is generated. Thus, the urea channel is regulated positively by protons, opening at acid pH to allow more urea into the buffer cytosolic and closing at neutral pH to avoid over-alkalinization [13].

2.1.2- Colonization and virulence factors

It is known that the stomach performs numerous functions: temporary storage of ingested nutrients; mechanical breakdown of solid food; chemical digestion of proteins; regulation of the passage of chime into the duodenum; secretion of intrinsic factor for vitamin B_{12} absorption; secretion of gut hormones; and secretion of acid to aid digestion and microbial defense. The stomach can be divided into four parts: (1) cardia, which surrounds the opening of the esophagus into the stomach; (2) fundus, which is the area above the level of the cardial orifice;

(3) body, which is the largest region of the stomach; and (4) pyloric part, which is divided into the pyloric antrum and pyloric canal and is the distal end of the stomach (Figure 2) [14-16]. Most intestinal type and diffuse gastric adenocarcinoma associated with *H. pylori* occur in the gastric antrum, body or fundus (less likely), and normally, *H. pylori* infects the gastric antrum part [17].

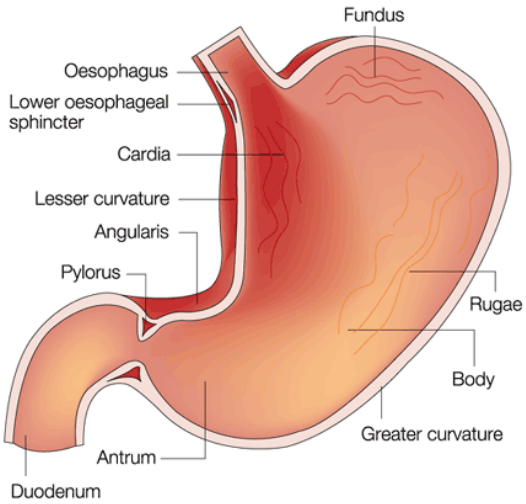

Figure 2- Parts of the stomach and its anatomy [17]**.**

The stomach wall and the proximal 3.0 cm of the duodenum are composed of four layers: serosa, muscularis, submucosa, and mucosa, together with vessels and nerves (Figure 3) [18].

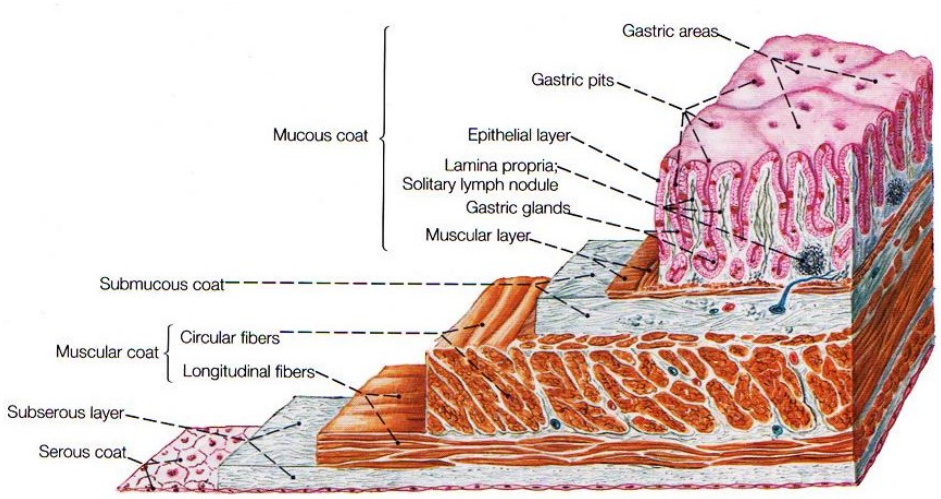

Figure 3-Structures of human gastric mucosa. Serosa is an extension of the visceral peritoneum and is a thin serous membrane made of a simple squamous epithelial tissue and areolar connective tissue. Muscularis is a thin layer of smooth muscle fibers lying external to the layer of glands, arranged with its fibers running in three different directions: longitudinal external, circular media and oblique internal. The submucosa is composed of various connective tissues, and contains thick bundles of collagen, numerous elastin fibers, blood vessels, and nerves, and surrounds the mucosa, the innermost layer of the stomach. Mucosa maintains structural integrity and resists auto-digestion by substances such as hydrochloric acid and pepsin. The gastric mucosa is a thick layer with a soft, smooth surface that is mostly reddish brown in life but pink in the pyloric region. It contains a layer of loose connective tissue of lamina propria, a thin layer of smooth muscle, the muscularis mucosae, and a simple columnar epithelium tissue. Adapted from [14,15,18,19].

The epithelial tissue of gastric mucosa is a layer of simple columnar cells that covers the entire luminal surface of the mucosa tubular invagination, gastric pits or foveolae. There are 60 to 100 gastric pits per square millimeter of gastric mucosa, with diameters of approximately 70 µm and depths around 0.2 mm. The base of each gastric pit receives several long, tubular gastric glands that extend deep into the lamina propria as far as the muscularis mucosae [14,15,18]. Simple columnar mucus-secreting epithelium covers the entire luminal surface, including the gastric pits and is composed of a continuous layer of surface mucous cells that release gastric mucus from their apical surfaces to form a thick, protective lubricant layer over the gastric lining (Figure 4) [14].

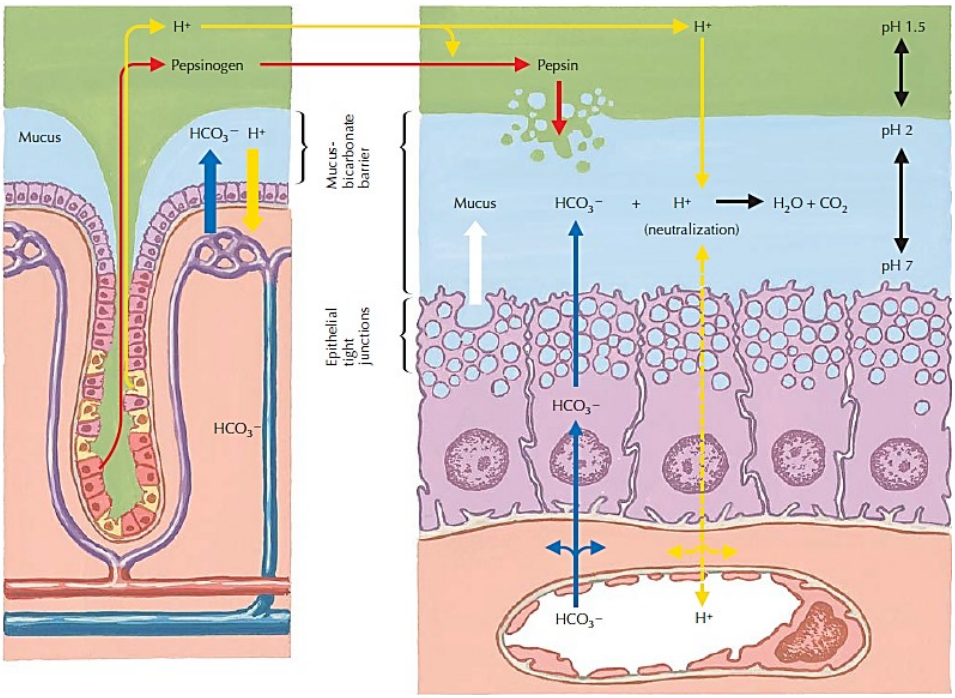

Figure 4- Gastric mucosa and submucosa protected from chemical injury by a mucus-bicarbonate surface barrier that neutralizes gastric H^+ and by epithelial "tight junctions" that prevent H^+ access to subepithelial tissue. Thick mucus from the surface epithelial cells traps the secreted bicarbonate on the surface of the gastric mucosa. The bicarbonate-containing mucus layer protects the cells from the caustic acid (pH ~1.5), keeping the pH at the surface ~7.0. Adapted from Mulroney& Myers (2009) [20].

The mucosal surface is highly hydrated (>95%) and covered by a viscous mucus gel with a thickness of approximately 300 µm. The mucus serves both as a lubricant and as a physical barrier protecting the mucosal epithelium against gastric acid and maintaining their neutral pH despite the highly acidic intragastric lumen. The main components of the mucus barrier are mucin glycoproteins. Mucins are highly *O*-glycosylated proteins located at the interface between the epithelial cell layers and the external environment [21]. The main mucins in the stomach are the membrane-associated MUC1 and the secreted gel-forming MUC5AC and MUC6, which have been shown to protect the epithelium against *H. pylori* adhesion, *in vitro* [21].

H. pylori road to colonization is summarized in the four steps described in Figure 5: survival, motility, adhesion and damaging.

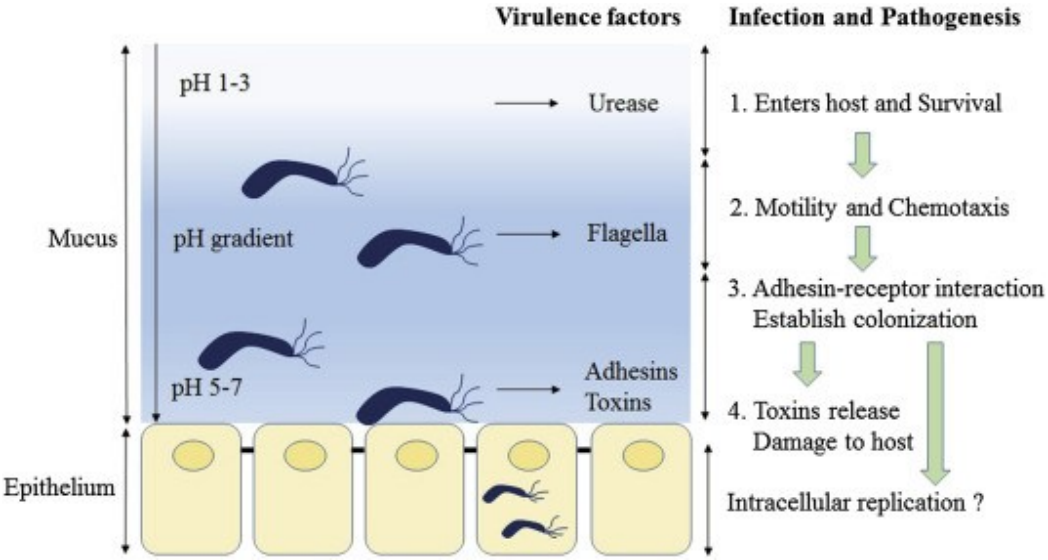

Figure 5- Schematic diagram of the *H. pylori* infection and pathogenesis. The urease activity and flagella-mediated motility of *H. pylori* facilitate its survival and movement towards the lower mucus gel, above the epithelium, and is followed by the interaction several adhesins, including blood-antigen binding protein A, sialic acid-binding adhesin, and other outer membrane proteins with receptors on the host epithelium cells. After successful colonization, toxins including CagA, and VacA, are involved in damaging the host tissue and intracellular replication. Adapted from Kao *et al.* [6].

H. pylori enter the gastric lumen where its urease activity is used to neutralize the acidic environment and the surface layer around the bacterium. The flagella and the helicoidal shape of *H. pylori* facilitate their entrance and travel through the mucus layer allowing them to reach the apical domain of gastric epithelial cells. This is followed by specific interactions between bacterial adhesins with host cell receptors, which lead to successful colonization and persistent infection [6,13]. *H. pylori* adhesion to gastric mucosa is a crucial step in the establishment of a successful infection since it protects the bacteria from displacement by forces such as those generated by peristalsis movements, shedding of the mucous layer and gastric emptying. Some of the adhesins include blood-antigen binding protein A (BabA), which binds to fucosylated Lewis B blood group antigen, and the sialic acid-binding adhesin (SabA), which binds to inflammation-associated sialyl-Lewis x antigen. This close proximity to the gastric epithelium enables the bacteria to scavenge nutrients from host cells, which are released when bacterial toxins like cytotoxin-associated gene A (CagA) type IV damage the host tissues, causing alteration of the cytoskeleton [22-24]. Then, vacuolating cytotoxin (VacA) induces alterations of tight junctions and the formation of large vacuoles increasing transcellular permeability, cytoskeleton changes and apoptosis [23,25,26]. Toxic factors such as the *H. pylori* neutrophil-activating protein crosses the epithelial lining and recruit neutrophils and monocytes that cause tissue damage by releasing reactive oxygen intermediates (ROIs) and nitrogen reactive species. The combined toxic activity of VacA and of ROIs leads to tissue damage that is enhanced by loosening of the protective mucus layer and acid permeation [13]. The damage

inflicted by such toxins may ultimately lead to the development of gastrointestinal symptoms. The complement of toxin genes that a particular strain of *H. pylori* possesses strongly affects its virulence [6,27]. *H. pylori* virulence factors and their potential role in pathogenesis are summarized in Table 1.

Table 1-*H. pylori* virulence factors. Adapted from Monack *et al.*(2004) [28].

Virulence factors	Description /potential role in pathogenesis
Flagella	Involved in motility Essential for colonization
Urease	Resists acidic conditions in the stomach Activates innate immune responses during early steps of infection
BabA	Outer membrane protein Binds to fucosylated Lewis B blood group antigen Mediates adhesion to epithelial cells and possibly stomach epithelium
SabA	Outer membrane protein Mediates the adhesion of *H. pylori* to inflamed gastric mucosa by binding the sialylated carbohydrate structure
CagA	Translocated into host cell by type IV secretion apparatus encoded on *Cag*-PAI Disrupts tight junctions Epidemiologic link to cancer
VacA	Vacuolating toxin Induces apoptosis Involved in the immunomodulation and colonization of the mouse stomach

2.1.3- Routes of transmission

The routes for *H. pylori* transmission are not completely understood, but it is known that the reservoir of *H. pylori* is the human stomach. This bacterium appears to have a narrow host range. New infections are thought to occur as consequence of direct human-to-human transmission or environmental contamination [29,30].

The possible routes for *H. pylori* transmission are summarized in Figure 6.

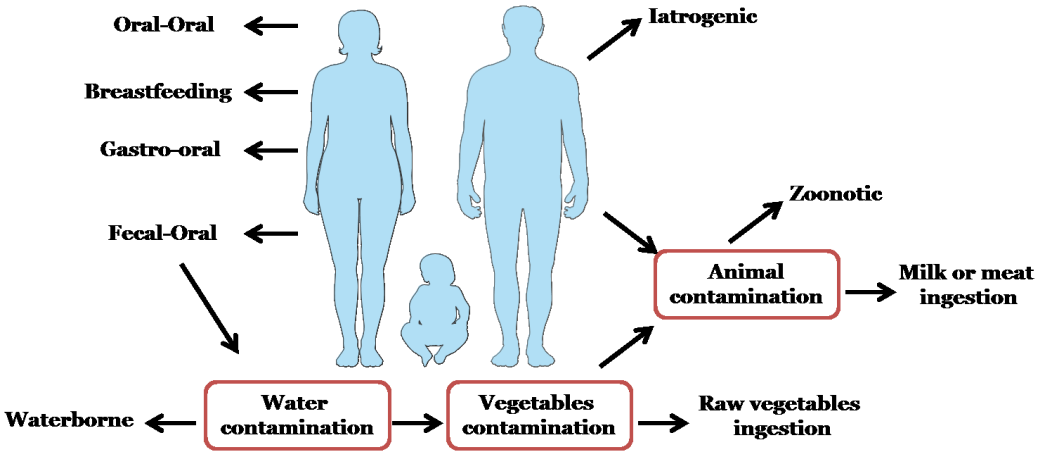

Figure 6-Transmission routes for *H. pylori*: direct person-to-person transmission, i.e. oral-oral, breastfeeding, gastro-oral, fecal-oral and iatrogenic via; and possible reservoirs outside the human host, namely water, vegetables, and animal contamination. Adapted from Azevedo *et al.*(2007) [31].

Most *H. pylori* infections are thought to be acquired in childhood via person-to-person. The close personal contact is important for the spread of *H. pylori* and its prevalence increases in family members with infected children [29,30,32]. The presence of *H. pylori* in the gastric juice, in up to 58% of patients infected with the bacterium, raised the possibility that the refluxed gastric juice may also represent a vehicle of transmission. The vomiting and regurgitation of gastric material into the mouth are fairly common in childhood and may represent an important route of transmission [30,31]. Saliva is another possible source of *H. pylori* transmission since the gastric flora can reach and colonize the mouth after regurgitation or vomiting. Still, the oral-oral transmission is not common for *H. pylori*, at least in adults [29].

Environmental or animal reservoirs, such as water, food, and animals, may be considered sources of *H. pylori* infection. Indeed, water is considered a vehicle in the transmission of *H. pylori,* in situation where poor hygienic practices during childhood are observed, in case of absence of a household bath, in non-hygienic drinking water situations and in the absence of a sewage disposal facility, which may lead to contamination or recontamination of drinking water [29,31,33]. Food products may also be contaminated while handling, under poor hygienic conditions. The food products most likely to transmit *H. pylori* are milk, meat, and vegetables. Vegetables are suspected to be vulnerable to *H. pylori* colonization when contaminated water is used for washing or irrigation [29,30].

The low socioeconomic status was reported as one of the most important factor in the spreading of *H. pylori* [30,33]. The high age-specific prevalence of *H. pylori* infection in developing countries has been attributed to low socioeconomic levels. Obviously, socioeconomic status is not restricted to income and social class but takes into consideration other factors such as levels of hygiene, the density of living, sanitation, urbanization and educational opportunities [30,33]. Educational level has been used as a marker of socioeconomic status and has been considered as one of the important determinants of *H.*

pylori prevalence in both developed and developing countries. Household crowding, sharing a bed and increasing household contact have also been identified as risks for *H. pylori* infection, because during childhood, crowded living conditions affect current bacterium status, and the number of children in the present household increases the risk of infection for the adult family members [30,33]. Another factor influencing the transmission of *H. pylori* is the genetic predisposition [30,33].

2.2. Outcomes of *H. pylori* infection

2.2.1- Gastric cancer in the World

Gastric cancer still ranks fifth for cancer incidence and third of cancer deaths worldwide (723 000 deaths, estimated in 2013) [34-36]. The majority of gastric cancer-related deaths occurred in East Asia, nearly half in China (Figure 7) [2,36,37].

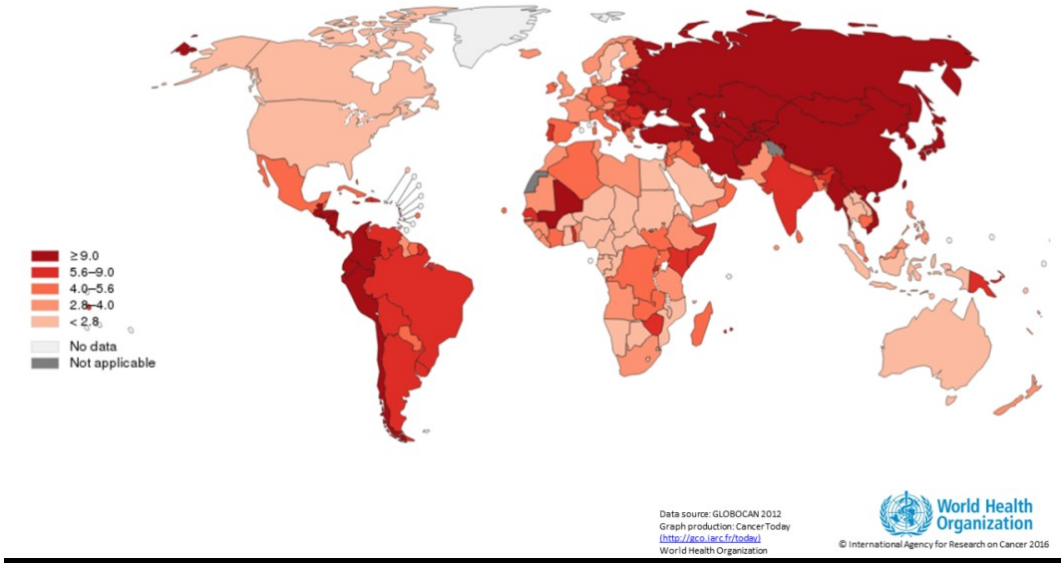

Figure 7- Estimated age-standardized death rates, for both sexes, caused by gastric cancer worldwide in 2012 [37].

Around 78% of all gastric cancer cases are estimated to be attributed to chronic *H. pylori* infection, considered to be the strongest identified risk factor for gastric cancer, with more than 60% of new gastric cancer cases worldwide being attributed to this bacterium [32]. In most individuals, *H. pylori* colonization is asymptomatic, but long-term carriage of the pathogen significantly increases the risk of developing site-specific diseases, suggested a sequential model of intestinal type-gastric carcinogenesis. Beside with outer environmental and host factors, trigger a precancerous cascade is initiated with chronic gastritis, evolving to atrophic gastritis, to intestinal metaplasia, followed by dysplasia, being the ultimate stage of this cascade invasive carcinoma (Figure 8) [7,32].

In 1994, *H. pylori* were classified by the International Agency for Research on Cancer as a Group 1 carcinogen, based on its association with gastric adenocarcinoma and mucosa-associated lymphoid tissue (MALT) lymphoma [1,2,34].

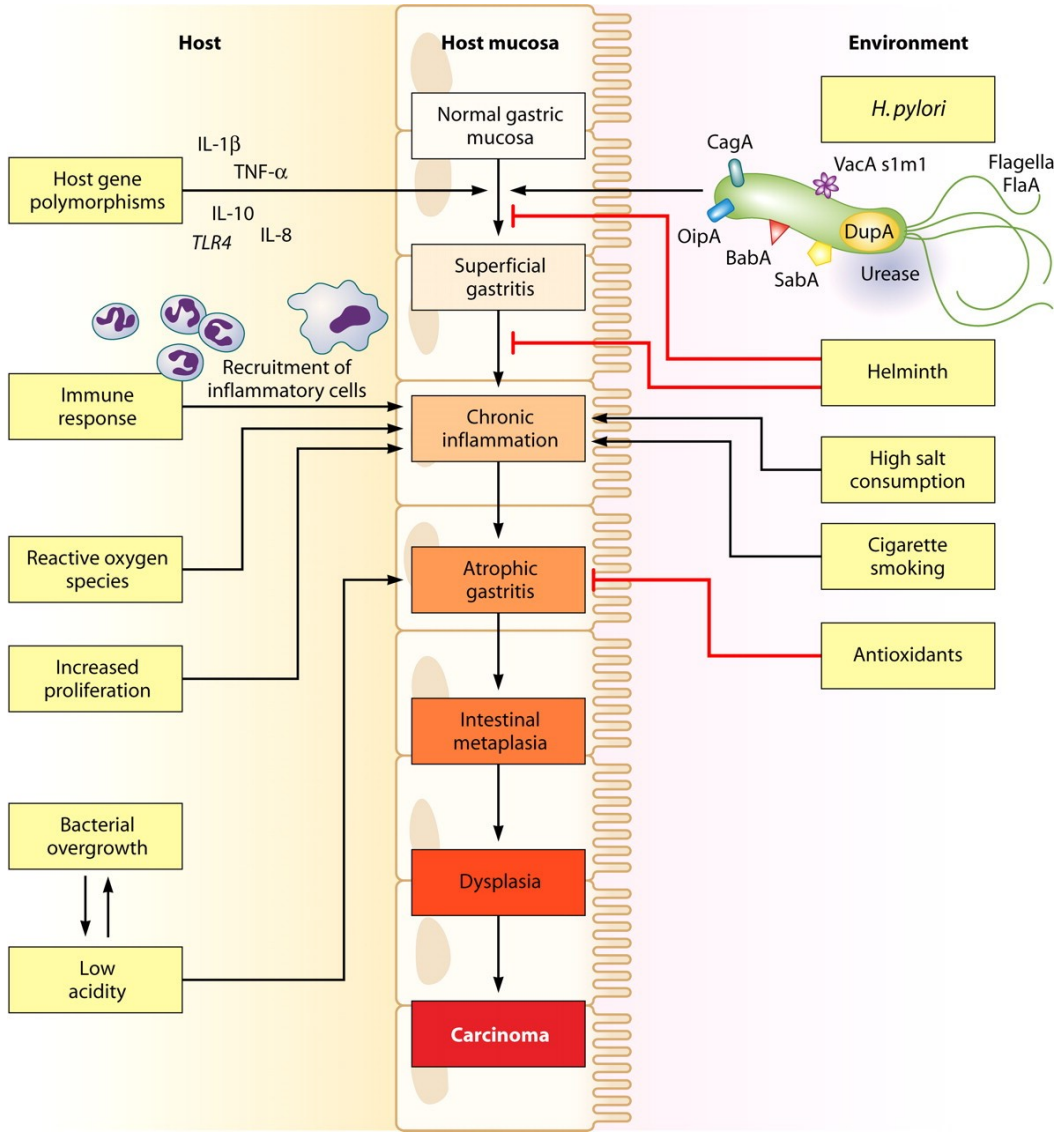

Figure 8- Multifactorial pathway leading to gastric carcinoma. Hosts, bacterial and environmental factors act in combination to contribute to the precancerous cascade that leads to the development of gastric cancer. Adapted from Wroblewski *et al.* [32].

2.2.2- Gastric cancer in Portugal

In Portugal, gastric cancer incidence (27.8%) and mortality (21.7%) rates are among the highest in Europe (19,5%) in 2013, especially in the North of the country (Figure 9), predicting an incidence of 40.1% in 2020 [4,38,39]. Regarding the number of deaths, stomach cancer accounts for 10.2% of all malignant cancer deaths [38].

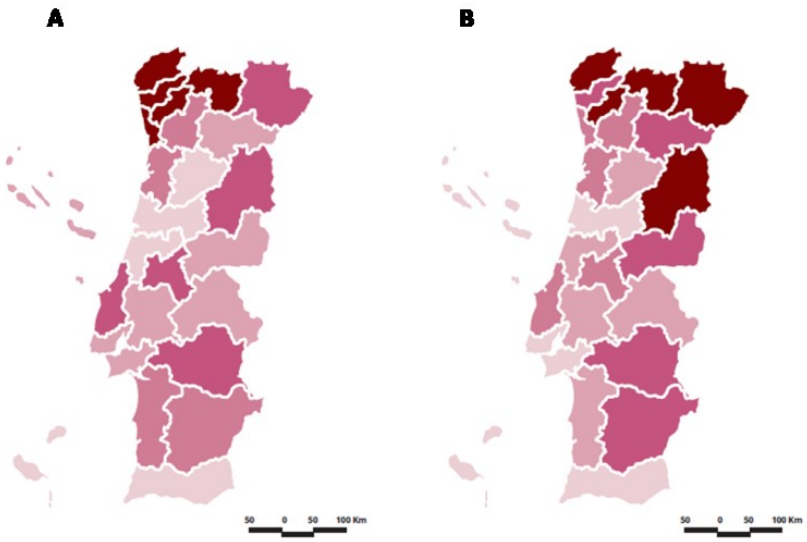

Figure 9-Stomach cancer standardized (**A**) incidence and (**B**) mortality rates per 100 000 population in 2013 [40].

In the last half century, Portugal went through several important economic and social changes, resulting in an improvement of the living standards, even though unequally across the different socioeconomic groups [4]. Some studies reported that the Northern Portugal has a higher gastric cancer risk factor than the Southern Portugal, due to the North of Portugal dietary habits, such as the preference for salty/cured foods, which favor the onset of gastric cancer [38,41].

2.3. Treatment of *H. pylori*

2.3.1- Current therapy

H. pylori eradication is the most promising strategy to reduce the incidence of gastric cancer. This treatment is recommended in infected patients with duodenal or gastric ulcers, early gastric cancer and gastric MALT lymphomas [7,42]. Treatment is also indicated for gastric cancer prevention in high-risk individuals and in patients with functional dyspepsia [42]. Recommended indications for treatment are summarized in Table 2.

Table 2- Indications for *H. pylori* infection eradication therapy. Adapted from Mitchell *et al.*(2016) [43].

Indication	Benefits of treatment
Past or present peptic ulcer disease	Heals ulcers and reduces relapse
Functional dyspepsia	May reduce symptoms and long-term risk of ulcer disease and gastric cancer
Use of NSAIDs, including aspirin, in some patients	Reduces risk of ulcers and bleeding
Gastric mucosal atrophy and intestinal metaplasia	Reduces risk of gastric cancer
Patients requiring long-term acid suppression with proton pump inhibitors	Reduces progression of intestinal metaplasia
Family history of gastric cancer	Reduces long-term risk of gastric cancer
Prior early gastric cancer	Reduces risk of further gastric cancer
Low-grade gastric MALT lymphoma	Induces regression of lymphoma
Patient choice, after risks and benefits, are discussed	Fulfills patient's desire to reduce risk of infection

Consensus conferences have recommended therapeutic regimens to achieve *H. pylori* cure rates higher than 80% on an intention-to-treat basis; for instance, the most efficient therapies available should be used first to avoid the cost inconvenience and risks associated with treatment failure [42,44,45].

Current initial treatments for *H. pylori* infection are summarized at Table 3.

Table 3- Current initial therapy regimens to treat *H. pylori* infection. Adapted from Costa *et al.* (2010) [46], Malfertheiner *et al* (2012, 2016) [47,48] and Thung *et al.* (2016)[3].

	Regimen	Time of treatment		Recommendations & comments
Triple therapy	Proton-pump inhibitor(PPI) Clarithromycin (500 mg) Amoxicillin (1g) or Metronidazole (500 mg)	7-14 days		Consider in areas of low clarithromycin resistance
Quadruple therapy	Proton-pump inhibitor (PPI) Levofloxacin (500 mg) Amoxicillin (1g) Metronidazole (500 mg)	10 days	Twice daily	Consider in areas of high clarithromycin resistance
	Proton-pump inhibitor (PPI) (morning and evening) Bismuth (525 mg) Metronidazole (250 mg) Tetracycline (500 mg)	14 days		

Currently, the most widely used treatment for *H. pylori* infection is the triple therapy, which includes the combination of two antibiotics, such as clarithromycin and amoxicillin or metronidazole, and a proton pump inhibitor (PPI) such as omeprazole [7,22,49,50]. However, the initial 90% cure rates obtained with this triple therapy have decreased to 75% or less, in some regions [7], which can be related to the increasing number of *H. pylori* strains that are resistant to the antibiotics used (Table 4), especially clarithromycin [46].

Table 4- Percentage of antibiotic resistance in some countries.

Antibiotic	Percentage of resistance	Reference
Clarithromycin	<18% in southern Europe	[46]
Metronidazole	20 to 40% in Europe and the USA 9 to 12% in Japan	[3]
Amoxicillin	<2% in Europe >38% Asia and South America	[3,51]

Levofloxacin-based triple therapy represents an alternative therapy in patients with persistent infection despite the use of multiple standard treatments [46,50]. Alternatively, a quadruple therapy containing bismuth, metronidazole, and tetracycline plus PPI, is quite effective even in the presence of clarithromycin and metronidazole resistance, with an eradication rate of up to 85%. However, compliance and side effects such as diarrhea, vomiting, and metallic taste remain as limitations of this regimen [3,46].

Another alternative treatment is the sequential therapy that consists of 5 days treatment with PPI and amoxicillin, followed by a further 5 days of PPI with two other antibiotics, clarithromycin and metronidazole [3,50,52]. The eradication rates for 10 days of sequential therapy were 87.2%, instead of 85.7% for 14 days of triple therapy, with no difference in compliance or adverse effects [3,50]. The drawback of this therapy is its complex regimen which may decrease patient compliance to the therapy and, thus, induce the development of multidrug-resistant bacteria [3].

Summing up, the choice of therapy is based on local antibiotic usage, documented antibiotic resistance, outcome data and also the world region [43,46]. It also depends whether it is a first-line therapy, a second course, or a rescue therapy for persistent infection [45,46] Other major determinants for a successful therapy are patient compliance, mucosal drug concentration and the individual primary or secondary bacterial resistance to the antibiotics employed [46].

2.3.2- Factors affecting *H. pylori* treatment failure

The successful eradication of *H. pylori* infection depends on various factors. These factors are associated with nature of the organism itself, the intragastric environment where the organism resides, the regimens used to eradicate it, and the behavior and reaction of the host [53].

The roles that the organism, gastric environment, hosts and drug regimens play in treatment failures are often inter-related. The key factors that increase the risk of *H. pylori* eradication therapy failure are described in Table 5.

Table 5- Factors that cause *H. pylori* treatment failure.

Factors	Major reason & comments	References
Antimicrobial resistance	• Resistant strains prior to treatment (primary) or be developed after a failed treatment (secondary)	[54-56]
Patient compliance to therapy	• Multiple different medications • Dose frequency (usually daily) • Duration of therapy (generally 10-14 days) • High frequency of side-effects • Limited information to patient about side-effect	[55-58]
Gastric environment	• Insufficient gastric acid inhibition • Easily degradation of antibiotics when the intragastric pH is less than 4.0	[53,59]
Smoking	• Decrease gastric blood flow and mucus secretion • Reduce the delivery of antibiotics to the gastric mucosa. • Stimulate acid secretion • Low efficacy of antibiotics	[54,57,59,60]

2.4. Alternatives to conventional therapy

The increased failure of the conventional therapies in the eradication of *H. pylori* infection in clinical practice demonstrates the urgent need for alternative therapeutic approaches. This includes the use of new drugs against *H. pylori* or new adjuvants that can reduce side-effects of available treatments and help in patient compliance.

The most exploited alternative approaches to fight *H. pylori* infections are the development of i) vaccines, ii) photodynamic inactivation, iii) phage therapy, iv) probiotics, v) antimicrobial peptides, vi) natural compounds such as plants and spices, phenolic compounds and lipophilic compounds, and vii) bioengineered micro/nanoparticles as drug delivery systems

or as binding agents [7,22,61,62]. Some examples of the described approaches are summarized in Table 6. However, although most of these alternative treatments have been very successful *in vitro*, their efficiency *in vivo* were not sufficient to be translated for clinical applications.

This is related with the fact that, *in vivo,* the molecules must achieve a bactericidal concentration at site of infection, and for that, they must be able to cross the protective mucus layer maintaining its biological activity at the large range of acidic pH [62].

Animal models can help elucidate the pathogenic mechanisms of *H. pylori* and aid in the development of improved strategies for the treatment of gastric disease [63].

The type of animal models developed to study *H. pylori* pathogenicity can go from primate- to rodent- based models. Several animals, including monkeys, pigs, cats, and dogs, have been successfully colonized by several *H. pylori* species. Their major advantage is their similar physiology with humans. However, several limiting factors, such as availability and high costs, may restrict their use. Other disadvantages of these animal models are related to the presence of natural *Helicobacter* infections such as *H. heilmannii* in primates and *H. suis* in pigs, and constraints regarding the examination of the long-term effects of colonization [63,64]. Because of that, most animal models used are rodents which allow host variables to be carefully monitored. Most mouse strains do not develop cancer but only mild inflammation following *H. pylori* infection. A rodent alternative is Mongolian gerbils that are an efficient, robust and cost-effective rodent model that can develop cancer when colonized with certain strains of *H. pylori* [64,65]. Table 7 summarizes some of the features of rodent animal models that can be used to study *H. pylori* infection.

Table 6- Alternative therapies against *H. pylori*

Therapy	Description	Agents	References
Vaccines	The key requirements to develop an effective vaccine are appropriate bacterial antigens, safe and effective adjuvants and a delivery route. Many vaccine formulations and strategies have been tested against *H. pylori* resulting in significant reduction in bacterial load, and production of regulatory T cells that many limit the eradicate *H. pylori* [66,67].	Antigens • UreB (most used) • HspC • VacA • CagA • NAP	*In vitro*: [68-71] Animal model: [72-76] Clinical trials: [77-81]
Photodynamic	Photodynamic therapy involves the use of non-toxic photosensitive molecules (photosensitizers) that will be activated by a specific wavelength of visible light. After activation in presence of oxygen, photosensitizers trigger a destructive action in biological systems, leading to bacterial death, due to the production of reactive oxygen species, such as singlet oxygen and hydroxyl radical [82-84].	Photosensitizer: • Ruthenium (II) complex covalently bound to micrometric glass beads (150-200µm) • Chorin e6 (ce6) in combination with red light • Aluminum sulfonated phthalocyanine	*In vitro*: [83-86] Animal model: [87] Clinical trials: [88,89]
Phage therapy	Bacteriophage therapy consists in the use of lytic bacteriophages (a virus that infects bacteria), or their lytic proteins to induce the lysis of *H. pylori*. The phages are engineered in a way that a particular antibody is fused to a protein on the phage's coat. Despite the possibility of using phage therapy to treat antibiotic multiresistant bacteria strains, *H. pylori* phage screening is a rare topic in the literature [61,90-93].	*H. pylori* phages • KHP30 • KHP40 • M13 • BAPOUI • JP1/95 • 1603/05 • Mex228	*In vitro*: [94-96] Animal model: [95]

(to be continued)

Therapy	Description	Agents	References
Probiotics	Probiotics are live microorganisms that are orally administered to promote a health benefit on the host. Probiotics can be used to prevent or decrease *H. pylori* colonization. Moreover, when included in *H. pylori* eradication therapy, they can improve eradication rates, by preventing antibiotic side effects, such as diarrhea. Also, probiotics can be produced in large scale at low cost [90-93].	Microorganisms • *L. acidophilus* • *L. casei* subsq *rhammosus* • *L. casei* 925 • *L. casei* DN-114001 • *L. Shirota* • *L. salivarius* WB1004 • *L. gasseri* • *L. johnsoniis* La1 • *L. plantarum* 8 RA-3 • *L. fermentum* BL-96 • *L. fermentum* L90265 • *Bifidobacterium infantis* 2036 • *Saccharomyces boulardii* • *Bacillus subtilis* • *Weissella confuse*	*In vitro*: [97-102] Animal model: [98,100,103,104] Clinical trials: [105-110]

(to be continued)

Therapy	Description	Agents	References
Antimicrobial peptides (AMP)	AMPs are a class of a broad spectrum antibiotic that are part of the innate immune system of several organisms such as animals, plants, fungi, bacteria and viruses. They are usually small (10-50 aminoacids in length), highly cationic and have tendency to form amphipathic structures. Most AMPs can act by the disruption of bacterial membranes due to electrostatic interactions between cationic AMP and anionic bacterial membranes, and low tendency to induce bacterial resistance [7,61].	Peptides • Magainin 2 • Odorranain-HP • Pexiganan • Defensins • Cathelicidins • RpL1 • TP4 • OAK • Epi-1	*In vitro*: [111-119] Animal model: [115,116,118,120,121]
Natural compounds	The use of natural food products such as fruits, vegetables, and fish could be used as adjuvant therapies or as potential sources for new effective agents against bacteria and associated inflammation. There are some molecules known by their capacity to inhibit essential bacterial enzymes (such as urease) or to disrupt bacterial membranes [7,61,90,92].	Phenolic compounds • Wine polyphenol • Apple peel polyphenols extracts • Olive oil polyphenols • Green tea • Garlic • Broccoli • Curcumin Lipophilic compounds • Terpenes • Terpenoids • Fatty acids	*In vitro*: [122-130] Animal model: [123,127,130-135] Clinical trials: [130,136-139]

(to be continued)

Therapy	Description	Agents	References
Bioengineering	Bioengineering has become a powerful tool by combining innovative bioengineering strategies with bioactive compounds. The encapsulation of antimicrobial compounds using gastric retentive polymers enhances their bioavailability, by protecting and increasing their retention time in the gastric environment. Binding systems that, after oral administration, are able to attract/bind bacteria and remove them from the host stomach through the intestinal tract, after gastric mucus turnover, were recently proposed as an alternative strategy [7,22].	Bioengineering strategies • Microspheres • Nanoparticles • Liposomes • NLC	*In vitro*: [128,129,140-154] Animal model: [135,140,148,150,155]

Abbreviations: UreB- urease B; HspC- heat shock proteins complex; NAP- neutrophil-activating protein; *L.* –*Lactobacillus*; TP4-Tilapia Piscidin 4; OAK- oligo-acyl-lysyl; Epi-1-Epinecidin-1

Table 7. Different features of rodents animal models used to study *H. pylori* infection. Adapted from Houghton (2012) [156] and Ivanov (2016)[157].

Animal model	*H. pylori*		Features/comments	References
	Strain	**Infection conditions**		
Mice (C57BL/6)	SS1	• *Helicobacter*-free • Oral gavage • 0.1 mL (10^6 CFU) of bacteria • 3 doses, 1 per day and each separated by 24-48h [158]	• Extensively studied for investigating *H. pylori* role in gastric carcinogenesis • Only show a marked influx of mononuclear cells while in humans gastritis there are an accumulation of neutrophils and mononuclear cells in the mucosa.	[127,134,135,140,159,160]
Mice (BALB/c)	SS1		• Widely used in cancer and immunology studies • Characterized by higher bacterial colonization levels but fewer epithelial lesion • Used as a model of *H. pylori*-induced MALT lymphoma.	[159-164]
Mice (C3H)	SS1 26695		• Easy to colonize with *H. pylori* including with strain 26695 or by isogenic mutants deficient in Lewis x or y expression.	[116,118,160,165]
Mongolian Gerbils	NCTC 11637 B128 G1.1 TN2 7.13	• *Helicobacter*-free • Oral gavage: 0.5 mL (10^9 CFU) of bacteria • 2 doses (wait 24–48h before the second challenge)[65]	• Model for study the pathogenesis of *H. pylori* infection, especially gastritis, intestinal metaplasia, gastric ulcers and gastric carcinoma.	[166-172]

2.4.1- Polyunsaturated fatty acids (PUFA)

The antibacterial proprieties of PUFA have been investigated in various organisms including *H. pylori,* due to their high potency and lower susceptibility to induce *H. pylori* resistance compared to conventional antibiotics.

2.4.1.1- General features and health benefits

Fatty acids can be classified by their carbon chain length and by their number of double bonds [173]. Long-chain fatty acids contain more than twelve carbon atoms. They are formed of hydrocarbon chains with a carboxyl group at one end (n end) and a methyl group at the opposite end (ω end). Unsaturated fatty acids (Table 8) hold in their chain one (monounsaturated) or more (polyunsaturated) carbon-carbon double bonds not saturated with hydrogen [174]. PUFA are defined as fatty acids that possess more than two double bonds, and their classification as n-3 or n-6 (omega-3 and omega-6, respectively) indicates the position of the first double-bond on the hydrocarbon chain, i.e. at the third or sixth carbons from the methyl end, respectively [174-176].

The n-3 and n-6 PUFA are present in vegetables and in animal tissues. Fish and other seafood are the major sources of the long-chain n-3 PUFA, such as eicosapentaenoic acid (EPA, C20:5 n-3) and docosahexaenoic acid (DHA, C22:6 n-3), whereas n-6 PUFA are mainly found in vegetable oils, nuts and seeds, especially linoleic acid (LA, C18:2 n-6) [174,176] (Table 9).

Table 8-Long-chain fatty acids classification in terms of number of carbon atoms and their double bonds. Adapted from Bazinet & Laye (2014) [173].

Name	Type	Number of carbon atoms	Number of double bonds	Symbol	Chemical structure
Oleic acid (OA)	Monounsaturated	18	1	18:1n-9	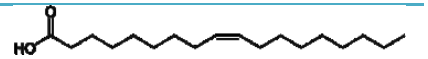
Linoleic acid (LA)	n-6 polyunsaturated	18	2	18:2n-6	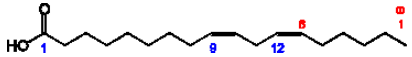
α-linolenic acid (ALA)	n-3 polyunsaturated	18	3	18:3n-3	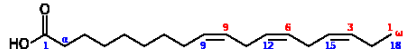
Arachidonic acid (ARA)	n-6 polyunsaturated	20	4	20:4n-6	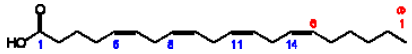
Eicosapentaenoic acid (EPA)	n-3 polyunsaturated	20	5	20:5n-3	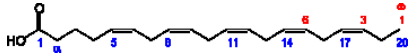
Docosapentaenoic acid (DPA) n-6	n-6 polyunsaturated	22	5	22:5n-6	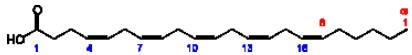
Docosapentaenoic acid (DPA) n-3	n-3 polyunsaturated	22	5	22:5n-3	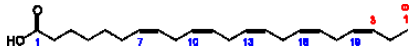
Docosahexaenoic acid (DHA)	n-3 polyunsaturated	22	6	22:6n-3	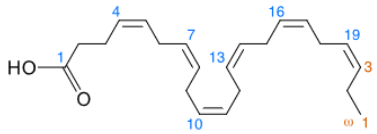

Table 9-Sources of PUFA high in n-3 and n-6 fatty acids [177].

n-3 oils	n-6 oils
Fish oil Chia oil Perilla oil Flaxseed oil Canola oil Walnut oil Soybean oil	Corn oil Safflower Sunflower seed oil Cottonseed oil Soybean oil Peanut oil Sesame oil Grapeseed oil Borage oil Primrose oil

LA can be endogenously converted to longer-chain n-6 PUFA, such as gamma-linolenic acid (GLA, C18:3 n-6) and arachidonic acid (ARA, C20:4 n-6) (Figure 10), whereas the n-3 PUFA, such as EPA and DHA, are converted from the progenitor alpha-linoleic acid (ALA, C18:3 n-3) by progressive desaturation and elongation (Figure 10) [176,178].

ALA is found in triglycerides, in cholesterol esters and in fewer amounts in phospholipids. EPA and DHA are found in the oils of fish (Table 10). EPA is found in triglycerides, cholesterol esters and phospholipids, or can be directly obtained from fish oils through diet. It is the precursor of eicosanoids comparable to those originating from ARA but with a lesser degree of bioactivity [175,177]. EPA may be converted to DHA, and also to eicosanoids, such as prostaglandins, thromboxanes, and leukotrienes. DHA is converted also to eicosanoids and to anti-inflammatory mediators such as resolvins and protectins [177]. DHA is found mostly in phospholipids, and its accumulation in the human body depends mainly on dietary intake [175,177,178].

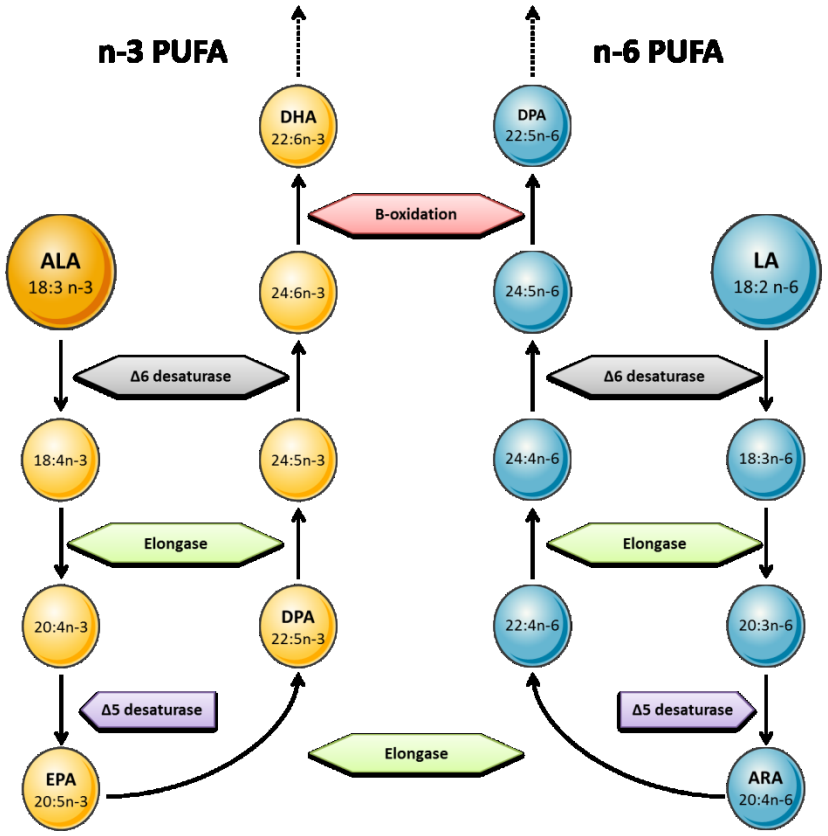

Figure 10- n3 and n-6 PUFA and their respective sources and metabolic derivatives. After consumption, the n-3 PUFA α-linolenic acid (ALA; 18:3n-3) and the n-6 PUFA linolenic acid (LA; 18:2n-6) can be desaturated, a process that involves the addition of a double bond, and elongated to become longer chain PUFA. The Δ6 desaturase enzyme is considered to be the rate-limiting step for the synthesis of docosahexaenoic acid (DHA; 22:6n-3). Adapted from Bazinet & Laye (2014) [173] and Mehta *et al.*(2009) [175].

Table 10-Content of n-3 PUFA in selected fish (grams per 100g edible portion, raw) Adapted from Simopoulos(2005) [177].

Fish	Total fat	Total PUFA	ALA (18:3n-3)	EPA (20:5n-3)	DHA (22:6n-3)	Cholesterol (mg/100g)
Anchovy, European	4.8	1.6	-	0.5	0.9	-
Bluefish	6.5	1.6	-	0.4	0.8	59
Carp	5.6	1.4	0.3	0.2	0.1	67
Catfish, channel	4.3	1.0	Tr	0.1	0.2	58
Cod, Atlantic	0.7	0.3	Tr	0.1	0.2	58
Croaker, Atlantic	3.2	0.5	Tr	0.1	0.1	61
Flounder	1.0	0.3	Tr	0.1	0.1	46
Grouper, red	0.8	0.2	-	Tr	0.2	-
Halibut, Greenland	13.8	1.4	Tr	0.5	0.4	46

(to be continued)

Fish	Total fat	Total PUFA	ALA (18:3n-3)	EPA (20:5n-3)	DHA (22:6n-3)	Cholesterol (mg/100g)
Halibut, Pacific	2.3	0.7	0.1	0.1	0.3	32
Mackerel, king	13.0	3.2	-	1.0	1.2	53
Mullet, striped	3.7	1.1	0.1	0.3	0.2	49
Plaice, European	1.5	0.4	Tr	0.1	0.1	70
Pollock	1.0	0.5	-	0.1	0.4	71
Salmon, Chinook	10.4	2.1	0.1	0.8	0.6	-
Salmon, pink	3.4	1.4	Tr	0.4	0.6	-
Sole, European	1.2	0.2	Tr	Tr	0.1	50
Swordfish	2.1	0.2	-	0.1	0.1	39
Tuna, albacore	4.9	1.8	0.2	0.3	1.0	54

Note: Tr, trace (<0.05g/100g food).

Different types of fish contain different amounts of fatty acids (Table 10) and may present different ratios of EPA:DHA. Populations such as the Japanese, who oily fish consumption is greater and regular than populations in Europe, North America, and Australian, have higher intakes of very long-chain n-3 PUFA, such as DHA that comprises ~30% of the fatty acids present [179].

Several clinical and epidemiologic studies have been developed to determine the effect of PUFA on the various physiologic index and their health or clinical benefits. PUFA confers various health benefits, including in rheumatoid arthritis [180], protection against the onset of diabetes [181,182], efficient immune response modifications [183], coronary heart disease [184], bronchial asthma [185], thyrotoxicosis [186], multiple sclerosis [175], depression [187], Alzheimer's disease [188,189] and cancer [190,191]. PUFA have roles in gastrointestinal diseases, such as gastric cancer and colonic cancer, as Wang *et al.* (2012) reported in a randomized clinical trial in which n-3 PUFA enriched emulsions displayed an anti-inflammatory effect in patients with gastrointestinal diseases [192]. PUFA have also an effect against pathogenic and opportunist microorganisms, inhibiting or killing bacteria [193].

2.4.1.2- PUFA activity against *H. pylori*

In 1987, a dietary intake of PUFA was reported as responsible for the decline of *H. pylori* infection in duodenal ulcer incidence [194]. After that, some studies were developed and demonstrated that concentrations of 2.5×10^{-4} M of LA could inhibit *H. pylori* growth *in vitro.* Further studies described that this inhibitory effect increased with the degree of PUFA unsaturation (number of double bonds): [oleic (C18:1) < linoleic (C18:2) < arachidonic (C20:4) < n-3 linolenic (C18:3) =n-6 linolenic (C18:3) = eicosapentaenoic (C20:5) acid] [195]. Concentrations of 1×10^{-3} M are able to kill bacteria by cell lysis as observed by Scanning

Electron Microscopy (SEM) [195,196]. PUFA can be incorporated into *H. pylori* phospholipids membrane, changing their morphology and inducing the disruption of the cell membrane [196].

Correia *et al.* (2012) demonstrated that DHA is also able to inhibit *H. pylori* growth *in vitro* in a concentration-dependent manner. At concentrations ≥ 250 μM, DHA was bactericidal to all *H. pylori* strains studied (26695, B128 and SS1 strains), whereas at concentration ~100 μM DHA was only able to inhibit their growth. Also, DHA induced the conversion of *H. pylori* from bacillus to coccoid form, being the coccoid form of *H. pylori* associated with low cell viability [127]. Moreover, DHA reduced ATP production by *H. pylori*, decreased *H. pylori* adhesion to AGS cells, inhibited their gastric colonization *in vivo*, and decreased gastric inflammation in a mouse model [127,134]. However, DHA efficiency in eradicating *H. pylori* infection in mice was significantly lower than the conventional antibiotherapy, failing in 50% of mice. Nevertheless, DHA used as co-adjuvant to conventional antibiotherapies yielded better results than those obtained with single conventional therapies.

Effectively, PUFA may contribute to a protective action against chronic inflammation, having an anti-inflammatory effect on *H. pylori*-infected gastric mucosa, in addition to its bactericidal effect [197]. According to Correia *et al.* (2012, 2013), DHA reduced inflammatory responses and the production of prostaglandin E2, associated with inflammation and tissue injury in the mouse gastric mucosa. In addition, this PUFA reduced the metabolic activity of *H. pylori* as well as the production of interleukin-8 (IL-8), cyclooxygenase 2 (COX-2) and induced nitric oxide synthase from gastric epithelial cells [127,134,198].

Clinical trials, using a daily administration of 2g EPA and DHA for 12 weeks in patients infected with *H. pylori,* had no significant effects on the eradication of *H. pylori,* and on the level of IL-6 (expecting high levels during *H. pylori* infection, but a gradual reduction after a successful treatment) [138].

Correia *et al.* (2014) also demonstrated that DHA is also incorporated into epithelial cells and is able to decrease cell membrane cholesterol levels, as well as cholesterol *de novo* synthesis. In addition, they showed that DHA decreases cholesterol uptake by *H. pylori* from epithelial cells and that *H. pylori* sensitivity to DHA may be influenced by a previous exposure to cholesterol [199]. It was also observed that *H. pylori* growth in a cholesterol-depleted medium is up to thousand-fold more resistant to antibiotics therapy [200,201].

The observed PUFA ineffectiveness *in vivo* can be related to their poor solubility in water (which difficult its administration), possible low penetration through the mucus layer and the low residence time in the stomach. Moreover, PUFA can suffer easy oxidation, carboxylic protonation, esterification, and lipid-protein complexation in gastric environment [193,202]. The exposition of EPA and DHA to light, peroxidants or high temperature may induce their rapid oxidation. Their autoxidation results in the formation of fatty acid based hydroperoxides and their degradation into secondary oxidation products [203].

One strategy to overcome and preventing PUFA oxidation is their encapsulation into nanodelivery systems, such as liposomes. These systems can stabilize and protect PUFA

against changes in environmental conditions and improve their bioavailability and activity at infection local.

LA incorporated into liposomes (LipoLLA), with sizes around 100 nm, were able to fuse with *H. pylori* membranes, allowing the free LA to be incorporated into the bacterium membrane, disrupting their integrity and killing bacteria in 5 min [128,129]. These LipoLLA were more efficient against *H. pylori* than other liposomal containing other PUFA such as oleic acid (LipoOA) and stearic acid (LipoSA). The minimal bactericidal concentration (MBC) for LipoLLA was 200 μg/mL, while 1 mg/mL of LipoOA was required to kill 90% of *H. pylori* and no antibacterial effect was observed for LipoSA for concentrations up to 1 mg/mL [128]. LipoLLA retention and distribution, as well as its efficiency in the treatment of *H. pylori* infection were evaluated using mice animal models. LipoLLA treatment was able to reduce the number of *H. pylori* in infected mice in a similar way as the currently used triple antibiotic therapy (99 %) and without promoting alterations in the histology or increased rates of apoptosis in the mice stomach. This effect was not observed when free LA treatment was used, that did not reduce *H. pylori* number in comparison to the triple therapy. Moreover, treatment with LipoLLA reduced the mRNA expression of proinflammatory cytokines known to be upregulated by *H. pylori* infection [135].

2.4.1.3- PUFA activity against other microorganisms

The effect of PUFA against other microorganisms have been also investigated since PUFA are well-suited for the: 1) treatment of superficial skin infections and acne [204-208], where the anti-inflammatory proprieties of certain PUFA may provide additional benefits [209,210]; 2) treatment and spread prevention of sexually-transmitted diseases [211,212], especially those caused by *Neisseria gonorrhoeae* or herpes simplex virus; 3) prevention of periodontal diseases and dental caries [213,214], and 4) reduction of infant gastrointestinal infections [215,216].

Table 11 summarizes some of the PUFA with antimicrobial activity.

Table 11- PUFA with antimicrobial activity.

Fatty acid	Microorganism	Reference
EPA DHA	*Bacillus subtilis* *Listeria monocytogenes* *Staphylococcus aureus* *Enterobacter aerogenes* *Escherichia coli* *Pseudomonas aeruginosa* *Salmonella enteritidis* *Salmonella typhimurium* *Burkholderia cenocepacia*	[217,218]
LA	*Staphylococcus aureus* *Bacillus cercus* *Streptococcus mutans* *Pseudomonas aeruginosa* *Salmonella typhimurium* *Vibro parahemolyticus* *Klebsiella pneumoniae* *Proteus mirabillis*	[219,220]
DHA γ-LA EPA	*Staphylococcus aureus* *Propionibacterium acnes*	[205]
EPA	*Phaeodactylum tricornutum* *Staphylococcus aureus* *Bacillus cereus* *Staphylococcus epidermidis* *Bacillus weihenstephanensis* *Planococcus citreus*	[221]

2.4.1.4- Antibacterial Mechanism of Action

PUFA antibacterial mechanism of action is unclear but can have inhibitory or cidal effects. It depends on many factors, such concentration, targeted microorganism, the microorganism physiological state and the environment conditions such as pH and temperature [209]. When a bactericidal interaction takes place, death is induced instantly or it may take longer periods of time. Often, the prime target is the bacterial membrane, which can be followed by the changes of a cascade of processes that are essential for bacteria survival. These processes are schematized at Figure 11 [193].

PUFA can disrupt the normal function of bacteria membrane and thus, the production of energy, by interfering with the electron transport chain and disrupting the oxidative

phosphorylation. Other processes that may contribute to bacterial growth inhibition or death include cell lysis, inhibition of enzyme activity, impairment of nutrient uptake and the generation of toxic peroxidation and auto-oxidation products (Table 12). Free fatty acids can exert a protonophore effect, whereby the pH of the cytoplasm is reduced to such an extent that the cell ceases to function normally [193,209,222]. Considering that fatty acids act on multiple cellular targets, bacteria resistance to fatty acids is expected to be rare [209,216,223].

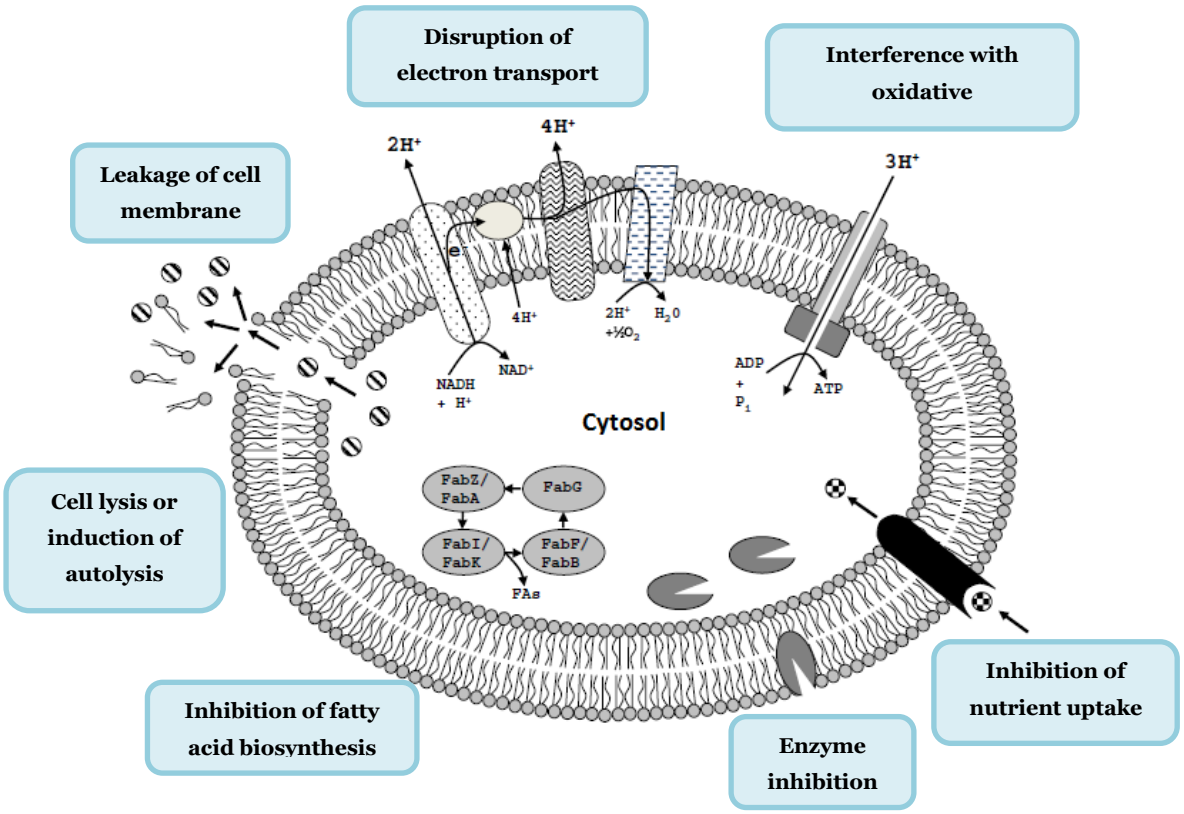

Figure 11- Schematic representation of the fatty acids antibacterial mechanism of action. Adapted from Desbois and Smith (2010) [193].

Table 12- Description of principal mechanisms of antibacterial of action of free PUFA. Adapted from Desbois and Smith (2010) [193].

Process	Description	References
Cell lysis	The insertion of free PUFA into the bacterial inner membrane causes it to become more fluid and permeable, allowing the leakage of the internal cell contents, causing growth inhibition or even death. When there is an excessive enhance of membrane fluidity, the membrane can become unstable and the cell will ultimately lyse. Notwithstanding, the detergent effect of fatty acids, which, at high concentrations, may solubilize large sections of the cell membrane, could further account for complete cell lysis.	[224-226]
Disruption of electron transport chain	The inner membrane of bacteria is an important site for energy production and it is where the electron transport chain is located. The ability of the electron transport chain to transfer electrons is impaired so that the proton gradient and membrane potential are reduced; resulting in a decrease in ATP production and the bacterium becomes deprived of an essential source of energy. Free PUFA could bind the electron carriers directly, but complete displacement from the membrane is likely achieved due to its increase membrane fluidity and instability.	[222,225,227-230]
Oxidative phosphorylation	Free PUFA can reduce ATP synthesis by increasing membrane permeability to protons, which could happen anywhere on the inner membrane or at specific proton pores. Thus, the proton gradient and membrane potential are able to be decreased by PUFA that after entered into cytosol, can release protons from its carboxyl groups and then returning across the membrane to the exterior, leading to an increase in the cytosolic concentration of protons.	[222,227,231,232]
Inhibition of nutrient uptake	Free PUFA are able to inhibit the bacteria ability to take up nutrients, such as amino acids. This reduction of nutrients uptake may be related to the disruption of the membrane-located transporter proteins or result from the reduced proton motive force required for the active transport.	[233-235]
Inhibition of enzyme activity	Free PUFA can interact with various intracellular and membrane targets, such enzymes. Inhibition of enzymes in the membrane or cytosol is crucial for bacterial survival and its growth. Their antibacterial effect are also due to the inhibition of fatty acids biosynthesis.	[236-238]
Peroxidation and auto-oxidation	PUFA high degree of unsaturation facilitates its degradation and the production of peroxides and reactive oxygen species, or its auto-oxidation creating oxylipins and short-chain aldehydes, which are antibacterial.	[216,227,239,240]

2.4.1.5-PUFA encapsulation

The bioavailability and absorption of PUFA is a complex process, depending on several factors, such as physicochemical properties, the presence or absence of other substances that enhance or inhibit absorption, metabolization after absorption, the state of health, and other individual factors [241-243]. After oral intake, PUFA enter the stomach where they are dispersed as fine droplets, due to the mechanical influence of stomach peristalsis movements, and travel until the upper small intestine. Besides the type of chemical bond, the concomitant intake of food, and the presence of other components also affect the uptake of PUFA. Calcium ions can also form a complex with PUFA and thus reduce their availability [243].

PUFA, like EPA and DHA, have a high degree of unsaturation, making them highly susceptible to oxidation, a process that involves the formation of toxic products (i.e. peroxides), unpleasantly smelling and tasting aldehydes and ketones [241,242,244,245]. There are a variety of materials that can be used for encapsulation of PUFA, to protect them against environmental effects (oxygen, light, humidity, pH) and, simultaneously, to improve their stability, handling conditions and bioavailability and may minimize the odor and taste problems [245,246]. There are some commercial capsules that use gelatin to encapsulate fish oil. However, these capsules tend to disintegrate in the stomach releasing the fish oil and consequently a fishy odor in the breath combined with undesired regurgitation which diminishes patient compliance [246]. Taking this into consideration, a novel lipid-based colloidal formulation has been developed. It consists of a highly concentrated lipid nanoparticle dispersion, which can be mixed in soft drinks or water, avoiding swallowing problems with solid dosage forms [246].

2.4.1.5.1- Lipid-based colloidal carriers

The application of nanotechnology, particularly the use of engineered small particles like microparticles (1-999 μm) and nanoparticles (1-999 nm) for drug delivery, has generated significant impact in medicine, revolutionizing the diagnosis and treatment of many diseases [49,247]. Why can nanoparticles offer improved properties to a classical organic antibacterial agent? One reason lies in their high surface area to volume ratio, resulting in the appearance of new mechanical, chemical, electrical, optical, magnetic, electro-optical and magneto-optical properties that are different from their bulk properties [248]. Small particles are recognized as allowing a sustained therapy since they can achieve higher retention time in the human body compared to free small molecules of antibiotics. Some authors defend that size plays a central role in the diffusion of the particles through the gastric mucosa to reach *H. pylori* since nanoparticles superior to 200 nm have a decreased diffusion [49,249,250].

Nanoparticles delivery systems possess some advantages: are quasi-monodisperse, are thermodynamically stable and show long-term kinetic stability. They improve drug controlled release, increase of pharmacokinetic proprieties of the drug, namely lipophilicity and reduce of side-effects leading to the increase of therapeutic compliance [49,251,252]. The use of nanoparticles in the treatment of *H. pylori* can also overcome the limitations associated with antimicrobial drugs degradation by the acidic pH of the stomach [49]. Moreover, it is improbable that bacteria might develop resistance to nanoparticles because numerous and complex gene mutation would be necessary to overcome either the multiple mechanisms of action of antimicrobial nanoparticles as well as the possibility to combine different antimicrobial drugs in the same carrier [253].

There are various nanoparticles delivery systems, especially, 1) lipid-based colloidal carriers such as liposomes or lipid nanoparticles, 2) polymeric nanoparticles, 3) dendrimers and 4) inorganic nanoparticles (Figure 12), that have been used in the release of antibiotics or novel non-antibiotic compounds [254,255].

Lipid-based colloidal carriers can overcome problems associated with polymeric nanoparticles, namely residues from the organic solvents used in the production process, polymer toxicity and the scaling up of the production process to industrial levels [251]. Lipid-based colloidal carriers have several application routes, namely topical [256,257] for cosmetics and dermatological applications, ophthalmic [258,259], nasal [260], parenteral [261] (intravenously, intramuscularly or subcutaneously), oral [262] and rectal [263-265]. These nanoparticles have shown excellent outcomes in treating and detecting bacterial pathogens by enabling targeted, responsive, combinatorial delivery of antimicrobial compounds, effective antibacterial vaccination and rapid detection of bacteria.

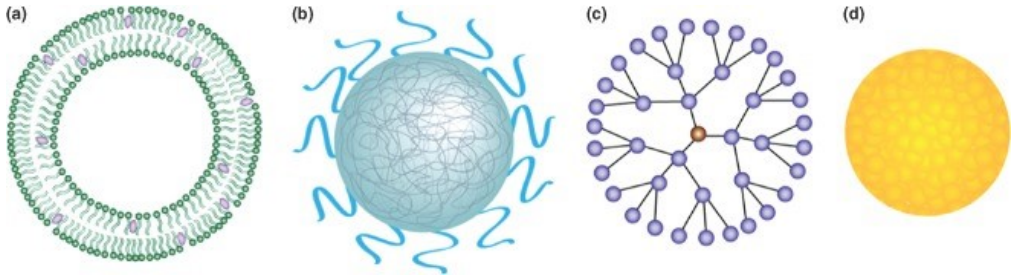

Figure 12- Schematic illustration of major nanoparticle-based delivery systems for the treatment of bacterial infections: (a) liposome, (b) polymeric nanoparticles, (c) dendrimer, and (d) inorganic nanoparticle [254].

In addition, multifunctional nanoparticles can respond to several stimuli that are characteristic of the pathological site, which is achieved through the inclusion of components that react to alterations in pH, temperature, redox conditions and to the overexpression of certain biological molecules. These nanoparticles can also respond to stimuli from outside the body, for instance, magnetic nanoparticles can be a tool for imaging contrast moiety to enable their biodistribution, target accumulation or to monitor the efficacy of a therapy (Figure 13) [266].

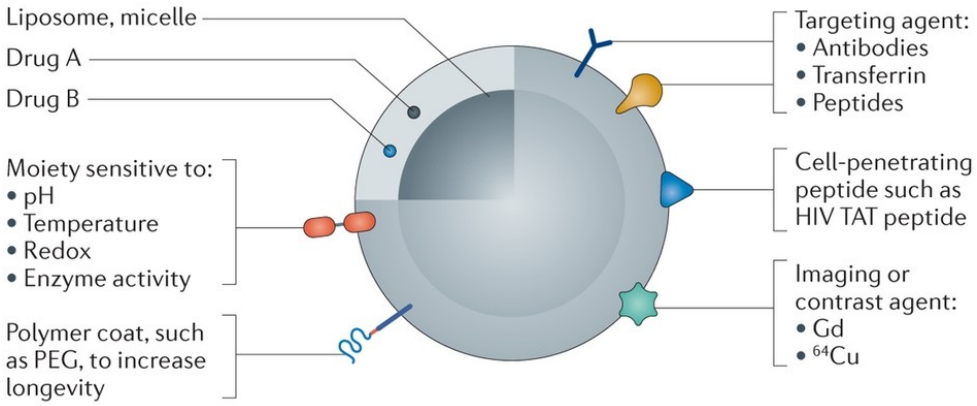

Figure 13- Schematic representation of a drug-loaded multifunctional, stimuli-sensitive nanoparticle. One or more drugs can be loaded into the nanoparticle. These can be functionalized with different targets, depending on the purpose of the nanoparticle, increasing cell penetration, to enable imaging or to release the drugs in response to a given stimuli [266].

Liposomes and lipid nanoparticles, namely solid lipid nanoparticles (SLN) and nanostructured lipid carriers (NLC), are colloidal nanoparticles that are suitable for the entrapping of lipophilic drugs [267], such PUFA.

2.4.1.5.2- Liposomes

Currently, liposomes are the most widely used antimicrobial drug delivery system. Liposomes are spherical lipid vesicles composed of self-assembled amphiphilic phospholipids, sphingolipids, and cholesterol that are self-assembled in the form of a bilayer membrane with an internal aqueous core. Once liposomes have both aqueous and lipid phases, they are able to carry both hydrophilic and hydrophobic drugs within the aqueous core or bilayer, respectively [254,268,269]. Liposomes are mainly composed of natural or synthetic lipids that are considered to be relatively biocompatible and biodegradable [252,270]. One of the most commonly used lipid is the phosphatidylcholine, which is an electrically neutral phospholipid that contains fatty acyl chains with varying degrees of saturation and length. Cholesterol is normally incorporated into the formulation to adjust membrane rigidity and stability [269].

One of the features of liposomes is its lipid bilayer structure, which mimics cell membranes and can readily fuse with infectious microorganisms and easily released the drugs to the cell membranes or inside the bacteria, consequently, a low drug resistance is induced [49,129,269].

Liposomes used in drug delivery typically range from 20 nm and a few hundred micrometers and are usually dispersed in an aqueous medium [252,268]. Drug release, *in vivo* stability, and biodistribution are determined by the size of the vesicles, their surface charge, surface hydrophobicity and membrane fluidity[252].

There are various methods for preparing liposomes. Still, all of them take into consideration parameters such as the physiochemical characteristics of the liposomal

ingredients, materials to be contained within the liposomes, particle size, polydispersity, surface zeta potential, shelf-time, batch-to-batch reproducibility, and the possibility of large-scale production [269]. Table 13 summarizes the methods that have been used for liposome production.

Table 14 presents some of the examples of liposomes that have been used for antimicrobial delivery.

Table 13- Methods of liposome preparation and their advantages and disadvantages for scale-up procedures. Adapted from Kraft *et al.*(2014)[271].

Method	Basic technique	Advantages for scaling	Disadvantages for scaling	Scalability potential
Solvent injection	Injection of lipids dissolved in a water-miscible solvent (generally ethanol) into aqueous phase	Single-step process Continuous processing	Presence of solvent without post-removal Not all lipids/drugs dissolve in ethanol	Very good
Thin film hydration	Production of a lipid film followed by solvent evaporation and rehydration in aqueous phase	Simple	Requires size reduction Equipment size is volume dependent	Suitable for small to mid-size batches
Reverse-phase evaporation	Preparation of an emulsion be mixing lipids dissolved in a water-immiscible solvent with aqueous phase followed by solvent evaporation	Simple	Multistep process	Suitable for small to mid-size batches
Detergent depletion (dialysis)	Lipid-micelle formation with detergent followed by detergent dilution or removal	Gentle	Presence of detergent	Good for sensitive proteins and oligonucleotides
Supercritical fluid	Solvation of lipids in supercritical carbon dioxide followed by injection into low-pressure aqueous phase	No organic solvent Sterility	Multistep process Expensive equipment	Good potential

Table 14- Liposomes for antimicrobial drug delivery against *H. pylori* and other bacteria.

Formulation	Drug combination	Targeted bacteria	Main Findings	References
PAA, PAH, PC, and cholesterol	Amoxicillin and metronidazole	*H. pylori*	• Effective in *H. pylori* eradication • Efficient to localize the drugs in the gastric environment • Rigid and tough for protecting the drug against the environment condition *in vivo*	[272]
EggPC and cholesterol	Linolenic acid	*H. pylori*	• Effective in killing both spiral and coccoid forms of bacteria via disrupting bacterial membrane *in vitro* • Penetrate on mucus layer of mouse stomach • Kill *H. pylori* and reduce bacterial load in the mouse stomach • Reduce the levels of pro-inflammatory cytokines • Biocompatible for mouse stomach	[128,129,135]
DPPC and cholesterol	Metronidazole Ampicillin	*H. pylori*	• Liposome interact with bacteria due to synthetic glycolipid-containing fucose • Interaction with coccoid forms of *H. pylori* namely strains with BabA2 • Efficient to kill bacteria	[273]
PC, SA, and cholesterol	Amoxicillin Bismuth citrate	*H. pylori*	• Enhance percent bacteria growth inhibition (*in vitro)* • Enhance anti-secretory and ulcer-protective activity (*in vivo*)	[274]
PEGylated liposome	Daptomycin and clarithromycin	MRSA	• Enhance anti-MRSA activity *in vitro* • Reduce MRSA bacterial load • Increase host survival *in vivo*	[275]

(to be continued)

Formulation	Drug combination	Targeted bacteria	Main Findings	References
PC, SA, and cholesterol	Ciprofloxacin and vancomycin	MRSA	• Enhance antibacterial activity • More effective in liposomal form than free form *in vivo* • Reduce drug toxicity • Reduce incidence of side-effect (severe diarrhea)	[276]
DPPC and cholesterol	Polymyxin B	*Pseudomonas aeruginosa*	• Decrease bacteria count in lung • Increase bioavailability • Decrease lung injury caused by bacteria	[277]
DSPC and cholesterol	Bismuth tobramycin	*Pseudomonas aeruginosa*	• Decrease number of bacteria • Reduce the production of quorum-sensing molecules and virulence factors • High therapeutic efficacy *in vivo*	[278]
PHEPC and PEGDSPE	Gentamicin	*Klebsiella pneunoniae*	• Increase survival rate of animal model • Increase therapeutic efficacy	[279]
DPPC, DCP, and cholesterol	Pyrazinamide	*Mycobacterium tuberculosis*	• Reduce the number of intracellularly located bacteria • High therapeutic efficacy *in vivo*	[280]

Abbreviations: DCP, dicetylphosphate; DPPC, 1,2-dipalmitoyl-sn-glycero-3-phosphocholine;; DSPC, 1,2-distearoyl-sn-glycero-3-phosphocholine; PAA, poly(acrylic acid); PAH, poly(allylamine hydrochloride); PC, phosphatidylcholine; PEGDSPE, 1,2-distearoylsn-glycero-3-phosphoethanolamine-N-(polyethylene glycol-2000); PHEPC, partially hydrogenated egg phosphatidylcholine; SA, stearylamine.

2.4.1.5.3- Lipid nanoparticles

Lipid nanoparticles are a relatively new class of drug nanocarriers that are able to incorporate hydrophobic drugs. These nanoparticles present very low cytotoxicity since are prepared using biodegradable and biocompatible lipids without using of organic solvents.. Moreover, they can be easily and economically prepared for large-scale production [281-283]. Lipid nanoparticles can be produced from oil-in-water nanoemulsions, where the liquid lipid of the oil droplets is replaced by a lipid that is solid at body temperature. Because of this, lipid nanoparticles remain solid after administration. At the same time, the matrix can be chemically protected against degradation. There are two generations of lipid nanoparticles, being the first generation are the solid lipid nanoparticles (SLN) and the second generation, the nanostructured lipid carriers (NLC) [282]. Figure 14 illustrates the differences between SLN and NLC.

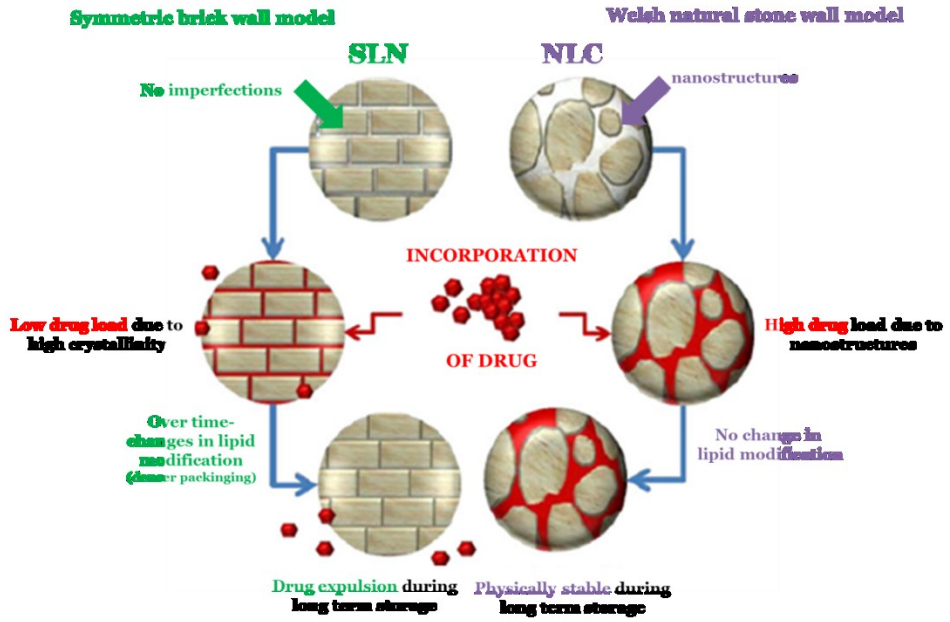

Figure 14- Differences between SLN and NLC. Adapted from Müller *et al.* (2011) [282].

2.4.1.5.3.1- Solid Lipid Nanoparticles (SLN)

By definition, SLN have sizes between 50 to 999 nm and the smaller the particle size the more likely will be their stability, their targeted responses and their capacity to encapsulate large amounts of the drug. SLN are colloidal particles derived from the oil-water emulsion by replacing liquid lipids with a lipid matrix that is solid at body temperature and a surfactant for particle stabilization [284-286]. Solid lipids used in SLN formulations include 1) fatty acids such as palmitic acid, decanoic acid, and behenic acid; 2) triglycerides such as trilaurin, trimyristin

and tripalmitin; 3) steroids such as cholesterol; 4) partial glycerides such as glyceryl monostearate and glyceryl behenate; and 5) waxes such as cetyl palmitate. Several types of surfactants are commonly used as emulsifiers to stabilize lipid dispersion, including soybean lecithin, phosphatidylcholine, poloxamer 188, sodium cholate and sodium glycocholate. The typical methods of preparing SLN include spray drying, high shear mixing, ultra-sonication and high-pressure homogenization [269,287].

SLN can be administrated by various routes such as oral, parental as well as transdermal/topical. Oral/intraduodenal administration of SLN are believed to enhance bioavailability of drugs by improving its transport through the intestinal epithelial layer and by protecting it from the hostile environment of the gastrointestinal tract [287].

SLN have several potential advantages [284]:

- Biocompatible and biodegradable;
- Prevent drug degradation in body fluids;
- Increase drug payload;
- Improve drug half-life;
- Control drug release;
- Enhance drug bioavailability;
- Drug targeting;
- Large scale manufacturing;
- Feasibility of sterilization.

However, common deficiencies of SLN include low drug loading capacity and a burst release after polymorphic transition during storage. This is related with the increased in the perfection of the crystal leaves, resulting in less space to accommodate drug molecules. In addition to polymorphic transition, the formation of drug-enriched shell leads to burst release. These disadvantages make SLN improper for some of applications as delivery system [252,285,287].

SLN have three different morphologies, based on the location of the incorporated drug molecules: (Table 15) 1) drug-enriched shell model; 2) drug-enriched core model, and 3) homogeneous matrix model [263,284].

Several unique proprieties of SLN make them promising antimicrobial drug delivery platforms, with possible applications in cosmetic and pharmaceutical products for skin care. One application of SLN is delivering azole antifungal drugs to superficial fungal infection patients. The occlusive effect of SLN, together with its small particle size, can extend drug residence time on the epidermis and enhance drug penetration through the skin [269]. SLN can also be used for oral administration, when included in tablets, capsules, and pellets. SLN can transport antibacterial compounds and penetrate the intestinal linings through endocytosis rather than passive diffusion. SLN have shown great therapeutic potentials against different microorganisms, as it is summarized in Table 16.

Table 15- Brief description of the structure of solid lipid nanoparticles (SLN). Adapted from Üner & Yener (2007) [263] and Shah *et al*. (2015) [284].

SLN structure	Description	Schematic illustration
Drug-enriched shell model	• Lipid core enclosed by a drug-enriched outer shell; • Suitable for applications where drugs need to be released as a burst; • Drug is solubilized in the surfactant-water mixture at elevated temperatures; • When dispersion is cooled, drug solubility decreases, leading to drug enrichment in the nanoparticle shell.	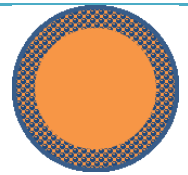
Drug-enriched core model	• Drug-enriched core enclosed by a lipid shell. This is obtained when the drug has a tendency to crystallize before the lipid; • The drug is solubilized in the melted lipid in a concentration closed to its saturation solubility; • Subsequent cooling of the lipid emulsion causes super-saturation of the drug in the lipid melt, leading to lipid recrystallization and formation of a membrane around the already crystallized drug-enriched core.	
Homogenous matrix model	• Drug is homogenously dispersed within the lipid matrix in molecules or amorphous clusters. • Suitable for incorporation of drugs that exhibit prolonged release from particles.	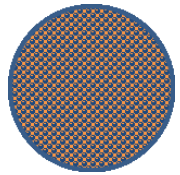

Table 16- Solid lipid nanoparticles for antimicrobial drug delivery against bacteria.

Formulation	Drug combination	Targeted bacteria	Main Findings	References
Stearic acid	Rifampicin, isoniazid, pyrazinamide	*Mycobacterium tuberculosis*	• Increase residence time • Increase drug bioavailability • Decrease administration frequency • Prolong drug release • High physical stability • High encapsulation efficiency	[288,289]
Stearic acid, soy phosphatidylcholine, and sodium taurocholate	Tobramycin	*Pseudomonas aeruginosa*	• Increase drug bioavailability	[290]
Tetradecanoic acid	Enrofloxacin	*S. aureus*	• Sustain and prolong drug release • Increase bioavailability • Extend mean residence time in combination with fatty acid	[291]
Palmitic acid, stearic acid, hydrogenated castor oil	Tilmicosin	*S. aureus*	• Sustain drug release • Enhance antibacterial activity • Decrease degree of inflammation (*in vivo*)	[292]
Compritol 888® ATO	Vancomycin	MRSA	• Ion pairing of vancomycin with antibacterial fatty acid (linoleic acid) • Enhance encapsulation efficiency • Increase antibacterial activity of vancomycin	[293]
Stearic acid	Norfloxacin	*E. coli*	• Sustaine drug release • Enhance antibacterial activity	[294]

2.4.1.5.3.2- Nanostructured Lipid Carriers (NLC)

NLC are prepared not from solid lipid only but from a blend of a solid lipid with liquid lipid (oils) in such a proportion that the mixture is solid at least at 40ºC [268]. NLC consists of an unstructured solid lipid matrix made of a mixture of blended solid and liquid lipids and an aqueous phase containing a surfactant or a mixture of surfactants. Different combinations of lipids and/or surfactants have been described (Table 17). They are commercially available and/or approved by different regulatory agencies such as Generally Recognized As Safe (GRAS) and FDA [264].

The imperfections present in the solid matrix of NLC accommodate the drugs either as molecules or as amorphous crystals. The process of full-crystallization or recrystallization of solid lipid reduces the drug solubility and leads to drug expulsion from the lipid nanoparticles, especially when the drug concentration in the formulations is too high [284,285]. On NLC formulation, the liquid lipid is incorporated into the core of a solid lipid. This leads to a higher loading capacity and a better control in drug release since the drug was dissolved in the liquid lipid that was simultaneously encapsulated in the solid lipid [285]. The major advantage of NLC over SLN is that many drugs are more soluble in a liquid lipid than in a solid lipid [285].

Therefore, NLC overcome the SLN drawbacks, since they increase encapsulation efficiency, drug loading, and drug physical stability. They seem to be a valuable option for improving the chemical stability and controlled release of functional lipophilic compounds [285,295]. NLC increase oral bioavailability when administered to mice [295].

NLC can be produced using various methods, such as hot/cold homogenization, emulsification-sonication, solvent injection, high-pressure homogenization, microemulsion and solvent diffusion, and membrane contractor techniques (Table 18). Hot homogenization is the most used method for fabrication of both, SLN and NLC due to several advantages, including easy scale up, lack of organic solvents and short production time, compared to the other methods [264,285,295]. In this approach, the mixture of solid, liquid lipids and surfactant are melted to 5-10ºC above the temperature of the solid lipid, and then the drug is dissolved or dispersed in this mixture. The mixture is dispersed in aqueous solution at the same temperature by high-speed stirring/shearing, obtaining a hot emulsion. Then this emulsion is homogenized using a high pressure homogenized, a high-intensity ultrasonic probe/jet/bath or a microfluidizer, to produce a hot nanoemulsion. Subsequently, NLC are cooled in cold water, at room temperature or by a heat exchanger to crystallize lipid droplet and precipitate the lipid nanoparticles [284,285].

Hot homogenization technique presents, however, some disadvantages like the high heating temperature which may promote degradation of the labile active compounds;

most surfactants have low cloud points and thus high temperatures may reduce their emulsifying capability and increase the NLC instability [285].

Like SLN, NLC have been proposed to possess three different morphologies based on the location of incorporated drug molecules: NLC type I or imperfect crystal type; type II or amorphous type; and type III or multiple type [263,284,285]. Table 19 summarizes the characteristics of each type of NLC.

NLC have shown great therapeutic potentials against different microorganisms, as it is summarized in Table 20.

Table 17- Lipid and surfactants used for NLC production, brief description and examples of marketed products. Adapted from Beloqui *et al* (2016) [264], Shah *et al*.(2015) [284] and Tamjidi *et al*.(2013) [285] .

Component	Chemical name	Trade name example	Examples of marketed products	Description
Solid lipid	Glyceryl palmitostearate	Precirol ATO®5	Xifaxan®	The requirements that should be considered for the choice of a suitable lipid blend are: 1. The solubility of the drug in lipid matrices. This influences the drug encapsulation efficiency and loading capacities, and subsequently the usefulness of lipid nanoparticles in drug delivery. 2. The solid and liquid lipids must be miscible at the specific concentrations needed, i.e., the blend of bulk lipids should be homogeneous and the liquid lipid should be situated as nanoholes within the solid matrix. 3. The lipid phase should be more stable to chemical degradation such as oxidation and lipolysis. 4. Lipids should be biodegradable and capable to produce particles in the nanometric scale. This is easier when the liquid lipid phase has a low viscosity and/or interfacial tension than when it has a high viscosity and/or interfacial tension. 5. Lipids should have an acceptable toxicological profile and should not lead to the production of any toxic residues during NLC preparation.
	Glyceryl dibeherante	Compritol ® 888 ATO	-	
	Cetyl palmitate	Crodamol™ CP	Azelex®	
	Stearic acid	-	Viokace®	
	Tripalmitin	-	Survanta®	
Liquid lipid	Caprylic/capric triglycerides	Miglyol®812	Avodart™	
	Vitamin E and derivatives	-	Neoral®	
	Monoacylglycerols	Myverol 18-99K	Terramycin®	
	Lauroyl Polyoxyglycerides	Gelucire®44/14	Lipofen®	
	Soy lecithin	Epikuron™200	Baycip®	

(to be continued)

Component	Chemical name	Trade name example	Examples of marketed products	Important considerations
Surfactants	Polysorbates	Tween® 20; Tween®60; Tween® 80	Targrentin®	The requirements that should be considered for the choice of a suitable surfactant are: 1. Amphipathic molecules that possess a hydrophilic moiety (polar) and a lipophilic moiety (non-polar), 2. Able to form nanoemulsions spontaneously by low-energy methods 3. Able to disperse the lipid melt in the aqueous phase during the production process, 4. Stabilize the lipid nanoparticles in dispersion after cooling 5. Non-ionic surfactants are preferred for oral and parenteral applications because they are less toxic, exhibit fewer side-effects and inhibit the *in vivo* degradation of lipid matrix than ionic surfactants.
	Poloxamers (188, 407)	Lutrol® F68; Lutrol® F127	Rapamune®	
	Polyoxiethylene stearate	Myrj 52	Dermazene™	
	Polyoxyl castor oil	Cremophor EL	Kaletra®	

Table 18- Methods used in the preparation of NLC: mechanism of production, advantages, and disadvantages. Adapted from Shah *et al*. (2015) [284].

Technique	Mechanism of nanoparticle formation	Advantages	Disadvantages
High-pressure homogenization	High mechanical shear due to strong turbulent eddies Lowering of pressure across the valves of homogenizers	Hot homogenization • Well established technology • Effective dispersion of particles • Reproducible • High lipid content • Simple to scale-up Cold homogenization • Effective dispersion of particles • Suitable for thermo-sensitive drugs • No complex lipid modifications • Increase drug-loading due to rapid cooling • Suitable for hydrophilic drugs • Reduce lipid melting • Reduce drug loss • Simple to scale-up	Hot homogenization • Extremely high energy inputs (heat and shear forces) • High polydispersity • Temperature-induced degradation of drugs • Complex crystallization, which leads to several lipid modifications and occurrence of supercooled melts • Inappropriate for hydrophilic drugs • Reduction in homogenization efficiency at elevated temperatures Cold homogenization • Extremely high energy inputs • Large particles with high polydispersity • Drug expulsion on storage
Emulsification and/or sonication	Shear between adjacent particles Formation, growth and implosive collapse of bubbles due to cavitation forces	• Use of organic solvents can be avoided • Use of large amounts of surfactants can be avoided • Simple technique with lower production cost • Higher energy inputs	• Unsuitable for higher lipid contents • High polydispersity • Physical instability due to high shearing • Metal contamination due to ultrasonication • Poor encapsulation efficiency

(to be continued)

Technique	Mechanism of nanoparticle formation	Advantages	Disadvantages
Microemulsion	Lipid crystallization due to rapid solidification	• Sophisticated equipment not required • Low energy inputs • Higher temperature gradients, faster lipid crystallization, avoids particle aggregation • Simple to scale-up	• Low lipid content
Solvent injection	Lipid crystallization due to rapid diffusion of solvent from internal organic phase to external aqueous phase	• Sophisticated equipment not required • Pharmaceutically accepted organic solvents used • Highly efficient and versatile technique • Simples to scale-up	• Solvent removal difficult • Low lipid content
Solvent diffusion	Lipid crystallization due to diffusion of solvent from internal organic phase to external aqueous phase	• Sophisticated equipment not required • Use of pharmaceutically accepted organic solvents • Small particle diameters and low polydispersity • Simple to scale-up	• Toxicological risks due to incomplete evaporation of organic solvents • Low lipid content
Membrane contractor	Solid/liquid lipid phase infuses through membrane pores into the tangentially flowing aqueous phase to form droplets Liquid lipid droplets crystallize to form lipid nanoparticles	• Controlled particles size with selection of membrane with correct pore size • Simple to scale-up	• Clogging of membrane pores, frequent replacement or cleaning procedures

Table 19- Brief description of the structure of NLC. Adapted from Üner&Yener (2007) [263], Tamjidi *et al*. (2013) [285] and Shah *et al*. (2015) [284].

NLC structure	Description	Schematic illustration
Imperfect crystal type	• Matrix with many voids and imperfections that are able to accommodate the drug molecules (★). • Mixing small amounts of chemically different and low compatible liquid and solid lipids to achieve the highest drug payload.	
Amorphous type	• The amorphous type minimizes drug expulsion by maintaining the polymorphicity of the lipid matrix, i.e., the amorphous model is created when mixing special lipids (e.g. hydroyoctacosanyl-hydroxystearate, isopropylmyristate) that do not recrystallize after homogenization and cooling of the nanoemulsion. • Lipid core congeals in an amorphous state (rather than crystalline state), minimizing drug expulsion during storage time.	
Multiple type	• The multiple type is related to the solubility of lipophilic drugs in liquid lipids, which is higher than that in solid lipids. • At low concentrations, liquid lipid molecules are easily dispersed into the lipid matrix. • By adding higher amounts of liquid lipid its solubility leads to phase separation, producing tiny oily nano-compartments (●) surrounded by the solid lipid matrix.	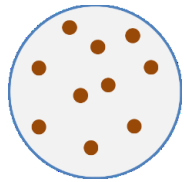

Table 20- NLC for antimicrobial drug delivery against bacteria.

Formulation	Drug combination	Targeted bacteria	Main Findings	References
Precirol ATO®5, Squalene and Pluronic F68	Tretinoin Tetracycline	*S. aureus* *Pseudomonas aeruginosa* *Propionibacterium acnes*	• Enhance tetracycline permeation through skin • Unaffect tretinoin permeation after encapsulation • Increase of antibacterial activity of tetracycline	[296]
Precirol ATO®5, Miglyol®812, Tween®80 and Poloxamer 188	Colistin	*Pseudomonas aeruginosa*	• Increase the antimicrobial activity of colistin • More efficient in the eradication of biofilms	[297]
Precirol ATO®5, Compritol® 888 ATO, Miglyol®812, Tween®80 and Poloxamer 188	Tobramycin	*Pseudomonas aeruginosa*	• Increase antimicrobial activity • No cytotoxic • Able to penetrate mucus • Large pulmonary distribution and retention in the *in vivo*	[298]
Precirol ATO®5, Miglyol®812, Tween®80 and Poloxamer 188	LL-37 peptide	*E. coli*	• Increase antimicrobial activity • No cytotoxic • Improve healing *in vivo* in terms of wound closure, re-epithelization grade and restoration of the inflammatory process	[299]
Hexadecyl palmitate, glycerol stearate, grape seed oil, sea buckthorn oil, St. John's wort oil, Syneperonic F68, Tween®20 and Tween®80	Green Tea extract	*E. coli*	• Increased antioxidant activity • Improved antibacterial activity	[300]
Glycerol monooleate, oleic acid, and Lutrol F127	Peptide: AP114 DPK-060 LL-37	MRSA *Pseudomonas aeruginosa* *E. coli* *Acinetobacter baumannii*	• Different structures have the capacity of solubilizing peptides • Differences on structure induced differences on antibacterial activity	[301]

References

1. Correa P (2013) Gastric Cancer: Overview. Gastroenterology Clinics of North America 42: 211-217.

2. de Martel C, Forman D, Plummer M (2013) Gastric Cancer: Epidemiology and Risk Factors. Gastroenterology Clinics of North America 42: 219-240.

3. Thung I, Aramin H, Vavinskaya V, Gupta S, Park JY, et al. (2016) Review article: the global emergence of *Helicobacter pylori* antibiotic resistance. Alimentary Pharmacology & Therapeutics 43: 514-533.

4. Bastos J, Peleteiro B, Barros R, Alves L, Severo M, et al. (2013) Sociodemographic Determinants of Prevalence and Incidence of *Helicobacter pylori Infection* in Portuguese Adults. Helicobacter 18: 413-422.

5. Bruce MG, Maaroos HI (2008) Epidemiology of *Helicobacter pylori* infection. Helicobacter 13 Suppl 1: 1-6.

6. Kao C-Y, Sheu B-S, Wu J-J (2016) *Helicobacter pylori* infection: An overview of bacterial virulence factors and pathogenesis. Biomedical Journal 39: 14-23.

7. Parreira P, Fátima Duarte M, Reis CA, Martins MCL (2016) *Helicobacter pylori* infection: A brief overview on alternative natural treatments to conventional therapy. Critical Reviews in Microbiology 42: 94-105.

8. Dunn BE, Cohen H, Blaser MJ (1997) *Helicobacter pylori*. Clinical Microbiology Reviews 10: 720-741.

9. Morales-Guerrero SE, Mucito-Varela E, Aguilar-Gutiérrez GR, Lopez-Vidal Y, Castillo-Rojas G (2013) The Role of CagA Protein Signaling in Gastric Carcinogenesis — CagA Signaling in Gastric Carcinogenesis.

10. Dunne C, Dolan B, Clyne M (2014) Factors that mediate colonization of the human stomach by *Helicobacter pylori*. World Journal of Gastroenterology : WJG 20: 5610-5624.

11. O'Rourke J, Bode G (2001) Morphology and Ultrastructure. In: Mobley HLT, Mendz GL, Hazell SL, editors. Helicobacter pylori: Physiology and Genetics. Washington (DC).

12. O'Toole PW, Clyne M (2001) Cell Envelope. In: Mobley HLT, Mendz GL, Hazell SL, editors. Helicobacter pylori: Physiology and Genetics. Washington (DC).

13. Montecucco C, Rappuoli R (2001) Living dangerously: how Helicobacter pylori survives in the human stomach. Nat Rev Mol Cell Biol 2: 457-466.

14. Standring S (2016) Gray's Anatomy: The Anatomical Basis of Clinical Practice; Standring S, editor: New York: Elsevier Limited.

15. Drake R, Vogl A, Mitchell A (2015) Gray's Anatomy for students. Philadelphia: Churchill Livingstone Elsevier.

16. Ellis H Anatomy of the stomach. Surgery - Oxford International Edition 29: 541-543.

17. Peek RM, Blaser MJ (2002) *Helicobacter pylori* and gastrointestinal tract adenocarcinomas. Nat Rev Cancer 2: 28-37.

18. Daniels IR, Allum WH (2005) The Anatomy and Physiology of the Stomach. Upper Gastrointestinal Surgery. London: Springer London. pp. 17-37.

19. Putz R, Pabst R (2006) Sobotta: Atlas of Human Anatomy; Putz R, editor: Elsevier GmbH.

20. Mulroney S, Myers AK (2009) Netter's Essential Physiology. Philadelphia, USA: Saunder Elsevier.

21. Yang I, Nell S, Suerbaum S (2013) Survival in hostile territory: the microbiota of the stomach. FEMS Microbiol Rev 37: 736-761.

22. Gonçalves IC, Henriques PC, Seabra CL, Martins MCL (2014) The potential utility of chitosan micro/nanoparticles in the treatment of gastric infection. Expert Review of Anti-infective Therapy 12: 981-992.

23. Yamaoka Y (2012) Pathogenesis of *Helicobacter pylori*-Related Gastroduodenal Diseases from Molecular Epidemiological Studies. Gastroenterology Research and Practice 2012: 9.

24. Magalhaes A, Reis CA (2010) *Helicobacter pylori* adhesion to gastric epithelial cells is mediated by glycan receptors. Braz J Med Biol Res 43: 611-618.

25. Atherton JC (2006) The pathogenesis of *Helicobacter pylori*-induced gastro-duodenal diseases. Annual Review of Pathology: Mechanisms of Disease 1: 63-96.

26. Kusters JG, van Vliet AHM, Kuipers EJ (2006) Pathogenesis of *Helicobacter pylori* Infection. Clinical Microbiology Reviews 19: 449-490.

27. Walton EL (2016) *Helicobacter pylori*'s road to colonization. Biomedical Journal 39: 1-4.

28. Monack DM, Mueller A, Falkow S (2004) Persistent bacterial infections: the interface of the pathogen and the host immune system. Nat Rev Micro 2: 747-765.

29. Vale FF, Vítor JMB (2010) Transmission pathway of *Helicobacter pylor*i: Does food play a role in rural and urban areas? International Journal of Food Microbiology 138: 1-12.

30. Mitchell H (2001) Epidemiology of Infection. In: HLT M, GL M, SL H, editors. Helicobacter pylori: Physiology and Genetics. Washington (DC): ASM Press.

31. Azevedo NF, Guimarães N, Figueiredo C, Keevil CW, Vieira MJ (2007) A New Model for the Transmission of *Helicobacter pylori*: Role of Environmental Reservoirs as Gene Pools to Increase Strain Diversity. Critical Reviews in Microbiology 33: 157-169.

32. Wroblewski LE, Peek RM, Wilson KT (2010) Helicobacter pylori and Gastric Cancer: Factors That Modulate Disease Risk. Clinical Microbiology Reviews 23: 713-739.

33. Khalifa MM, Sharaf RR, Aziz RK (2010) *Helicobacter pylori*: a poor man's gut pathogen? Gut Pathogens 2: 2-2.

34. IARC (2014) *Helicobacter pylori* Eradication as a Strategy for Preventing Gastric Cancer.; Group I*Hp*W, editor. Lyon, France: International Agency for Research on Cancer.

35. Venerito M, Link A, Rokkas T, Malfertheiner P (2016) Gastric cancer – clinical and epidemiological aspects. Helicobacter 21: 39-44.

36. Ferlay J, Soerjomataram I, Dikshit R, Eser S, Mathers C, et al. (2015) Cancer incidence and mortality worldwide: sources, methods and major patterns in GLOBOCAN 2012. Int J Cancer 136: E359-386.

37. Ferlay J, Soerjomataram I, Ervik M, Dikshit R, Eser S, et al. (2013) GLOBOCAN 2012 v1.0, Cancer Incidence and Mortality Worldwide: IARC CancerBase No 11. Lyon, France: International Agency for Research on Cancer

38. Papoila AL, Riebler A, Amaral-Turkman A, São-João R, Ribeiro C, et al. (2014) Stomach cancer incidence in Southern Portugal 1998–2006: A spatio-temporal analysis. Biometrical Journal 56: 403-415.

39. Morais S, Ferro A, Bastos A, Castro C, Lunet N, et al. (2016) Trends in gastric cancer mortality and in the prevalence of *Helicobacter pylori* infection in Portugal. European Journal of Cancer Prevention 25: 275-281.

40. Miranda N, Portugal C, Nogueira PJ, Farinha CS, Oliveira AL, et al. (2016) PORTUGAL- Doenças Oncológicas em Números-2015. In: Saúde D-Gd, editor. Lisboa: Direção-Geral da Saúde, Direção de Serviços de Informação e Análise.

41. Peleteiro B, La Vecchia C, Lunet N (2012) The role of *Helicobacter pylori* infection in the web of gastric cancer causation. European Journal of Cancer Prevention 21: 118-125.

42. Fallone CA, Chiba N, van Zanten SV, Fischbach L, Gisbert JP, et al. (2016) The Toronto Consensus for the Treatment of *Helicobacter pylori* Infection in Adults. Gastroenterology 151: 51-69.e14.

43. Mitchell H, Katelaris P (2016) Epidemiology, clinical impacts and current clinical management of *Helicobacter pylori* infection. Med J Aust 204: 376-380.

44. Gisbert JP (2012) Rescue Therapy for *Helicobacter pylori* Infection 2012. Gastroenterology Research and Practice 2012: 974594.

45. Malfertheiner P, Megraud F, O'Morain CA, Atherton J, Axon ATR, et al. (2012) Management of *Helicobacter pylori* infection—the Maastricht IV/ Florence Consensus Report. Gut 61: 646-664.

46. Costa F, D'Elios MM (2010) Management of *Helicobacter pylori* infection. Expert Rev Anti Infect Ther 8: 887-892.

47. Malfertheiner P, Megraud F, O'Morain CA, Atherton J, Axon ATR, et al. (2012) Management of *Helicobacter pylori* infection- the Maastricht IV/ Florence Consensus Report. Gut 61: 646e664.

48. Malfertheiner P, Megraud F, O'Morain CA, Gisbert JP, Kuipers EJ, et al. (2016) Management of *Helicobacter pylori* infection—the Maastricht V/Florence Consensus Report. Gut.

49. Lopes D, Nunes C, Martins MCL, Sarmento B, Reis S (2014) Eradication of *Helicobacter pylori*: Past, present and future. Journal of Controlled Release 189: 169-186.

50. O'Connor A, Fischbach W, Gisbert JP, O'Morain C (2016) Treatment of *Helicobacter pylori* infection 2016. Helicobacter 21: 55-61.

51. Selgrad M, Tammer I, Langner C, Bornschein J, Meißle J, et al. (2014) Different antibiotic susceptibility between antrum and corpus of the stomach, a possible reason for treatment failure of *Helicobacter pylori* infection. World Journal of Gastroenterology : WJG 20: 16245-16251.

52. Conteduca V, Sansonno D, Lauletta G, Russi S, Ingravallo G, et al. (2013) *H. pylori* infection and gastric cancer: state of the art (review). Int J Oncol 42: 5-18.

53. Graham DY, Fischbach L (2010) *Helicobacter pylori* treatment in the era of increasing antibiotic resistance. Gut 59: 1143-1153.

54. Malfertheiner P, Peitz U, Treiber G (2003) What constitutes failure for *Helicobacter pylori* eradication therapy? Can J Gastroenterol 17 Suppl B: 53B-57B.

55. Senatore FJ, Wilmot J, Birk JW (2016) *Helicobacter pylori* treatment: Still a work in progress. Postgraduate Medicine 128: 152-157.

56. Vakil N (2006) Helicobacter pylori Treatment: A Practical Approach. Am J Gastroenterol 101: 497-499.

57. O'Connor JPA, Taneike I, O'Morain C (2009) Improving Compliance with *Helicobacter pylori Eradication* Therapy: When and How? Therapeutic Advances in Gastroenterology 2: 273-279.

58. Bohr URM, Malfertheiner P (2009) Eradication of *H. pylori* Infection: the Challenge is on if Standard Therapy Fails. Therapeutic Advances in Gastroenterology 2: 59-66.

59. Song M, Ang TL (2014) Second and third line treatment options for *Helicobacter pylori* eradication. World Journal of Gastroenterology : WJG 20: 1517-1528.

60. Suzuki T, Matsuo K, Ito H, Sawaki A, Hirose K, et al. (2006) Smoking Increases the Treatment Failure for *Helicobacter pylori* Eradication. The American Journal of Medicine 119: 217-224.

61. Ayala G, Escobedo-Hinojosa WI, de la Cruz-Herrera CF, Romero I (2014) Exploring alternative treatments for *Helicobacter pylori* infection. World Journal of Gastroenterology : WJG 20: 1450-1469.

62. Gaby AR (2001) *Helicobacter pylori* eradication: are there alternatives to antibiotics? Altern Med Rev 6: 355-366.

63. O'Rourke JL, Lee A (2003) Animal models of *Helicobacter pylori* infection and disease. Microbes and Infection 5: 741-748.

64. Peek RM (2008) *Helicobacter pylori* infection and disease: from humans to animal models. Disease Models & Mechanisms 1: 50-55.

65. Noto JM, Romero-Gallo J, Piazuelo MB, Peek RM (2016) The Mongolian Gerbil: A Robust Model of *Helicobacter pylori*-Induced Gastric Inflammation and Cancer. In: Ivanov AI, editor. Gastrointestinal Physiology and Diseases: Methods and Protocols. New York, NY: Springer New York. pp. 263-280.

66. Velin D, Michetti P (2010) Advances in vaccination against *Helicobacter pylori*. Expert Review of Gastroenterology & Hepatology 4: 157-166.

67. Czinn SJ, Blanchard T (2011) Vaccinating against *Helicobacter pylori* infection. Nat Rev Gastroenterol Hepatol 8: 133-140.

68. Zhang H-x, Qiu Y-y, Zhao Y-h, Liu X-t, Liu M, et al. (2014) Immunogenicity of oral vaccination with *Lactococcus lactis* derived vaccine candidate antigen (UreB) of *Helicobacter pylori* fused with the human interleukin 2 as adjuvant. Molecular and Cellular Probes 28: 25-30.

69. Koch M, Meyer TF, Moss SF (2013) Inflammation, Immunity, Vaccines for *Helicobacter pylori* infection. Helicobacter 18: 18-23.

70. Yazbek PB, Trindade AB, Chin CM, dos Santos JL (2015) Challenges to the Treatment and New Perspectives for the Eradication of *Helicobacter pylori*. Digestive Diseases and Sciences 60: 2901-2912.

71. Chionh YT, Arulmuruganar A, Venditti E, Ng GZ, Han J-X, et al. (2014) Heat shock protein complex vaccination induces protection against *Helicobacter pylori* without exogenous adjuvant. Vaccine 32: 2350-2358.

72. Corthésy-Theulaz I, Porta N, Glauser M, Saraga E, Vaney A-C, et al. (1995) Oral immunization with *Helicobacter pylori* urease B subunit as a treatment against Helicobacter infection in mice. Gastroenterology 109: 115-121.

73. DeLyria ES, Redline RW, Blanchard TG (2009) Vaccination of mice against *H. pylor*i induces a strong Th-17 response and immunity that is neutrophil-dependent. Gastroenterology 136: 247-256.

74. Suganya K, Prem Kumar A, Sekar B, Sundaran B (2017) Protection of mice against gastric colonization of *Helicobacter pylori* by therapeutic immunization with systemic whole cell inactivated vaccines. Biologicals 45: 39-46.

75. Sun P, Wang J-Q, Zhang Y-T, Zhao S-G (2014) Evaluating the immune responses of mice to subcutaneous immunization with *Helicobacter pylori* urease B subunit. Journal of Animal Science and Biotechnology 5: 14.

76. Chen J, Li N, She F (2014) *Helicobacter pylori* outer inflammatory protein DNA vaccine-loaded bacterial ghost enhances immune protective efficacy in C57BL/6 mice. Vaccine 32: 6054-6060.

77. Aebischer T, Bumann D, Epple HJ, Metzger W, Schneider T, et al. (2008) Correlation of T cell response and bacterial clearance in human volunteers challenged with *Helicobacter pylori* revealed by randomised controlled vaccination with Ty21a-based *Salmonella* vaccines. Gut 57: 1065-1072.

78. Angelakopoulos H, Hohmann EL (2000) Pilot Study of phoP/phoQ-Deleted *Salmonella enterica* Serovar Typhimurium Expressing *Helicobacter pylori* Urease in Adult Volunteers. Infection and Immunity 68: 2135-2141.

79. Banerjee S, Medina-Fatimi A, Nichols R, Tendler D, Michetti M, et al. (2002) Safety and efficacy of low dose *Escherichia coli* enterotoxin adjuvant for urease based oral immunisation against *Helicobacter pylori* in healthy volunteers. Gut 51: 634-640.

80. Malfertheiner P, Schultze V, Rosenkranz B, Kaufmann SHE, Ulrichs T, et al. (2008) Safety and Immunogenicity of an Intramuscular *Helicobacter pylori* Vaccine in Noninfected Volunteers: A Phase I Study. Gastroenterology 135: 787-795.

81. Zeng M, Mao XH, Li JX, Tong WD, Wang B, et al. (2015) Efficacy, safety, and immunogenicity of an oral recombinant *Helicobacter pylori* vaccine in children in China: a randomised, double-blind, placebo-controlled, phase 3 trial. Lancet 386: 1457-1464.

82. Dai T, Huang Y-Y, Hamblin MR (2009) Photodynamic therapy for localized infections—State of the art. Photodiagnosis and Photodynamic Therapy 6: 170-188.

83. Calvino-Fernández M, García-Fresnadillo D, Benito-Martínez S, McNicholl AG, Calvet X, et al. (2013) *Helicobacter pylori* inactivation and virulence gene damage using a supported sensitiser for photodynamic therapy. European Journal of Medicinal Chemistry 68: 284-290.

84. Simon C, Mohrbacher C, Hüttenberger D, Bauer-Marschall I, Krickhahn C, et al. (2014) *In vitro* studies of different irradiation conditions for Photodynamic inactivation of *Helicobacter pylori*. Journal of Photochemistry and Photobiology B: Biology 141: 113-118.

85. Calvino-Fernández M, Garcia-Fresnadillo D, Benito-Martinez S, McNicholl AG, Gisbert JP, et al. (2012) Su1708 Photodynamic Therapy: an Alternative Strategy Against *Helicobacter pylori*. Gastroenterology 142: S-486.

86. Hamblin MR, Viveiros J, Yang C, Ahmadi A, Ganz RA, et al. (2005) *Helicobacter pylori* Accumulates Photoactive Porphyrins and Is Killed by Visible Light. Antimicrobial Agents and Chemotherapy 49: 2822-2827.

87. Millson CE, Wilson M, MacRobert AJ, Bown SG (1996) *Ex-vivo* treatment of gastric *Helicobacter* infection by photodynamic therapy. Journal of Photochemistry and Photobiology B: Biology 32: 59-65.

88. Lembo AJ, Ganz RA, Sheth S, Cave D, Kelly C, et al. (2009) Treatment of *Helicobacter pylori* infection with intra-gastric violet light phototherapy: a pilot clinical trial. Lasers Surg Med 41: 337-344.

89. Ganz RA, Hamblin M, Tolkoff J, Nishioka N, Ahmad A, et al. (2003) *Helicobacter pylori* in patients is killed by visible light. Am J Gastroenterol 98: S47-S47.

90. Vale FF, Oleastro M (2014) Overview of the phytomedicine approaches against *Helicobacter pylori*. World Journal of Gastroenterology : WJG 20: 5594-5609.

91. Vitor JM, Vale FF (2011) Alternative therapies for *Helicobacter pylor*i: probiotics and phytomedicine. FEMS Immunol Med Microbiol 63: 153-164.

92. Roxo-Rosa M, Oleastro M, Vale FF (2013) *Helicobacter pylori* eradication-the alternatives beyond antibiotics. In: Méndez-Vilas A, editor. Microbial pathogens and strategies for combating them: science, technology and education: Formatex Research Center.

93. Kamiji MM, de Oliveira RB (2005) Non-antibiotic therapies for *Helicobacter pylori* infection. Eur J Gastroenterol Hepatol 17: 973-981.

94. Abdel-Haliem MEF, Askora A (2013) Isolation and characterization of bacteriophages of *Helicobacter pylori* isolated from Egypt. Future Virology 8: 821-826.

95. Cao J, Sun Y, Berglindh T, Mellgard B, Li Z, et al. (2000) *Helicobacter pylori*-antigen-binding fragments expressed on the filamentous M13 phage prevent bacterial growth. Biochim Biophys Acta 1474: 107-113.

96. Vale FF, Matos APA, Carvalho P, Vítor JMB (2008) *Helicobacter pylor*i Phage Screening. Microscopy and Microanalysis 14: 150-151.

97. Lorca GL, Wadstrom T, Valdez GF, Ljungh A (2001) *Lactobacillus acidophilus* autolysins inhibit *Helicobacter pylori* in vitro. Curr Microbiol 42: 39-44.

98. Coconnier M-H, Lievin V, Hemery E, Servin AL (1998) Antagonistic Activity against *Helicobacter Infection In Vitro* and *In Vivo* by the Human *Lactobacillus acidophilus* Strain LB. Applied and Environmental Microbiology 64: 4573-4580.

99. Ushiyama A, Tanaka K, Aiba Y, Shiba T, Takagi A, et al. (2003) *Lactobacillus gasseri* OLL2716 as a probiotic in clarithromycin-resistant *Helicobacter pylori* infection. J Gastroenterol Hepatol 18: 986-991.

100. Sgouras D, Maragkoudakis P, Petraki K, Martinez-Gonzalez B, Eriotou E, et al. (2004) In Vitro and *In Vivo* Inhibition of *Helicobacter pylori* by *Lactobacillus casei* Strain Shirota. Applied and Environmental Microbiology 70: 518-526.

101. Pinchuk IV, Bressollier P, Verneuil B, Fenet B, Sorokulova IB, et al. (2001) *In Vitro* Anti-H*elicobacter pylori* Activity of the Probiotic Strain *Bacillus subtilis* 3 Is Due to Secretion of Antibiotics. Antimicrobial Agents and Chemotherapy 45: 3156-3161.

102. Nam H, Ha M, Bae O, Lee Y (2002) Effect of *Weissella confusa* Strain PL9001 on the Adherence and Growth of *Helicobacter pylori*. Applied and Environmental Microbiology 68: 4642-4645.

103. Johnson-Henry KC, Mitchell DJ, Avitzur Y, Galindo-Mata E, Jones NL, et al. (2004) Probiotics reduce bacterial colonization and gastric inflammation in *H. pylori*-infected mice. Dig Dis Sci 49: 1095-1102.

104. Sgouras DN, Panayotopoulou EG, Martinez-Gonzalez B, Petraki K, Michopoulos S, et al. (2005) *Lactobacillus johnsonii* La1 Attenuates *Helicobacter pylori*-Associated Gastritis and Reduces Levels of Proinflammatory Chemokines in C57BL/6 Mice. Clinical and Diagnostic Laboratory Immunology 12: 1378-1386.

105. Goldman CG, Barrado DA, Balcarce N, Rua EC, Oshiro M, et al. Effect of a probiotic food as an adjuvant to triple therapy for eradication of *Helicobacter pylori* infection in children. Nutrition 22: 984-988.

106. Szajewska H, Albrecht P, Topczewska-Cabanek A (2009) Randomized, Double-blind, Placebo-controlled Trial: Effect of *Lactobacillus* GG Supplementation on *Helicobacter pylori* Eradication Rates and Side Effects During Treatment in Children. Journal of Pediatric Gastroenterology and Nutrition 48: 431-436.

107. Dang Y, Reinhardt JD, Zhou X, Zhang G (2014) The Effect of Probiotics Supplementation on *Helicobacter pylori* Eradication Rates and Side Effects during Eradication Therapy: A Meta-Analysis. PLoS One 9: e111030.

108. Wang Z-H, Gao Q-Y, Fang J-Y (2013) Meta-Analysis of the Efficacy and Safety of *Lactobacillus*-containing and *Bifidobacterium*-containing Probiotic Compound Preparation in *Helicobacter pylori* Eradication Therapy. Journal of Clinical Gastroenterology 47: 25-32.

109. Szajewska H, Horvath A, Piwowarczyk A (2010) Meta-analysis: the effects of *Saccharomyces boulardii* supplementation on *Helicobacter pylori* eradication rates and side effects during treatment. Alimentary Pharmacology & Therapeutics 32: 1069-1079.

110. Li S, Huang X-l, Sui J-z, Chen S-y, Xie Y-t, et al. (2014) Meta-analysis of randomized controlled trials on the efficacy of probiotics in *Helicobacter pylori* eradication therapy in children. European Journal of Pediatrics 173: 153-161.

111. Putsep K, Branden C-I, Boman HG, Normark S (1999) Antibacterial peptide from *H. pylori*. Nature 398: 671-672.

112. Zhang L, Wu WKK, Gallo RL, Fang EF, Hu W, et al. (2016) Critical Role of Antimicrobial Peptide Cathelicidin for Controlling *Helicobacter pylori* Survival and Infection. The Journal of Immunology 196: 1799-1809.

113. Chen L, Li Y, Li J, Xu X, Lai R, et al. (2007) An antimicrobial peptide with antimicrobial activity against *Helicobacter pylori*. Peptides 28: 1527-1531.

114. Ge Y, MacDonald DL, Holroyd KJ, Thornsberry C, Wexler H, et al. (1999) In Vitro Antibacterial Properties of Pexiganan, an Analog of Magainin. Antimicrobial Agents and Chemotherapy 43: 782-788.

115. Zhang X-L, Jiang A-M, Ma Z-Y, Li X-B, Xiong Y-Y, et al. (2015) The Synthetic Antimicrobial Peptide Pexiganan and Its Nanoparticles (PNPs) Exhibit the Anti-*Helicobacter pylori* Activity *in vitro* and *in vivo*. Molecules 20: 3972.

116. Narayana JL, Huang H-N, Wu C-J, Chen J-Y (2015) Efficacy of the antimicrobial peptide TP4 against *Helicobacter pylori infection*: *in vitro* membrane perturbation via micellization and *in vivo* suppression of host immune responses in a mouse model. Oncotarget 6: 12936-12954.

117. Makobongo MO, Kovachi T, Gancz H, Mor A, Merrell DS (2009) *In vitro* Antibacterial Activity of Acyl-Lysyl Oligomers against *Helicobacter pylori*. Antimicrobial Agents and Chemotherapy 53: 4231-4239.

118. Narayana JL, Huang H-N, Wu C-J, Chen J-Y (2015) Epinecidin-1 antimicrobial activity: *in vitro* membrane lysis and *in vivo* efficacy against *Helicobacter pylori* infection in a mouse model. Biomaterials 61: 41-51.

119. Leszczyńska K, Namiot A, Fein DE, Wen Q, Namiot Z, et al. (2009) Bactericidal activities of the cationic steroid CSA-13 and the cathelicidin peptide LL-37 against *Helicobacter pylori* in simulated gastric juice. BMC Microbiology 9: 187-187.

120. Moyat M, Bouzourene H, Ouyang W, Iovanna J, Renauld JC, et al. (2016) IL-22-induced antimicrobial peptides are key determinants of mucosal vaccine-induced protection against *H. pylori* in mice. Mucosal Immunol.

121. Zhang L, Yu J, Wong CCM, Ling TKW, Li ZJ, et al. (2013) Cathelicidin protects against *Helicobacter pylori* colonization and the associated gastritis in mice. Gene Ther 20: 751-760.

122. Tombola F, Campello S, De Luca L, Ruggiero P, Del Giudice G, et al. (2003) Plant polyphenols inhibit VacA, a toxin secreted by the gastric pathogen *Helicobacter pylori*. FEBS Lett 543: 184-189.

123. Stoicov C, Saffari R, Houghton J (2009) Green tea inhibits *Helicobacter* growth *in vivo* and *in vitro*. International Journal of Antimicrobial Agents 33: 473-478.

124. Paulo L, Oleastro M, Gallardo E, Queiroz JA, Domingues F (2011) Anti-*Helicobacter pylori* and urease inhibitory activities of resveratrol and red wine. Food Research International 44: 964-969.

125. Zaidi SFH, Ahmed K, Yamamoto T, Kondo T, Usmanghani K, et al. (2009) Effect of Resveratrol on *Helicobacter pylor*i- Induced Interleukin-8 Secretion, Reactive Oxygen Species Generation and Morphological Changes in Human Gastric Epithelial Cells. Biological and Pharmaceutical Bulletin 32: 1931-1935.

126. Pastene E, Speisky H, Troncoso M, Alarcon J, Figueroa G (2009) *In vitro* inhibitory effect of apple peel extract on the growth of *Helicobacter pylori* and respiratory burst induced on human neutrophils. J Agric Food Chem 57: 7743-7749.

127. Correia M, Michel V, Matos AA, Carvalho P, Oliveira MJ, et al. (2012) Docosahexaenoic acid inhibits *Helicobacter pylori* growth in vitro and mice gastric mucosa colonization. PLoS One 7: e35072.

128. Jung SW, Thamphiwatana S, Zhang L, Obonyo M (2015) Mechanism of antibacterial activity of liposomal linolenic acid against *Helicobacter pylori*. PloS one 10: e0116519.

129. Obonyo M, Zhang L, Thamphiwatana S, Pornpattananangkul D, Fu V, et al. (2012) Antibacterial Activities of Liposomal Linolenic Acids against Antibiotic-Resistant *Helicobacter pylori*. Molecular Pharmaceutics 9: 2677-2685.

130. Akinori Y (2011) Sulforaphane Enhances Protection and Repair of Gastric Mucosa Against Oxidative stress *in vitro*, and Demonstrates Anti-inflammatory Effects on H*elicobacter pylori* infected Gastric Mucosae in Mice and Human Subjects. Current Pharmaceutical Design 17: 1532-1540.

131. Santos AM, Lopes T, Oleastro M, Gato IV, Floch P, et al. (2015) Curcumin Inhibits Gastric Inflammation Induced by *Helicobacter pylori* Infection in a Mouse Model. Nutrients 7: 306-320.

132. Iimuro M, Shibata H, Kawamori T, Matsumoto T, Arakawa T, et al. (2002) Suppressive effects of garlic extract on *Helicobacter pylori*-induced gastritis in Mongolian gerbils. Cancer Letters 187: 61-68.

133. Matsubara S, Shibata H, Ishikawa F, Yokokura T, Takahashi M, et al. (2003) Suppression of *Helicobacter pylori*-induced gastritis by green tea extract in Mongolian gerbils. Biochemical and Biophysical Research Communications 310: 715-719.

134. Correia M, Michel V, Osorio H, El Ghachi M, Bonis M, et al. (2013) Crosstalk between *Helicobacter pylori* and gastric epithelial cells is impaired by docosahexaenoic acid. PLoS One 8: e60657.

135. Thamphiwatana S, Gao W, Obonyo M, Zhang L (2014) *In vivo* treatment of *Helicobacter pylori* infection with liposomal linolenic acid reduces colonization and ameliorates inflammation. Proceedings of the National Academy of Sciences 111: 17600-17605.

136. McNulty CAM, Wilson MP, Havinga W, Johnston B, O'Gara EA, et al. (2001) A Pilot Study to Determine the Effectiveness of Garlic Oil Capsules in the Treatment of Dyspeptic Patients with *Helicobacter pylori*. Helicobacter 6: 249-253.

137. Castro M, Romero C, de Castro A, Vargas J, Medina E, et al. (2012) Assessment of *Helicobacter pylori* Eradication by Virgin Olive Oil. Helicobacter 17: 305-311.

138. Khandouzi N, Shidfar F, Agah S, Hosseini AF, Dehnad A (2015) Comparison of the Effects of Eicosapentaenoic Acid and Docosahexaenoic Acid on the Eradication of *Helicobacter pylor*i Infection, Serum Inflammatory Factors and Total Antioxidant Capacity. Iranian Journal of Pharmaceutical Research : IJPR 14: 149-157.

139. Agah S, Shidfar F, Khandouzi N, Baghestani AR, Hosseini S (2015) Comparison of the Effects of Eicosapentaenoic Acid With Docosahexaenoic Acid on the Level of Serum Lipoproteins in *Helicobacter pylor*i: A Randomized Clinical Trial. Iranian Red Crescent Medical Journal 17: e17652.

140. Gonçalves IC, Magalhães A, Costa AMS, Oliveira JR, Henriques PC, et al. (2016) Bacteria-targeted biomaterials: Glycan-coated microspheres to bind *Helicobacter pylori*. Acta Biomaterialia 33: 40-50.

141. Gonçalves IC, Magalhães A, Fernandes M, Rodrigues IV, Reis CA, et al. (2013) Bacterial-binding chitosan microspheres for gastric infection treatment and prevention. Acta Biomaterialia 9: 9370-9378.

142. Nogueira F, Gonçalves IC, Martins MCL (2013) Effect of gastric environment on *Helicobacter pylori* adhesion to a mucoadhesive polymer. Acta Biomaterialia 9: 5208-5215.

143. Fernandes M, Gonçalves IC, Nardecchia S, Amaral IF, Barbosa MA, et al. (2013) Modulation of stability and mucoadhesive properties of chitosan microspheres for therapeutic gastric application. International Journal of Pharmaceutics 454: 116-124.

144. Seabra CL, Nunes C, Gomez-Lazaro M, Correia M, Machado JC, et al. (2017) Docosahexaenoic acid loaded lipid nanoparticles with bactericidal activity against *Helicobacter pylori*. International Journal of Pharmaceutics 519: 128-137.

145. Parreira P, Magalhães A, Gonçalves IC, Gomes J, Vidal R, et al. (2011) Effect of surface chemistry on bacterial adhesion, viability, and morphology. Journal of Biomedical Materials Research Part A 99A: 344-353.

146. Parreira P, Magalhães A, Reis CA, Borén T, Leckband D, et al. (2013) Bioengineered surfaces promote specific protein–glycan mediated binding of the gastric pathogen *Helicobacter pylori*. Acta Biomaterialia 9: 8885-8893.

147. Martins C, Gonçalves I, Gomes P, Oliveira JR, Reis C, et al. (2013) Microspheres for treating *Helicobacter pylori* infections.

148. Arora S, Gupta S, Narang RK, Budhiraja RD (2011) Amoxicillin Loaded Chitosan–Alginate Polyelectrolyte Complex Nanoparticles as Mucopenetrating Delivery System for *H. Pylori*. Scientia Pharmaceutica 79: 673-694.

149. Arora S, Budhiraja RD (2012) Chitosan-alginate microcapsules of amoxicillin for gastric stability and mucoadhesion. Journal of Advanced Pharmaceutical Technology & Research 3: 68-74.

150. Lin Y-H, Chiou S-F, Lai C-H, Tsai S-C, Chou C-W, et al. (2012) Formulation and evaluation of water-in-oil amoxicillin-loaded nanoemulsions using for *Helicobacter pylori* eradication. Process Biochemistry 47: 1469-1478.

151. Chang C-H, Huang W-Y, Lai C-H, Hsu Y-M, Yao Y-H, et al. (2011) Development of novel nanoparticles shelled with heparin for berberine delivery to treat *Helicobacter pylori*. Acta Biomaterialia 7: 593-603.

152. Lin Y-H, Tsai S-C, Lai C-H, Lee C-H, He ZS, et al. (2013) Genipin-cross-linked fucose–chitosan/heparin nanoparticles for the eradication of *Helicobacter pylori*. Biomaterials 34: 4466-4479.

153. Chang C-H, Lin Y-H, Yeh C-L, Chen Y-C, Chiou S-F, et al. (2010) Nanoparticles Incorporated in pH-Sensitive Hydrogels as Amoxicillin Delivery for Eradication of *Helicobacter pylori*. Biomacromolecules 11: 133-142.

154. Ping Y, Hu X, Yao Q, Hu Q, Amini S, et al. (2016) Engineering bioinspired bacteria-adhesive clay nanoparticles with a membrane-disruptive property for the treatment of *Helicobacter pylori* infection. Nanoscale 8: 16486-16498.

155. Henriques PC, Costa LM, Junqueira-Neto S, Carvalho R, Seabra CL, et al. Chitosan microspheres can fight *Helicobacter pylori* gastric infection in mice. Frontiers in Bioengineering and Biotechnology.

156. Houghton J (2012) Helicobacter Species: Methods and Protocols; Houghton J, editor: Humana Press. X, 258 p.

157. Ivanov AI (2016) Gastrointestinal Physiology and Diseases: Methods and Protocols: Springer New York.

158. Taylor NS, Fox JG (2012) Animal Models of *Helicobacter*-Induced Disease: Methods to Successfully Infect the Mouse. Methods in molecular biology (Clifton, NJ) 921: 131-142.

159. Shi Y, Liu X-F, Zhuang Y, Zhang J-Y, Liu T, et al. (2010) *Helicobacter pylori* Induced Th17 Responses Modulate Th1 Cell Responses, Benefit Bacterial Growth, and Contribute to Pathology in Mice. The Journal of Immunology 184: 5121-5129.

160. Mahler M, Janke C, Wagner S, Hedrich HJ (2002) Differential susceptibility of inbred mouse strains to *Helicobacter pylori* infection. Scand J Gastroenterol 37: 267-278.

161. Zhuang Y, Shi Y, Liu X-F, Zhang J-Y, Liu T, et al. (2011) *Helicobacter pylori*-infected macrophages induce Th17 cell differentiation. Immunobiology 216: 200-207.

162. Chrisment D, Dubus P, Chambonnier L, Hocès de la Guardia A, Sifré E, et al. (2014) Neonatal Thymectomy Favors *Helicobacter pylori*–Promoted Gastric Mucosa-Associated Lymphoid Tissue Lymphoma Lesions in BALB/c Mice. The American Journal of Pathology 184: 2174-2184.

163. Guo L, Liu K, Zhao W, Li X, Li T, et al. (2013) Immunological features and efficacy of the reconstructed epitope vaccine CtUBE against *Helicobacter pylori* infection in BALB/c mice model. Applied Microbiology and Biotechnology 97: 2367-2378.

164. Yang J, Dai L-x, Pan X, Wang H, Li B, et al. (2015) Protection against *Helicobacter pylori* infection in BALB/c mice by oral administration of multi-epitope vaccine of CTB-UreI-UreB. Pathogens and Disease 73: ftv026-ftv026.

165. Takata T, El-Omar E, Camorlinga M, Thompson SA, Minohara Y, et al. (2002) *Helicobacter pylori* Does Not Require Lewis X or Lewis Y Expression To Colonize C3H/HeJ mice. Infection and Immunity 70: 3073-3079.

166. Toyoda T, Shi L, Takasu S, Cho Y-M, Kiriyama Y, et al. (2016) Anti-Inflammatory Effects of Capsaicin and Piperine on *Helicobacter pylori*-Induced Chronic Gastritis in Mongolian Gerbils. Helicobacter 21: 131-142.

167. Bae M, Lim JW, Kim H (2013) Oxidative DNA Damage Response in *Helicobacter pylor*i-Infected Mongolian Gerbils. Journal of Cancer Prevention 18: 271-275.

168. Girish Kumar T, Satyawan S, Gopal N, Ravi Kant D (2011) Evaluation of pH Triggers in situ Porous Controlled Release Micro Balloon Delivery of Amoxicillin for Eradication of *Helicobacter pylori*. Current Drug Delivery 8: 667-677.

169. Rajinikanth PS, Balasubramaniam J, Mishra B (2007) Development and evaluation of a novel floating in situ gelling system of amoxicillin for eradication of *Helicobacter pylori*. International Journal of Pharmaceutics 335: 114-122.

170. Fox JG, Kuipers EJ (2011) Long-term proton pump inhibitor administration, *H pylori* and gastric cancer: lessons from the gerbil. Gut 60: 567-568.

171. Noto JM, Gaddy JA, Lee JY, Piazuelo MB, Friedman DB, et al. (2013) Iron deficiency accelerates *Helicobacter pylori*–induced carcinogenesis in rodents and humans. The Journal of Clinical Investigation 123: 479-492.

172. Romero-Gallo J, Harris EJ, Krishna U, Washington MK, Perez-Perez GI, et al. (2008) Effect of *Helicobacter pylori* eradication on gastric carcinogenesis. Laboratory investigation; a journal of technical methods and pathology 88: 328-336.

173. Bazinet RP, Laye S (2014) Polyunsaturated fatty acids and their metabolites in brain function and disease. Nat Rev Neurosci 15: 771-785.

174. Catal A (2013) Five Decades with Polyunsaturated Fatty Acids: Chemical Synthesis, Enzymatic Formation, Lipid Peroxidation and Its Biological Effects. Journal of Lipids 2013: 19.

175. Mehta LR, Dworkin RH, Schwid SR (2009) Polyunsaturated fatty acids and their potential therapeutic role in multiple sclerosis. Nat Clin Pract Neurol 5: 82-92.

176. Daneshmand R, Kurl S, Tuomainen TP, Virtanen JK (2016) Associations of serum n-3 and n-6 polyunsaturated fatty acids with plasma natriuretic peptides. Eur J Clin Nutr 70: 963-969.

177. Simopoulos AP (2005) Omega-3 Polyunsaturated. In: Allen L, Prentice A, editors. Encyclopedia of Human Nutrition. Second ed: Academic Press.

178. Song C, Shieh CH, Wu YS, Kalueff A, Gaikwad S, et al. (2016) The role of omega-3 polyunsaturated fatty acids eicosapentaenoic and docosahexaenoic acids in the treatment of major depression and Alzheimer's disease: Acting separately or synergistically? Prog Lipid Res 62: 41-54.

179. Calder PC (2012) Mechanisms of action of (n-3) fatty acids. J Nutr 142: 592S-599S.

180. Calder PC (2008) Session 3: Joint Nutrition Society and Irish Nutrition and Dietetic Institute Symposium on 'Nutrition and autoimmune disease' PUFA, inflammatory processes and rheumatoid arthritis. Proc Nutr Soc 67: 409-418.

181. Suresh Y, Das UN (2003) Long-chain polyunsaturated fatty acids and chemically induced diabetes mellitus. Nutrition 19: 213-228.

182. Rudkowska I (2010) Fish oils for cardiovascular disease: Impact on diabetes. Maturitas 67: 25-28.

183. Hwang D (2000) Fatty acids and immune responses--a new perspective in searching for clues to mechanism. Annu Rev Nutr 20: 431-456.

184. Hamer M, Steptoe A (2006) Influence of specific nutrients on progression of atherosclerosis, vascular function, haemostasis and inflammation in coronary heart disease patients: a systematic review. Br J Nutr 95: 849-859.

185. Calder PC (2006) n-3 polyunsaturated fatty acids, inflammation, and inflammatory diseases. Am J Clin Nutr 83: 1505S-1519S.

186. De Caterina R, Basta G (2001) n-3 Fatty acids and the inflammatory response — biological background. European Heart Journal Supplements 3: D42-D49.

187. Hoffmire CA, Block RC, Thevenet-Morrison K, van Wijngaarden E (2012) Associations between omega-3 poly-unsaturated fatty acids from fish consumption and severity of depressive symptoms: an analysis of the 2005-2008 National Health and Nutrition Examination Survey. Prostaglandins Leukot Essent Fatty Acids 86: 155-160.

188. Quinn JF, Raman R, Thomas RG, Yurko-Mauro K, Nelson EB, et al. (2010) Docosahexaenoic Acid Supplementation and Cognitive Decline in Alzheimer Disease: A Randomized Trial. Jama 304: 1903-1911.

189. Moro K, Nagahashi M, Ramanathan R, Takabe K, Wakai T (2016) Resolvins and omega three polyunsaturated fatty acids: Clinical implications in inflammatory diseases and cancer. World Journal of Clinical Cases 4: 155-164.

190. Cockbain AJ, Toogood GJ, Hull MA (2012) Omega-3 polyunsaturated fatty acids for the treatment and prevention of colorectal cancer. Gut 61: 135-149.

191. Vaughan VC, Hassing MR, Lewandowski PA (2013) Marine polyunsaturated fatty acids and cancer therapy. Br J Cancer 108: 486-492.

192. Wang J, Yu JC, Kang WM, Ma ZQ (2012) Superiority of a fish oil-enriched emulsion to medium-chain triacylglycerols/long-chain triacylglycerols in gastrointestinal surgery patients: a randomized clinical trial. Nutrition 28: 623-629.

193. Desbois AP, Smith VJ (2010) Antibacterial free fatty acids: activities, mechanisms of action and biotechnological potential. Appl Microbiol Biotechnol 85: 1629-1642.

194. Tarnawski A, Hollander D, Gergely H (1987) Protection of the gastric mucosa by linoleic acid--a nutrient essential fatty acid. Clin Invest Med 10: 132-135.

195. Thompson L, Cockayne A, Spiller RC (1994) Inhibitory effect of polyunsaturated fatty acids on the growth of *Helicobacter pylori*: a possible explanation of the effect of diet on peptic ulceration. Gut 35: 1557-1561.

196. Khulusi S, Ahmed HA, Patel P, Mendall MA, Northfield TC (1995) The effects of unsaturated fatty acids on *Helicobacter pylori in vitro*. J Med Microbiol 42: 276-282.

197. Park S-H, Kangwan N, Park J-M, Kim E-H, Hahm KB (2013) Non-microbial approach for *Helicobacter pylori* as faster track to prevent gastric cancer than simple eradication. World Journal of Gastroenterology : WJG 19: 8986-8995.

198. Lee SE, Lim JW, Kim JM, Kim H (2014) Anti-Inflammatory Mechanism of Polyunsaturated Fatty Acids in *Helicobacter pylori*-Infected Gastric Epithelial Cells. Mediators of Inflammation 2014: 12.

199. Correia M, Casal S, Vinagre J, Seruca R, Figueiredo C, et al. (2014) *Helicobacter pylori*'s cholesterol uptake impacts resistance to docosahexaenoic acid. Int J Med Microbiol 304: 314-320.

200. McGee DJ, George AE, Trainor EA, Horton KE, Hildebrandt E, et al. (2011) Cholesterol Enhances *Helicobacter pylori* Resistance to Antibiotics and LL-37. Antimicrobial Agents and Chemotherapy 55: 2897-2904.

201. Trainor EA, Horton KE, Savage PB, Testerman TL, McGee DJ (2011) Role of the HefC Efflux Pump in *Helicobacter pylori* Cholesterol-Dependent Resistance to Ceragenins and Bile Salts. Infection and Immunity 79: 88-97.

202. Dyall SC (2011) Methodological issues and inconsistencies in the field of omega-3 fatty acids research. Prostaglandins, Leukotrienes and Essential Fatty Acids (PLEFA) 85: 281-285.

203. Hadian Z (2016) A Review of Nanoliposomal Delivery System for Stabilization of Bioactive Omega-3 Fatty Acids. Electronic Physician 8: 1776-1785.

204. Chen CH, Wang Y, Nakatsuji T, Liu YT, Zouboulis C, et al. (2011) An innate bactericidal oleic acid effective against skin infection of methicillin-resistant *Staphylococcus aureus*: a therapy concordant with evolutionary medicine. J Microbiol Biotechnol 21: 391-399.

205. Desbois AP, Lawlor KC (2013) Antibacterial Activity of Long-Chain Polyunsaturated Fatty Acids against *Propionibacterium acnes* and *Staphylococcus aureus*. Marine Drugs 11: 4544-4557.

206. Lukowski G, Lindequist U, Mundt S, Kramer A, Jülich WD (2008) Inhibition of Dermal MRSA Colonization by Microalgal Micro- and Nanoparticles. Skin Pharmacology and Physiology 21: 98-105.

207. Yang D, Pornpattananangkul D, Nakatsuji T, Chan M, Carson D, et al. (2009) The antimicrobial activity of liposomal lauric acids against *Propionibacterium acnes*. Biomaterials 30: 6035-6040.

208. Nakatsuji T, Kao MC, Fang J-Y, Zouboulis CC, Zhang L, et al. (2009) Antimicrobial Property of Lauric Acid Against *Propionibacterium Acnes*: Its Therapeutic Potential for Inflammatory Acne Vulgaris. Journal of Investigative Dermatology 129: 2480-2488.

209. Desbois AP (2012) Potential applications of antimicrobial fatty acids in medicine, agriculture and other industries. Recent Pat Antiinfect Drug Discov 7: 111-122.

210. Thormar H, Hilmarsson H, Bergsson G (2013) Antimicrobial lipids: Role in innate immunity and potential use in prevention and treatment of infection. In: Méndez-Vilas A, editor. Microbial pathogens and strategies for combating them: science, technology and education: Formatex Research Center. pp. 1474-1488.

211. Bergsson G, Steingrimsson O, Thormar H (1999) In vitro susceptibilities of *Neisseria gonorrhoeae* to fatty acids and monoglycerides. Antimicrob Agents Chemother 43: 2790-2792.

212. Bergsson G, Arnfinnsson J, Karlsson SM, Steingrimsson O, Thormar H (1998) In vitro inactivation of *Chlamydia trachomatis* by fatty acids and monoglycerides. Antimicrob Agents Chemother 42: 2290-2294.

213. Bergsson G, Arnfinnsson J, Steingrimsson O, Thormar H (2001) In vitro killing of *Candida albicans* by fatty acids and monoglycerides. Antimicrob Agents Chemother 45: 3209-3212.

214. Huang CB, George B, Ebersole JL (2010) Antimicrobial activity of n-6, n-7 and n-9 fatty acids and their esters for oral microorganisms. Archives of oral biology 55: 555-560.

215. Sprong RC, Hulstein MFE, Van der Meer R (2001) Bactericidal Activities of Milk Lipids. Antimicrobial Agents and Chemotherapy 45: 1298-1301.

216. Sun CQ, O'Connor CJ, Roberton AM (2003) Antibacterial actions of fatty acids and monoglycerides against *Helicobacter pylori*. FEMS Immunol Med Microbiol 36: 9-17.

217. Shin SY, Bajpai VK, Kim HR, Kang SC (2007) Antibacterial activity of bioconverted eicosapentaenoic (EPA) and docosahexaenoic acid (DHA) against foodborne pathogenic bacteria. International Journal of Food Microbiology 113: 233-236.

218. Mil-Homens D, Bernardes N, Fialho AM (2012) The antibacterial properties of docosahexaenoic omega-3 fatty acid against the cystic fibrosis multiresistant pathogen *Burkholderia cenocepacia*. FEMS Microbiol Lett 328: 61-69.

219. Byeon JI, Song HS, Oh TW, Kim YS, Choi BD, et al. (2009) Growth inhibition of foodborne and pathogenic bacteria by conjugated linoleic acid. J Agric Food Chem 57: 3164-3172.

220. Shin SY, Hou CT, Choi UK, Kim HR, Bajpai VK, et al. (2005) Antibacterial activity of bioconverted linoleic acid produced by *Pseudomonas aeruginosa* PR3. Agric Chem Biotechnol 48: 167-169.

221. Desbois AP, Mearns-Spragg A, Smith VJ (2009) A fatty acid from the diatom *Phaeodactylum tricornutum* is antibacterial against diverse bacteria including multi-resistant *Staphylococcus aureus* (MRSA). Mar Biotechnol (NY) 11: 45-52.

222. Wojtczak L, Wie¸ckowski MR (1999) The Mechanisms of Fatty Acid-Induced Proton Permeability of the Inner Mitochondrial Membrane. Journal of Bioenergetics and Biomembranes 31: 447-455.

223. Petschow BW, Batema RP, Ford LL (1996) Susceptibility of *Helicobacter pylori* to bactericidal properties of medium-chain monoglycerides and free fatty acids. Antimicrob Agents Chemother 40: 302-306.

224. Cybulski LE, Albanesi D, Mansilla MC, Altabe S, Aguilar PS, et al. (2002) Mechanism of membrane fluidity optimization: isothermal control of the *Bacillus subtilis* acyl-lipid desaturase. Molecular Microbiology 45: 1379-1388.

225. Kenny JG, Ward D, Josefsson E, Jonsson I-M, Hinds J, et al. (2009) The *Staphylococcus aureus* Response to Unsaturated Long Chain Free Fatty Acids: Survival Mechanisms and Virulence Implications. PLOS ONE 4: e4344.

226. Shin SY, Bajpai VK, Kim HR, Kang SC (2007) Antibacterial activity of eicosapentaenoic acid (EPA) against foodborne and food spoilage microorganisms. LWT - Food Science and Technology 40: 1515-1519.

227. Schönfeld P, Wojtczak L (2008) Fatty acids as modulators of the cellular production of reactive oxygen species. Free Radical Biology and Medicine 45: 231-241.

228. Cartron ML, England SR, Chiriac AI, Josten M, Turner R, et al. (2014) Bactericidal Activity of the Human Skin Fatty Acid cis-6-Hexadecanoic Acid on *Staphylococcus aureus*. Antimicrobial Agents and Chemotherapy 58: 3599-3609.

229. Peters Jeanne S, Chin C-K (2003) Inhibition of photosynthetic electron transport by palmitoleic acid is partially correlated to loss of thylakoid membrane proteins. Plant Physiology and Biochemistry 41: 117-124.

230. Stulnig TM, Huber J, Leitinger N, Imre E-M, Angelisová P, et al. (2001) Polyunsaturated Eicosapentaenoic Acid Displaces Proteins from Membrane Rafts by Altering Raft Lipid Composition. Journal of Biological Chemistry 276: 37335-37340.

231. Beck V, Jabůrek M, Demina T, Rupprecht A, Porter RK, et al. (2007) Polyunsaturated fatty acids activate human uncoupling proteins 1 and 2 in planar lipid bilayers. The FASEB Journal 21: 1137-1144.

232. Köhnke D, Ludwig B, Kadenbach B (1993) A threshold membrane potential accounts for controversial effects of fatty acids on mitochondrial oxidative phosphorylation. FEBS Letters 336: 90-94.

233. Fay JP, Farias RN (1975) The inhibitory action of fatty acids on the growth of *Escherichia coli*. J Gen Microbiol 91: 233-240.

234. Galbraith H, Miller TB (1973) Effect of Long Chain Fatty Acids on Bacterial Respiration and Amino Acid Uptake. Journal of Applied Bacteriology 36: 659-675.

235. Sheu CW, Salomon D, Simmons JL, Sreevalsan T, Freese E (1975) Inhibitory effects of lipophilic acids and related compounds on bacteria and mammalian cells. Antimicrob Agents Chemother 7: 349-363.

236. Zhang Y-M, Rock CO (2008) Membrane lipid homeostasis in bacteria. Nat Rev Micro 6: 222-233.

237. Zheng CJ, Yoo J-S, Lee T-G, Cho H-Y, Kim Y-H, et al. (2005) Fatty acid synthesis is a target for antibacterial activity of unsaturated fatty acids. FEBS Letters 579: 5157-5162.

238. Sado-Kamdem SL, Vannini L, Guerzoni ME (2009) Effect of α-linolenic, capric and lauric acid on the fatty acid biosynthesis in S*taphylococcus aureus*. International Journal of Food Microbiology 129: 288-294.

239. Rustan AC, Drevon CA (2001) Fatty Acids: Structures and Properties. eLS: John Wiley & Sons, Ltd.

240. Adolph S, Bach S, Blondel M, Cueff A, Moreau M, et al. (2004) Cytotoxicity of diatom-derived oxylipins in organisms belonging to different phyla. Journal of Experimental Biology 207: 2935-2946.

241. Rubio-Rodríguez N, Beltrán S, Jaime I, de Diego SM, Sanz MT, et al. (2010) Production of omega-3 polyunsaturated fatty acid concentrates: A review. Innovative Food Science & Emerging Technologies 11: 1-12.

242. Kralovec JA, Zhang S, Zhang W, Barrow CJ (2012) A review of the progress in enzymatic concentration and microencapsulation of omega-3 rich oil from fish and microbial sources. Food Chemistry 131: 639-644.

243. Schuchardt JP, Hahn A (2013) Bioavailability of long-chain omega-3 fatty acids. Prostaglandins, Leukotrienes and Essential Fatty Acids (PLEFA) 89: 1-8.

244. Sanguansri L, Ann Augustin M (2006) Microencapsulation and Delivery of Omega-3 Fatty Acids. Functional Food Ingredients and Nutraceuticals: CRC Press. pp. 297-327.

245. Kaushik P, Dowling K, Barrow CJ, Adhikari B (2015) Microencapsulation of omega-3 fatty acids: A review of microencapsulation and characterization methods. Journal of Functional Foods 19, Part B: 868-881.

246. Muchow M, Schmitz EI, Despatova N, Maincent P, Muller RH (2009) Omega-3 fatty acids-loaded lipid nanoparticles for patient-convenient oral bioavailability enhancement. Pharmazie 64: 499-504.

247. Hajipour MJ, Fromm KM, Akbar Ashkarran A, Jimenez de Aberasturi D, Larramendi IRd, et al. Antibacterial properties of nanoparticles. Trends in Biotechnology 30: 499-511.

248. Hajipour MJ, Fromm KM, Akbar Ashkarran A, Jimenez de Aberasturi D, Larramendi IRd, et al. (2012) Antibacterial properties of nanoparticles. Trends in Biotechnology 30: 499-511.

249. Norris DA, Puri N, Sinko PJ (1998) The effect of physical barriers and properties on the oral absorption of particulates. Advanced Drug Delivery Reviews 34: 135-154.

250. Hasani S, Pellequer Y, Lamprecht A (2009) Selective Adhesion of Nanoparticles to Inflamed Tissue in Gastric Ulcers. Pharmaceutical Research 26: 1149-1154.

251. Saupe A, Rades T (2006) Solid lipid nanoparticles. In: Mozafari MR, editor. Nanocarrier Technologies: Frontiers of Nanotherapy. Netherlands: Springer. pp. 41-50.

252. Attama AA, Momoh MA, Builders PF (2012) Lipid Nanoparticulate Drug Delivery Systemens A Revolution in Dosage Form Design and Development, . In: Sezer AD, editor. Recent Advances in Novel Drug Carrier Systems: InTech.

253. Pelgrift RY, Friedman AJ (2013) Nanotechnology as a therapeutic tool to combat microbial resistance. Advanced Drug Delivery Reviews 65: 1803-1815.

254. Gao W, Thamphiwatana S, Angsantikul P, Zhang L (2014) Nanoparticle approaches against bacterial infections. Wiley Interdiscip Rev Nanomed Nanobiotechnol 6: 532-547.

255. Petros RA, DeSimone JM (2010) Strategies in the design of nanoparticles for therapeutic applications. Nat Rev Drug Discov 9: 615-627.

256. Trombino S, Mellace S, Cassano R (2016) Solid lipid nanoparticles for antifungal drugs delivery for topical applications. Therapeutic Delivery 7: 639-647.

257. Zhang J, Purdon CH, Smith EW (2006) Solid lipid nanoparticles for topical drug delivery. American Journal of Drug Delivery 4: 215-220.

258. Seyfoddin A, Shaw J, Al-Kassas R (2010) Solid lipid nanoparticles for ocular drug delivery. Drug Delivery 17: 467-489.

259. Balguri SP, Adelli GR, Majumdar S (2016) Topical ophthalmic lipid nanoparticle formulations (SLN, NLC) of indomethacin for delivery to the posterior segment ocular tissues. European Journal of Pharmaceutics and Biopharmaceutics 109: 224-235.

260. Prego C, García M, Torres D, Alonso MJ (2005) Transmucosal macromolecular drug delivery. Journal of Controlled Release 101: 151-162.

261. Wissing SA, Kayser O, Müller RH (2004) Solid lipid nanoparticles for parenteral drug delivery. Advanced Drug Delivery Reviews 56: 1257-1272.

262. Pandey R, Sharma S, Khuller GK (2005) Oral solid lipid nanoparticle-based antitubercular chemotherapy. Tuberculosis 85: 415-420.

263. Üner M, Yener G (2007) Importance of solid lipid nanoparticles (SLN) in various administration routes and future perspectives. Int J Nanomedicine 2: 289-300.

264. Beloqui A, Solinis MA, Rodriguez-Gascon A, Almeida AJ, Preat V (2016) Nanostructured lipid carriers: Promising drug delivery systems for future clinics. Nanomedicine 12: 143-161.

265. Mohamed RA, Abass HA, Attia MA, Heikal OA (2013) Formulation and evaluation of metoclopramide solid lipid nanoparticles for rectal suppository. Journal of Pharmacy and Pharmacology 65: 1607-1621.

266. Torchilin VP (2014) Multifunctional, stimuli-sensitive nanoparticulate systems for drug delivery. Nat Rev Drug Discov 13: 813-827.

267. Martins S, Sarmento B, Ferreira DC, Souto EB (2007) Lipid-based colloidal carriers for peptide and protein delivery – liposomes versus lipid nanoparticles. International Journal of Nanomedicine 2: 595-607.

268. Martins S, Sarmento B, Ferreira DC, Souto EB (2007) Lipid-based colloidal carriers for peptide and protein delivery--liposomes versus lipid nanoparticles. Int J Nanomedicine 2: 595-607.

269. Zhang L, Pornpattananangkul D, Hu CMJ, Huang CM (2010) Development of Nanoparticles for Antimicrobial Drug Delivery. Current Medicinal Chemistry 17: 585-594.

270. Jaafar-Maalej C, Elaissari A, Fessi H (2012) Lipid-based carriers: manufacturing and applications for pulmonary route. Expert Opinion on Drug Delivery 9: 1111-1127.

271. Kraft JC, Freeling JP, Wang Z, Ho RJY (2014) Emerging Research and Clinical Development Trends of Liposome and Lipid Nanoparticle Drug Delivery Systems. Journal of pharmaceutical sciences 103: 29-52.

272. Jain P, Jain S, Prasad KN, Jain SK, Vyas SP (2009) Polyelectrolyte Coated Multilayered Liposomes (Nanocapsules) for the Treatment of *Helicobacter pylori* Infection. Molecular Pharmaceutics 6: 593-603.

273. Bardonnet P-L, Faivre V, Boullanger P, Piffaretti J-C, Falson F (2008) Pre-formulation of liposomes against Helicobacter pylori: Characterization and interaction with the bacteria. European Journal of Pharmaceutics and Biopharmaceutics 69: 908-922.

274. Jain AK, Agarwal A, Agrawal H, Agrawal GP (2012) Double-Liposome – Based Dual-Drug Delivery System as Vectors for Effective Management of Peptic Ulcer. Journal of Liposome Research 22: 205-214.

275. Li Y, Su T, Zhang Y, Huang X, Li J, et al. (2015) Liposomal co-delivery of daptomycin and clarithromycin at an optimized ratio for treatment of methicillin-resistant Staphylococcus aureus infection. Drug Deliv 22: 627-637.

276. Kadry AA, Al-Suwayeh SA, Abd-Allah ARA, Bayomi MA (2004) Treatment of experimental osteomyelitis by liposomal antibiotics. Journal of Antimicrobial Chemotherapy 54: 1103-1108.

277. Omri A, Suntres ZE, Shek PN (2002) Enhanced activity of liposomal polymyxin B against *Pseudomonas aeruginosa* in a rat model of lung infection. Biochemical Pharmacology 64: 1407-1413.

278. Alhariri M, Omri A (2013) Efficacy of Liposomal Bismuth-Ethanedithiol-Loaded Tobramycin after Intratracheal Administration in Rats with Pulmonary *Pseudomonas aeruginosa* Infection. Antimicrobial Agents and Chemotherapy 57: 569-578.

279. Schiffelers R, Storm G, Bakker-Woudenberg I (2001) Liposome-encapsulated aminoglycosides in pre-clinical and clinical studies. J Antimicrob Chemother 48: 333-344.

280. El-Ridy MS, Mostafa DM, Shehab A, Nasr EA, Abd El-Alim S (2007) Biological evaluation of pyrazinamide liposomes for treatment of *Mycobacterium tuberculosis*. International Journal of Pharmaceutics 330: 82-88.

281. Müller RH, Mäder K, Gohla S (2000) Solid lipid nanoparticles (SLN) for controlled drug delivery – a review of the state of the art. European Journal of Pharmaceutics and Biopharmaceutics 50: 161-177.

282. Muller RH, Shegokar R, Keck CM (2011) 20 years of lipid nanoparticles (SLN and NLC): present state of development and industrial applications. Curr Drug Discov Technol 8: 207-227.

283. Mehnert W, Mäder K (2001) Solid lipid nanoparticles: Production, characterization and applications. Advanced Drug Delivery Reviews 47: 165-196.

284. Shah R, Eldridge D, Palombo E, Harding I (2015) Lipid Nanoparticles: Production, Characterization and Stability. SpringerBriefs in Pharmaceutical Science & Drug Development.

285. Tamjidi F, Shahedi M, Varshosaz J, Nasirpour A (2013) Nanostructured lipid carriers (NLC): A potential delivery system for bioactive food molecules. Innovative Food Science & Emerging Technologies 19: 29-43.

286. Battaglia L, Gallarate M (2012) Lipid nanoparticles: state of the art, new preparation methods and challenges in drug delivery. Expert Opin Drug Deliv 9: 497-508.

287. Harde H, Das M, Jain S (2011) Solid lipid nanoparticles: an oral bioavailability enhancer vehicle. Expert Opinion on Drug Delivery 8: 1407-1424.

288. Pandey R, Khuller GK (2006) Oral nanoparticle-based antituberculosis drug delivery to the brain in an experimental model. J Antimicrob Chemother 57: 1146-1152.

289. Pandey R, Khuller GK (2005) Solid lipid particle-based inhalable sustained drug delivery system against experimental tuberculosis. Tuberculosis (Edinb) 85: 227-234.

290. Cavalli R, Gasco MR, Chetoni P, Burgalassi S, Saettone MF (2002) Solid lipid nanoparticles (SLN) as ocular delivery system for tobramycin. International Journal of Pharmaceutics 238: 241-245.

291. Xie S, Zhu L, Dong Z, Wang X, Wang Y, et al. (2011) Preparation, characterization and pharmacokinetics of enrofloxacin-loaded solid lipid nanoparticles: Influences of fatty acids. Colloids and Surfaces B: Biointerfaces 83: 382-387.

292. Wang XF, Zhang SL, Zhu LY, Xie SY, Dong Z, et al. (2012) Enhancement of antibacterial activity of tilmicosin against *Staphylococcus aureus* by solid lipid nanoparticles in vitro and in vivo. The Veterinary Journal 191: 115-120.

293. Kalhapure RS, Mocktar C, Sikwal DR, Sonawane SJ, Kathiravan MK, et al. (2014) Ion pairing with linoleic acid simultaneously enhances encapsulation efficiency and antibacterial activity of vancomycin in solid lipid nanoparticles. Colloids and Surfaces B: Biointerfaces 117: 303-311.

294. Wang Y, Zhu L, Dong Z, Xie S, Chen X, et al. (2012) Preparation and stability study of norfloxacin-loaded solid lipid nanoparticle suspensions. Colloids and Surfaces B: Biointerfaces 98: 105-111.

295. Poonia N, Kharb R, Lather V, Pandita D (2016) Nanostructured lipid carriers: versatile oral delivery vehicle. Future Science OA 2: FSO135.

296. Lin CH, Fang YP, Al-Suwayeh SA, Yang SY, Fang JY (2013) Percutaneous absorption and antibacterial activities of lipid nanocarriers loaded with dual drugs for acne treatment. Biol Pharm Bull 36: 276-286.

297. Sans-Serramitjana E, Fusté E, Martínez-Garriga B, Merlos A, Pastor M, et al. (2016) Killing effect of nanoencapsulated colistin sulfate on *Pseudomonas aeruginosa* from cystic fibrosis patients. Journal of Cystic Fibrosis 15: 611-618.

298. Moreno-Sastre M, Pastor M, Esquisabel A, Sans E, Viñas M, et al. (2016) Pulmonary delivery of tobramycin-loaded nanostructured lipid carriers for *Pseudomonas aeruginosa* infections associated with cystic fibrosis. International Journal of Pharmaceutics 498: 263-273.

299. Garcia-Orue I, Gainza G, Girbau C, Alonso R, Aguirre JJ, et al. (2016) LL37 loaded nanostructured lipid carriers (NLC): A new strategy for the topical treatment of chronic wounds. European Journal of Pharmaceutics and Biopharmaceutics 108: 310-316.

300. Manea A-M, Vasile BS, Meghea A (2014) Antioxidant and antimicrobial activities of green tea extract loaded into nanostructured lipid carriers. Comptes Rendus Chimie 17: 331-341.

301. Boge L, Bysell H, Ringstad L, Wennman D, Umerska A, et al. (2016) Lipid-Based Liquid Crystals As Carriers for Antimicrobial Peptides: Phase Behavior and Antimicrobial Effect. Langmuir 32: 4217-4228.

CHAPTER III

THEORETICAL BACKGROUND OF TECHNIQUES USED

A brief description of the different techniques applied for the lipid nanoparticles and bacteria characterization, in terms of morphology, characteristics features, namely size, surface charge, stability and interactions between nanoparticles and bacteria, is provided in this chapter.

3.1- Measurement of size and surface charge

3.1.1- Dynamic Light Scattering (DLS)

Particle size is the most basic information that can be obtained from nanoparticles. It is a determinant factor for nanoparticles biodistribution and retention at the targeted site [1]. Particle sizing in the submicrometer range is routinely performed using the DLS technique. This technique can provide, in a few minutes, an average of nanoparticles size and their distribution through the analysis of light scattering of a laser beam [1-3]. Submicrometer-sized particles suspended in a fluid are in constant random Brownian motion as result of the random collisions between the solvent molecules and the particles, causing fluctuations in the intensity of the light scattered at a certain detection angle (varying from 10º to 90º) [4,5]. This intensity of the fluctuation trace comprises a mixture of constructive and destructive interferences on the scattered light, through which the particle size can be determined by analyzing the motion-dependent autocorrelation function using the Stokes-Einstein equation (Eq.1) [1,2].

$$d(H) = \frac{kT}{3\pi\eta D} \qquad \text{(Eq.1)}$$

where:

$d(H)$ = hydrodynamic diameter

D = translational diffusion coefficient

k = Boltzmann's constant

T = absolute temperature

η = viscosity

In the Stokes-Einstein theory of Brownian motion, particle motion at very low concentrations is determined by the suspending fluid viscosity and temperature, and particle size [3]. Usually, samples are diluted with purified water (type I) or a buffer solution at a suitable concentration, placed in an appropriate measuring cell and finally measured [4]. This technique is based on the principle that smaller particles move at higher speeds than larger particles (Figure 1), and thus the rate of fluctuation of the light scattered for the last is also slower (Figure 1) [4,6]. The correlation between time and light intensity variation results in a diffusion coefficient that is converted to particle size, in the form of an average of effective hydrodynamic diameter and polydispersity index (a dimensionless parameter), which is a measure of the width of the distribution [1,4]. A polydispersity index value from 0.1 to 0.25 indicates a narrow size distribution, while values greater than 0.5 indicate a broad distribution [1].

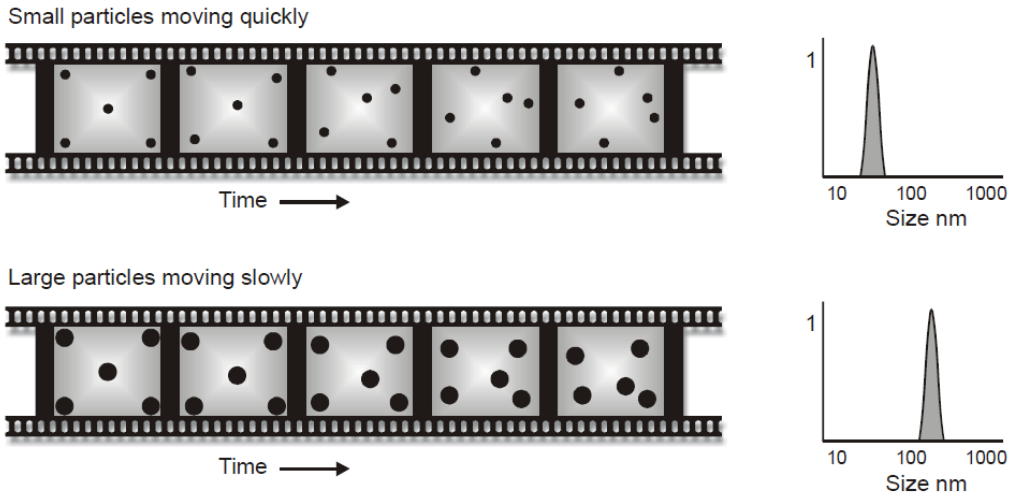

Figure 15- The particles random motion in a liquid and their speed are used to determine the particle's size [6].

3.1.2- Nanoparticle Tracking Analysis: NanoSight®

NanoSight® offers the ability to visualize the size and determine the number of nanoparticles in a liquid suspension. This technique can analyze simultaneously a population of nanoparticles on an individual basis and is ideally suited for real-time analysis of polydispersity systems ranging from 10-30 nm up to 1-2 µm in size. Additionally, it is also allowed to acquire information on nanoparticles concentration, the relative intensity of light scattered and also to visualize and analyze fluorescently labeled particles [7]. NanoSight® uses a finely focused laser

beam that is introduced into a liquid sample containing a dilute suspension of particles, through a glass prism. This beam refracts at a low angle as it enters the sample, resulting in a thin beam of laser light that illuminates the particles (Figure 2) [8].

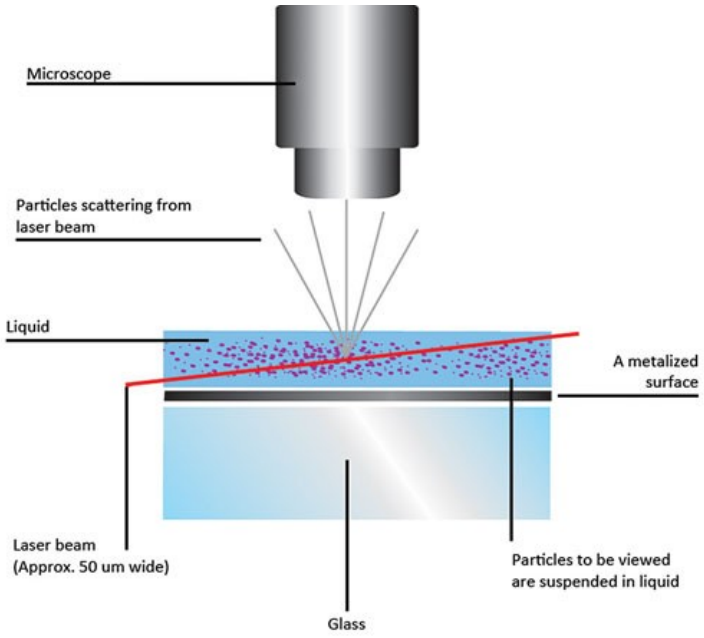

Figure 16- Schematic representation of the NanoSight® instrument configuration [7].

The particles in suspension scatter light in such a manner that they can easily be visualized at 90º via a long working distance. The camera which operates at approximately 30 frames per second captures a video file of the particles moving under Brownian motion in a field of approximately 100 μm ×80 μm ×10 μm [7,9].

Particles concentration can be measured from one video frame alone. Yet, in practice, data from all the recorded frames is used to determine the average concentration, eliminating this way concerns like counting the same particle over and over. The concentration is calculated by taking this average and dividing by the volume used in which the number of particles is measured [7]. It is important that a sufficient number of particles are analyzed within testing time to ensure that the data produced is statistically robust. A concentration in the region of 10^6 to 10^9 particles per mL provides a statistically sound and repeatable particle size distribution within 30-60 seconds (typical timescale) [7,9]. Under normal conditions, when analyzing optimal concentrations of nanoparticles with similar optical characteristics, concentration accuracies can be as good as 5-10% if the samples are diluted to a suitable concentration range [7,9].

3.1.3- Electrophoretic Light Scattering (ELS)

Zeta potential refers to a particle surface charge. It can be determined using a combination of the measurement techniques electrophoresis and laser doppler velocimetry, that determine how fast a particle moves in a liquid when an electrical field is applied (electrophoretic mobility) [4,6]. The surface charge affects the ion distribution around the nanoparticles in the aqueous medium. Most liquids contain ions, which are negatively and positively charged atoms or cations and anions, respectively. When a charged particle is suspended in liquid, ions of an opposite charge will be attracted to the surface of the suspended particle forming a thin liquid layer. This particle is also covered by an outer diffuse layer consisting of loosely associated ions [2,6,10]. In this sense, a negatively charged sample attracts positive ions from the liquid, while a positively charged sample attracts negative ions from the liquid [6]. Hence, the result is the creation of an electrical double layer formed by the charged surface and the counter-ions distributed in a diffuse way in the aqueous medium (Figure 3). Generally, particles with zeta potential more positive than + 30 mV or more negative than -30 mV have colloidal stability maintained by electrostatic repulsion, whereas, a low zeta potential value of less than 30 mV indicates a condition towards instability, aggregation, coagulation or flocculation [1,2,10].

The zeta potential measurement depends on the strength and valence of ions contained in the nanoparticles suspension. High ionic strength and high valence ions compress the electric double layer, resulting in a reduction of the zeta potential. The pH, concentration of hydrogen ions in the medium, influence greatly the zeta potential as well. When the suspension is acidic, the nanoparticles acquire more positive charge and vice versa. Therefore, a zeta potential value without indication of solution pH is a virtually meaningless number [1].

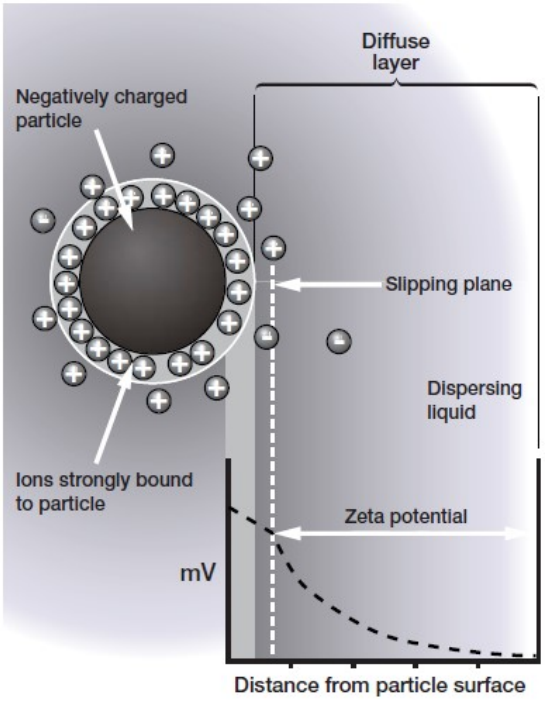

Figure 17- Schematic of the electrical double layer at the surface of solution-phase nanoparticles [6].

3.2- Lipid Crystallinity by Differential Scanning Calorimetry (DSC)

DSC is primarily used to determine the energetics of phase transitions and conformational changes and allows quantification of their temperature dependence. DSC provides also information on the physical state and crystallinity of lipid nanoparticles [11,12]. The degree of crystallinity of a particle is extremely important because it influences the encapsulation efficiency and the release rate and expulsion of the drug during storage. DSC analysis also provides the fusion temperature and enthalpy of the particles. A high value of fusion enthalpy suggests a high level of organization in the crystal lattice since the fusion of a highly organized crystal (perfect crystal) requires more energy to overcome the forces of cohesion in the crystal lattice [12]. In this sense, DSC is considered a thermal analytical technique commonly used to measure the heat capacity of a substance and the enthalpy variation, *ΔH* [13-15]. During measurements, the sample and reference are inside aluminum pans, which are located on the sample holder. The reference pan was empty and the sample pan contained the nanoparticles dispersion or the lipid bulk. The pan might be used with numerous inert atmospheres, as well as oxidizing and reducing atmospheres. Commercial sample pans can be hermetic, open or sealed. The sample size required for DSC analysis is very low with 2-10 mg being sufficient [11,15].

The pans are heated or cooled with a constant scan rate and the temperature within the two pans is maintained constant. When phase changes occur in one pan but do not in the reference pan, this means the calorimeter requires different energies to heat or cool the reference pan and the sample pan and the isothermal energy necessary is registered as an electrical signal [11,15]. The signal resultant from DSC measurements is the heat flow as a function of temperature and the enthalpy variation, *ΔH*, can be calculated by the peak area determined by integration of the peak from the DSC thermograms [16].

DSC analyses are easy and rapidly performed, and are frequently used to characterize the physical state, the degree of crystallinity, polymorphism, crystal ordering, eutectic mixtures or glass transition processes in lipid nanoparticle dispersions [13,16]. To compare the crystallinity between the developed formulations, the recrystallization index (RI) is a useful and commonly used parameter. RI is defined as the percentage of the lipid matrix that has recrystallized during storage time and can be calculated according to the following equation (Eq. 2), where *ΔH* is the molar melting enthalpy given by J/g and the concentration is given by the percentage of lipid phase [17]:

$$RI(\%) = \frac{\Delta H\ lipid\ nanoparticles}{\Delta H\ bulk\ material \times concentration\ lipid\ phase} \times 100 \quad \text{(Eq.2)}$$

3.3- Bioimaging techniques

There are various methods and techniques that evaluate the morphology of nanoparticles as well as of bacteria. In this work cryo-SEM, NanoSight® and AFM were used to analyze the morphology and topography of nanoparticles, whereas bacteria morphology and interaction with nanoparticles were evaluated by scanning electron microscopy (SEM), transmission electron microscopy (TEM), atomic force microscopy (AFM) and flow cytometry image by ImageStream$^{X®}$.

3.3.1- Scanning and Transmission Electron Microscopy (SEM and TEM)

Although there is no theoretical limit to the magnification power of a light microscope, the resolving power has a maximal value of about 200 nm due to the fixed minimal wavelength of visible light [18]. Electron microscopy uses beams of accelerated electrons and electrostatic or electromagnetic lenses to generate images of high resolution, based on the much shorter wavelengths of electrons than visible light photons [2]. The major limitation to using electron microscopy is that specimens must be fixed, dehydrated and chemically treated. Therefore, this technique cannot be applied to living cells or microorganisms. Usually, to diminish artifacts, specimens can be rapidly frozen, so the water and other components present in the cells or particles do not have time to rearrange or even crystallize into ice; this was conducted in this work to evaluate de lipid nanoparticles morphology [18]. There are two major types of electron microscopy, SEM, and TEM.

SEM is an imaging method used for the detailed analysis of a specimen's surface, in which an incident electron beam scans and interacts with the sample surface it to generate signals that reflect its atomic composition and topographic detail [2,18]. Interactions between the sample and the electron beam result in different types of electron signals emitted at or near the specimen surface. These electronic signals are collected, processed and translated as pixels by a monitor that forms a three-dimensional (3D) image of the specimen's surface topography [18]. Then, the incident electrons emit elastic scattering electrons also referred to as backscattered electrons, inelastic scattering electrons also known as low-energy secondary electrons. Moreover, a characteristic X-ray emitted from below the specimen surface, providing information on the specimen composition [2,18]. Usually, the specimen surface is coated with a thin film of gold or platinum to improve contrast and the signal-to-noise ratio [2,18].

In TEM, an electron beam is aimed at a thin section of a specimen that has been chemically treated to enhance contrast. Negative staining for TEM has been considered for many years as the "gold standard" for imaging samples. This negative-stain TEM requires an adequate concentration of sample, bacterial cells or nanoparticles to adsorb to a thin support

film [2,18,19]. The thin sections (< 100 nm) of preserved tissue are stained with atoms of heavy metals, which are preferentially attracted to certain cellular components. When these heavy metal stains, which are electron dense, are hit by an electron beam, the electrons are absorbed or scattered, making electron-dense areas appear darker [18]. The magnification of TEM is mainly determined by the ratio of the distance between the objective lens and the specimen and the distance between the objective lens and its image plane, producing two-dimensional (2D) images of thin tissue sections [2]. The specimen thickness of less than 50 nm is required while doing high-resolution TEM or electron spectroscopy. However, the extensive preparation of thin specimens increases the possibility of altering the sample's structure and makes TEM analysis a very time-consuming process. Moreover, TEM specimens can be damaged or even destroyed by intense, high-voltage electron beams [2].

3.3.2- Atomic Force Microscopy (AFM)

AFM is a versatile technique that allows for the investigation of the surface morphology of a biological specimen at an unprecedented level of resolution.

AFM consists several parts, but one of the most important is the AFM tip, mounted at the end of a microfabricated flexible cantilever, which is then used to scan the sample's surface (Figure 4) [20,21]. As the tip scans the sample surface, the cantilever deflects and this deflection is detected by means of a laser beam aligned at the back of the cantilever, being passed onto a position-sensitive photodiode, processed as a function of the position on the (*x,y*) plane and through that, a 3D morphology of the surface can be reconstructed [2,20-22]. A closed loop control system helps to keep the tip in proximity to the surface by adjusting de *z* position of the sample [2,21,22].

Like SEM and TEM, AFM technique can be used for investigating the size, shape, structure, sorption, dispersion and aggregation of nanomaterials [2]. One of the great peculiarities and advantages of the AFM technique in biology, namely in what concerns the use of live samples (such as cells, bacteria, etc) is the fact that it can work in any environmental condition, including in liquids, allowing to perform experiments in *quasi*-physiological conditions [20]. Moreover, the AFM offers substantial benefits in 3D real quantitative data acquisition, namely minimal sample preparation time, flexibility in ambient operating conditions (*i.e*. no vacuum is necessary) and effective 3D magnification at the submicron level [22].

AFM can be applied to more sophisticated *in vivo* studies, namely studies concerning antibiotics efficacy and action mechanisms. The effectiveness of antibiotics that compromise the bacterial structure and integrity as an epiphenomenon of internal biochemical action, can be studied with AFM technique, by analyzing the bacterial morphology and structure at the nanoscale level or, in cases of resistance, to investigate their lack of activity[22].

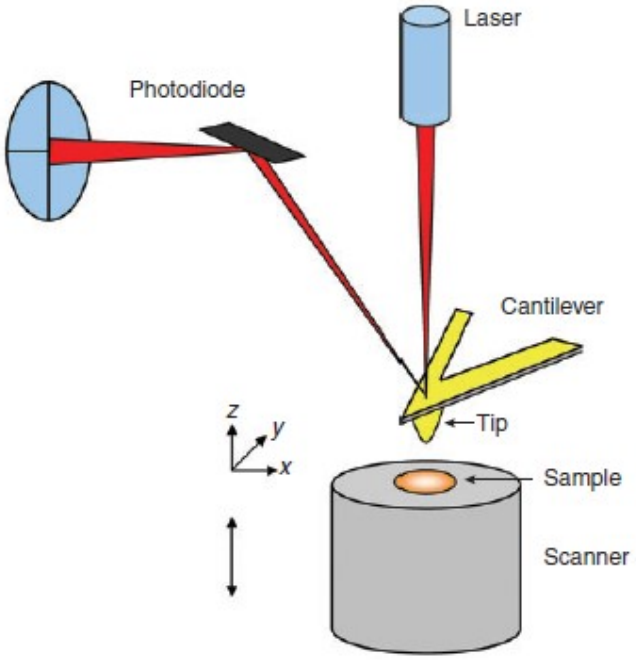

Figure 18- Schematic representation of the AFM general principle. AFM imaging is performed by scanning a tip across the sample surface while the force of interaction between the tip and the sample is monitored with piconewton sensitivity. The sample is mounted on a piezoelectric scanner, which ensures three-dimensional positioning with high resolution, and the force between tip and surface is monitored by measuring the cantilever deflection using an optical method (*i.e*. laser, photodiode). Adapted from Hinterdorfer and Dufrene [23].

AFM can operate in a variety of topographical modes, including contact (the tip is in continuous contact with the surface), non-contact (the cantilever vibrates and variations from its resonance frequency are used to generate images), and intermittent (the cantilever moves rapidly with a large oscillation between the repulsive and attractive forces) (Figure 5) [21]. The most widely used imaging mode is the contact mode, in which sample topography can be measured in two ways: constant-height or constant-force. In the constant-height mode, cantilever deflection is recorded while the sample is scanned at a constant height. However, it is often necessary to minimize large deflections and, therefore, keep the applied force restricted to small values to prevent sample damage. In the constant-force mode, in which the sample height is adjusted to keep the deflection of the cantilever, the force that is applied to the tip is maintained constant using a feedback loop [24]. The drawback here is the lateral force exerted on the sample can be quite high, resulting in sample damage or the movement of relatively loosely attached objects, such as proteins. To overcome this problem is to oscillate the cantilever during imaging, which led to dynamic mode [25].

In dynamic or Tapping® mode, the tip is kept in constant oscillation driven by an oscillation piezo. When the tip is driven towards the surface, it begins to “touch or tap” the surface, recreating the sample morphology as previously explained. With the dynamic mode, the samples are less likely to be damaged by the tip due to the small tip-surface interactions, the lateral shear forces are greatly reduced and it is the most common used topographic mode when working in fluid environments [26]. The accuracy and reproducibility of the dynamic mode

height profiles for different surfaces have been verified by comparing AFM images with TEM or other electron microscopy micrographs. This mode has been used to image bacteria [26].

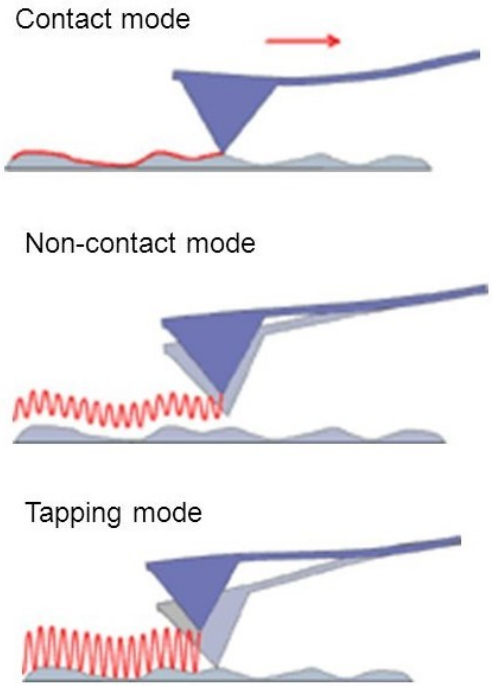

Figure 19- Schematic representation of the three AFM operating modes, contact, non-contact and dynamic or Tapping® mode.

3.3.3- Imaging Flow cytometry by ImageStream$^{X®}$

Imaging flow cytometry is distinguished from conventional flow cytometry by its ability to acquire images of cells in fluid flow. This very powerful image-based cytometric technology combines the high-throughput, multi-parameter capabilities of conventional flow cytometry with the capacity to capture up to 6 spatially registered multi-spectral images per cell at 40x magnification, using a combination of transmitted light, scattered light and fluorescence [27,28]. The introduction of multiple lasers, detectors, configurations of filters and beam splitters allow the detection of emitted fluorescence at various wavelengths through multiple channels, advanced software, and computers that perform compensation, as well as statical analysis and data display; these are the main functions/components of modern flow cytometric systems [29,30]. The time-delay-integration detection technology used by the ImageStream$^{X®}$ CCD camera allows up to 1000 times more signal to be acquired from cells in flow than the conventional frame imaging approaches. Velocity detection and autofocus systems maintain a proper camera synchronization and focused during the process of image acquisition [30].

Figure 6 illustrates ImageStream$^{X®}$ working process. Similar to flow cytometry, the ImageStream$^{X®}$ analyzes cells in suspension. Samples are introduced into a fluidic system where cells are hydrodynamically focused into a core stream and illuminated by a brightfield

light source and a laser (orthogonally) [29,30]. A high numerical aperture objective lens collects fluorescence emissions, scattered and transmitted light from the sample. Additional fluorescence light is decomposed into six images in defined ranges of wavelengths by a dichroic filter stack [29]. Signals are further directed onto the surface of a CCD camera with six channels (Table 1) used as system detectors. The CCD camera operates in a time-delay-integration mode that electronically tracks moving objects by moving pixel content from row to row down the 256 rows of pixels in synchrony with the velocity of the object in flow as measured by the velocity detection system [30].

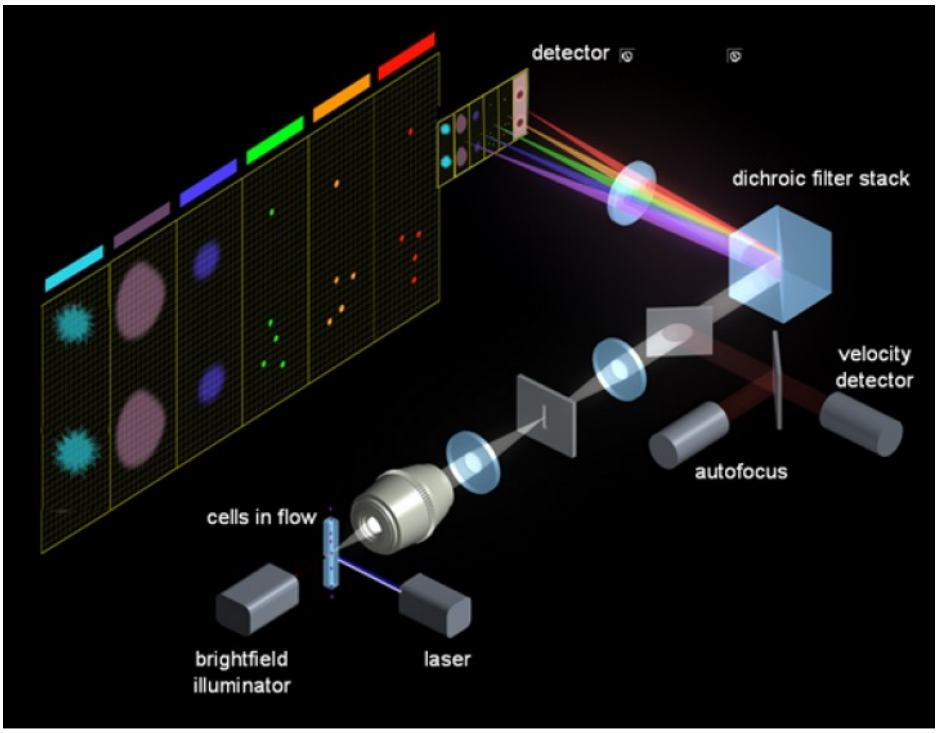

Figure 20- ImageStream$^{X®}$ platform overview. Cells in laminar flow are hydrodynamically focused into a glass cuvette and illuminated by laser (488 nm) and brightfield illuminator light. Fluorescent, transmitted and scattered lights collected by the objective are then split into multi-spectral bands by an optical decomposition element. Six independent wavelengths are collected by a detector-charge coupled device (CCD) camera (channels 1-6) and digital images are saved for further analysis by IDEAS software. Adapted from Amnis Corp manual[30] and Zuba-Surma *et al* (2007) [29].

Table 21- The spectral bandwidth of the camera channel. Adapted from Amnis Corp manual [30].

Channel	Wavelength (nm)
1	430-505
2	505-560
3	560-595
4	595-660
5	660-745
6	745-800

ImageStream$^{X®}$ has been used in various research fields, i.e. to localize and quantify molecules like peptides, proteins, protein complexes, nucleic acids (DNA, RNA, miRNA), glycolipids, etc., in single cells as well as in multicellular clusters or small aggregates, and to map their spatial distribution to the cellular compartments. Besides, by using fluorescent molecules as markers, ImageStream$^{X®}$ allows the analysis of host-pathogen interaction, quantification of intracellular microorganisms, has the potential for providing high-throughput analysis of host protein interactions and to assess drugs action against microorganism and microbial infections [31]. This technique is very helpful in cases where live cells are associated with dead cells, for instance in apoptotic bodies, adherent platelets/platelet fragments, or extracellular vesicles, as well as in distinguishing false-positive events in cell death evaluation and during analysis of activated cells. Therefore, the applications of ImageStream$^{X®}$ are extensive and include but not limited to immunophenotypic multiparametric analysis combined with a morphometric assessment of cells. It can also be applied to microbiology, oncology, stem cell differentiation, morphology, cell cycle and mitosis [29,31,32].

References

1. Cho EJ, Holback H, Liu KC, Abouelmagd SA, Park J, et al. (2013) Nanoparticle Characterization: State of the Art, Challenges, and Emerging Technologies. Molecular Pharmaceutics 10: 2093-2110.

2. Lin P-C, Lin S, Wang PC, Sridhar R (2014) Techniques for physicochemical characterization of nanomaterials. Biotechnology Advances 32: 711-726.

3. ISO22412 (2008) Particles size analysis- Dynamic light scattering (DLS). Geneve: International Organization for Standardization.

4. Fonte P, Andrade F, Araújo F, Andrade C, Neves Jd, et al. (2012) Chapter fifteen - Chitosan-Coated Solid Lipid Nanoparticles for Insulin Delivery. In: Nejat D, editor. Methods in Enzymology: Academic Press. pp. 295-314.

5. Jiang J, Oberdörster G, Biswas P (2009) Characterization of size, surface charge, and agglomeration state of nanoparticle dispersions for toxicological studies. Journal of Nanoparticle Research 11: 77-89.

6. Malvern (2013) Zetasizer Nano -User Manual. United Kingdom: Malvern Instruments Limited.

7. Malvern (2016) Nanoscale Material Characterization: a Review of the use of Nanoparticle Tracking Analysis (NTA). Worcestershire, UK: Malvern Instruments Limited.

8. Dragovic RA, Gardiner C, Brooks AS, Tannetta DS, Ferguson DJP, et al. (2011) Sizing and phenotyping of cellular vesicles using Nanoparticle Tracking Analysis. Nanomedicine: Nanotechnology, Biology and Medicine 7: 780-788.

9. Malvern (2015) NTA: Principles and Methodology- Part 1 of NTA 1000 papers publication review. Malvern Instruments Limited. United Kingdom: Malvern Instruments Limited.

10. Clogston JD, Patri AK (2011) Zeta Potential Measurement. In: McNeil SE, editor. Characterization of Nanoparticles Intended for Drug Delivery. Totowa, NJ: Humana Press. pp. 63-70.

11. Chiu M, Prenner E (2011) Differential scanning calorimetry: An invaluable tool for a detailed thermodynamic characterization of macromolecules and their interactions. Journal of Pharmacy And Bioallied Sciences 3: 39-59.

12. Durán N, Teixeira Z, Marcato PD (2011) Topical Application of Nanostructures: Solid Lipid, Polymeric and Metallic Nanoparticles. In: Beck R, Guterres S, Pohlmann A, editors. Nanocosmetics and Nanomedicines: New Approaches for Skin Care. Berlin, Heidelberg: Springer Berlin Heidelberg. pp. 69-99.

13. Montenegro L, Sarpietro MG, Ottimo S, Puglisi G, Castelli F (2011) Differential scanning calorimetry studies on sunscreen loaded solid lipid nanoparticles prepared by the phase inversion temperature method. International Journal of Pharmaceutics 415: 301-306.

14. Elmer P (2013) Differential scanning calorimetry - A beginner´s guide. United State of America: Perkin Elmer.

15. Aulton ME, Taylor K (2013) Aulton's Pharmaceutics: The Design and Manufacture of Medicines: Churchill Livingstone/Elsevier.

16. Bunjes H, Unruh T (2007) Characterization of lipid nanoparticles by differential scanning calorimetry, X-ray and neutron scattering. Advanced Drug Delivery Reviews 59: 379-402.

17. Neves AR, Lucio M, Martins S, Lima JL, Reis S (2013) Novel resveratrol nanodelivery systems based on lipid nanoparticles to enhance its oral bioavailability. Int J Nanomedicine 8: 177-187.

18. Carter M, Shieh JC (2010) Chapter 5 - Microscopy. Guide to Research Techniques in Neuroscience. New York: Academic Press. pp. 119-145.

19. Golding CG, Lamboo LL, Beniac DR, Booth TF (2016) The scanning electron microscope in microbiology and diagnosis of infectious disease. Scientific Reports 6: 26516.

20. Longo G, Kasas S (2014) Effects of antibacterial agents and drugs monitored by atomic force microscopy. Wiley Interdisciplinary Reviews: Nanomedicine and Nanobiotechnology 6: 230-244.

21. Variola F (2015) Atomic force microscopy in biomaterials surface science. Physical Chemistry Chemical Physics 17: 2950-2959.

22. Braga PC, Ricci D (2011) Imaging Bacterial Shape, Surface, and Appendages Before and After Treatment with Antibiotics. In: Braga PC, Ricci D, editors. Atomic Force Microscopy in Biomedical Research: Methods and Protocols. Totowa, NJ: Humana Press. pp. 391-399.

23. Hinterdorfer P, Dufrene YF (2006) Detection and localization of single molecular recognition events using atomic force microscopy. Nat Meth 3: 347-355.

24. Dufrene YF (2008) Towards nanomicrobiology using atomic force microscopy. Nat Rev Micro 6: 674-680.

25. Torre B, Canale C, Ricci D, Braga PC (2011) Measurement Methods in Atomic Force Microscopy. In: Braga PC, Ricci D, editors. Atomic Force Microscopy in Biomedical Research: Methods and Protocols. Totowa, NJ: Humana Press. pp. 19-29.

26. Camesano TA, Natan MJ, Logan BE (2000) Observation of Changes in Bacterial Cell Morphology Using Tapping Mode Atomic Force Microscopy. Langmuir 16: 4563-4572.

27. Hennig H, Rees P, Blasi T, Kamentsky L, Hung J, et al. (2017) An open-source solution for advanced imaging flow cytometry data analysis using machine learning. Methods 112: 201-210.

28. Basiji DA (2016) Principles of Amnis Imaging Flow Cytometry. In: Barteneva NS, Vorobjev IA, editors. Imaging Flow Cytometry: Methods and Protocols. New York, NY: Springer New York. pp. 13-21.

29. Zuba-Surma EK, Kucia M, Abdel-Latif A, Lillard JW, Jr., Ratajczak MZ (2007) The ImageStream System: a key step to a new era in imaging. Folia Histochem Cytobiol 45: 279-290.

30. Amnis (2010) INSPIRE^{TM}- ImageStream^{X} System Software: User's Manual. Amnis Corporation. USA: Amnis Corporation. pp. 9-15.

31. Vorobjev IA, Barteneva NS (2016) Quantitative Functional Morphology by Imaging Flow Cytometry. In: Barteneva NS, Vorobjev IA, editors. Imaging Flow Cytometry: Methods and Protocols. New York, NY: Springer New York. pp. 3-11.

32. Amnis (2012) The ImageStream^{X}: Imaging Flow Cytometer. USA: Amnis Corporation.

CHAPTER IV

DOCOSAHEXAENOIC ACID LOADED LIPID NANOPARTICLES WITH BACTERICIDAL ACTIVITY AGAINST *HELICOBACTER PYLORI*

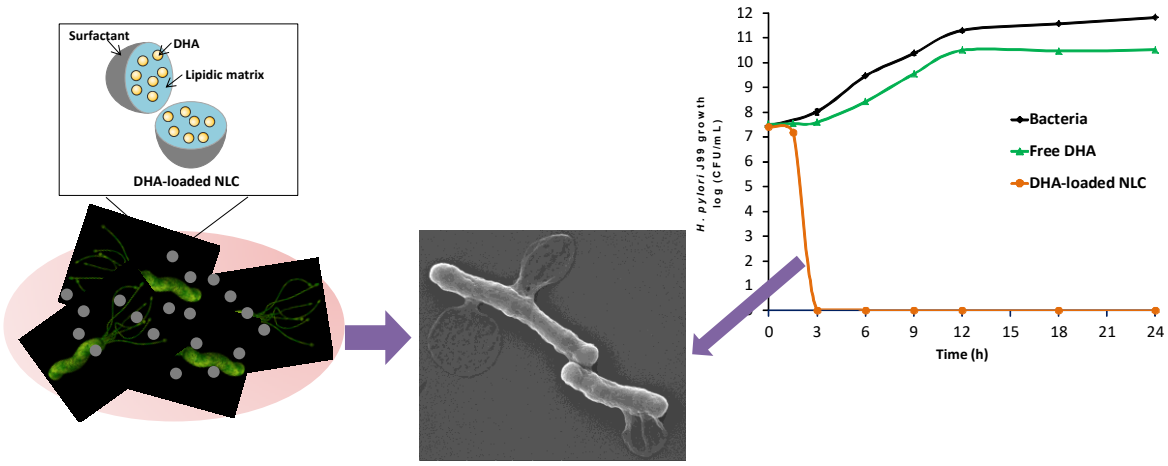

This chapter was based on the following published paper:

- **SEABRA C.L**, Nunes C., Gomez-Lazaro, M., Correia M., Machado J.C, Gonçalves I.C, Reis C.A, Reis S., Martins M.C.L. (2017) Docosahexaenoic acid loaded lipid nanoparticles with bactericidal activity against *Helicobacter pylori, International Journal of Pharmaceutics, 519:128-137. doi:* http://dx.doi.org/10.1016/j.ijpharm.2017.01.014

Abstract

Docosahexaenoic acid (DHA), an omega-3 polyunsaturated fatty acid present in fish oil, has been described as a promising molecule to the treatment of *Helicobacter pylori* gastric infection. However, due to its highly unsaturated structure, DHA can be easily oxidized loosing part of its bioactivity. This work aims the nanoencapsulation of DHA to improve its bactericidal efficacy against *H. pylori.*

DHA was loaded into nanostructured lipid carriers (NLC) produced by hot homogenization and ultrasonication using a blend of lipids (Precirol®ATO5, Miglyol® 812) and a surfactant (Tween®60). Homogeneous NLC with 302±14nm diameter, -28±3mV surface charge (dynamic and electrophoretic light scattering) and containing 66±7% DHA (UV/VIS spectroscopy) were successfully produced.

Bacterial growth curves, performed over 24h in the presence of different DHA concentrations (free or loaded into NLC), demonstrated that nanoencapsulation enhanced DHA bactericidal effect, since DHA-loaded NLC were able to inhibit *H. pylori* growth in a much lower concentrations (25μM) than free DHA (>100μM).

Bioimaging studies, using scanning and transmission electron microscopy and also imaging flow cytometry, demonstrated that DHA-loaded NLC interact with *H. pylori* membrane, increasing their periplasmic space and disrupting membrane and allowing the leakage of cytoplasmic content. Furthermore, the developed nanoparticles are not cytotoxic to human gastric adenocarcinoma cells at bactericidal concentrations. DHA-loaded NLC should, therefore, be envisaged as an alternative to the current treatments for *H. pylori* infection.

KEYWORDS: Docosahexaenoic acid (DHA), *Helicobacter pylori*, Nanostructured lipid carriers (NLC), polyunsaturated fatty acid (PUFA)

1. Introduction

Gastric carcinoma, the third leading cause of cancer-related deaths worldwide [1], has been associated with persistent *Helicobacter pylori* (*H. pylori*) gastric infection. This bacterium, which colonizes the gastric mucosa of over half of world population, is also responsible for the development of gastritis and peptic ulcer [2-4]. It has been estimated that approximately 75% of the global gastric cancer burden is attributable to *H. pylori* infection [5]. Therefore, *H. pylori* eradication is the most promising strategy to avoid *H. pylori*-related gastrointestinal disorders. The present recommended treatment is a combination of antibiotics [6-9], however, this therapy may fail due to several reasons but principally by bacterial resistance to available antibiotics [10].

The use of natural compounds with *H. pylori* bactericidal effect, namely polyunsaturated fatty acids [11,12] and phenolic compounds [13-15] has been explored as an alternative to conventional antibiotics [6]. Fatty acids are attractive compounds due to their potency, a broad spectrum of activity and lack of typical resistance mechanisms against the actions of these compounds [16-18]. Particularly, polyunsaturated fatty acids (PUFAS) found naturally at high levels in many marine organisms, have been reported as having a high potent activity against *H. pylori*, including linolenic acid (C18:3) [11], eicosapentaenoic acid (C20:5) [19], and docosahexaenoic acid (DHA) (C22:6) [20]. Indeed, it was previously reported that some PUFAS, as the linolenic acid, can inhibit up to 50% of bacteria growth at 1 mM concentration [21], whereas 2 mM kills all bacteria [12,21]. This anti-bacterial activity of PUFA is dependent on many factors, including concentration, the target microorganism and its physiological state, the physiological conditions associated with delivery (e.g., pH and temperature) and interaction with the microbial cell [17].

DHA, an omega-3 polyunsaturated fatty acid present in fish oil, was able to inhibit *H. pylori* (26695, B128 and SS1) growth *in vitro* in a dose-dependent manner. Moreover, a study using gastric infected mice, demonstrated that free DHA treatment was able to decrease 50% of *H. pylori* gastric colonization [20,22]. As a result of its highly unsaturated structure, DHA can be easily oxidized losing its bioactivity. Therefore DHA encapsulation is recommended for its protection against environmental factors (oxygen, light, humidity, gastric acid, etc.) [18,20,23].

The present work aims to evaluate if the encapsulation of DHA into nanostructured lipid carriers (NLC) can improve DHA activity against *H. pylori in vitro*. NLC are delivery systems suitable for the encapsulation of poorly water-soluble drugs. They are prepared by blending biocompatible and biodegradable solid and liquid lipids, stabilized in aqueous suspensions by hydrophilic surfactants. The advantage of NLC regarding other lipid nanoparticles, namely solid lipid nanoparticles (SLN), is their higher drug loading capacity, improvement of drug stability and controlled release. This is attributed to their partial-crystallized structure with imperfections in the core solid matrix that provides higher space for drug incorporation [24-26].

2. Material & methods

2.1. DHA nanoencapsulation and characterization

2.1.1. NLC preparation

NLC were produced by hot homogenization and ultrasonication [27] using 200 mg of Precirol®ATO5 (Gattefosé, France), 90 mg of Miglyol® 812 (Acofarma, Spain) and 60 mg of Tween® 60 (Merck, Germany). Briefly, the two lipids (Precirol®ATO5 and Miglyol® 812 and Tween® 60 were weighted and heated together at 65ºC to promote their mixture. Ultrapure water (4.2 mL) preheated at 65ºC was added, and the mixture homogenized using an ultra-turrax (T25; Janke and Kunkel IKA-Labortechnik, Germany) under high speed stirring at 12000 rpm during 20 seconds. Afterward, a sonicator was used (Vibra-Cell model VCX 130 equipped with a VC 18 probe, Sonics and Materials Inc., Newtown, USA), with a tip diameter of ¼" (6 mm), at 60% amplitude for 5 minutes obtaining the NLC. For the production of DHA-loaded NLC, DHA (Cayman Chemical Company, USA) was added in different concentrations (1.0, 2.0 and 2.5% v/v) before addition of hot ultrapure water, obtaining three different formulations.

2.1.2. NLC size and charge measurement

The size and surface charge (ξ-potential) of the produced NLC were characterized by dynamic light scattering (DLS) and electrophoretic light scattering (ELS) respectively, using a Malvern Zetasizer Nano ZS (Malvern Instruments, UK). Diluted NLC (1:50 in ultrapure water) were placed on a disposable capillary cell and triplicate measurements were conducted at a backscattering angle of 173º at 37ºC. DLS and ELS were acquired using equipment maintained by Biointerface and Nanotechnology Unit.

2.1.3. NLC morphology assessment

The NLC morphology was evaluated by Cryo-Scanning Electron Microscopy (Cryo-SEM) and NanoSight®.

For CryoSEM analysis, it was used a JEOL JSM-6301F (Tokyo, Japan) with an Oxford Instruments INCA Energy 350 (Abingdon, UK) and a Gatan Alto 2500 (Pleasanton, CA, USA). A diluted sample of NLC (1:100 in ultrapure water) was placed on a grid, rapidly cooled in liquid nitrogen slush (-210ºC), and transferred under vacuum to the cold stage of the preparation chamber. A fracture and sublimation for 120 seconds at -90ºC was then performed and the sample coated with a gold-palladium alloy by sputtering for 40 seconds. Finally, the sample was transferred under vacuum into the SEM chamber and observed at -150ºC, at CEMUP (*Centro de Materiais da Universidade do Porto*).

For NanoSight® analysis, NLC were diluted (1:20000) with ultrapure water and morphology

was evaluated using a NanoSight® NS300 (Malvern Instruments, UK).

2.1.4. DHA entrapment efficiency

DHA nanoencapsulation was quantified by UV/VIS-spectroscopy. Freeze-dried NLC were dissolved in absolute ethanol for 15 minutes, centrifuged during 30 minutes at 4000 rpm, at 20ºC and its supernatant analyzed by measuring its absorbance using a UV/VIS spectrophotometer (Lambda 45, Perkin Elmer, USA) at 237 nm. All measurements were performed in triplicate.

The DHA loading was calculated using a calibration curve prepared with a concentration range between 0.01 and 3% v/v of DHA in absolute ethanol (0.08-22.80 mM), with a correlation coefficient of R=0.996. The amount of DHA in NLC and the entrapment efficiency (EE) were calculated according to the following equation (Eq.1).

Eq.1

$$EE = \frac{\text{DHA measured (mM)}}{\text{DHA added during NLC production (mM)}} \times 100$$

2.1.5. NLC stability

2.1.5.1. In water

The storage of NLC was evaluated in ultrapure water at 4ºC and 20ºC during 2 months by periodic measurements of their size and surface charge using the DLS and ELS techniques as described above. Measurements were performed at 4º and 20ºC and in triplicate.

2.1.5.2. In bacteria growth medium

NLC were incubated in Brucella Broth medium (BB, Oxoid, France) supplemented with 10% of Fetal Bovine Serum (FBS, Gibco, USA) (BB+10%FBS medium) during 3 hours at 37ºC and 150 rpm. At time-point 0 and 3 hours, samples were diluted (1:20000) ultrapure water and analyzed using the NanoSight® NS300 (Malvern Instruments, UK).

2.1.6. DHA release in bacteria growth medium

DHA-loaded NLC (formulation produced with 2% v/v of DHA) was incubated inside the Slide-A-Lyzer Dialysis Cassettes device (Thermo Scientific, USA), with a nominal molecular weight cut-off of 20 kDa filled with 2 ml of the sample in BB+10%FBS at 37ºC and 150 rpm. At regular intervals (0, 0.5, 1, 1.5, 2 and 3 hours), sample aliquots were withdrawn and replaced with the same volume of fresh medium. The DHA released was quantified using an ELISA Kit for DHA (Cloud-Clone Corporation, USA), according to the supplier

instructions. DHA release was calculated from the optical density using a calibration curve in a concentration range from 12.35 to 4000 pg/mL, with a correlation coefficient of R= 0.989.

2.2. Evaluation of NLC antimicrobial proprieties

2.2.1. *H. pylori* strains and culture conditions

Human isolated *H. pylori* strain J99 (provided by Department of Medical Biochemistry and Biophysics, Umeã University, Sweden) and mouse-adapted *H. pylori* strain SS1 (provided by Unité de Pathogenèse de *Helicobacter*, Institute Pasteur, France) were cultured in spots in *H. pylori* medium plates, in a microaerophilic environment at 37ºC for 48 hours. The *H. pylori* medium plates were composed of blood agar base 2 (Oxoid, France) supplemented with 10% defibrinated horse blood (Probiológica, Portugal) and with 0.2% antibiotics-cocktail of 0.155 g/L Polymixin B (Sigma-Aldrich, USA), 6.25 g/L Vancomycin (Sigma-Aldrich, USA), 1.25 g/L Amphotericin B (Sigma-Aldrich, USA) and 3.125 g/L Trimethroprim (Sigma-Aldrich, USA). Afterward, some colonies of *H. pylori* were spread on *H. pylori* medium plates and incubated for 48 hours, under the same conditions. Then, bacteria were transferred to T-flask containing Brucella Broth medium (BB, Oxoid, France) supplemented with 10% of Fetal Bovine Serum (FBS, Gibco, USA) with an optical density (OD) adjusted to 0.1 (λ= 600 nm; UV/VIS spectrophotometer, Lambda 45, Perkin Elmer, USA). *H. pylori* incubation was performed under microaerophilic conditions, at 150 rpm, 37ºC during 18-20 hours and subsequently used in the following experiments.

2.2.2. Effect of NLC on *H. pylori* growth

H. pylori (~1x10^7 bacteria/mL, OD 0.03) were incubated with different concentrations (0.5, 1.25, 2.5, 5.0 and 25.0 %v/v) of unloaded- NLC and DHA-loaded NLC (formulation produced with 2% v/v of DHA), and free DHA (10, 25, 50, 100 and 500 μM). The cultures were grown for 24 hours into liquid BB + 10% FBS medium (20 mL), under microaerophilic conditions, 37ºC, and 150 rpm.

2.2.2.1. Colony forming units (CFU)

At different time-points (0, 1.5, 3, 6, 9, 12, 18, 24 hours), 200 μL of each culture was collected, serially diluted and plated on *H. pylori* medium plates. After 5 days, at 37ºC, the number of viable bacteria was determined by colony forming unit (CFU) counting.

2.2.2.2. *H. pylori* morphology and NLC membrane interaction

At time-points 3 and 12 h, samples of *H. pylori* strain J99 were incubated with 25 μM of free DHA, 1.25 %v/v of unloaded-NLC and 1.25 %v/v of DHA-loaded NLC (which contains 25 μM DHA) were washed in phosphate buffered saline (PBS, pH 7.4) and centrifuged (3000*g*, for 5 minutes). The bacteria pellet was then fixed differently depending on the following described techniques to evaluate *H. pylori* morphology and/or interaction of NLC with bacteria membrane.

2.2.2.2.1. Scanning Electron Microscopy (SEM)

The bacterial pellet was fixed with 2.5% v/v glutaraldehyde (Merck, Germany) in 0.14 M sodium cacodylate buffer (Merck, Germany) for 30 minutes at RT. Then, bacteria were allowed to adhere on glass coverslips during 2 hours at RT and afterward dehydrated with increasing ethanol/water gradient (50% v/v to 99% v/v) and subjected to critical point drying (CPD 7501, Poloran). Finally, samples were sputter-coated with a gold/palladium film over 30 seconds and bacterial morphology visualized by SEM (JEOL JSM-6310F) at magnifications of 30000 and 60000×, at CEMUP (*Centro de Materiais da Universidade do Porto*).

2.2.2.2.2. Transmission Electron Microscopy (TEM)

The bacterial pellet was fixed with a mixture of 4% w/v of paraformaldehyde (Merck, Germany) with 2.5% v/v glutaraldehyde (Merck, Germany) in 0.14 M sodium cacodylate buffer (Merck, Germany) for 30 minutes at RT. Then, bacteria suspension were washed by centrifugation (3000*g*, for 5 minutes) with sodium cacodylate buffer and bacterial pellet were post-fixed in 2% osmium tetroxide (Electron Microscopy Sciences, UK) in sodium cacodylate buffer, embedded in a HistoGel (Thermo Scientific, USA) and processed in Epon resin (Electron Microscopy Sciences, UK). Ultrathin sections with 50 nm thicknesses were prepared using an Ultramicrotome (RMC PowerTome PC model, USA) with diamond knives (Diatome, USA). Sections were mounted on formvar-coated nickel grids, stained with uranyl acetate and lead citrate (Delta Microscopies, France) and examined by TEM (JEOL JEM 1400 transmission electron microscope; Tokyo, Japan) equipped with a CCD digital camera Orious 1100W (Tokyo, Japan) at the Histology and Electron Microscopy Service of *Instituto de Biologia Molecular e Celular da Universidade do Porto.*

2.2.2.2.3. Imaging flow cytometry

For imaging flow cytometry, NLC were previously stained with 0.1% w/v of coumarin-6. The

bacterial pellet was fixed with 4% w/v of paraformaldehyde in PBS for 30 minutes. To label *H. pylori DNA,* bacterial suspensions were incubated with propidium iodide (0.1µg/mL) for 30 minutes at RT, in the dark. The respective unstained negative controls were prepared. Each sample was filtered through a 70 µm mesh filter before running in the flow cytometer (ImageStream$^{X®}$, Amnis, EDM Millipore, Darmstadt, Germany) equipped with a 488 nm laser, a 40× magnification objective of 0.75 N.A (image pixel 0.5 µm^2), and one CDD camera. Images were acquired using the INSPIRE^{TM} software v4.0 (Amnis, EDM Millipore, Darmstadt, Germany), which included a brightfield image (Channel 1, 420-480 nm), a green fluorescence image corresponding to coumarin-6 (Channel 2, 480-560 nm), and an orange fluorescence image matching the propidium iodide fluorescence emission (Channel 4- 560-595 nm). During the acquisition, bacterial debris and aggregates were limited by setting the area in channel 1 between 2 and 10 µm^2. For each sample, 150 000 events were collected and two independent experiments were performed. All data was analyzed using the IDEAS® software (Amnis, EDM Millipore, Darmstadt, Germany, version 6.2.64.0). Shortly, for the quantification of the intensity of the coumarin-6 labeling, the fluorescence intensity on channel 2 was measured for every cell. This feature represents the sum of the intensity pixel values in the region of interest. The region of interest was limited to the area of fluorescence positive signal in channel 2. Control samples without coumarin-6 labeling were run in the same conditions in the imaging flow cytometer to define the positive coumarin-6 signal. Imaging flow cytometry data were acquired using equipment maintained by the Bioimaging Center for Biomaterials and Regenerative Therapies (b.IMAGE).

2.3. Evaluation of NLC biocompatibility

2.3.2.1. MKN45 cell culture

In order to access the biocompatibility of NLC, viability and cytotoxicity studies were performed using the MKN45 gastric carcinoma cell line.

Cells were grown in RPMI 1640 with Glutamax and HEPES (Gibco, USA) supplemented with 10% inactivated FBS (Gibco, USA) and 1% penicillin-streptomycin (Gibco, USA) at 37ºC and under 5% CO_2 in humidified air. Cells were supplied with fresh medium every two days and trypsinized when 80-90% confluency was reached, followed by counting in a Neubauer chamber with trypan blue solution (0.4% w/v; Sigma-Aldrich). Cells were then seeded at a density of 5×10^5 cells per well (12-well plate) in medium, during 48 hours.

2.3.2.2. MTT assay

The metabolic activity of cell in the presence of NLC was assessed using the thiazolyl blue tetrazolium bromide (MTT) colorimetric assay. This test evaluates the metabolic activity of living cells via the measurement of the activity of the mitochondrial dehydrogenases.

NLC effect was evaluated on MKN45 cells seeded in a 12-well plate as described above.

The culture medium was removed and different concentrations (0, 0.5, 1.25, 2.5 and 5%v/v in culture medium) of unloaded and DHA-loaded NLC (formulation produced with 2% v/v of DHA) were added and cells were incubated during 24 hours. Then, the supernatant was removed; cells were treated with 0.5 mg/mL of MTT (98%, Sigma-Aldrich, USA) and incubated for 3 hours at 37ºC, in the dark. Then, MTT solution was discarded and dimethyl sulfoxide (DMSO) was added to solubilize the formazan crystals formed by MTT reaction within the cells. The plate was shaken for 5 minutes, at RT, under light protection and then the optical density was measured at 590 nm and 630 nm in a microplate reader (Synergy™ H Multi-mode Microplate Reader, BioTek Instruments, USA). A positive control (cells growing in fresh culture medium) and a negative control (cells treated with 2% w/v Triton™ X-100; Sigma-Aldrich, USA) were included, in order to normalize the results. Metabolic activity was determined according to the following equation (Eq.2).

Eq. 2 $$\text{Metabolic activity } (\%) = \frac{\text{Experimental value- Negative control}}{\text{Positive control-Negative control}} \times 100$$

2.3.2.3. LDH assay

Cell death was assessed by quantification of lactate dehydrogenase (LDH) that was released to the cell culture medium after cell lysis. After cell seeding and incubation with NLC, as described above, the supernatant was collected and centrifuged (250*g*, for 10 minutes at RT) and placed in a 96-well plate with LDH Cytotoxicity Detection Kit (Takara Bio Inc, Japan) in a ratio 1:1. After 5 minutes of incubation, at RT and protected from light, the absorbance was measured at 490 and 630 nm using the microplate reader. NLC cytotoxicity was determined according to the following equation (Eq.3), where the positive control was cells treated with 2% w/v Triton™ X-100 solution, and the negative control were untreated cells.

Eq. 3 $$\text{Cytotoxicity } (\%) = \frac{\text{Experimental value- Negative control}}{\text{Positive control-Negative control}} \times 100$$

2.4. Statistical analysis

Data are reported as mean ± standard deviation (SD). Non-parametric Kruskal-Wallis test was applied to the data and statically significant differences were considered at $p<0.05$. The statistical analyses were performed using Graph Pad Prism 6.0 (Graph-Pad Software, La Jolla, USA).

3. Results

3.1. DHA nanoencapsulation

NLC size and ξ-potential were determined by DLS and ELS as described in Figure 1A. Unloaded-NLC (without DHA) presented diameters of 211±8 nm. After DHA incorporation, NLC diameter increased in a concentration-dependent manner ($p<0.05$) exhibiting diameters of 260±12, 302±14 and 323±41 nm for DHA-loaded NLC produced with 1, 2 and 2.5% of DHA, respectively. Moreover, NLC presented a homogeneous size distribution with low polydispersion index (~0.2) for NLC prepared with 1 and 2% of DHA. Surface ξ-potential of NLC in water were around -28 mV independently of DHA incorporation ($p>0.05$). Figure 1B shows the amount of DHA incorporated into NLC. The maximum of DHA incorporation (66±7 %) was reached when 2% v/v of DHA was used in the formulation. These DHA-loaded NLC, which contain 2.02±0.23 mM DHA per suspension of NLC produced, were, therefore, used in all subsequent studies.

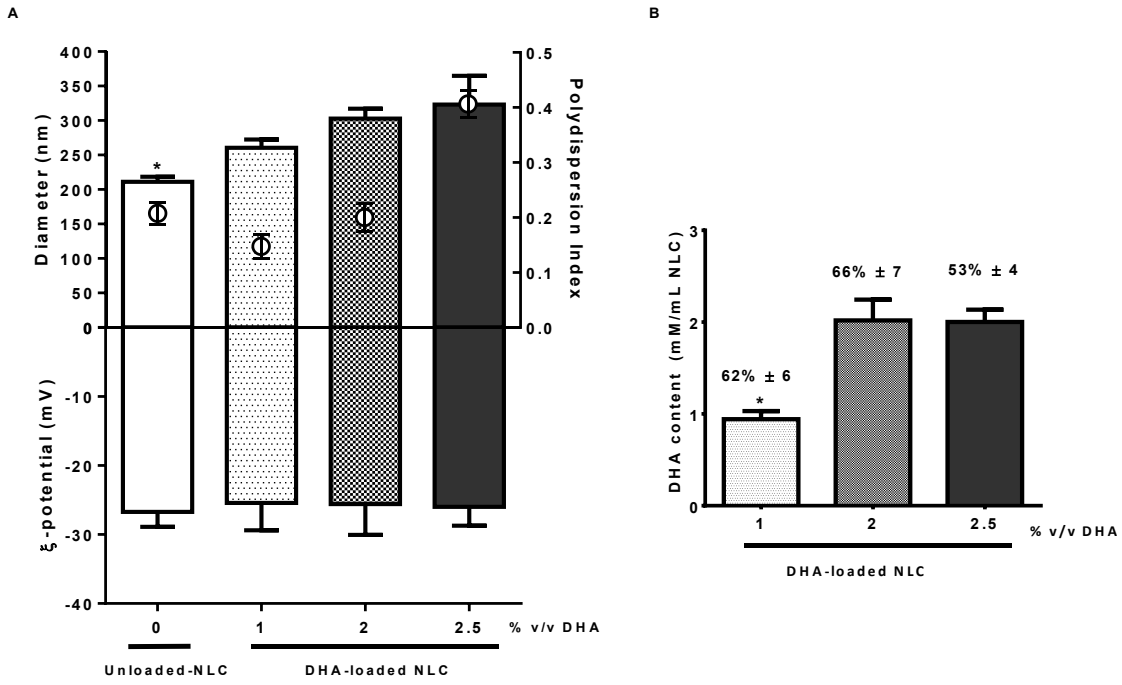

Figure 1. (A) NLC were characterized in terms of: diameter (bars), polydispersion index (dots) and charge surface (ξ-potential) (bars) performed using dynamic light scattering at 37ºC. *$p<0.05$; statically significant differences between unloaded-NLC and different concentrations of DHA added (Kruskal-Wallis test). (B) NLC characterization in terms of DHA content (bars) and entrapment efficiency (values in percentage). *$p<0.05$; statically significant differences between concentrations of DHA added (Kruskal-Wallis test). All data is reported as the mean ± standard deviation (n=3).

The morphology of these NLC (unloaded and DHA-loaded) was observed by Cryo-SEM and NanoSight®. Images from Figure 2 demonstrate that NLC displayed an almost spherical morphology and were not aggregated.

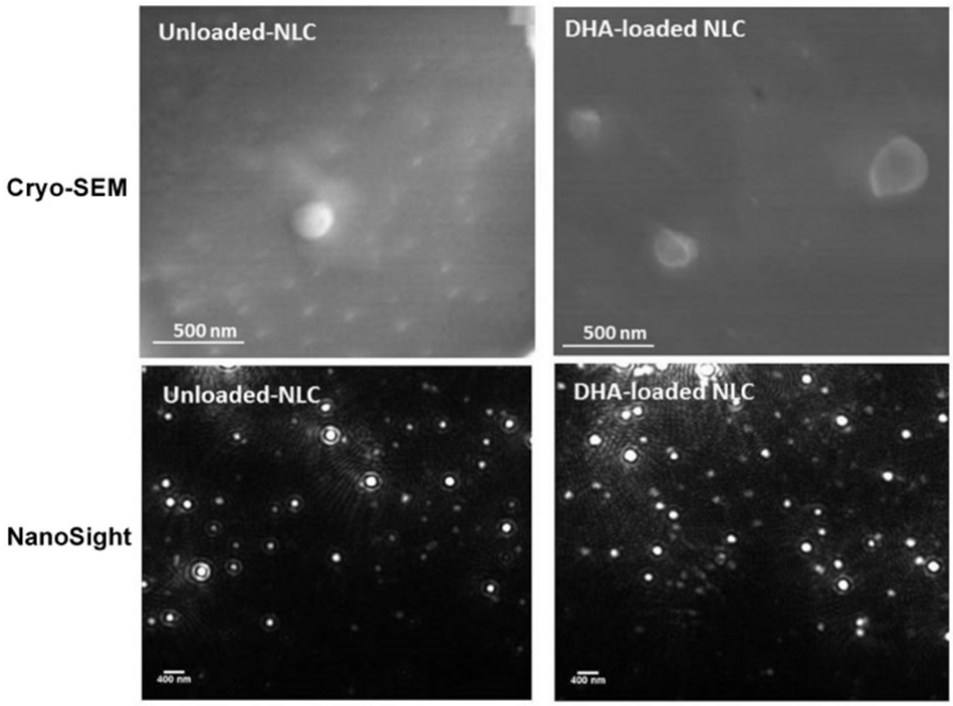

Figure 2. Unloaded-NLC and 2% v/v DHA-loaded NLC morphology was evaluated by cryo-scanning electron microscopy (Cryo-SEM) (scale bar 500 nm) and NanoSight® (scale bar 400 nm).

NLC stability was followed by measuring the change of NLC size and charge after their storage in aqueous solution up to 2 months at 4ºC and 20ºC. As shown in Figure 3, NLC did not change their size until one month of storage, independently of the temperature. However, surface ξ-potential of DHA-loaded NLC was only maintained during 2 weeks, suggesting that these NLC can be stored in water for at least 2 weeks, independently of the temperature. Figure 3 also demonstrated that unloaded-NLC were stable during all the storage period in both temperatures used.

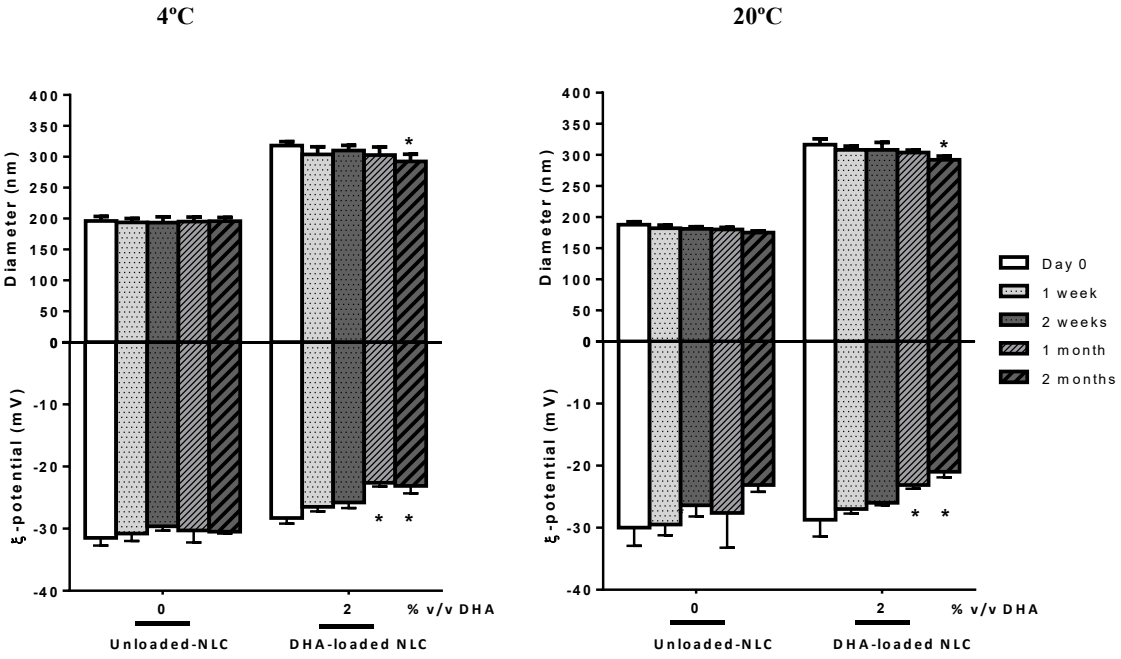

Figure 3. Storage time effect regarding diameter and charge on unloaded-NLC and 2% DHA-loaded in water at 4ºC and 20ºC. Data is reported as the mean ± standard deviation (n=3). *Statistically significance different from the same NLC at day 0 ($p<0.05$; Kruskal-Wallis test).

Concerning the DHA release profile, studies were performed in bacteria liquid medium (BB + 10% FBS medium), which is the medium used during NLC bactericidal evaluation. Figure 4A shows the concentration of NLC before and after incubation in bacteria medium during 3 hours. The decrease in DHA-loaded NLC concentration (~50%) after their incubation in medium indicates that DHA was released by NLC disruption. Figure 4B confers that this delivery was initially 3% of total amount of DHA from DHA-loaded NLC during the first 30 minutes incubation and approximate 40% of total amount of DHA, after 3 h.

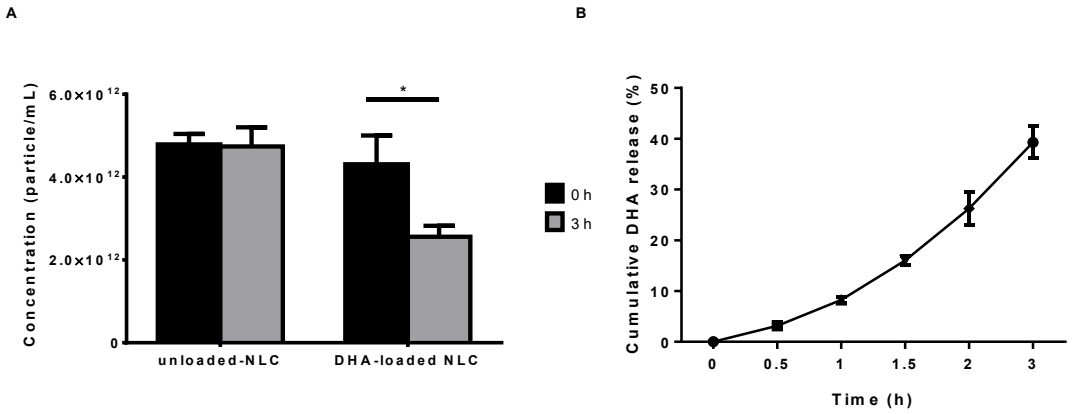

Figure 4. (A) NLC stability in bacteria medium (Brucella-broth+10% FBS medium) was evaluated through the concentration of particles measured by NanoSight®. The values are given as mean ± standard deviation. * Statically significant differences between samples ($p<0.05$; Kruskal-Wallis test). (B) *In vitro* release curve of DHA from 2% DHA-loaded NLC in bacteria medium (Brucella-broth+10% FBS medium) during 3 h.

3.2. Antimicrobial proprieties of NLC against *H. pylori*

Figure 5 shows the effect of NLC on the growth kinetic of *H. pylori* strain J99. Figure 5A demonstrated that the presence of free DHA (10, 25, 50, 100 and 500 μM) decreased *H. pylori* J99 growth in 1 log compared to control (*H. pylori* growth in liquid BB+10% FBS medium).

Figure 5B and 5C also demonstrated that NLC (unloaded and DHA-loaded) are bactericidal against *H. pylori* J99 strain, as well as SS1 strain (Figure S1), in all concentrations tested since they were able to kill 99.9% (>3 logs) bacteria in 24 hours of incubation. However, DHA-loaded NLC displayed a faster bactericidal effect than unloaded-NLC. When low concentration (0.5% v/v) of NLC were used, the bactericidal effect on *H. pylori* J99 was reached after 6 hours for DHA-loaded NLC (corresponding to 10 μM DHA) and only after 18 hours for the same concentration of unloaded-NLC. DHA-loaded NLC at 1.25% (25 μM DHA) and 2.5% (50 μM DHA) are bactericidal for both *H. pylori* strains, after 3 and 1.5 hours, respectively. On the other hand, the lowest time needed to kill both bacteria, using the highest amount of unloaded-NLC (25%), was 9 hours.

To evaluate if DHA-loaded NLC storage in water for 2 weeks at 4ºC would interfere in their effect towards *H. pylori*, bactericidal activity after storage in these conditions was also studied (Figure S2). Results demonstrated that the stored DHA-loaded NLC have the same profile of the freshly prepared NLC, killing bacteria after 3 and 1.5 hours at concentrations of 1.25% and 2.5%, respectively.

A **B**

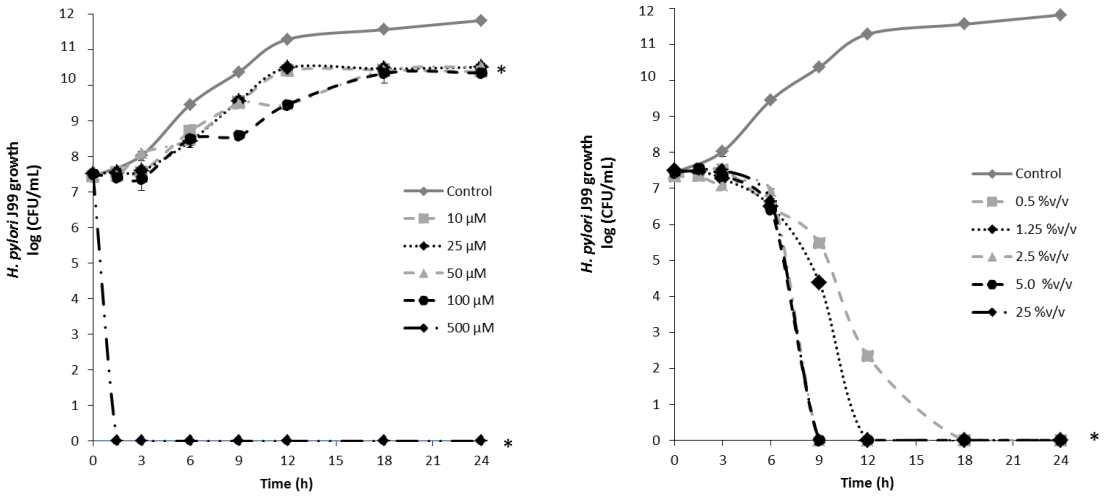

C

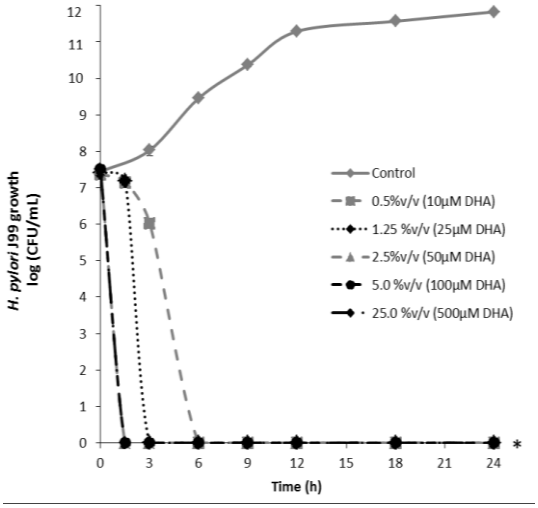

Figure 5. *H. pylori* J99 growth over 24 hours in the presence of increasing concentrations of (A) free DHA, (B) unloaded-NLC (nanoparticles without DHA) and (C) 2% v/v DHA-loaded NLC. Data is expressed as mean ± standard deviation (n=3). * $p<0.05$, refers to significant differences in *H. pylori* growth between control (bacteria untreated) and bacteria treated with free DHA or unloaded or DHA-loaded NLC (Kruskal-Wallis test).

Morphological changes of *H. pylori* J99 after exposition to free DHA (25 µM), unloaded-NLC (1.25%) and DHA-loaded NLC (1.25%; 25 µM DHA) for 3 and 12 hours were observed by SEM (Figure 6) and TEM (Figure 7). Figures 6A and 6E show *H. pylori* in its characteristic curved rod shape after 3 and 12 hours growing in bacterial medium (control). After bacteria incubation with free DHA for 3 hours (Figure 6B) and 12 hours (Figure 6F), *H. pylori* morphology was similar to the control. The same was observed when bacteria were grown for 3 hours in the presence of unloaded-NLC (Figure 6C). However, after 12 hours growing in the presence of unloaded-NLC (Figure 6G) or after 3 and 12 hours in the presence of DHA-loaded NLC (Figures 6D and 6H), SEM images suggest that bacteria released their cytoplasmic contents, although morphological changes were not observed.

TEM images (Figure 7) corroborate with SEM results, showing *H. pylori* with the intact cell membrane and dense cytoplasm in controls, in the presence of free DHA (25 µM) (Figure 7B and 7F) and unloaded-NLC (1.25%) for 3 hours (Figure 7C). Moreover, TEM images also revealed *H pylori* cell membrane fragmentation, an increase of the bacterial periplasmic space and loss of cytoplasmic content in the presence of unloaded-NLC for 12 hours (Figure 6G) and DHA-loaded for 3 and 12 hours (Figure 7D and 7H).

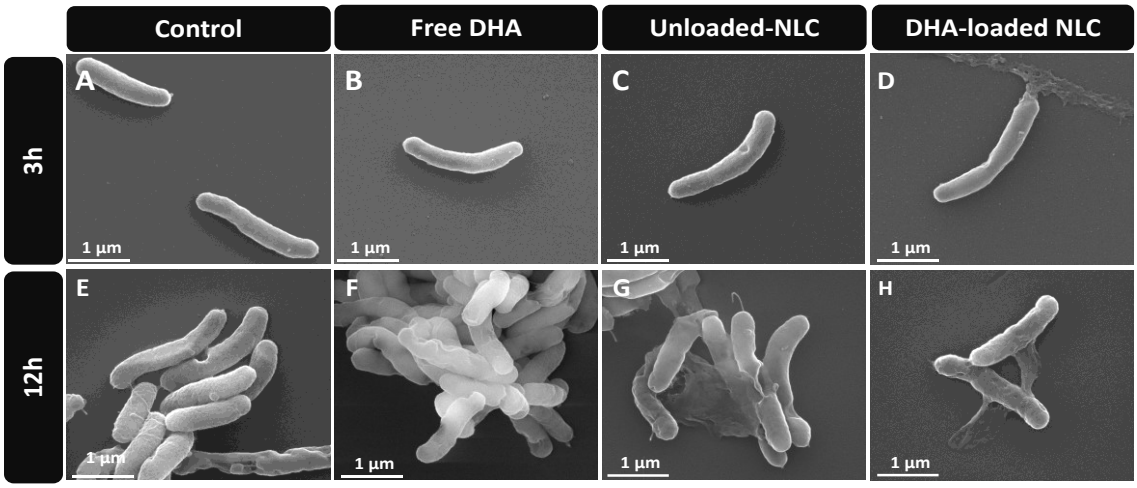

Figure 6. SEM images of *H. pylori* J99 after 3 hours (A to D) and 12 hours (E to H) exposure to the different treatments: control (untreated) (A and E), 25 µM of free DHA (B and F), 1.25 % v/v of unloaded-NLC (C and G) and 1.25 %v/v (25 µM DHA) of DHA-loaded NLC (D and H). Scale bars represent 1 µm.

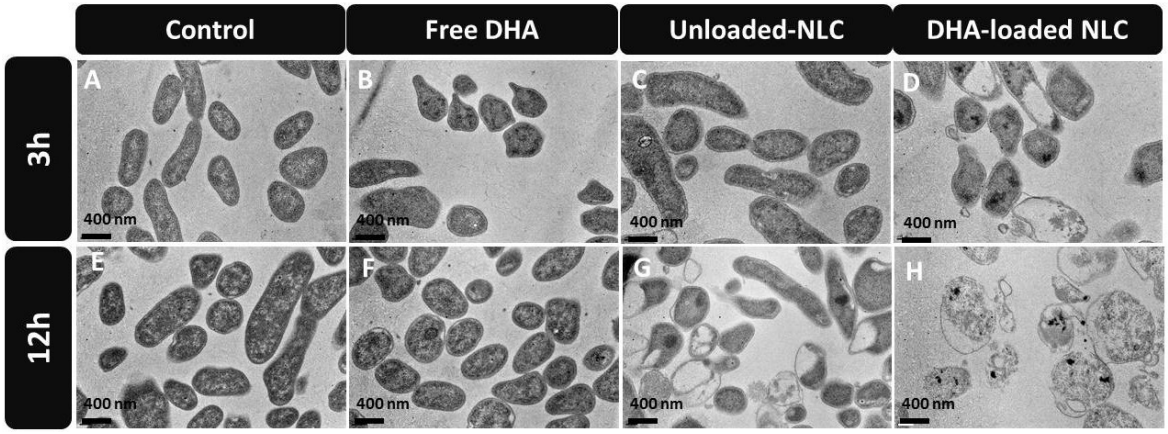

Figure 7. TEM micrographs of *H. pylori* J99 after 3 hours (A to D) and 12 hours (E to H) exposure to different treatments: control (untreated) (A and E), 25 µM of free DHA (B and F), 1.25 % v/v of unloaded-NLC (C and G) and 1.25 %v/v (25 µM DHA) of DHA-loaded NLC (D and H). Scale bars represent 400 nm.

As in SEM and TEM, bacteria images obtained from imaging flow cytometry also demonstrated that *H. pylori* J99 are in rod shape as exemplified in Figure 8A. Figure 8A also shows that bacteria were labeled with coumarin-labelled NLC (presenting a green fluorescence), indicating that NLC have high affinity to *H. pylori*. However, although *H. pylori* were labeled with fluorescent NLC, the bactericidal effect of unloaded-NLC was not observed for 3 h, since only 30% of bacteria are dead. These results suggest that although the interaction between NLC with bacteria is similar with and without DHA, their bactericidal effect is faster in the presence of DHA.

A

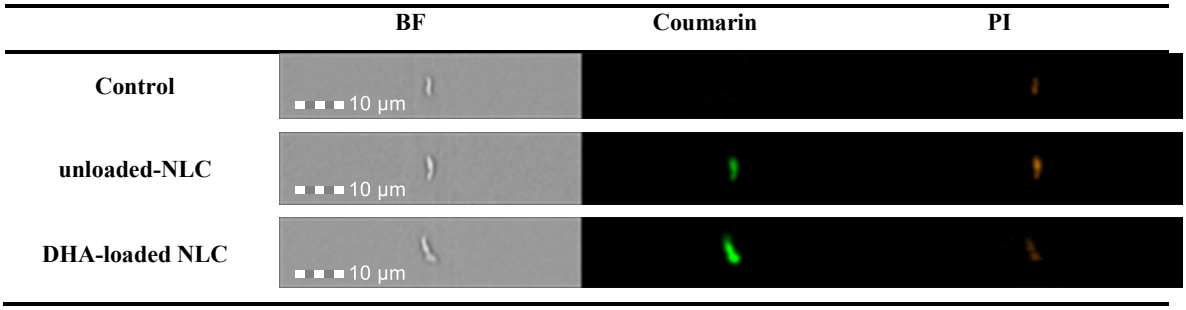

B

	Control		unloaded- NLC (1.25% v/v)		DHA-loaded NLC (25µM DHA)	
Time (h)	**Bacteria labelled with NLC (%)**	**Death by CFU (%)**	**Bacteria labelled with NLC (%)**	**Death by CFU (%)**	**Bacteria labelled with NLC (%)**	**Death by CFU (%)**
3	0	0	99	30	100	100
12	0	0	100	100	100	100

Figure 8. (A) Representative images of individualized *H. pylori* with unloaded-NLC (1.25% v/v) and DHA-loaded NLC (1.25% v/v; 25 µM). The individual bacterial cells are shown by Brightfield images (BF, left column) and propidium iodide (PI, right column), and bacteria labelled by nanoparticles labelled with 0.1%w/v of coumarin-6, green fluorescence images (coumarin-6, centre column). (B) Quantification of green fluorescent bacteria labelled by NLC labelled with coumarin-6, incubated during 3 hours and 12 hours, obtained by flow cytometry and bacterial death quantified by colony-forming-unit (CFU) counting.

3.3. Biocompatibility of NLC

Figure 9 shows the effect of NLC on human gastric adenocarcinoma cells viability and lysis determined by MTT (Figure 9A) and LDH (Figure 9B) assays, respectively.

Figure 9A demonstrated that there was not a significant decrease in cell viability by the presence of NLC concentrations up to 2.5% (unloaded and DHA-loaded NLC). However, a severe reduction in cell viability was observed when MKN45 cells were exposed to the highest concentration of DHA-loaded NLC tested (5.0% corresponding to 100 µM DHA). Concerning the effect of NLC on gastric cell lysis (Figure 9B), no toxicity was observed for NLC concentration up to 2.5% (unloaded and DHA-loaded NLC). For this concentration, only ~20% of cell lysis was observed, independently of the presence of DHA. High toxicity was observed for 5.0% of DHA-loaded NLC (100 µM DHA).

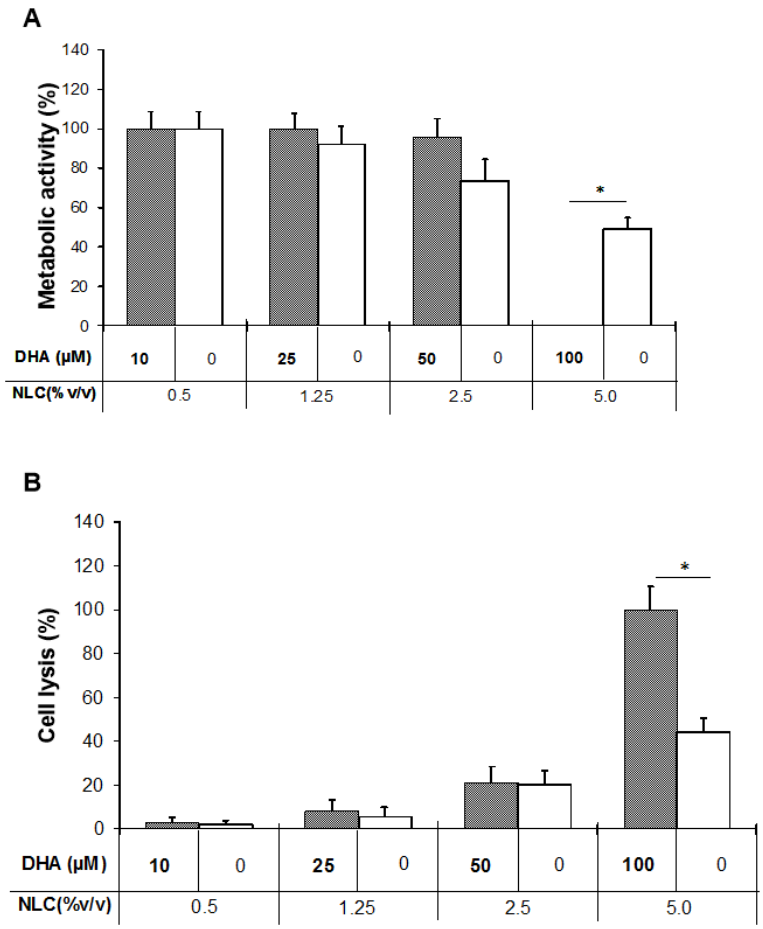

Figure 9. MKN45 gastric carcinoma cell line (A) viability and (B) cytotoxicity were assessed by the MTT and LDH assays, respectively, after 24 h of exposure to different concentrations of unloaded and DHA-loaded NLC. Data is reported as mean ± standard deviation (n=3). * Statically significant differences of MKN45 gastric cells treated with DHA-loaded NLC between unloaded-NLC ($p<0.05$; Kruskal-Wallis test).

4. Discussion

The increase of *H. pylori* strains resistant to available antibiotics is a serious problem that affects its rate of eradication and clearly, demonstrates the urgent need of finding new drugs and different strategies to fight this bacterium. Correia *et al* [20] demonstrated that DHA reduced the ability of *H. pylori* to colonize the gastric mucosa in only 50% of mice. This could be explained by DHA poor solubility in water, low penetration through the mucus layer, low residence time in the stomach but also by its degradation in the gastric environment due to oxidation, carboxylic protonation, esterification or lipid-protein complexation [18]. To overcome these problems, in the present work DHA was encapsulated into NLC that are a promising delivery system for lipophilic drugs [24]. NLC are suitable for transport, and protect bioactive compounds against degradation, offering a liquid matrix with a nanostructure that improves drug loading and its preservation during storage. [27-29] In this study, NLC were synthesized using a hot homogenization and ultrasonication, avoiding the

use of organic solvents. In addition, they present low cytotoxicity due to their lipid biodegradable and biocompatible composition recognized by the FDA as safe [30-32]. Bactericidal DHA-loaded NLC with 302±14 nm of diameter, and negative charge (around -28mV) were successfully produced with an entrapment efficiency of 66% (containing ~2 mM DHA/mL NLC; DHA-loaded NLC produced with 2% of DHA).

This DHA-loaded NLC displayed a bactericidal activity against *H. pylori* J99 (Figure 5) and SS1 (Figure S1) strains at all concentrations tested. However, their efficacy rate was concentration dependent, taking 6 hours (J99) and 9 hours (SS1) to kill all the bacteria even with the lowest DHA concentration used (10 μM). We proved that the incorporation of DHA into NLC greatly improves DHA bactericidal effect since free DHA was only bactericidal at DHA concentrations around 500 μM, as also previously described for other *H. pylori* strains [20], and DHA was released (40% after 3h) from NLC (Figure 4B), due to destabilization and disintegration in bacteria medium (Figure 4A). Nevertheless, unloaded-NLC (211±8 nm) are also bactericidal to both *H. pylori* strains used in all the concentrations tested although with a lower efficiency rate than DHA-loaded NLC. This effect is not associated with NLC reagents, namely Precirol®ATO5 [33], Tween®60 [34,35] and Miglyol®812 (Figure S3), as they alone do not affect bacteria growth in the concentrations used during NLC production. Moreover, our results (Figure 4A) demonstrated that these unloaded-NLC did not dissolve after at least 3 h in bacteria liquid medium.

The mechanism of action of DHA-loaded NLC is unclear, however, the mechanism of action of PUFAs can be related to their ability to disrupt the integrity of the cell membrane, leading to the leakage of important cellular metabolites and even bacteria lysis [11,12,17,18,20,21]. Aside from perturbation of membranes, PUFAs can interact with other intracellular targets and enzymes, including those involved in bacterial fatty acid synthesis. Free fatty acids can exert an effect, whereby the pH of the cytoplasm is reduced to such an extent that the cell ceases to function normally [17].

Cleary, all NLC have high affinity to the *H. pylori* membrane, as shown by ImageStream® (Figure 8) where coumarin-labelled NLC adhered to bacteria enabling them to exhibit a green fluorescence. Coumarin-6, often used as a model for delivery systems, was used in this work since it is a non-cytotoxic lipophilic dye [36]. Furthermore, it was shown that NLC interact with *H. pylori* membrane and disrupt the cell membrane, allowing the leakage of the cytoplasmic content (Figure 5). NLC also induced the separation of the plasma membrane from the outer membrane, enhancing the periplasmic space (Figure 7). These morphological changes were similar to the described by Jung *et al* [37], for the effect of liposomes loaded with linolenic acid (C18:3) on *H. pylori* SS1 after 30 minutes of 400 μg/mL (220 μM) of linolenic acid. Jung *et al* proposed that these liposomes could fuse with bacteria membranes incorporating/releasing the linolenic acid directly into bacterial membrane, changing their phospholipid composition [37].

The morphological transition of *H. pylori* form a bacillary to a coccoid shape was not found by SEM, TEM nor ImageStream$^{X®}$ images, where only bacillus shape was visualized,

indicating that DHA-loaded NLC have a fast effect on bacteria not allowing a modification of the bacterial cell wall peptidoglycan [38].

Highlighting its bactericidal effect, DHA-loaded NLC are not cytotoxic to human gastric adenocarcinoma cells (MKN45 cell line) at bactericidal concentrations, namely up to 50 μM (Figure 9), since an increase of cell lysis higher than 30% was not observed, the value defined in ISO 10993-5 [39] for cytotoxic materials. However, DHA-loaded NLC are cytotoxic for concentrations around 100 μM (5% v/v), the same concentration described in the literature as cytotoxic for free DHA [40,41]. Noteworthy, the maximum daily recommendation for DHA is 250 mg/day (762 μM/day) in humans [42], which is much higher than the values evaluated in this study.

These DHA-loaded NLC can be stored in water at least during two weeks at 4ºC or 20ºC (Figure 3) without losing their *H. pylori* antimicrobial activity (Figure S2). For longer periods of time (3, 6 or 12 months of storage at 20ºC), NLC should be freeze-dried using a preservative agent [24,43,44].

5. Conclusion

DHA-loaded NLC with ~300 nm of size and negative charge were developed. These nanoparticles enhanced the bactericidal effect of DHA against *H. pylori* in a concentration-dependent way. Moreover, unloaded- NLC were also bactericidal against the bacterial strains tested although in a slower level. Its bactericidal effect is associated with changes in *H. pylori* membrane, namely by separation of plasma membrane from the outer membrane, increasing the periplasmic space and the leakage of cytoplasmic contents. Finally, NLC are not cytotoxic to human epithelial cells at bactericidal concentrations (below 50 μM of DHA) and can be stored in water for two weeks at 4ºC without any preservative agent.

DHA-loaded NLC should, therefore, be explored as an alternative to the current treatment of *H. pylori* infection.

Acknowledgments

This work was financed by FEDER - Fundo Europeu de Desenvolvimento Regional funds through the COMPETE 2020 - Operational Programme for Competitiveness and Internationalization (POCI), Portugal 2020. FCT - Fundação para a Ciência e a Tecnologia/ Ministério da Ciência, Tecnologia e Inovação through the projects: POCI-01-0145-FEDER-007274; PYLORIBINDERS (PTDC/CTM-BIO/4043/2014); PYLORICIDAL (PTDC/CTM-BPC/121149/2010) and FCT grant SFRH/BD/89001/2012. The authors thank Virginia Gouveia (REQUIMTE, FFUP) for the culture of cells and cytotoxicity studies, and Carla Teixeira and Sónia Melo (IPATIMUP, i3S) for the NanoSight studies.

Appendix A. Supplementary data

Supplementary data associated with this article can be found, in the online version, at http://dx.doi.org/10.1016/j. ijpharm.2017.01.014.

Figure S1

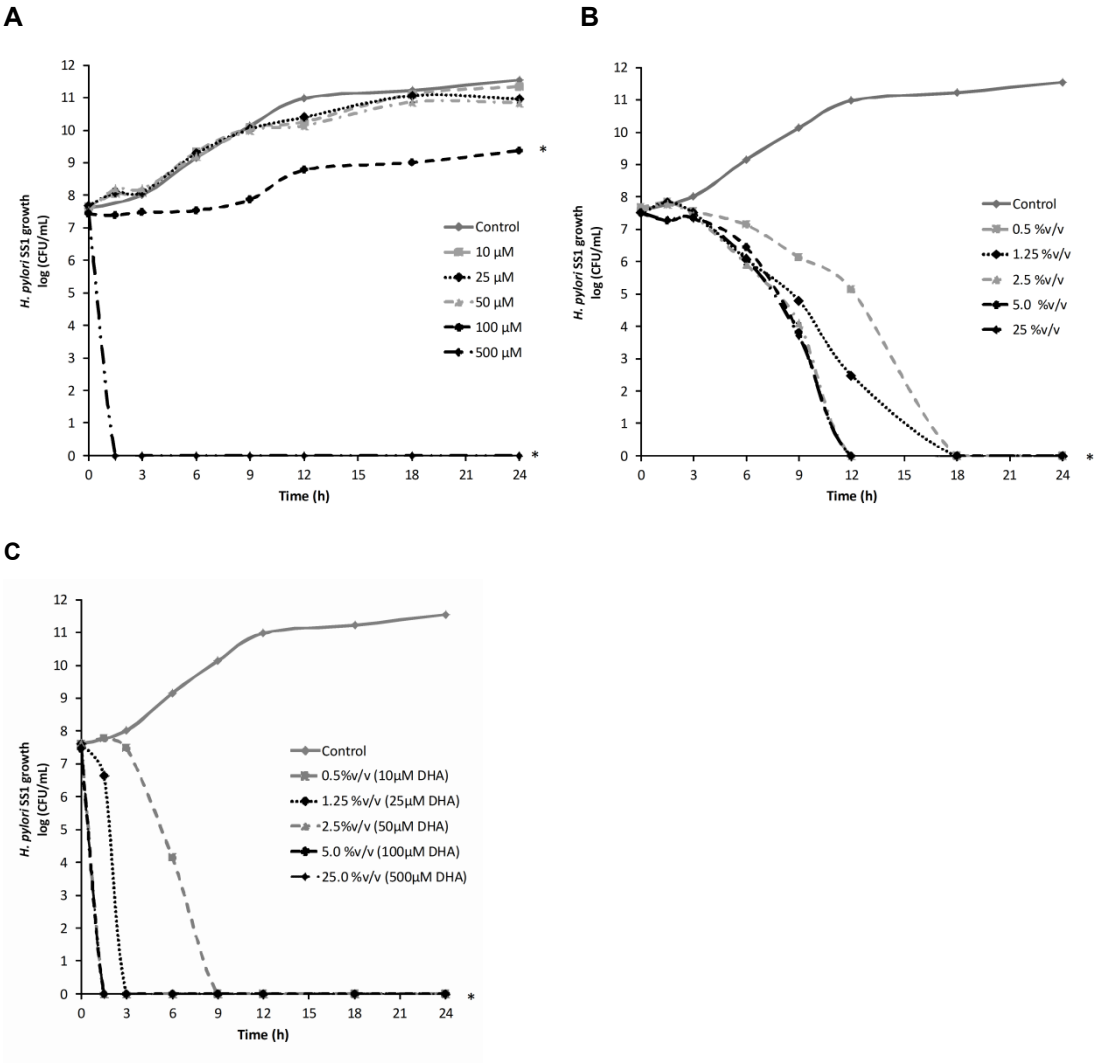

Fig. S1 *H. pylori* SS1 growth over 24 hours in the presence of increasing concentrations of (A) free DHA, (B) unloaded-NLC (nanoparticles without DHA) and (C) 2% v/v DHA-loaded NLC. 100 µM of free DHA presented an inhibitory effect against SS1 strains and a bactericidal effect with 500 µM. In the presence of NLC (unloaded and DHA-loaded), a similar bactericidal profile against *H. pylori* SS1 strain was observed compared to the J99 strain. Data is expressed as mean ± standard deviation (n=3). * $p<0.05$, refers to significant differences in *H. pylori* growth between control (bacteria untreated) and bacteria treated with free DHA or unloaded or DHA-loaded NLC (Kruskal-Wallis test).

Figure S2

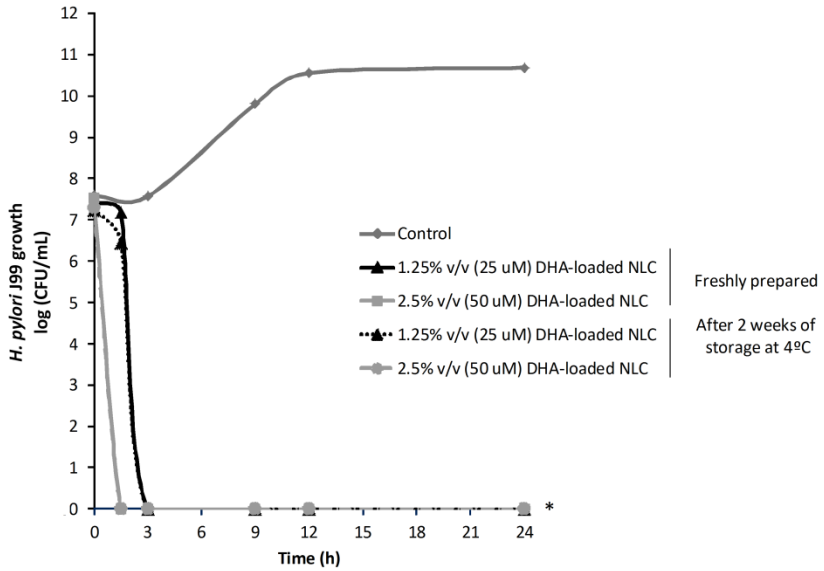

Fig. S2 *H. pylori* J99 strain growth over 24 hours in the presence of increasing concentrations of 2% v/v DHA-loaded NLC after preparation and after 2 weeks storage in aqueous solution at 4ºC. The bactericidal profile of DHA-loaded NLC does not change after 2 weeks stored at 4ºC compared to the profile of the freshly prepared NLC, killing bacteria after 1.5h and 3h at concentrations of 1.25% (25μM DHA) and 2.5% (50 μM) of DHA-loaded NLC, respectively. The values are reported as mean ± standard deviation (n=3). * $p<0.05$, refers to significant differences in *H. pylori* growth between bacteria treated with DHA-loaded NLC stored at 4ºC and bacteria treated with DHA-loaded NLC freshly prepared (Kruskal-Wallis test).

Figure S3

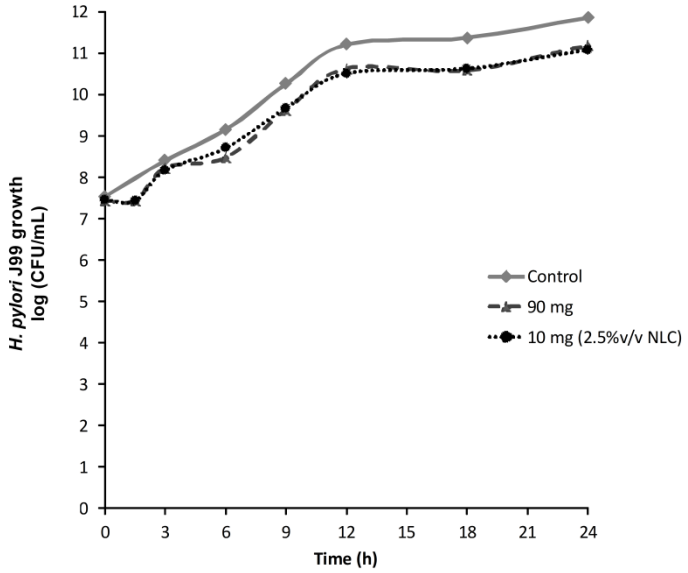

Fig. S3 *H. pylori* J99 strain growth over 24 hours in the presence of two concentrations of Miglyol®812: concentration used on NLC production (90mg) and concentration correspondent to the amount of Miglyol®812 on 2.5%v/v of NLC. Data is expressed as mean ± standard deviation (n=2).

References

1. AmericanCancerSociety (2015) Global Cancer Facts & Figures Atlanta: American Cancer Society.

2. Correa P, Houghton J (2007) Carcinogenesis of *Helicobacter pylori*. Gastroenterology 133: 659-672.

3. Matysiak-Budnik T, Megraud F (2006) *Helicobacter pylori* infection and gastric cancer. Eur J Cancer 42: 708-716.

4. Pinho SS, Carvalho S, Marcos-Pinto R, Magalhaes A, Oliveira C, et al. (2013) Gastric cancer: adding glycosylation to the equation. Trends Mol Med 19: 664-676.

5. Amieva M, Peek RM, Jr. (2016) Pathobiology of *Helicobacter pylori*-Induced Gastric Cancer. Gastroenterology 150: 64-78.

6. Goncalves IC, Henriques PC, Seabra CL, Martins MC (2014) The potential utility of chitosan micro/nanoparticles in the treatment of gastric infection. Expert Rev Anti Infect Ther 12: 981-992.

7. Lopes D, Nunes C, Martins MC, Sarmento B, Reis S (2014) Eradication of *Helicobacter pylori:* Past, present and future. J Control Release 189: 169-186.

8. Malfertheiner P, Megraud F, O'Morain CA, Atherton J, Axon ATR, et al. (2012) Management of *Helicobacter pylori* infection- the Maastricht IV/ Florence Consensus Report. Gut 61: 646e664.

9. Parreira P, Fátima Duarte M, Reis CA, Martins MCL (2016) *Helicobacter pylori* infection: A brief overview on alternative natural treatments to conventional therapy. Critical Reviews in Microbiology: 1-12.

10. Vakil N (2006) *Helicobacter pylori* treatment: a practical approach. Am J Gastroenterol 101: 497-499.

11. Sun CQ, O'Connor CJ, Roberton AM (2003) Antibacterial actions of fatty acids and monoglycerides against *Helicobacter pylori*. FEMS Immunol Med Microbiol 36: 9-17.

12. Thompson L, Cockayne A, Spiller RC (1994) Inhibitory effect of polyunsaturated fatty acids on the growth of *Helicobacter pylori*: a possible explanation of the effect of diet on peptic ulceration. Gut 35: 1557-1561.

13. Romero C, Medina E, Vargas J, Brenes M, De Castro A (2007) In vitro activity of olive oil polyphenols against Helicobacter pylori. J Agric Food Chem 55: 680-686.

14. Paulo L, Oleastro M, Gallardo E, Queiroz JA, Domingues F (2011) Anti-*Helicobacter pylori* and urease inhibitory activities of resveratrol and red wine. Food Research International 44: 964-969.

15. Brown JC, Huang G, Haley-Zitlin V, Jiang X (2009) Antibacterial effects of grape extracts on *Helicobacter pylori*. Appl Environ Microbiol 75: 848-852.

16. Desbois AP, Lawlor KC (2013) Antibacterial Activity of Long-Chain Polyunsaturated Fatty Acids against *Propionibacterium acnes* and *Staphylococcus aureus*. Marine Drugs 11: 4544-4557.

17. Desbois AP (2012) Potential applications of antimicrobial fatty acids in medicine, agriculture and other industries. Recent Pat Antiinfect Drug Discov 7: 111-122.

18. Desbois AP, Smith VJ (2010) Antibacterial free fatty acids: activities, mechanisms of action and biotechnological potential. Appl Microbiol Biotechnol 85: 1629-1642.

19. Meier R, Wettstein A, Drewe J, Geiser HR (2001) Fish oil (Eicosapen) is less effective than metronidazole, in combination with pantoprazole and clarithromycin, for *Helicobacter pylor*i eradication. Aliment Pharmacol Ther 15: 851-855.

20. Correia M, Michel V, Matos AA, Carvalho P, Oliveira MJ, et al. (2012) Docosahexaenoic acid inhibits *Helicobacter pylori* growth in vitro and mice gastric mucosa colonization. PLoS One 7: e35072.

21. Petschow BW, Batema RP, Ford LL (1996) Susceptibility of *Helicobacter pylori* to bactericidal properties of medium-chain monoglycerides and free fatty acids. Antimicrob Agents Chemother 40: 302-306.

22. Correia M, Michel V, Osório H, El Ghachi M, Bonis M, et al. (2013) Crosstalk between *Helicobacter pylori* and Gastric Epithelial Cells Is Impaired by Docosahexaenoic Acid. PloS one 8: e60657.

23. Taneja A, Singh H (2012) Challenges for the delivery of long-chain n-3 fatty acids in functional foods. Annual review of food science and technology 3: 105-123.

24. Beloqui A, Solinis MA, Rodriguez-Gascon A, Almeida AJ, Preat V (2016) Nanostructured lipid carriers: Promising drug delivery systems for future clinics. Nanomedicine 12: 143-161.

25. Poonia N, Kharb R, Lather V, Pandita D (2016) Nanostructured lipid carriers: versatile oral delivery vehicle. Future Science OA 2: FSO135.

26. Tamjidi F, Shahedi M, Varshosaz J, Nasirpour A (2013) Nanostructured lipid carriers (NLC): A potential delivery system for bioactive food molecules. Innovative Food Science & Emerging Technologies 19: 29-43.

27. Neves AR, Lucio M, Martins S, Lima JL, Reis S (2013) Novel resveratrol nanodelivery systems based on lipid nanoparticles to enhance its oral bioavailability. Int J Nanomedicine 8: 177-187.

28. Das S, Chaudhury A (2011) Recent advances in lipid nanoparticle formulations with solid matrix for oral drug delivery. AAPS PharmSciTech 12: 62-76.

29. Zhuang C-Y, Li N, Wang M, Zhang X-N, Pan W-S, et al. (2010) Preparation and characterization of vinpocetine loaded nanostructured lipid carriers (NLC) for improved oral bioavailability. International Journal of Pharmaceutics 394: 179-185.

30. Mehnert W, Mäder K (2001) Solid lipid nanoparticles: Production, characterization and applications. Advanced Drug Delivery Reviews 47: 165-196.

31. Müller RH, Mäder K, Gohla S (2000) Solid lipid nanoparticles (SLN) for controlled drug delivery – a review of the state of the art. European Journal of Pharmaceutics and Biopharmaceutics 50: 161-177.

32. Muller RH, Shegokar R, Keck CM (2011) 20 years of lipid nanoparticles (SLN and NLC): present state of development and industrial applications. Curr Drug Discov Technol 8: 207-227.

33. Cerreto F, Paolicelli P, Cesa S, Abu Amara HM, D'Auria FD, et al. (2013) Solid lipid nanoparticles as effective reservoir systems for long-term preservation of multidose formulations. AAPS PharmSciTech 14: 847-853.

34. Blackburn P (1997) Polysorbate-containing compositions and their use against *Helicobacter*. European Patent Office WO/1997/036600.

35. Santucci A, Figura N, Spreafico A, Cavallo G, Marcolongo RF (2013) Compositions for treating *Helicobacter pylori* infection. European Patent Office WO2011IT00175.

36. Iemsam-Arng J, Ketchart O, Rattana-Amron T, Wutikhun T, Tapaneeyakorn S (2015) Modified NLC-loaded coumarin for pharmaceutical applications: the improvement of physical stability and controlled release profile. Pharm Dev Technol: 1-8.

37. Jung SW, Thamphiwatana S, Zhang L, Obonyo M (2015) Mechanism of antibacterial activity of liposomal linolenic acid against *Helicobacter pylori*. PloS one 10: e0116519.

38. Chaput C, Labigne A, Boneca IG (2007) Characterization of *Helicobacter pylori* lytic transglycosylases Slt and MltD. J Bacteriol 189: 422-429.

39. ISO10993-5 (2009) Part 5:Tests for in vitro cytotoxicity. Biological evaluation of medical devices. 3rd ed. Geneva, Switzerland: International Organization for Standardization.

40. Dai J, Shen J, Pan W, Shen S, Das UN (2013) Effects of polyunsaturated fatty acids on the growth of gastric cancer cells in vitro. Lipids Health Dis 12: 71.

41. Lee SE, Lim JW, Kim H (2009) Activator protein-1 mediates docosahexaenoic acid-induced apoptosis of human gastric cancer cells. Ann N Y Acad Sci 1171: 163-169.

42. Government US (2010) Dietary Guidelines for Americans; Agriculture Do, Health Do, Services H, editors. Washington, DC: Government Printing Office.

43. Obeidat WM, Schwabe K, Müller RH, Keck CM (2010) Preservation of nanostructured lipid carriers (NLC). European Journal of Pharmaceutics and Biopharmaceutics 76: 56-67.

44. del Pozo-Rodriguez A, Solinis MA, Gascon AR, Pedraz JL (2009) Short- and long-term stability study of lyophilized solid lipid nanoparticles for gene therapy. Eur J Pharm Biopharm 71: 181-189.

CHAPTER V

SPECIFIC BACTERICIDAL ACTIVITY OF UNLOADED-LIPID NANOPARTICLES AGAINST *HELICOBACTER PYLORI*

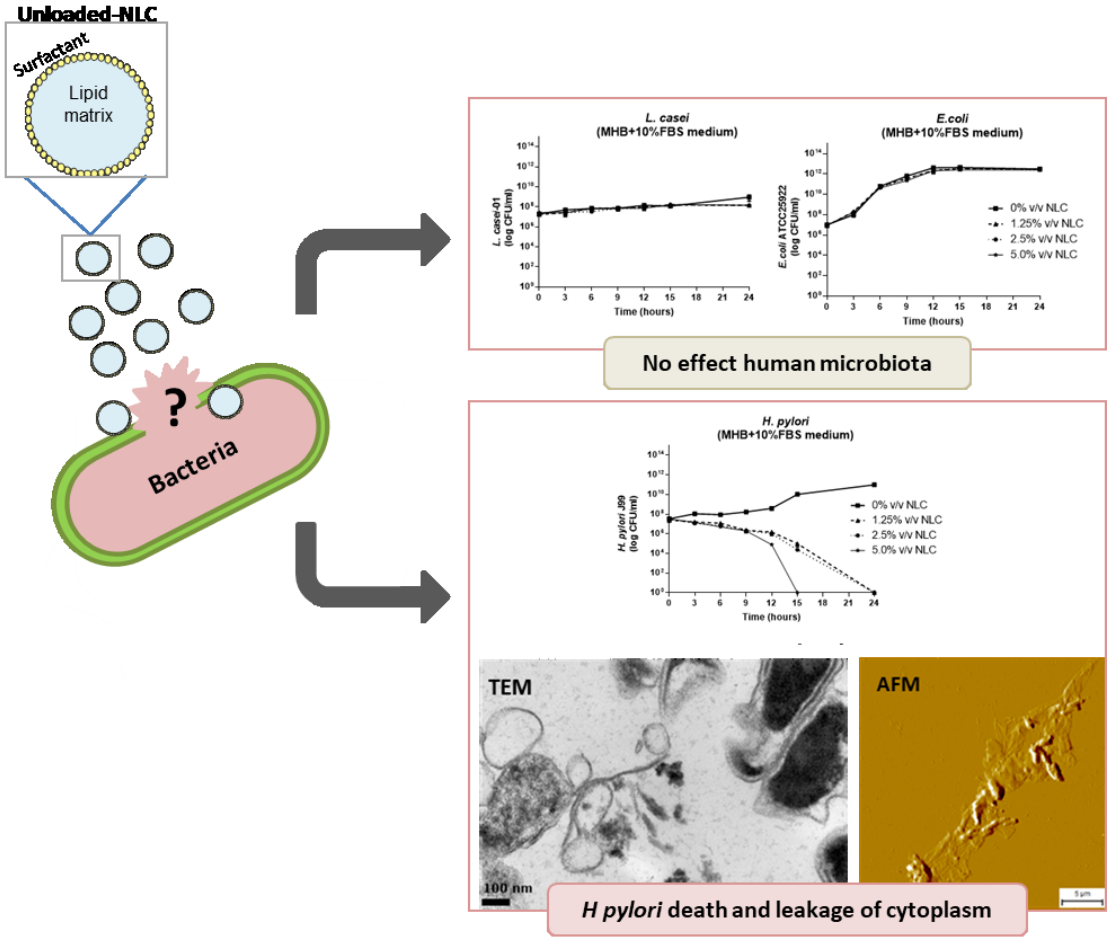

This chapter was based on the following submitted paper:

- **SEABRA CL**, Nunes C., Brás, M, Gomez-Lazaro, M., Reis, CA, Gonçalves IC, Reis S., Martins MCL. (2017) Specific bactericidal activity of unloaded-lipid nanoparticles against *Helicobacter pylori, Submitted*

Abstract

Helicobacter pylori (*H. pylori*) chronic infection is one of the major risk factors for the development of gastric cancer and available antibiotic treatments are not efficient in all the patients.

We recently demonstrated that lipid nanoparticles, namely nanostructured lipid carriers (NLC), even without any drug, display bactericidal proprieties against *H. pylori.* Subsequently, this work aims to evaluate if these NLC are selective to *H. pylori*, and to clarify their mode of action.

NLC with around 200 nm and negatively charge (-28±3 mV) were produced by a high shear hot homogenization followed by ultrasonication method, using Precirol®ATO5 and Miglyol®812 as lipids and Tween®60 as a surfactant.

Bactericidal assays, using bacteria that are different in their structural (Gram-positive *vs* Gram-negative) and morphological features (rod *vs* spherical) and surface charge (from -2 mV to -30 mV), demonstrated that the NLC bactericidal effect is specific to *H. pylori* since they did not kill any other bacteria tested, namely *Lactobacillus*, *E. coli, S.* epi*dermidis* and *S. aureus.*

Bioimaging assays, namely imaging flow cytometry, scanning and transmission electron microscopies (SEM and TEM, respectively) and atomic force microscopy (AFM), demonstrated that NLC rapidly bind to *H. pylori* surface and then, cross both bacteria membranes, destabilizing and disrupting bacterial membranes, allowing the leakage of cytoplasmic contents leading to bacteria death. Nevertheless, *H. pylori* maintained their typical bacillary shape.

This study demonstrated that NLC with specific bactericidal effect to *H. pylori* shoud be considered for the development of a new antibiotic free therapy to fight *H. pylori* infection without affecting human microbiota.

KEYWORDS: *Helicobacter pylori*, unloaded-NLC, disruption membrane

1. Introduction

Helicobacter pylori (*H. pylori*) are microaerophilic, Gram-negative, spiral and bacillus shape bacteria that colonize the gastric mucosa of half of the world population [1-3]. This bacterium is considered the strongest identified risk factor for the development of gastric cancer since 78% of gastric cancer cases were attributed to chronic *H. pylori* infection [4-6]. Currently recommended antibiotic-based therapy is inefficient in 20% of the cases due to, principally, the increased *H. pylori* resistance to antibiotics and the low antibiotic bioavailability at local infection [7].

Nanostructured lipid carriers (NLC) are lipid nanoparticles specially designed for the encapsulation of lipophilic drugs, enhancing oral bioavailability of drugs by protecting them against the hostile environment of the gastrointestinal tract [8]. NLC are prepared from a blend of a solid lipid with a liquid lipid and an aqueous phase which is stabilized by a surfactant [9-11]. The increasing interest in NLC is associated with their higher biocompatibility and lower toxicity compared to polymeric nanoparticles, due to the GRAS (generally recognized as safe) lipids used in their composition, the production in absence of organic solvents and their lower costs associated with large-scale production [9,11-15]. NLC have been described as a promising antibacterial drug delivery system, showing great therapeutic potential as delivery systems for antibiotics and natural compounds, against different microorganisms, such as *Staphylococcus aureus, Escherichia coli, H. pylori, Propionibacterium acnes* and *Pseudomonas aeruginosa* [16-21]. However, any direct bactericidal effect of NLC without drugs to these bacteria has never been studied, until recently by our research group.

Docosahexaenoic acid (DHA), an omega-3 polyunsaturated fatty acid, has been described as a very effective bactericidal against *H. pylori* [22]. We recently demonstrated that the nanoencapsulation of DHA into NLC improved its bactericidal efficacy against different *H. pylori* strains [23]. However, NLC without DHA was also bactericidal to *H. pylori* J99 (human strain) and SS1 (mouse-adapted strain), although at a slower rate than DHA-loaded NLC [23].

Taking this into consideration, the aim of this work was to evaluate if this NLC bactericidal effect was selective to *H. pylori* strain and to understand their mode of action. To assess their selectivity, NLC were tested against other bacteria presenting different structural (Gram-positive *vs* Gram-negative) and morphological (rod *vs* spherical) features, such as the gastrointestinal *Lactobacillus casei* and *E. coli*. Moreover, since NLC are also commonly used in topical applications, they were also tested against pathogenic bacteria from skin and mucosae, *S. epidermidis* and *S. aureus*.

2. Material & methods

2.1. NLC preparation and characterization

2.1.1. NLC production

NLC were produced by a high shear hot homogenization followed by ultrasonication method according to Neves *et al.* [24] and Seabra *et al.*[23]. Briefly, 200 mg of glyceryl palmitostearate (Precirol®ATO5, Gattefosé, France), 90 mg of Caprylic/Capric Triglyceride (Miglyol®812, Acofarma, Spain) and 60 mg of polysorbate 60 (Tween®60, Merck, Germany) were weighted and heated together (65ºC) to promote their mixture. Then, 4.2 mL of Milli-Q® Integral ultrapure water (type 1) preheated at 65ºC was added to the lipid mixture. This mixture was homogenized under high speed stirring (12000 rpm, 20 s) using an T25 Ultra-Turrax® (IKA, Germany) and sonicated using a sonicator (Vibra-Cell model VCX 130 equipped with a VC 18 probe, Sonics and Materials Inc., Newtown, USA) with a tip diameter of 6 mm at 60% amplitude for 5 min.

2.1.2. NLC size and zeta potential determination

NLC hydrodynamic size distribution and surface charge (ξ-potential) were characterized using dynamic and electrophoretic light scattering (DLS and ELS) (Zetasizer Nano ZS; Malvern, UK). NLC were diluted (1:50 in type 1 water) and placed into clear disposable folded capillary cells (DTS1070; Malvern, UK). Size and ξ-potential were measured in type 1 water conducted at a backscattering angle of 173º at 37ºC. All measurements were performed in triplicate.

2.1.3. NLC morphology

NLC morphology was evaluated by Atomic Force Microscopy (AFM) imaging. Freshly cleaned mica sheet was coated with 10 µL of an NLC suspension (diluted 1:200 in type 1 water). Samples were dried during 24h at room temperature.

Atomic Force Microscopy (AFM) images were obtained with a PicoPlus scanning probe microscope interfaced with a Picoscan 2500 controller (Keysight Technologies, USA) using the PicoView 1.20 software (Keysight Technologies, USA), coupled to an Inverted Optical Microscope (Observer Z1, Zeiss, Germany), in order to precisely choose the microorganisms to be observed. Each sample was imaged with a 100×100 μm^2 piezoelectric scanner. All measurements were performed in Tapping® mode at RT using bar-shaped cantilever silicon tips (AppNano, USA) with a spring constant of 25 – 75 N/m. Scan speed was set at 2.3 l/s.

2.2. NLC bactericidal activity

2.2.1. Microorganisms and growth conditions

Microorganisms used in this study as well as their specific growth media are described in Table 1. In all cases, bacteria were first cultured in solid and only afterward grown overnight in their specific medium for use in all subsequent experiments.

2.2.2. Bacteria zeta potential

All bacteria were incubated overnight on their specific liquid medium (Table 1) and, after washed in PBS, were adjusted to approximately 1×10^7 CFU/mL in MHB supplemented with 10% of FBS. Bacteria samples were diluted (1:2) in type 1 water and placed into clear disposable folded capillary cells (DTS1070, Malvern). ξ-potential was determined using the ELS described above in section 2.1.2.

2.2.3. NLC bactericidal activity on different bacteria

All bacteria were incubated overnight on specific liquid medium (Table 1) at 37ºC and 150 rpm. After washing (3000*g*, 5 min) with phosphate buffered saline (PBS 1x, pH 7.4), bacteria concentration was adjusted to approximately 1×10^7 CFU/mL in Müeller-Hinton broth medium (MHB, Merck Millipore, Germany), recommended medium for the determination of minimal inhibitory concentration (MIC), according to guidelines recognized by CLSI (Clinical & Laboratory Standards Institute) and EUCAST (European Society of Clinical Microbiology and Infectious Diseases) organizations [25]. As *H. pylori* is a fastidious microorganism which requires a complex nutrient-rich growth media [26], the MHB medium was supplemented with 10% of FBS. *H. pylori* was also tested in its specific medium BB+10% FBS [27].

Different concentrations of unloaded-NLC (0%, 1.25%, 2.5% and 5% v/v) were added to each bacteria suspension and incubated at 37ºC and 150 rpm. A sample of each bacterial culture was collected at different time-points (0, 3, 6, 9, 12, 15, 24 h), serially diluted and plated on specific solid medium plates (Table 1). Plates were incubated at 37ºC for 5 days for *H. pylori*, 2 days for *L. casei* and 24 h for the other bacteria. The number of viable bacteria per mL was determined by colonies forming unit (CFU) counting.

Table 1- Bacteria used in this study: characteristics and specific media used in their growth.

Microorganism	Solid medium		Liquid medium		Ref.
	Medium composition	Growth conditions	Medium composition	Growth conditions	

Helicobacter pylori (J99[1])	• Blood agar base 2 (Oxoid, France)
	• Defibrinated horse blood (10%) (Probiológica, Portugal)
	• Antibiotics-cocktail (0.2%) (Sigma-Aldrich):
	  • 0.155 g/L Polymixine B
	  • 6.25 g/L Vancomycin
	  • 1.25 g/L Amphotericin B
	  • 3.125 g/L Trimethroprim
		48 h in spots
		48 h in spread
		Static
		37ºC
		Microaerophilic conditions
			• Brucella Broth medium (BB, Oxoid, France)
			• Fetal Bovine Serum (10%) (FBS, Gibco, USA)
				Overnight (OD 0.1)
				150 rpm
				37ºC
				Microaerophilic conditions
					[23]

Lactobacillus casei-01[2]	• De Man-Rogosa and Sharpe agar (MRS agar, Biokar, France)	48 h in spread Static 37ºC Aerobic conditions	• De Man-Rogosa and Sharpe broth (MRS broth, Biokar, France)	Overnight (1 colony) 150 rpm 37ºC Aerobic conditions	[45]
Escherichia coli (ATCC® 25922™)	• Tryptic Soy Agar (TSA, Merck Millipore, Germany)	24 h in spread Static 37ºC Aerobic conditions	Tryptic Soy Broth (TSB, Merck Millipore, Germany)	Overnight (1 colony) 150 rpm 37ºC Aerobic conditions	[46]
Staphylococcus epidermidis (ATCC® 35984™)					
Methicillin-resistant *Staphylococcus aureus* (ATCC® 33591™; MRSA)					

Note: [1] *H. pylori* J99 strain provided by Department of Medical Biochemistry and Biophysics, Umeã University, Sweden; [2] *Lactobacillus casei-01* provided Chr. Hansen, Hørsholm Denmark.

2.2.4. NLC interaction with *H. pylori*

According to results obtained, *H. pylori* J99 (1×10^7 bacteria/mL, OD 0.03, BB+10%FBS medium) were incubated with NLC (1.25%v/v) under microaerophilic conditions, 37ºC and 150 rpm.

2.2.4.1. Imaging flow cytometry

NLC were previously stained with coumarin-6 (0.1% w/v, Sigma-Aldrich) and incubated according to conditions described above (section 2.2.4). At time-points 1.5, 3 and 12 h, bacteria were washed in PBS (3000 *g*, 5 min) and fixed with paraformaldehyde (4% w/v) in PBS for 30 min. To label *H. pylori DNA,* bacterial suspensions were incubated with propidium iodide (0.1 µg/mL) for 30 min at room temperature, in the dark (unstained negative controls were also prepared). Before running in the imaging flow cytometer (ImageStream$^{X®}$, Amnis, EDM Millipore, Darmstadt, Germany), samples were filtered through a mesh filter (70 µm). Images were acquired using the INSPIRE^{TM} software v4.0 (Amnis, EDM Millipore, Darmstadt, Germany). For each sample, 150000 events were collected and two independent experiments were performed including a brightfield image (Channel 1, 420-480 nm), a green fluorescence image corresponding to coumarin-6 (Channel 2, 480-560 nm), and an orange fluorescence image matching the propidium iodide fluorescence emission (Channel 4- 560-595 nm). Data was analyzed using the IDEAS® software (Amnis, EDM Millipore, Darmstadt, Germany, version 6.2.64.0), quantifying the intensity of the coumarin-6 labeling (fluorescence intensity on channel 2) for every bacteria. Bacterial debris and aggregates were limited by setting the area in channel 1 between 2 and 10 μm^2, and the interest region was limited to the area of fluorescence positive signal in channel 2. Control samples without coumarin-6 labeling were run in the same conditions in the imaging flow cytometer to define the positive coumarin-6 signal.

2.2.4.2. Scanning Electron Microscopy (SEM)

H. pylori J99 strain was incubated with NLC (1.25%v/v) in the conditions described above (section 2.2.4). At time-points 3 and 12 h, samples were washed in PBS (3000 *g*, 5 min). The pellet of bacteria was fixed in glutaraldehyde (2.5%; Merck) in sodium cacodylate buffer (0.14 M, Merck) for 30 min at room temperature. Fixed bacteria adhered on glass coverslips during 2 h at room temperature. Then, samples were dehydrated with an increasing ethanol/water gradient (50% v/v to 99% v/v) and subjected to critical point drying (CPD 7501, Poloran). Finally, the samples were sputter-coated with gold/palladium film over 30 s. *H. pylori* samples were observed by scanning electron microscopy (SEM; JEOL JSM-6310F), at magnification 30000 and 60000x.

2.2.4.3. Transmission Electron Microscopy (TEM)

Gold nanoparticles (500 µL, Gold-NP, 10 nm, BBI Solutions, UK) were encapsulated into NLC according to the same NLC production method described in section 2.1.1. *H. pylori* J99 strain was incubated with 1.25% v/v Gold-NP-loaded NLC for 3 and 12 h, in the conditions described above (section 2.2.4).The pellet was fixed by resuspending in a mixture of paraformaldehyde (4% w/v, Merck) with glutaraldehyde (2.5% v/v, Merck) in 0.14M sodium cacodylate buffer (0.14 M, pH 7.4 Merck). Samples were then washed with sodium cacodylate buffer, centrifuged and bacterial pellet post-fixed in 2% osmium tetroxide (Electron Microscopy Sciences, UK) in sodium cacodylate buffer was embedded in a HistoGel (Thermo Scientific, USA) and processed in Epon resin (Electron Microscopy Sciences, UK). Ultrathin sections of 50 nm thickness were performed using an Ultramicrotome (RMC PowerTome PC model), by using diamond knives (Diatome, USA). Sections were mounted on formvar-coated nickel grids, stained with uranyl acetate and lead citrate (Delta Microscopies, France) and examined using TEM (JEOL JEM 1400 transmission electron microscope; Tokyo, Japan) equipped with a CCD digital camera Orious 1100 W.

2.2.4.4. Atomic Force Microscopy (AFM)

H. pylori J99 strain was incubated with NLC (1.25%v/v), for 3 and 12 h, in the conditions described above (section 2.2.4). Bacteria were fixed in glutaraldehyde (2.5% v/v, Merck) in sodium cacodylate buffer (0.14 M, Merck) for 30 min at room temperature. Fixed bacteria were adhered on glass bottom microwell dishes (MatTek Corporation USA) during 2 h at RT and dehydrated with an increasing ethanol/water gradient (50% v/v to 99% v/v). The samples underwent drying at RT, overnight.

Atomic Force Microscopy (AFM) images were obtained using the same equipment described in section 2.1.3. Briefly, all measurements were performed in Contact mode at RT. A V-shaped cantilever with a triangular silicon tip (AppNano, USA) was calibrated using the Thermal K tune method provided by PicoView 1.2 software, resulting in a spring constant value of 0.046 N/m. Scan speeds were set at 1.0 l/s, and scan sizes were taken within an interval range among 1.4 µm and 7.0 µm. The contact force used was 4.6 nN. The height profile measurements were obtaining using the Gwydion 2.36 software version using the full width at half height (FWHH) method.

2.3. Statistical analysis

Data are reported as mean ± standard deviation. Data from different groups were compared

statistically using non-parametric Kruskal-Wallis test. Analysis was performed with a significance level of 0.05 using Graph Pad Prism 6.0 (Graph-Pad Software, La Jolla, USA).

3. Results

3.1. NLC production and characterization

NLC were successfully produced by hot homogenization and ultrasonication without the use of organic solvents. AFM images revealed that NLC are spherical and not aggregated (Figure 1A). DLS and ELS characterization demonstrated their negative charge (around -28 mV) and diameter around 211 nm (Figure 1B). Moreover, the low polydispersion index (around 0.20) indicates an almost monodisperse distribution.

A

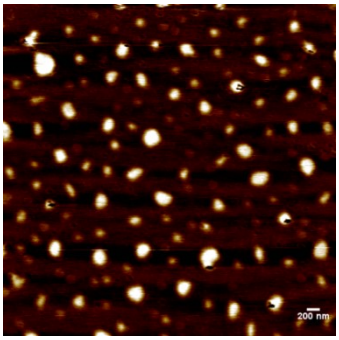

B

Diameter (nm)	211 ± 8
Polydispersion index	0.20 ± 0.02
ξ-potential (mV)	-28 ± 3

Figure 1- Nanostructured lipid carriers (NLC) characterization. (A) NLC visualized by Atomic Force Microscopy (AFM) (scale bar 200 nm) **(B)** NLC diameter, polydispersion index and ξ-potential determined by DLS at 37ºC. Data are reported as the mean ± standard deviation of 3 independent experiences.

3.2. Bacterial characterization (zeta potential)

Bacteria ξ-potential indicated that, in the conditions used during bactericidal assays, all bacteria were negatively charged (Table 2) having *E. coli* and *S. epidermidis* the most negative surface charge and *L. casei-01* the less negative surface charge (almost neutral).

Table 2- Principal features of bacteria used: *H. pylori, L. casei, E.coli, S. epidermidis* and MRSA.

	Helicobacter pylori **(J99)**	***Lactobacillus casei*-01**	***Escherichia coli*** **(ATCC® 25922™)**	***Staphylococcus epidermidis*** **(ATCC® 35984™)**	**MRSA (ATCC® 33591™)**
Characteristics	Gram-negative, spiral-shaped, microaerophilic	Gram-positive, rod-shaped, facultative anaerobic or microaerophilic	Gram-negative, rod-shaped, facultative anaerobic	Gram-positive, coagulase-negative cocci, aerobic	Gram-positive, coagulase-negative cocci, facultative aerobe,
Most common Local (Human)	Stomach	Intestine and mouth	Intestine	Skin	Skin, nose and respiratory tract
Associate Disease	Gastric disorder: gastritis to gastric cancer	Used a probiotic Some of the cases sepsis, meningitis, and infections localized in organs	Cholecystitis, bacteremia, urinary tract infection, traveler's diarrhea	Intravascular devices such as prosthetics, catheter; septicemia and endocarditis	Skin infections and sepsis to pneumonia to bloodstream infections
Zeta potential (mV) *	-17.3 ± 0.7	-2.4 ± 0.2	-30.0 ± 1.2	-31.1 ± 1.6	-19.9 ± 1.3

* ξ-potential measured in Müller-Hinton Broth medium (pH 7) using ZetaSizer® (n=3).

3.3. NLC antimicrobial proprieties

Bactericidal activity of developed nanoparticles was evaluated by following bacteria growth over 24 h in MHB medium supplemented with 10% FBS containing different NLC concentrations (0, 1.25, 2.5 and 5% v/v) (Figure 2). Minimal bactericidal concentration (MBC) is the minimal drug concentration to kill 99.9% (≥3 logs) bacteria in 24 h of incubation. Figure 2A e 2B shows that these NLC are bactericidal against *H. pylori* J99 in all concentrations tested since after 24 h all bacteria are death. However, *H. pylori* dead rate was NLC concentration-dependent. Figure 2A shown that with specific *H. pylori* medium (BB+10% FBS), a bactericide activity after 12 h was observed with the lowest concentration tested (1.25%v/v). However, a slight delay in bactericide activity with MHB+10%FBS was observed, for the highest NLC concentration tested (5%v/v), *H. pylori* were killed after 12 h, and for lower NLC concentrations (1.25% and 2.5%), a reduction of 99.9% (>3log) was observed after 15 h (Figure 2B). Nonetheless, an inhibitory effect of 50% (> 1log) was detected after 9 h incubation with any NLC concentration tested (Figure 2B).

NLC bactericidal effect was also evaluated against other bacteria, namely the gut bacteria *L. casei-01* (Figure 2C*)* and *E. coli* (Figure 2D), and the infectious bacteria, *S. epidermidis* (Figure 2E*)* and *S. aureus* (Figure 2F). It was demonstrated that NLC are not bactericidal against *L. casei-01*, *E. coli,* and *S. epidermidis* at all concentrations tested. However, NLC was able to delay *S. aureus* growth when used in high concentrations (5% v/v) (Figure 2F).

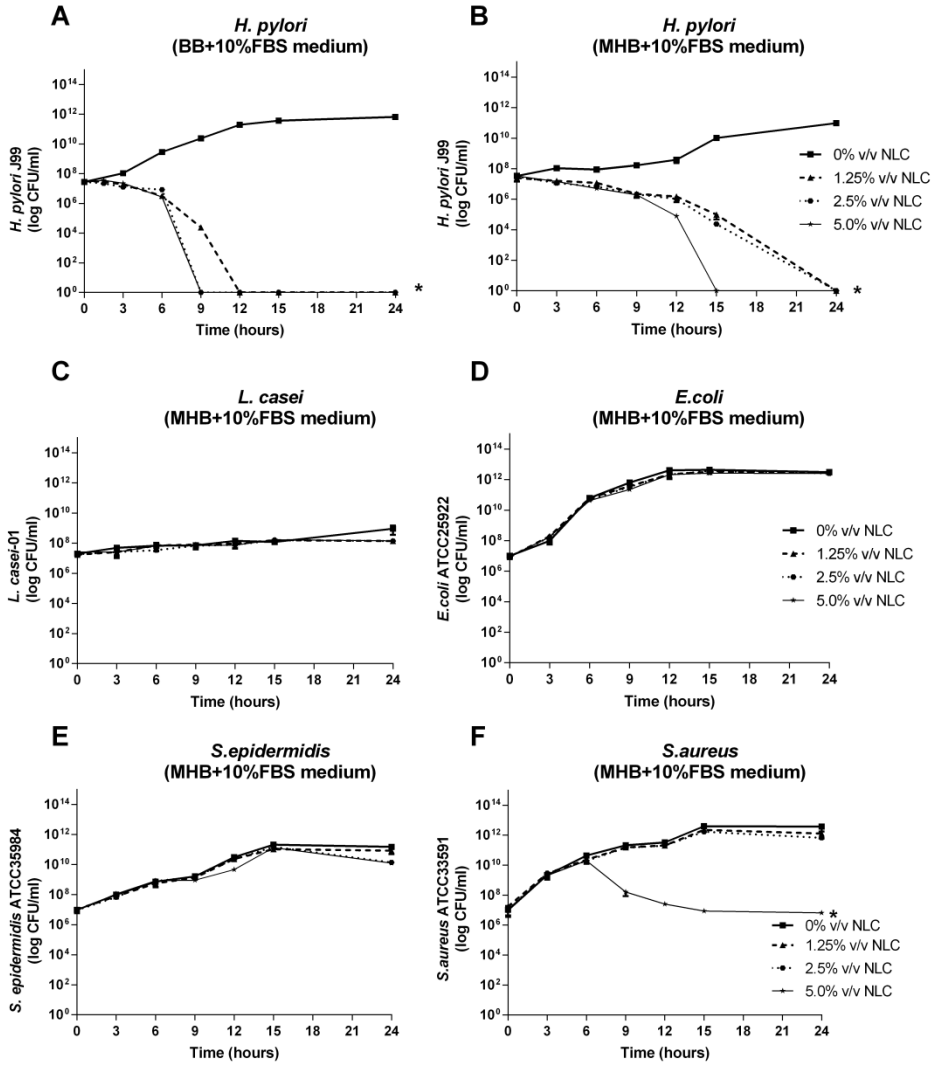

Figure 2- Antibacterial activity of NLC on different bacteria. Bacteria growth in the presence of increasing concentrations of NLC in Brucella Broth supplemented with 10%FBS **(A)** *H. pylori* J99 and in Müller-Hinton broth supplemented with 10% FBS **(B)** *H. pylori* J99, **(C)** *L. casei-01*, **(D)** *E. coli* ATCC™25922, **(E)** *S. epidermidis* ATCC™35984, **(F)** *S. aureus* ATCC™33591. Numerical data is reported as mean ± standard deviation (n=3).* $p<0.05$; statically differences between bacteria treated with NLC and untreated (bacteria with 0% v/v NLC) (Kruskal-Wallis test).

3.4. NLC interaction with *H. pylori*

In order to understand NLC mechanism of action against *H. pylori*, different advanced imaging techniques, namely ImageStream$^{X®}$, SEM, TEM, and AFM were used. Assays were performed in BB medium supplemented with 10% FBS (the best medium for *H. pylori* growth) incubating with NLC at 1.25%. This NLC concentration was chosen due to its high bactericidal effect despite low cytotoxicity towards gastric cells, as previously described [23].

Figure 3 shows ImageStream$^{X®}$ results of *H. pylori* J99 after incubation with fluorescence green-labeled NLC (1.25% coumarin-labeled NLC) for 1.5, 3 and 12 h. These time-points were chosen in order to have samples where most of the bacteria are cultivable (1.5 and 3 h) and samples where all bacteria are dead (12 h) (Figure 2A). After 1.5 h, 99% bacteria are fluorescence green-labeled demonstrating the high affinity of NLC to *H. pylori*. Nevertheless, NLC bactericidal effect was only observed after 12 h incubation, since after 1.5 h and 3h, 99% and 70% bacteria were alive, respectively.

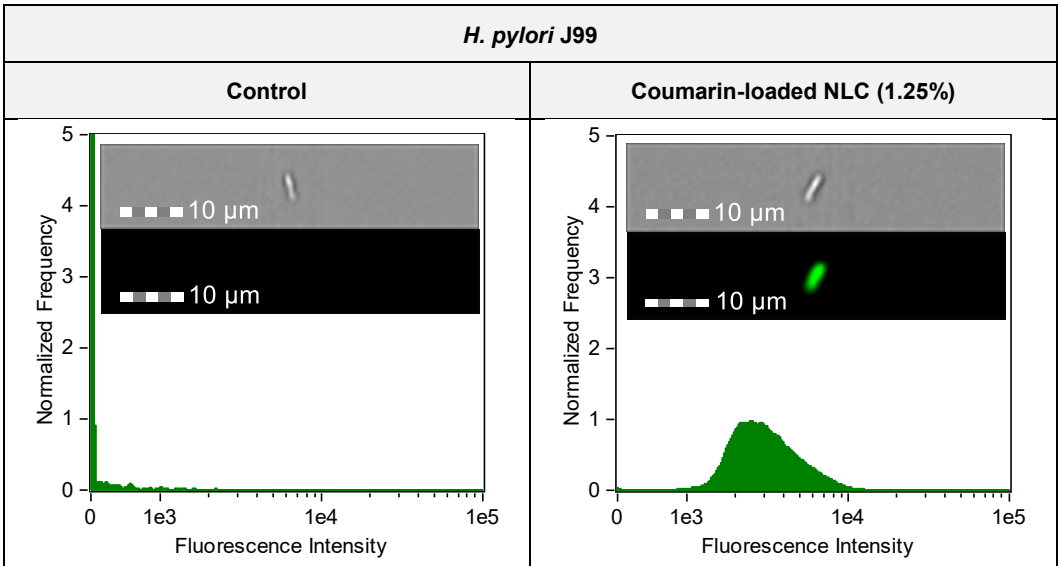

Time (hours)	NLC-labeled *H. pylori* (%) *ImageStream$^{X®}$*	Viable *H. pylori* (%) *CFU*	NLC-labelled *H. pylori (%)* *ImageStream$^{X®}$*	Viable *H. pylori* (%) *CFU*
1.5	**0**	**100**	**99**	**99**
3	**0**	**100**	**99**	**70**
12	**0**	**100**	**100**	**0**

Figure 3- NLC interaction with *H. pylori* membrane after 1.5, 3 and 12 hours incubation with coumarin-labelled NLC (1.25%) determined by imaging flow cytometry (ImageStream$^{X®}$). Representative histogram and *H. pylori* images in brightfield (Channel 1, 420-480 nm) and in green fluorescence corresponding to bacteria with adherent coumarin-6 labeled NLC (Channel 2, 480-560 nm) after 1.5 h of incubation. Scale bar represents 10 µm. Table describing percentages of green fluorescence bacteria quantified by flow cytometry and the correspondent viable bacteria quantified by CFU counting, after 1.5, 3 and 12 h of *H. pylori* exposure to NLC.

SEM images (Figure 4) revealed that when growing in the absence of NLC (control), bacteria present their characteristic bacillus shape (Figure 4A and 4C) and no morphological changes

were detected in most *H. pylori* after 3 h incubation with NLC (Figure 4B). However, after growing during 12 h in contact with NLC, most bacteria suffer a disruption of parts of their membrane although maintaining the bacillar shape (Figure 4D).

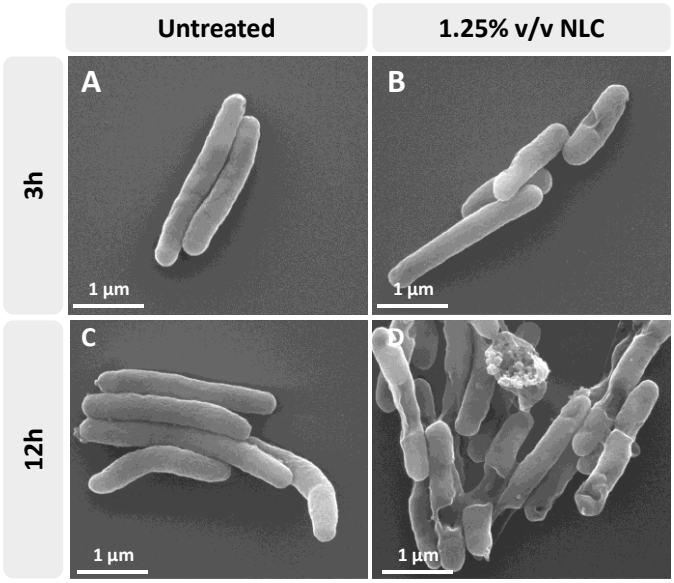

Figure 4. *H. pylori* morphology. Scanning Electron micrographs of *H. pylori* untreated and treated with 1.25% v/v of NLC for 3 (**A** and **B**) and 12h (**C** and **D**) respectively. Scale bar in the SEM image represents 1 µm.

TEM images also show *H. pylori* J99 with intact membrane and dense cytoplasm when bacteria grew in the absence of NLC (controls) (Figure 5A and 5D). After 3 h growing with 1.25% NLC (Figure 5B), *H. pylori* maintained their intact membrane and dense cytoplasm as observed in controls, although Gold-NP-loaded NLC were visualized in their periplasmatic space (red arrows at Figure 5C). After 12 h incubation with this NLC concentration, bacteria display a separation between the outer and inner membrane with loss of cytoplasmic contents (Figure 5E). At this time-point, Gold-NP-loaded NLC were observed inside bacteria, namely at their cytoplasm (red arrows at Figure 5F).

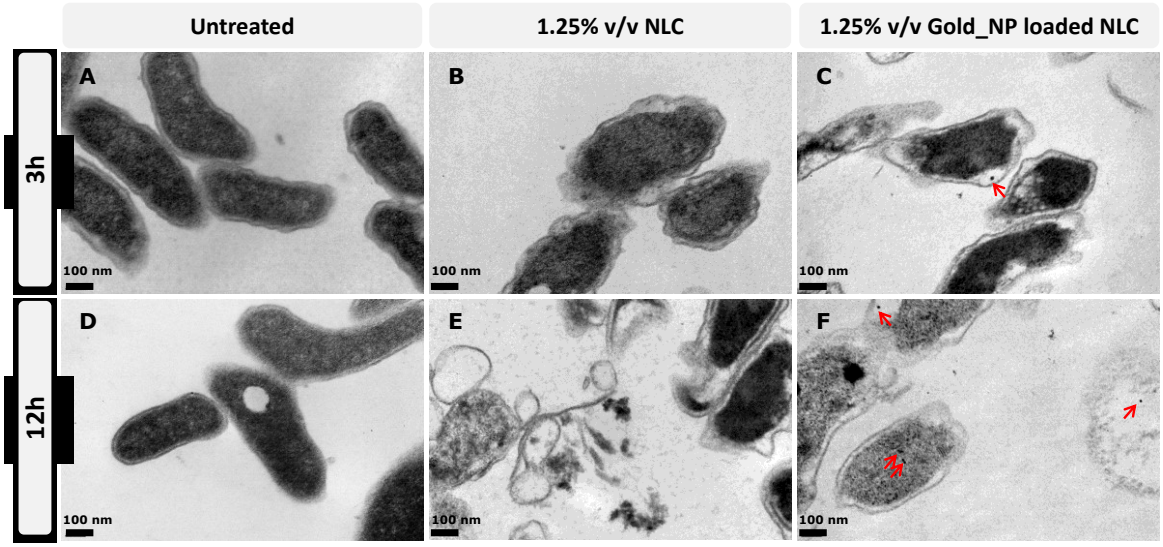

Figure 5- Transmission Electron micrographs of *H. pylori* J99 incubated with NLC (**B** and **E**) and Gold-NP-loaded NLC(**C** and **F**) for 3 and 12 h, respectively. Untreated *H. pylori* J99 were used as control at the same time-points (A and D). Red arrows point to Gold nanoparticles (Gold_NP). Scale bar in the SEM image represents 100 nm.

AFM was used to identify changes in bacteria morphology of *H.* pylori J99 upon NLC treatment. Figure 6 shows AFM deflection images of *H. pylori* in bacillus shape after 3 and 12 h growing in the absence (6A and 6B, respectively) and the presence of 1.25% NLC (6C and 6D, respectively) in the medium. Although in a bacillary shape, when incubated for 12 h with NLC, the wall of *H. pylori* is not uniform along their length (Figure 6D).

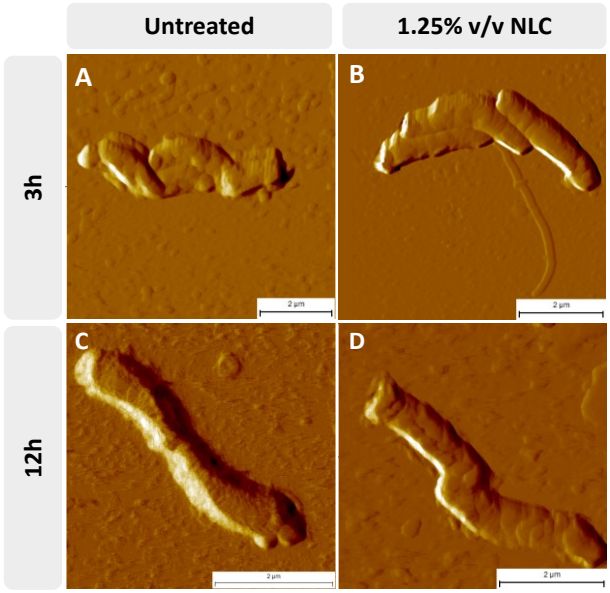

Figure 6- AFM deflection images of *H. pylori* J99 incubated with 1.25% v/v of NLC for 3 (**B**) and 12 (**D**) hours. Untreated *H. pylori* J99 were also tested at 3 (**A**) and 12 (**C**) hours. Scale bar in the AFM image represents 2 µm.

The height of untreated bacteria was ~214 nm in all the bacteria length, while the height of treated bacteria with 1.25% NLC suffered a reduction of height ~200nm and a hole can be observed with a bacteria height of ~160 nm (Table 3). Nevertheless, the number of *H. pylori*-treated, found in AFM samples prepared using *H. pylori* that grew with NLC for 12h, was very low and most of the adhered bacteria were completely lysed, with their cytoplasmic content spread on the surface (Petri dish), although maintaining their bacillary shape (Figure S1).

Table 3- AFM topographic image of *H. pylori* J99 after growing during 12 h with NLC (1.25%). The height measurements of two selected cross-section of *H. pylori* J99 untreated and treated with 1.25% v/v of NLC over 12 h. Scale bar of AFM topography image represents 2 µm.

	2D topography	3D topography	Height (nm)	
			Section 1	Section 2
Untreated	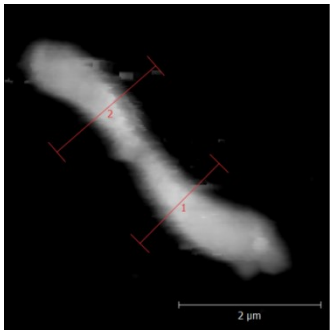	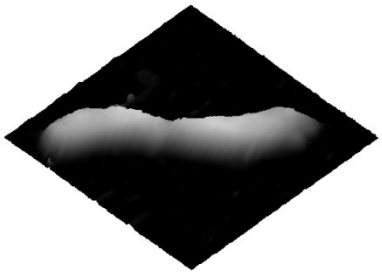	214	213
Treated with 1.25% unloaded-NLC	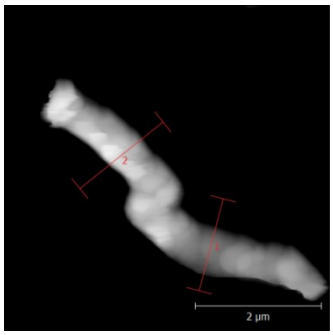	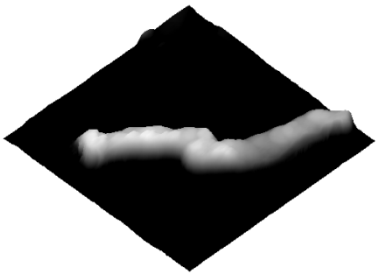	160	200

4. Discussion

NLC are a relatively new class of drug nanocarriers (100-400 nm) developed for the incorporation of lipophilic drugs. These nanoparticles present low cytotoxicity since are composed by FDA approved biodegradable and biocompatible lipids [14,15,28]. Moreover, they

are produced without organic solvents. Concerning infection treatments/prevention, NLC have been used for the encapsulation of different antibiotics, peptides and natural compounds with activity against several bacteria, namely *S. aureus, Pseudomonas aeruginosa, E. coli* and *Propionibacterium acnes* [16-21].

We previously demonstrated that the bactericidal effect of docosahexaenoic acid (DHA) against *H. pylori* was improved after its NLC encapsulation [23]. However, we verified that unloaded-NLC (with diameter ~211 nm and a negative charge around -28 mV) were also bactericidal against *H. pylori* J99 (human strain) and SS1 (mouse-adapted strain) although at a slower rate than DHA-loaded NLC [23]. This direct bactericidal effect of unloaded-NLC was not expected and justifies further investigation, namely regarding its effect in other bacteria.

To investigate their selectivity against *H. pylori*, NLC were tested against other bacteria that present different morphological characteristics regarding shape (rod *vs* spherical), membrane structure (Gram-positive *vs* Gram-negative) and surface charge (from -2mV to -30 mV). Assays were performed following bacteria growth over 24 h using Müller-Hinton Broth (MHB) medium, which is the recommend medium for determination of the minimal inhibitory concentration (MIC) according to the guidelines recognized by CLSI (Clinical & Laboratory Standards Institute) and EUCAST (European Society of Clinical Microbiology and Infectious Diseases) organizations [25]. However, since *H. pylori* is a fastidious microorganism that requires a complex nutrient-rich growth media, the MHB medium was supplemented with 10% of fetal bovine serum (FBS) [26]. Therefore, for comparative studies between bacteria, all antimicrobial assays were performed using MHB supplemented with 10% FBS. In this medium, NLC bactericidal activity against *H. pylori* J99 was similar to Brucella Broth medium (BB) also supplemented with 10% FBS (Figure 2A), the recommended medium for *H. pylori* culture [27]. However, a slight delay in the bactericidal activity of NLC was observed with MHB+10%FBS medium. NLC did not affect the growth of other bacteria tested, except in *S. aureus,* where NLC at 5% was able to decrease bacteria growth after 6 h, although without a bactericidal effect. Nevertheless, NLC concentration as high as 5% v/v was previously associated with some cytotoxicity (~50%) in human gastric adenocarcinoma cells [23].

Thus, this specific bactericidal effect of NLC against *H. pylori* cannot be explained by differences in bacteria morphology and surface charge, but rather through *H. pylori* specific features. *H. pylori* has specific and unique characteristics that are very different from all the other bacteria. To be able to colonize human gastric mucosa and to survive in the adverse environment of host stomach, *H. pylori* present several structural and morphological characteristics that favor their penetration through the mucus layer, namely their flagella and their spiral form [29]. This spiral morphology needs a less rigid cell envelope than other non-spiraled bacteria. This fact could be related to the composition of their peptidoglycan and cell membranes that differ substantially from other bacteria. Their peptidoglycan has a unique and less complex muropeptides composition than other Gram-negative bacteria. It contains a high proportion of muropeptides, with a pentapeptide side chain ending in glycine and containing anhydro-N-acetylmuramic acid, which is very different than *E. coli [30]*. Concerning their

membrane composition, *H. pylori* have an unusual fatty acid profile and have glycosylated cholesterol which is a unique characteristic of *Helicobacter* sp.[30]. According to literature, *H. pylori* steal host cholesterol, modifies it by alpha-glycosylation and incorporates it into its surface to resist multiple stresses [31]. *H. pylori* lipopolysaccharides (LPS), is also an important component of the wall of *H. pylori* that differs substantially from other bacteria. *H. pylori* LPS are composed by an unusual cellular fatty acid, lipid profile and molecular mimicry of Lewis antigens[30,32]. The lipid A component of *H. pylori* LPS is different of lipid A of many bacterial species by the absence of 3-hydroxytetradecanoic (β-hydroymyristic) acid [14:0(3-OH)], as well as the underphosphorylation and underacylation of the lipid A [33]. Moreover, the core oligosaccharide of *H. pylori* strains exhibit an unusual conformation, compared with other bacterial species. A branching occurs from the D-*glycerol*-D-*manno*-heptose (DD-Hep) residue in the inner core through a second such a residue to which the first repeating unit of the O-polysaccharide chain is attached [33]. Additionally, *H. pylori* have several adhesins on its outer membrane to bind specific glycosylated compounds found in gastric mucosa [34]. Periplasmic pH homeostasis of *H. pylori* contrasts with the patterns in *E. coli* and other Gram-negative bacteria. The periplasmic pH is thought to be in equilibrium with the medium and not regulated in concert with the cytoplasm. *H. pylori* express the highest level of urease of any known microorganism, a key component of periplasmic pH homeostasis, thus elevating the pH to neutral as necessary for its survival [35]. The production of urease by the bacterium results in the production of ammonia, maintaining periplasmic and cytoplasmic pH of the bacterium near to neutral even in the presence of acid shocks [29,36].

Nanoparticles that have been designed to directly interact with bacteria are usually cationic in order to bind any bacteria via electrostatic interactions, since pathogenic bacteria have a negative surface charge under physiological conditions [37]. These NLC are negatively charged so, their interaction with bacteria via electrostatic interactions is not expected. In addition, all the individual compounds used in NLC production (Tween®60, Miglyol®812 and Precirol®ATO5) are not bactericidal at concentrations used [23,38-40] demonstrating that the bactericidal effect is related with nanoparticle 3D format.

In order to understand NLC mechanism of action against *H. pylori*, different bioimaging techniques were applied. These assays were performed using NLC at 1.25% and *H. pylori* J99 cultured in BB medium supplemented with 10% FBS, recommended medium for *H. pylori* growth. In these conditions, NLC were bactericidal against *H. pylori* in 12h. Studies using ImageStream$^{X®}$ revealed the high binding affinity of NLC to *H. pylori* membrane since, after 1.5h in contact with fluorescent labeled NLC, all bacteria were fluorescent labeled. However, their bactericidal effect was only observed after 12h, demonstrating that this bactericidal process although being concentration-dependent is also time-dependent.

TEM studies using Gold-NP-loaded NLC showed that NLC can be internalized by *H. pylori* in a time-dependent process. After 3 h, NLC were found in bacterial periplasmic space and after 12 h in the cytoplasm showing their ability to cross both membranes of *H. pylori*. TEM images also revealed a separation between the outer and cytoplasmic membrane of *H. pylori* after 3 and 12

h incubation with NLC. A leakage of bacterial cytoplasmic content and a decrease in bacteria thickness (AFM) was also observed using SEM and AFM. Nevertheless, although these morphological alterations, bacteria maintained their typical bacillary shape. These results suggest that after their physically binding to *H. pylori* surface, NLC are able to cross both bacterial plasma membranes destabilizing them or creating pores in their structure which allow cytoplasmic leakage without destroying bacteria wall.

The non-visualization of *H. pylori* in coccoid shape, as observed in other studies when bacteria were exposed to a hostile environment [41], can support the idea that the binding process NLC-*H. pylori* is fast not allowing their morphological transition. Similar *H. pylori* morphological changes were described by Jung *et al* (2015) for liposome containing linolenic acid [42]. Their bactericidal effect was explained by liposomal fusion into *H. pylori* outer membrane allowing the incorporation of linolenic acid in the membrane and thus affecting their permeability due to the alteration of the phospholipid composition. Interestingly, these liposomal have negative zeta-potential (-73 ± 2 mV), like our NLC, Their negative charge did not avoid their integration/fusion into the bacteria membrane. Moreover, although negatively charged, NLC have on their surface the hydrophilic moiety of the non-ionic surfactant (Tween®60) used during the production as a nanoparticle stabilizer. This non-ionic surfactant may decrease the surface tension between nanoparticle and bacteria enabling their interaction with proteins and lipids of *H. pylori* membrane [43]. NLC surface surfactant can also facilitate their interaction/travel through *H. pylori* LPS since Gram-negative bacteria only allows a limited diffusion of hydrophobic substances through their LPS-covered surface [44]. Moreover, NLC lipid composition may also allow the insertion of NLC into the bacterial membrane, causing an excessive enhance of membrane fluidity and it to become more permeable, allowing internal contents to leak from the cell and consequently bacteria death. Notwithstanding, the surfactant effect may solubilize sections of the cell membrane, which may cause cytoplasm leakage and consequently cell lysis.

This specific NLC bactericidal activity against *H. pylori* is an advantage for the development of new and alternative therapies for *H. pylori* infection since, in opposite to the antibiotic therapy; it will not affect human microbiota.

Acknowledgments

This work was financed by FEDER funds through the COMPETE 2020 (POCI), Portugal 2020. FCT/MCTES through the projects: POCI-01-0145-FEDER-007274; PYLORIBINDERS (PTDC/CTM-BIO/ 4043/2014); PYLORICIDAL (PTDC/CTM-BPC/121149/2010), NORTE-01-0145-FEDER-000012 and FCT grant SFRH/BD/89001/ 2012.

DLS, ELS, and AFM have performed at BN-Biointerfaces and Nanotechnology unit facility; imaging flow cytometry at b.IMAGE-Bioimaging Center for Biomaterials and Regenerative Therapies , TEM at HEMS – Histology and Electron Microscopy Service Unit facility. All of these unit facilities are located at i3S-*Instituto de Investigação e Inovação em Saúde da Universidade do Porto (www.i3s.up.pt/research/scientific-platforms)*. SEM studies were performed at the CEMUP- *Centro de Materiais da Universidade do Porto* unit facility (http://www.cemup.up.pt)

The authors thank Prof. Manuela Pintado (Universidade Católica do Porto, Portugal) for providing the *Lactobacillus casei-01* strain; and Prof. Thomas Boren (Umeã University, Sweden) for providing the *H. pylori* J99 strain.

Appendix A. Supplementary data

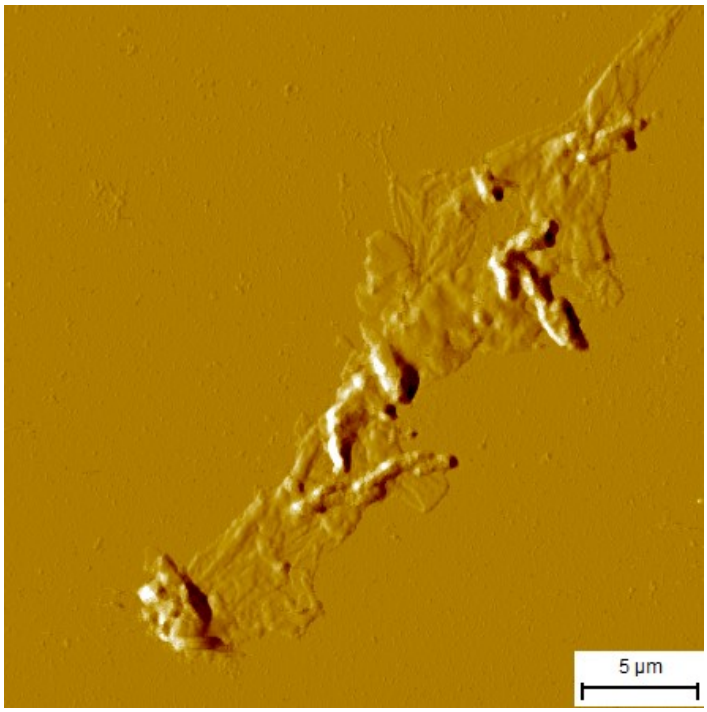

Figure S1- AFM deflection image of *H. pylori* J99 incubated with 1.25% v/v of NLC for 12 h. Scale bar in the AFM image represents 5 µm

References

1. Correa P, Houghton J (2007) Carcinogenesis of Helicobacter pylori. Gastroenterology 133: 659-672.

2. Amieva M, Peek Jr RM (2016) Pathobiology of Helicobacter pylori–Induced Gastric Cancer. Gastroenterology 150: 64-78.

3. Matysiak-Budnik T, Mégraud F (2006) Helicobacter pylori infection and gastric cancer. European Journal of Cancer 42: 708-716.

4. IARC (2014) *Helicobacter pylori* Eradication as a Strategy for Preventing Gastric Cancer.; Group I*Hp*W, editor. Lyon, France: International Agency for Research on Cancer.

5. Ferlay J, Soerjomataram I, Dikshit R, Eser S, Mathers C, et al. (2015) Cancer incidence and mortality worldwide: sources, methods and major patterns in GLOBOCAN 2012. Int J Cancer 136: E359-386.

6. Correa P (2013) Gastric Cancer: Overview. Gastroenterology Clinics of North America 42: 211-217.

7. Vakil N (2006) *Helicobacter pylori* treatment: a practical approach. Am J Gastroenterol 101: 497-499.

8. Poonia N, Kharb R, Lather V, Pandita D (2016) Nanostructured lipid carriers: versatile oral delivery vehicle. Future Science OA 2: FSO135.

9. Beloqui A, Solinis MA, Delgado A, Evora C, Isla A, et al. (2014) Fate of nanostructured lipid carriers (NLCs) following the oral route: design, pharmacokinetics and biodistribution. J Microencapsul 31: 1-8.

10. Beloqui A, Solinis MA, Rodriguez-Gascon A, Almeida AJ, Preat V (2016) Nanostructured lipid carriers: Promising drug delivery systems for future clinics. Nanomedicine 12: 143-161.

11. Martins S, Sarmento B, Ferreira DC, Souto EB (2007) Lipid-based colloidal carriers for peptide and protein delivery--liposomes versus lipid nanoparticles. Int J Nanomedicine 2: 595-607.

12. Carbone C, Leonardi A, Cupri S, Puglisi G, Pignatello R (2014) Pharmaceutical and biomedical applications of lipid-based nanocarriers. Pharm Pat Anal 3: 199-215.

13. Battaglia L, Gallarate M (2012) Lipid nanoparticles: state of the art, new preparation methods and challenges in drug delivery. Expert Opinion on Drug Delivery 9: 497-508.

14. Müller RH, Mäder K, Gohla S (2000) Solid lipid nanoparticles (SLN) for controlled drug delivery – a review of the state of the art. European Journal of Pharmaceutics and Biopharmaceutics 50: 161-177.

15. Muller RH, Shegokar R, Keck CM (2011) 20 years of lipid nanoparticles (SLN and NLC): present state of development and industrial applications. Curr Drug Discov Technol 8: 207-227.

16. Boge L, Bysell H, Ringstad L, Wennman D, Umerska A, et al. (2016) Lipid-Based Liquid Crystals As Carriers for Antimicrobial Peptides: Phase Behavior and Antimicrobial Effect. Langmuir 32: 4217-4228.

17. Garcia-Orue I, Gainza G, Girbau C, Alonso R, Aguirre JJ, et al. (2016) LL37 loaded nanostructured lipid carriers (NLC): A new strategy for the topical treatment of chronic wounds. European Journal of Pharmaceutics and Biopharmaceutics 108: 310-316.

18. Lin CH, Fang YP, Al-Suwayeh SA, Yang SY, Fang JY (2013) Percutaneous absorption and antibacterial activities of lipid nanocarriers loaded with dual drugs for acne treatment. Biol Pharm Bull 36: 276-286.

19. Manea A-M, Vasile BS, Meghea A (2014) Antioxidant and antimicrobial activities of green tea extract loaded into nanostructured lipid carriers. Comptes Rendus Chimie 17: 331-341.

20. Moreno-Sastre M, Pastor M, Esquisabel A, Sans E, Viñas M, et al. (2016) Pulmonary delivery of tobramycin-loaded nanostructured lipid carriers for *Pseudomonas aeruginosa* infections associated with cystic fibrosis. International Journal of Pharmaceutics 498: 263-273.

21. Sans-Serramitjana E, Fusté E, Martínez-Garriga B, Merlos A, Pastor M, et al. (2016) Killing effect of nanoencapsulated colistin sulfate on *Pseudomonas aeruginosa* from cystic fibrosis patients. Journal of Cystic Fibrosis 15: 611-618.

22. Correia M, Michel V, Matos AA, Carvalho P, Oliveira MJ, et al. (2012) Docosahexaenoic Acid Inhibits *Helicobacter pylori* Growth In Vitro and Mice Gastric Mucosa Colonization. PLOS ONE 7: e35072.

23. Seabra CL, Nunes C, Gomez-Lazaro M, Correia M, Machado JC, et al. (2017) Docosahexaenoic acid loaded lipid nanoparticles with bactericidal activity against *Helicobacter pylori*. International Journal of Pharmaceutics 519: 128-137.

24. Neves AR, Lucio M, Martins S, Lima JL, Reis S (2013) Novel resveratrol nanodelivery systems based on lipid nanoparticles to enhance its oral bioavailability. Int J Nanomedicine 8: 177-187.

25. Matuschek E, Brown DFJ, Kahlmeter G (2014) Development of the EUCAST disk diffusion antimicrobial susceptibility testing method and its implementation in routine microbiology laboratories. Clinical Microbiology and Infection 20: O255–O266.

26. Kusters JG, van Vliet AHM, Kuipers EJ (2006) Pathogenesis of *Helicobacter pylori* Infection. Clinical Microbiology Reviews 19: 449-490.

27. Blanchard TG, Nedrud JG (2006) Laboratory Maintenance of Helicobacter Species. Current Protocols in Microbiology CHAPTER: Unit8B.1-Unit8B.1.

28. Mehnert W, Mäder K (2001) Solid lipid nanoparticles: Production, characterization and applications. Advanced Drug Delivery Reviews 47: 165-196.

29. Lopes D, Nunes C, Martins MCL, Sarmento B, Reis S (2014) Eradication of *Helicobacter pylori*: Past, present and future. Journal of Controlled Release 189: 169-186.

30. O'Toole PW, Clyne M (2001) Cell Envelope. In: Mobley HLT, Mendz GL, Hazell SL, editors. Helicobacter pylori: Physiology and Genetics. Washington (DC).

31. McGee DJ, George AE, Trainor EA, Horton KE, Hildebrandt E, et al. (2011) Cholesterol enhances *Helicobacter pylori* resistance to antibiotics and LL-37. Antimicrob Agents Chemother 55: 2897-2904.

32. O'Rourke J, Bode G (2001) Morphology and Ultrastructure. In: Mobley HLT, Mendz GL, Hazell SL, editors. Helicobacter pylori: Physiology and Genetics. Washington (DC).

33. AP. M (2001) Molecular Structure, Biosynthesis, and Pathogenic Roles of Lipopolysaccharides. In: HLT M, GL M, SL H, editors. Helicobacter pylori: Physiology and Genetics. Washington (DC): ASM Press.

34. Magalhães A, Ismail MN, Reis CA (2010) Sweet receptors mediate the adhesion of the gastric pathogen *Helicobacter pylori*: glycoproteomic strategies. Expert Review of Proteomics 7: 307-310.

35. Krulwich TA, Sachs G, Padan E (2011) Molecular aspects of bacterial pH sensing and homeostasis. Nat Rev Micro 9: 330-343.

36. Gonçalves IC, Henriques PC, Seabra CL, Martins MCL (2014) The potential utility of chitosan micro/nanoparticles in the treatment of gastric infection. Expert Review of Anti-infective Therapy 12: 981-992.

37. Gao W, Thamphiwatana S, Angsantikul P, Zhang L (2014) Nanoparticle approaches against bacterial infections. Wiley Interdisciplinary Reviews: Nanomedicine and Nanobiotechnology 6: 532-547.

38. Blackburn P (1997) Polysorbate-containing compositions and their use against *Helicobacter*. European Patent Office WO/1997/036600.

39. Cerreto F, Paolicelli P, Cesa S, Abu Amara HM, D'Auria FD, et al. (2013) Solid lipid nanoparticles as effective reservoir systems for long-term preservation of multidose formulations. AAPS PharmSciTech 14: 847-853.

40. Santucci A, Figura N, Spreafico A, Cavallo G, Marcolongo RF (2013) Compositions for treating *Helicobacter pylori* infection. European Patent Office WO2011IT00175.

41. Nogueira F, Gonçalves IC, Martins MCL (2013) Effect of gastric environment on *Helicobacter pylori* adhesion to a mucoadhesive polymer. Acta Biomaterialia 9: 5208-5215.

42. Jung SW, Thamphiwatana S, Zhang L, Obonyo M (2015) Mechanism of antibacterial activity of liposomal linolenic acid against *Helicobacter pylori*. PloS one 10: e0116519.

43. Ishikawa S, Matsumura Y, Katoh-Kubo K, Tsuchido T (2002) Antibacterial activity of surfactants against *Escherichia coli* cells is influenced by carbon source and anaerobiosis. Journal of Applied Microbiology 93: 302-309.

44. Hamouda T, Baker JR (2000) Antimicrobial mechanism of action of surfactant lipid preparations in enteric Gram-negative bacilli. Journal of Applied Microbiology 89: 397-403.

45. Rodrigues D, Rocha-Santos T, Sousa S, Gomes AM, Pintado MM, et al. (2011) On the viability of five probiotic strains when immobilised on various polymers. International Journal of Dairy Technology 64: 137-144.

46. Monteiro C, Fernandes M, Pinheiro M, Maia S, Seabra CL, et al. (2015) Antimicrobial properties of membrane-active dodecapeptides derived from MSI-78. Biochimica et Biophysica Acta (BBA) - Biomembranes 1848: 1139-1146.

CHAPTER VI

DEVELOPMENT OF LIPID NANOPARTICLES FOR THE TREATMENT OF *HELICOBACTER PYLORI* INFECTION IN MICE

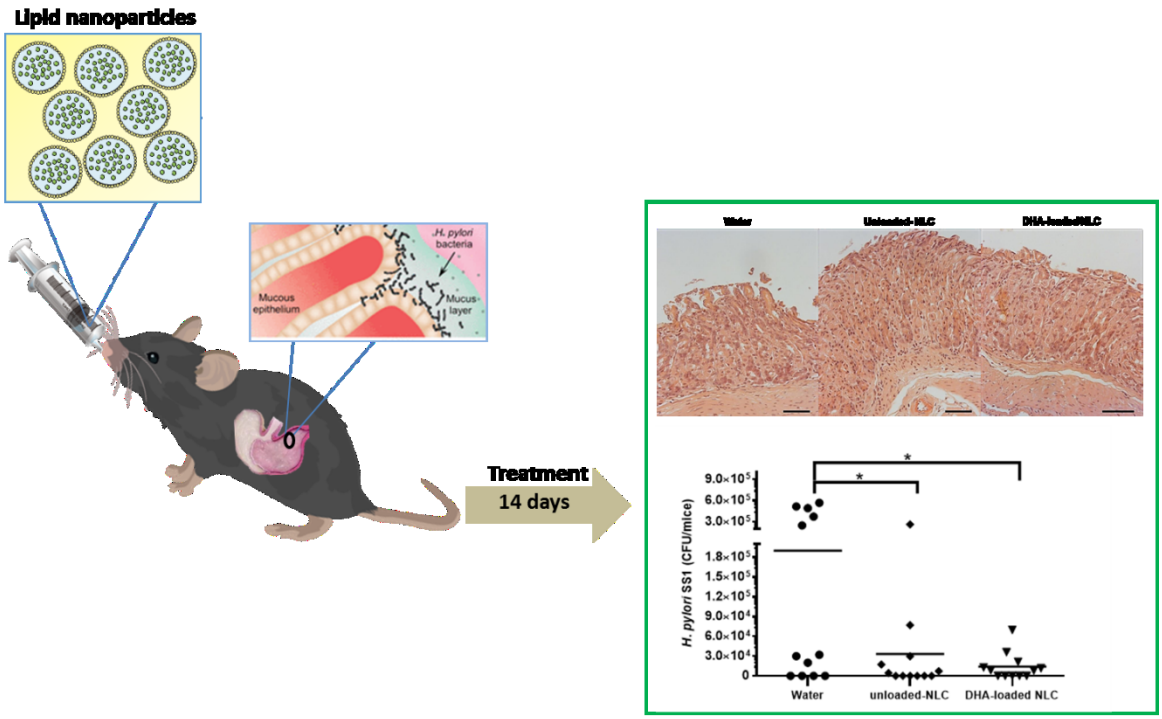

Manuscript in preparation

Abstract

Persistent *Helicobacter pylori* (*H. pylori*) infection may lead to several gastric complications such as gastritis, peptic ulcer, and gastric carcinoma. Current antibiotic-based treatments are unsuccessful in approximately 20% of the patients due, principally, to the increase number of *H. pylori* strains resistant to available antibiotics. We recently demonstrated that lipid nanoparticles, namely nanostructured lipid carriers (NLC) loaded with docosahexaenoic acid (DHA), an omega-3 fatty acid with anti-*H. pylori* activity and unloaded-NLC were both bactericidal against *H. pylori*.

The major goal of this work was to evaluate if these NLC may be used in the treatment of *H. pylori* infection. For that, their stability in simulated gastric fluidic and their ability to cross gastric mucus layer was firstly evaluated using *in vitro* mice model, respectively. Nanoparticles toxicity and efficacy in *H. pylori* eradication were assessed using C57BL/6 mice infected with mouse-adapted *H. pylori* strain (SS1). Additionally, *in vitro* assays were done to assess the crystalline structure of these lipid nanoparticles and to estimate their effect on *H. pylori* membrane permeability.

Homogenous and spherical negatively charged DHA-loaded NLC (302±14 nm) and unloaded (211±8nm) were stable in simulated gastric fluid for 3h. DSC results demonstrated a crystallinity reduction of DHA-loaded NLC relatively to unloaded-NLC meaning that DHA -loaded NLC have a lower crystal organization than unloaded-NLC and their bulk material.

A fast (30 min) bactericidal activity of DHA-loaded NLC was observed, which was explained by their higher effect on the permeability of bacteria membrane than unloaded-NLC at this time point. *In vivo* efficacy assays, using *H. pylori*-infected C57BL/6 mice treated with nanoparticles (2.5% v/v) during 14 days, demonstrated a reduction in *H. pylori* colonization of around 92.6% when mice were treated with DHA-loaded NLC (50 μM DHA) and 82.5% when treated with unloaded-NLC. This reduction of infection was verified without causing gastric or hepatic toxicity. However, 1/3 of infected but untreated mice (control) were not infected after the 14 days treatment (with water), demonstrating the need for further assays.

This work demonstrated that these lipid nanoparticles, mainly the ones containing DHA, are very effective *in vitro* against *H. pylori* due to their action on the increase of bacteria membrane permeability. *In vivo,* preliminary results also suggested that lipid nanoparticles should be considered as a promising alternative for the treatment of *H. pylori* gastric infection.

KEYWORDS: *Helicobacter pylori*, NLC, *in vivo* efficiency, gastric mucosa

1. Introduction

Helicobacter pylori (*H. pylori*) is one the most common bacterial pathogen Worldwide, with a strong association to several gastric diseases, including gastritis, peptic ulcers, and gastric cancer. Gastric cancer is the fifth most incident type of cancer and the second leading cause of cancer-related deaths in the world [1,2]. The increasing prevalence of antibiotic-resistant strains has led to a significant decrease in the success of *H. pylori* eradication [3-5]. Different regimen treatments, including antibiotics combinations, have been used to overcome this problem. However, poor patient compliance, side-effects and high cost associated with multiple antibiotics used are also related to therapy failure [6], demonstrating the urgent need for alternative treatments.

Several antibiotic-free approaches have been investigated to fight *H. pylori* infection such as antimicrobial peptides [7-9], lipophilic compounds [10-14], the use of probiotics [15-18], the application of bioengineering strategies for drug delivery or binding bacteria [19-24] and also, the development of vaccines [25-28]. However, although very successful *in vitro,* none of these alternatives were sufficiently effective to be used, by itself, in the *H. pylori* infection eradication.

Some polyunsaturated fatty acids (PUFA), namely docosahexaenoic acid (DHA), linolenic acid (LA) and eicosapentaenoic acid (EPA) are bactericidal against a broad range of bacteria and have a lower tendency to induce bacteria resistant than conventional antibiotics [29-31]. Although some PUFA as DHA have been very effective against *H. pylori in vitro* [29,32-36], their poorly bioavailability *in vivo* needs to be overcome. This can be related to their low stability, namely high susceptibility to oxidation, or their low ability to cross gastric mucus layer to reach the infection site.

The development of local delivery systems may improve PUFA *in vivo* bioavailability. It was recently demonstrated by us that nanostructured lipid carriers (NLC) containing DHA (DHA-loaded NLC) are highly bactericidal against *H. pylori* by membrane disruption. However, unloaded-NLC were also bactericidal, demonstrating that the DHA-loaded NLC bactericidal effect was not only due to the DHA released, but due to a synergistic effect of NLC and DHA [37].

The main goal of this work was to evaluate if NLC (unloaded and DHA-loaded) may be used in the treatment of *H. pylori* infection. *In vivo* studies, using C57BL/6 mice infected with mouse-adapted *H. pylori* strain (SS1) were then performed. The toxicity profile of developed nanoparticles in mouse stomach was also evaluated through histological analysis. Additionally, we evaluate the effect of NLC in the permeability of bacteria membrane, to understand how NLC may disrupt bacteria membrane. To evaluate the physical state of the lipid core in the produced NLC and to correlate this parameter with the DHA incorporation, additional NLC characterization was performed by DSC analysis.

2. Material & methods

2.1. Preparation and characterization of NLC

2.1.1. NLC production

NLC was prepared by hot homogenization and sonication as described by Seabra *et al* (2017) [37]. Briefly, 200 mg of Precirol®ATO5 (Gattefosé, France), 90 mg of Miglyol®812 (Acofarma, Spain) and 60 mg Tween®60 (Merck, Germany) were weighted and heated together at 60ºC. Then 84µL of DHA and 4.2 mL of water type I (preheated at 60ºC) were added and mixed using an ultra-turrax (T25, Janke and Kunkel IKA-Labortechnik, Germany) at 12000 rpm, over 20 s, and sonicated using a Vibra-Cell model VCX 130, with a VC 18 probe of ¼'' (6 nm), at 60% amplitude for 5 min (Sonics and Materials Inc, Newtown, USA), obtaining DHA-loaded NLC.

2.1.2. NLC characterization

DHA-loaded NLC was characterized in terms of size and morphology as described by Seabra *et al* (2017) [37].

2.1.2.1. Differential Scanning Calorimetry (DSC)

Differential scanning calorimetry (DSC) analysis was performed using a Perkin-Elmer Pyris 1 DSC differential scanning calorimeter (Perkin-Elmer Analytical Instruments, Waltham, USA). The samples were weighed directly in aluminum pans (7-23 mg) and scanned between 10ºC and 80ºC at a heating rate of 5ºC/min and cooling rate of 40ºC/min under a stream of nitrogen gas. An empty aluminum pan was used as reference. DSC analyses were performed for the lipid nanoparticles, as well as for the bulk materials used in the preparation of the nanoparticles. The melting point (peak maximum) and the enthalpy (ΔH) were calculated using the PerkinElmer software.

2.1.2.2. Stability in simulated gastric fluid

DHA-loaded NLC stability was performed using a simulated gastric fluid (SGF) prepared with HCl 0.2M and NaCl 0.2M (pH1.2). DHA-loaded NLC were incubated with SGF over 3 h at 37ºC and 150 rpm. At time-point 0 and 3 h, samples were diluted (1:20000) in water type I and analyzed in terms of particle concentration using NanoSight® NS300 (Malvern Instruments, UK). The measurements were performed in triplicate.

2.2. Anti-*Helicobacter pylori* activity: *in vitro* study

2.2.1. *H. pylori* culture

H. pylori J99 strain (human isolate provided by Department of Medical Biochemistry and Biophysics, Umeã, Sweden) were cultured as described by Seabra *et al*. (2017) [37]. Briefly, *H. pylori* J99 spots and spreads were subsequently incubated at 37ºC for 48 h, under microaerophilic conditions. *H. pylori* medium plates were prepared using 20g of blood agar base 2 (Oxoid, France) supplemented with 10% v/v of defibrinated horse blood (Probiológica, Portugal) and with 0.2% v/v antibiotics-cocktail composed of 0.155 g/L polymixin B (Sigma-Aldrich, USA), 6.25 g/L vancomycin (Sigma-Aldrich, USA), 1.25 g/L amphotericin B (Sigma-Aldrich, USA) and 3.125 g/L trimethroprim (Sigma-Aldrich, USA). Afterwards, the optical density of bacteria was adjusted to 0.1 (λ=600 nm) and *H. pylori* were incubated in Brucella Broth medium (BB, Oxoid, France) supplemented with 10% of fetal bovine serum (FBS, Gibco, USA), at 37ºC, 150 rpm, under microaerophilic conditions, over 18-20 h.

2.2.2. NLC activity against *H. pylori* membrane

The *H. pylori* optical density was adjusted to 0.03 (1×10^7 bacteria/mL) and incubated with unloaded-NLC (2.5% v/v) and DHA-loaded NLC (2.5% v/v containing 50μM DHA). The respective control was performed with untreated bacteria (incubated with water). Bacteria culture was performed at 15, 30, 90 and 150 minutes in bacteria medium, under microaerophilic conditions, at 37ºC and 150 rpm.

2.2.2.1. Colony forming units (CFU)

At different time-points (15, 30, 90 and 150 min), 200 μL of each culture (control, unloaded and DHA-loaded NLC) was collected, serially diluted and plated on *H. pylori* medium plates and incubated at 37ºC. After 5 days, the number of viable bacteria was determined by colony forming unit (CFU) counting.

2.2.2.2. Permeability assay

2.2.2.2.1. Outer membrane

The outer membrane permeability was evaluated by adapting the methods described by Loh *et al* (1984)[38] and Alakoni *et al*. (2006) [39], measuring the uptake of the

fluorescent probe 1-N-phenylnaphthetlamine (NPN). After 30 min of incubation with unloaded- and DHA-loaded NLC, as described above (2.2.2.), bacteria were collected by centrifugation at 3000 *g* at 25ºC for 5 min and washed twice with 0.01M phosphate buffer (PBS 1x; pH 7.4). A negative control (bacteria growing in bacteria medium) and a positive control (bacteria treated with 10% v/v of Triton TM X-100) were included, in order to normalize the results. The bacterial pellet was resuspended in 5 mM of n-heptadecanoic acid methyl ester buffer (HEPES buffer; pH 7.2). For NPN assay (at room temperature), 50µL of NPN (10µM final concentration) were added and mixed with 150µL of bacteria suspension. Fluorescence was measured after shaking for 3 minutes, using a microplate reader (Synergy™H Multi-mode Microplate Reader, BioTek Instruments, USA) at an excitation wavelength of 350 nm and an emission wavelength of 420 nm. The measurements were repeated three times.

2.2.2.2.2. Inner membrane

The plasma membrane permeability was evaluated by measuring the ATP release from bacterial cells, using BacTiter-Glo microbial cell viability assay kit (Promega Inc, USA), as described by Parsons *et al* (2012) [40] and Jung *et al.* (2015) [10]. After *H. pylori* treatment with unloaded and DHA-loaded NLC for 30 min, as described above (2.2.2), bacteria were centrifuged at 14 000 *g* for 5 minutes and the supernatant containing released ATP was collected. Then, 100 µL of supernatant were placed in a 96-well plate and BacTiter-Glo reagent was added directly to the supernatant at ratio 1:1. The mixture was shaken for 2 minutes and using a microplate reader (Synergy™ H Multi-mode Microplate Reader, BioTek Instruments, USA), the luminescence was measured. The measurements were repeated three times.

2.3. Anti-*Helicobacter pylori* activity: *in vivo* study

2.3.1. Mice infection

Six-week-old specific pathogen-free C57BL/6 male mice (Charles Rivers, France) were divided into six groups: non-infected mice (negative control group; *n*=3), two non-infected mice and treated group with unloaded (*n*=2) and DHA-loaded NLC (*n*=2) for toxicity evaluation, *H. pylori*-infected mice (positive control group, *n*=12) and two *H.* pylori-infected groups that were treated with unloaded (*n*=12) and DHA-loaded NLC (*n*=12). *H. pylori* SS1 (mouse-adapted strain provided by Unité de Pathogenèse de *Helicobacter*, Institute Pasteur, France) was cultured as described in section 2.2.1. Mice received 100µL of 1×10^{10} CFU/mL of *H. pylori* strain SS1 in peptone water (Sigma-Aldrich, USA) administrated intragastrically through oral gavage twice with a 2 dyes interval and infection was allowed to

develop for 4 weeks. The control groups of mice were given peptone water alone. 24 h before infection, mice were weighted and food and bedding were removed. Water was removed 6 h before administration. 3 h after *H. pylori* administration, mice were switched back to the original cages with food, water, and bedding. All animal procedures were performed in compliance with the laws and institutional guidelines of the Ethical Committee of i3S Animal Facilities.

2.3.2. NLC treatment and mice sacrifice

Four weeks after infection, treatment was performed with unloaded-NLC (2.5% v/v) and DHA-loaded NLC (2.5% v/v containing 50 μM DHA). For the treatment, mice were first fasted for 6 h and then 100μL of NLC (unloaded or DHA-loaded) were administrated through oral gavage once a day for consecutive 14 days. The control groups of mice were given water. The treatment plan applied to the mice is represented in Scheme 1.

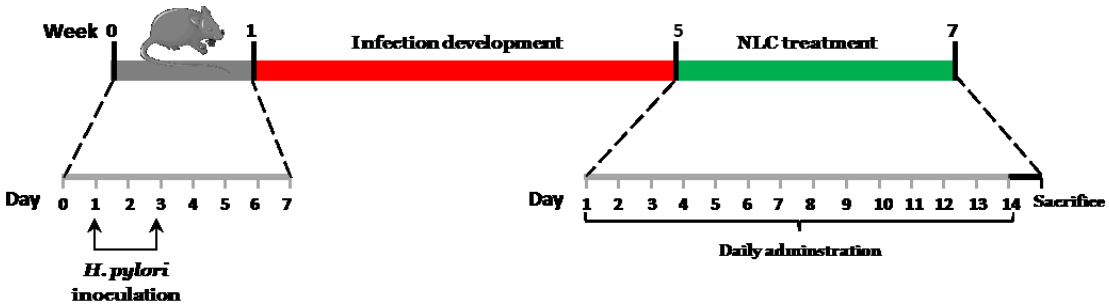

Scheme 1- Experimental protocol including the *H. pylori* SS1 inoculation, infection development, and treatment of C57BL/6 infected mice.

After the last administration, mice were fasted for 18 h and then euthanized by cervical dislocation, with previous anesthesia (50-75 mg/kg Ketamine and 0.5-1 mg/kg Medetomidine) through intraperitoneal injection. The abdominal cavity was opened and a liver section was removed. Then, mouse stomach was removed, rinsed in 0.9% NaCl (to remove food) and opened transversally. The mouse stomach was divided into 4 longitudinal sections (Scheme 2): one section for cryopreservation, another for histological analysis and the two other sections (part A and B) were placed in a tube containing 400 μL of peptone water, for CFU counting, evaluating the reduction of *H. pylori* colonization. Each stomach section (part A and B) was smashed with a tissue homogenizer using sterile pistons, and then serial dilutions (10^1, 10^2, and 10^3) were made and plated on *H. pylori* medium plates, described above, and supplemented with 20 mg/mL of naladixic acid (Sigma-Aldrich, USA) and 50mg/mL bacitracin (Sigma-Aldrich, USA). After 15 days, at 37ºC under microaerophilic conditions, the number of colony forming units (CFU) per mice stomach was determined.

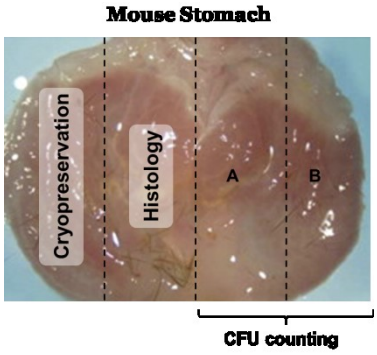

Scheme 2- Mouse stomach segments for cryopreservation, histological analysis, and CFU counting evaluation.

Liver section and longitudinal section of mice stomach were fixed in formalin and then embedded in paraffin and cut transversally in to 3 µm sections and gastric mucosa and liver sections were placed on glass slides.

Sections were deparaffinated with xylene and hydrated in ethanol (100%, 96%, and 70%), running water and the hematoxylin and eosin (H&E) staining was performed. After staining sections were mounted with mounting medium (Entellan®, Merck, Germany) and observed using an optical microscope, evaluating the NLC (unloaded- and DHA-loaded NLC) toxicity

2.4. Statistical analysis

The statistical analysis was performed using Graph Pad Prism 6.0 Software (La, Jolla, USA) applying non-parametric Kruskal-Wallis test or One-way ANOVA (Tukey test), considering statically significant differences at $p<0.05$.

3. Results

3.1. NLC production and *in vitro* characterization

DHA was loaded into NLC forming homogeneous and spherical nanoparticles with a hydrodynamic diameter of 302 ± 14 nm (Figure 1B and 1D). Unloaded-NLC were also produced as a control of DHA encapsulation, having a diameter of 211±8 nm (Figure 1A and 1C).

NLC thermometric behavior was compared with their physical mixture of their excipients (bulk material). DSC thermograms and respective thermometric parameters as melting point, enthalpy, and recrystallization index (RI) for the bulk materials and NLC are shown in Figure 1B. For bulk materials of unloaded and DHA-loaded NLC, the melting process took place at 57.1º and 58.3ºC, respectively. When NLC are produced, the melting transition

peak and onset temperature are lower than that of the bulk material, as well as the melting enthalpy values that decrease, from 83.5 to 8.2 J/g in unloaded-NLC and 87.2 to 6.7 J/g in DHA-loaded NLC. The presence of DHA caused a decrease in the melting enthalpy, from 8.2 to 6.7 J/g. These melting enthalpy values were calculated from the area under the curve by integrating the peak beneath the baseline and dividing by the mass of sample in each case (Figure 1B). The degree of crystallinity or recrystallization index (RI) of NLC formulations were calculated from the enthalpy of the NLC dispersion compared with the enthalpy of their bulk materials. The enthalpy of bulk material was set at 100% crystallinity and this value was used as a reference to determine the degree of crystallinity of the NLC. As shown in the table of Figure 1B, the RI of the unloaded- and DHA-loaded NLC decreased to 77% and 56%, respectively, in comparison with each own bulk material. The reduction of maximum temperature peak and melting enthalpy can be related to distorted crystallization due to the presence of surfactant distributed in the melted lipid phase.

The developed NLC seem to be suitable for oral administration as observed in the assessment of NLC stability in gastric fluid (Figure 1C), which was followed by measuring the concentration of NLC before and after incubation in simulated gastric fluid (pH1.2) over 3 h. No changes of NLC concentration were observed after their incubation in simulated gastric fluid, indicating that the NLC are not disrupted in gastric pH (Figure 1C).

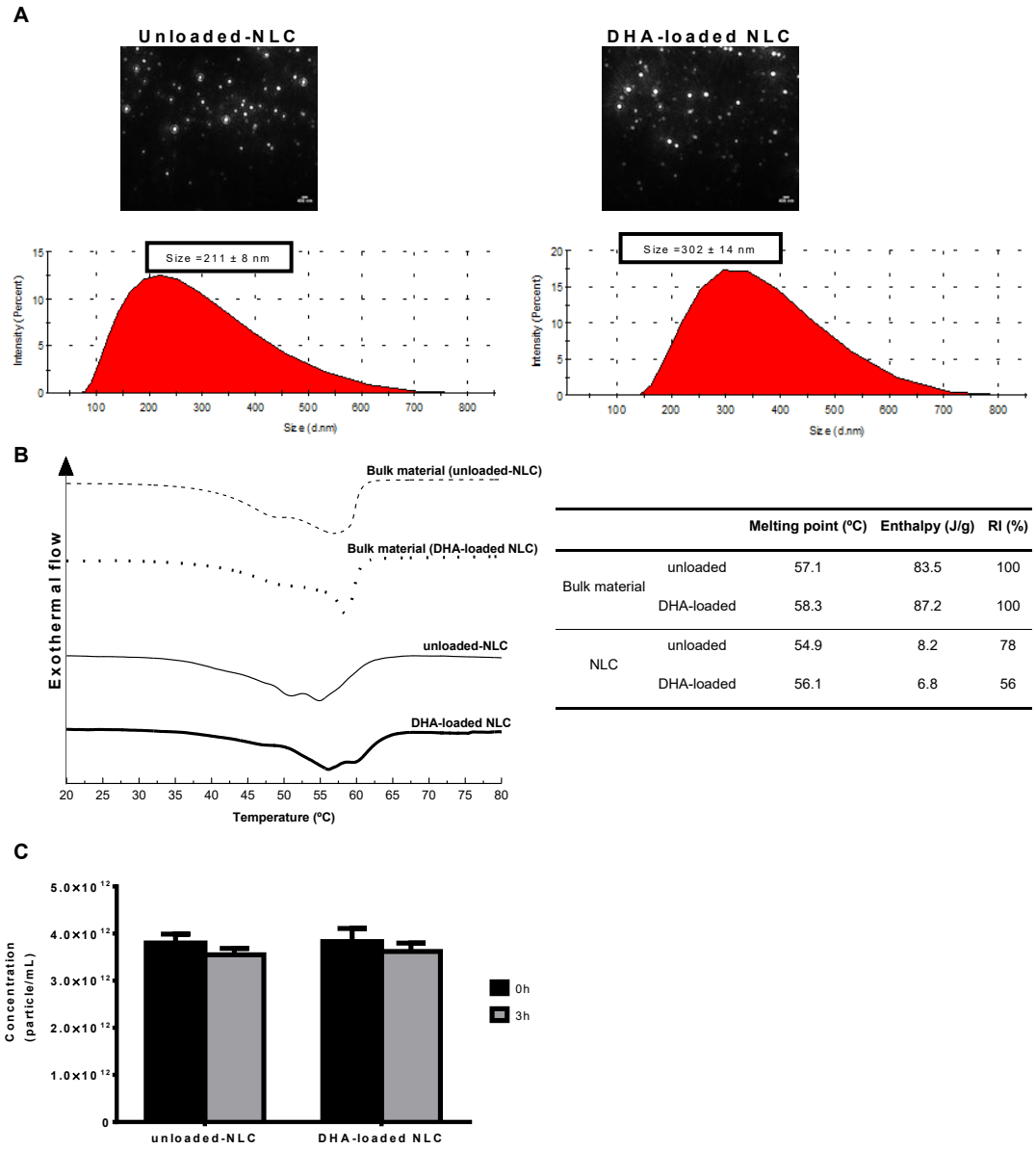

		Melting point (ºC)	Enthalpy (J/g)	RI (%)
Bulk material	unloaded	57.1	83.5	100
	DHA-loaded	58.3	87.2	100
NLC	unloaded	54.9	8.2	78
	DHA-loaded	56.1	6.8	56

Figure 1. NLC characterization. Morphology and average of size (d, nm) of unloaded- and DHA-loaded NLC measured using NanoSight® image (scale bar 400 nm) and NanoSizer® Malvern, respectively. (**B**) Differential scanning calorimetry thermograms and thermometric parameters as melting point, enthalpy, and recrystallization index (RI) of bulk material blends and NLC. (**C**) NLC stability in simulated gastric fluid for 3 h, measuring the particle concentration changes by NanoSight®.

3.2. Anti-*H. pylori in vitro* efficiency

The bactericidal effect of NLC, unloaded and DHA-loaded, against *H. pylori in vitro* was previously reported by us [37]. However, due to their high bactericidal potency, their kill-time kinetics was further investigated for very short times (15, 30, 90 and 150 min) and using a bactericidal concentration (unloaded-NLC (2.5% v/v) and DHA-loaded NLC (2.5% v/v containing 50 μM DHA) that was not toxic to gastric human cells [37]. DHA-loaded NLC rapidly decreased the number of viable bacteria within 30 min of incubation, having a reduction of 3 logs (99.9%) of *H. pylori* at 2.5% v/v (50 μM), while with unloaded-NLC no bactericidal activity against bacteria was observed up to 150 min (Figure 2A). No viable bacteria were detected, when bacteria was treated with this concentration of DHA-loaded NLC after 90 min.

As anti-*H. pylori* activity of DHA-loaded NLC was fast, the possible mechanism of action was explored by evaluating permeability of the outer and inner membrane. To evaluate de outer membrane permeability, NPN was used. This is a hydrophobic fluorescent probe, which can enter into the hydrophobic interior of the outer membrane when membrane integrity is compromised [38,39]. After 30 min incubation, *H. pylori* treated with DHA-loaded NLC had a significant increase in the fluorescence signal of NPN (NPN uptake) compared to the control and unloaded-NLC, indicating DHA-loaded NLC increased rapidly the outer membrane permeability of *H. pylori,* explaining their more effective bactericidal activity than unloaded-NLC. Nevertheless, unloaded-NLC also affected the outer membrane permeability of *H. pylori* but in a slower way.

The plasma membrane permeability was also examined using a BacTiter-Glo microbial cell viability assay kit, evaluating the disrupting of the plasma membrane as a result of the immediate collapse of the proton gradient accompanied with a fast release of intracellular ATP into the medium [40]. Treatment with DHA-loaded NLC enhanced ATP release from *H. pylori* comparing to control and unloaded-NLC. Once again, unloaded-NLC increased also the plasma permeability of *H. pylori*, but with a lower efficiency rate than DHA-loaded NLC.

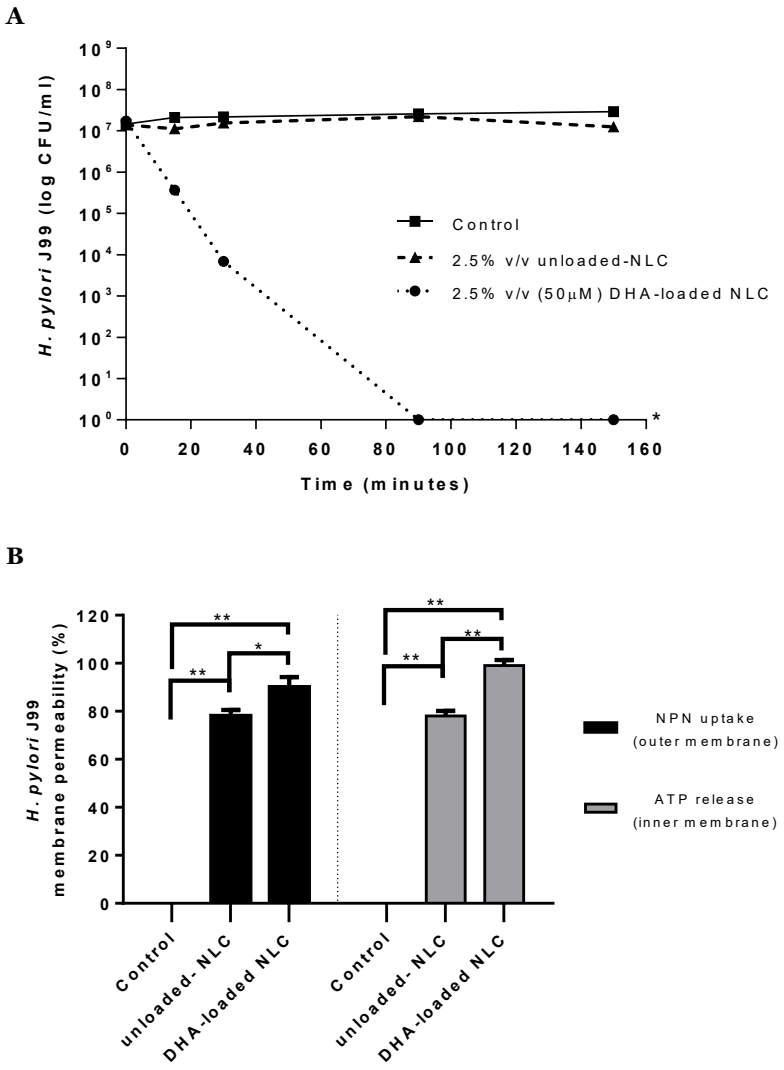

Figure 2. *H. pylori* growth and membrane permeability. (**A**) *In vitro* bactericidal activity of 2.5% v/v unloaded and DHA-loaded NLC against *H. pylori* strain J99 evaluated by colony forming unit counting. *p<0.05, refers to significant differences in *H. pylori* growth between control (bacteria untreated) and bacteria treated with NLC (Kruskal-Wallis test). (**B**) Outer and inner membrane quantification by uptake of N-phenylnapthylamine (NPN) and release of ATP from *H. pylori* J99 due to treatment with of 2.5% v/v unloaded and DHA-loaded NLC for 30 minutes. * p<0.05, **p<0.001, statically significant differences between samples (One-way ANOVA, Tukey test).

3.3. Anti-*H. pylori in vivo* efficiency

NLC were administered to C57BL/6 mice, as described in Scheme 1, evaluating their efficiency in the treatment of *H. pylori* infection. Infection was confirmed by CFU counting and toxicity by hematoxylin and eosin (H&E) staining of stomach and liver sections (Figure 4). By CFU counting (CFU/mice stomach), it was possible to notice the presence of *H. pylori* SS1 strain in infected mice that were administered with only water, presenting average infection levels of CFU/mice of ~1.98×10^5 (Figure 4C). Regarding NLC efficiency

to reduce the bacteria infection, significant differences were observed when mice were treated with 2.5% unloaded and DHA-loaded NLC (50 μM DHA), comparing with untreated mice (mice received only water) (Figure 4C). The reduction of infection in these cases was 82.5% (~3.34×10^4 CFU/mice) and 92.6% (~1.40×10^4 CFU/mice), respectively, a reduction of 1 log.

To evaluate NLC toxicity, gastric and liver histopathology by H&E staining was performed as showed in Figure 4A and 4B. Stomach sections of non-infected mice presented normal gastric architecture, with an organized structure, an intact epithelial layer and glandular cells with continuous gastric pits, even when treated with NLC. In what concerns infected and treated mice, some inflammatory infiltrates can still be found, although less pronounced. The gastric mucosa morphology and structure of untreated *H. pylori*-infected shows more disorganized epithelium with a slight atrophy comparing with non-infected mice. Regarding the histological analysis of the liver, in all groups, a normal architecture of the tissue can be observed, with a normal distribution of hepatocytes around central veins and some accumulation of hepatic fat (steatosis) in some mice.

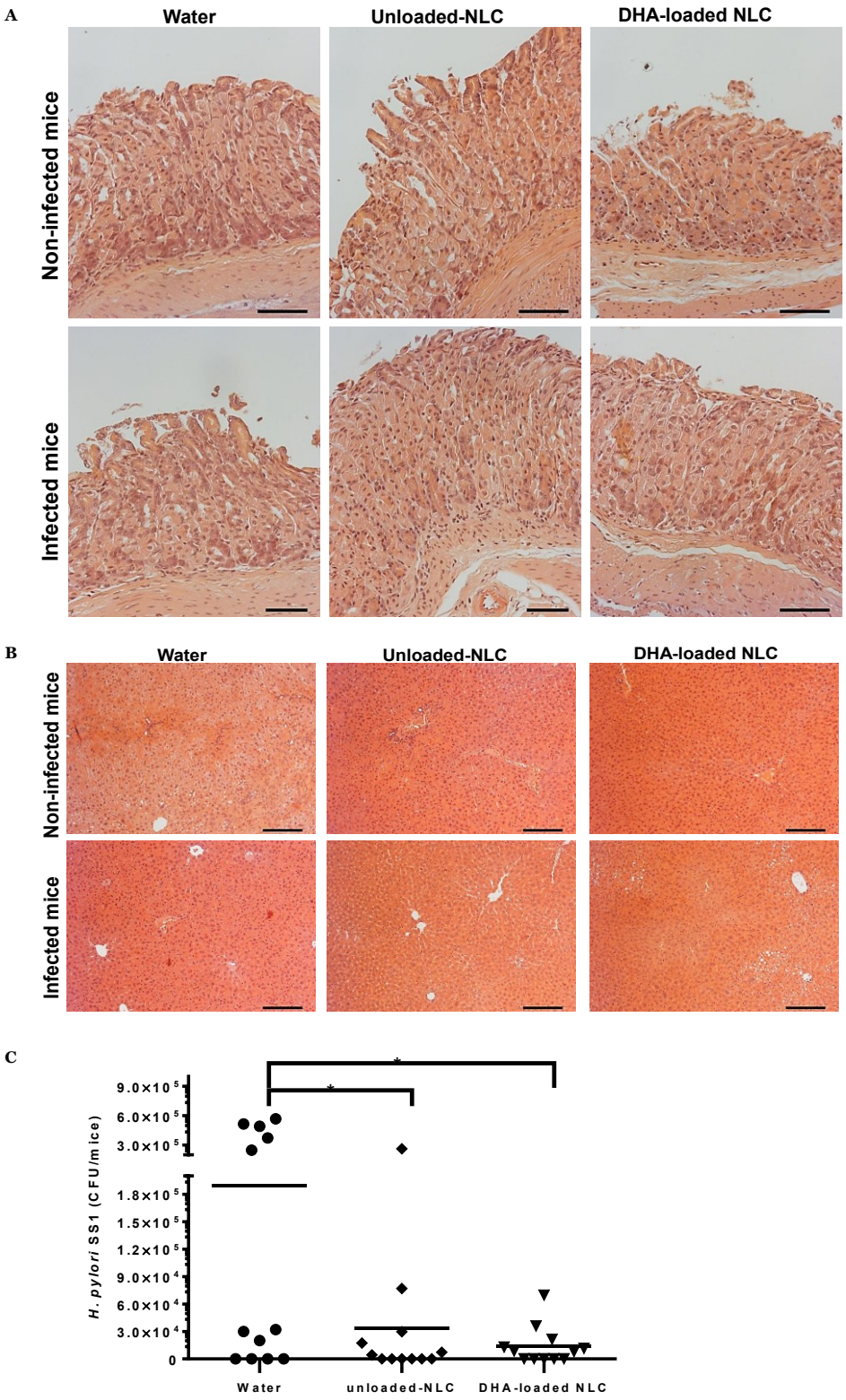

Figure 3. Anti-*H. pylori* efficacy *in vivo*. (A) Stomach and **(B)** liver toxicity characterized by histology (H&E staining) of C57BL/6 mice infected with *H. pylori* SS1 treated with, water, unloaded and DHA-loaded NLC. Scale bar: 200μm. **(C)** Quantification of *H. pylori* burden in the stomach of infected mice treated with water, unloaded and DHA-loaded NLC (n=12 per group). Bars represent mean values. * $p<0.05$, refers to significant differences between infected mice non-treated and treated mice (One-way ANOVA, Tukey test).

4. Discussion

Due to the rapid rise of *H.* pylori strains resistant to the existing antibiotics, current treatment regimens present a rapid decline in their eradication rates [41]. The bactericidal potential of DHA, as a safe and natural bacteria inhibitor, was well described [35]. Correia *et al.* [35] demonstrated that DHA after oral administration was able to eradicate *H. pylori* from 50% of *H. pylori*-infected mice.

We previously demonstrated that DHA loading into NLC strongly promotes its anti-*H. pylori* activity. However, this effect was associated with a synergistic effect between the released DHA and the lipid nanoparticle, since unloaded-NLC were also bactericidal to *H. pylori* [37]. During this work, we demonstrated that these unloaded- (~211nm) and DHA-loaded (~300 nm) NLC, were both stable in simulated gastric fluid (pH 1.2) for 3h. However, we previously demonstrated that DHA-loaded NLC, containing 66% DHA entrapment efficiency, were unstable in bacteria medium (Brucella broth supplemented with 10%FBS), releasing 40% of their DHA after 3h [37]. This may be explained by our DSC results that demonstrated that when DHA was incorporated into NLC matrix, creates a less order crystalline structure, nanoparticle is less rigid, which will favor their disintegration and DHA released [37]. DHA-loaded NLC have a faster bactericidal activity against *H. pylori* J99 (human strain) than unloaded-NLC. This was explained by their higher ability to increase the permeability of the outer and inner *H. pylori* membrane in a short period of time (30 min). This fact can explain the faster disruption of *H. pylori* membrane and leakage of cytoplasmic contents when *H. pylori* was treated with DHA-loaded NLC instead of unloaded NLC [37]. Similar bactericidal results were described by Jung *et al* [10] for liposomes containing linoleic acid (LA). They proposed that the high bactericidal potential of these liposomes were related to their ability to rapidly fuse and incorporate LA into *H. pylori* phospholipid membrane, promoting membrane disruption and causing bacterial death [10]. Moreover, due to their fast bactericidal effect (30 min), DHA-loaded NLC at 2.5% (v/v) have low propensity to induce resistant *H. pylori* strains since 30 min is a relatively short time compared with the 2.5 h needed for *H. pylori* to complete a replication cycle [30,42]. Another advantage of these NLC (unloaded and DHA-loaded), is the absence of cytotoxicity against human adenocarcinoma gastric cells at bactericidal concentrations (2.5% v/v) [37] and both NLC were also stable in simulated gastric fluid (pH1.2)

In what concerns NLC oral administration, data revealed no changes in morphology in mouse stomach and liver histological sections, comparing with the histological section in the literature [43,44] after 14 days treatment with 2.5% (v/v) NLC. These results suggest that this NLC concentration is safe and well-tolerated, with no toxic effect observed, in agreement with several clinical trials that have used DHA supplementation at higher doses with no reports of toxicological effects [45]. However, some of the mice presented liver steatosis, which was associated with the diet rich in carbohydrates that mice are subjected to in the animal facility.

Regarding gastric infection treatment, C57BL/6 mice were infected with an *H. pylori* mouse-adapted strain (*H. pylori* SS1), since these mice are not infected by *H. pylori*-human strains [46]. A similar bactericidal effect of developed NLC (unloaded and DHA-loaded) against both bacteria *H. pylori* strains (SS1 and J99) was previously demonstrated by us [37].

Treatment with DHA-loaded NLC reduced *H. pylori* number in the gastric mucosa of infected mice in around 92.6%, while treatment with unloaded-NLC have only a decrease in 82.5% compared with untreated mice. These findings suggest that, although NLC were able to decrease *H. pylori* gastric colonization, DHA-loaded NLC was more effective than unloaded-NLC. However, four in twelve mice of the control untreated group (mice infected but treated with water) were *H. pylori* negative after 14 days. This *H. pylori* clearance in the untreated group may be associated with *H. pylori* SS1 quality that may have lost its ability to infect mice. Several parameters may affect *H. pylori* SS1 mice colonization and strain virulence namely the frequency of dosing, volume of inoculum, and excessive passage of the SS1 strain [46]. Another hypothesis is related to the immunity of mice to *H. pylori* because a persistent *H. pylori* infection in mice typically results in an *H. pylori* immunization due to the presence of some of the antibodies that may participate to the *H. pylori* clearance [47,48].

5. Conclusion

DHA-loaded NLC, at concentrations around 2.5% v/v (50 μM DHA), were bactericidal against *H. pylori* in a very short time (30 min). NLC (unloaded- and DHA-loaded) were able to affect the permeability of the outer and the inner bacteria membrane in 30 min, although this effect was more effective for DHA-loaded NLC. Unloaded and DHA-loaded NLC were both stable in acidic conditions and may be able to use for oral administration. *In vivo,* preliminary data suggest that both, unloaded and DHA-loaded NLC, were able to reduce *H. pylori* infection in mice (~1 Log), although DHA-loaded NLC has been more efficient. Moreover, these NLC did not demonstrate any toxicity to mice in the concentrations used. Overall, the results indicate the therapeutic potential of DHA-loaded NLC for the treatment of *H. pylori* infection.

References

1. Venerito M, Link A, Rokkas T, Malfertheiner P (2016) Gastric cancer – clinical and epidemiological aspects. Helicobacter 21: 39-44.

2. De Francesco V, Giorgio F, Hassan C, Manes G, Vannella L, et al. (2010) Worldwide *H. pylori* antibiotic resistance: a systematic review. J Gastrointestin Liver Dis 19: 409-414.

3. Malfertheiner P, Megraud F, O'Morain CA, Gisbert JP, Kuipers EJ, et al. (2016) Management of *Helicobacter pylori* infection—the Maastricht V/Florence Consensus Report. Gut.

4. Malfertheiner P, Peitz U, Treiber G (2003) What constitutes failure for *Helicobacter pylori* eradication therapy? Can J Gastroenterol 17 Suppl B: 53B-57B.

5. Fallone CA, Chiba N, van Zanten SV, Fischbach L, Gisbert JP, et al. (2016) The Toronto Consensus for the Treatment of *Helicobacter pylori* Infection in Adults. Gastroenterology 151: 51-69.e14.

6. O'Connor A, Fischbach W, Gisbert JP, O'Morain C (2016) Treatment of *Helicobacter pylori* infection 2016. Helicobacter 21: 55-61.

7. Zhang L, Wu WKK, Gallo RL, Fang EF, Hu W, et al. (2016) Critical Role of Antimicrobial Peptide Cathelicidin for Controlling *Helicobacter pylori* Survival and Infection. The Journal of Immunology 196: 1799-1809.

8. Putsep K, Branden C-I, Boman HG, Normark S (1999) Antibacterial peptide from *H. pylori*. Nature 398: 671-672.

9. Narayana JL, Huang H-N, Wu C-J, Chen J-Y (2015) Efficacy of the antimicrobial peptide TP4 against *Helicobacter pylori infection*: *in vitro* membrane perturbation via micellization and *in vivo* suppression of host immune responses in a mouse model. Oncotarget 6: 12936-12954.

10. Jung SW, Thamphiwatana S, Zhang L, Obonyo M (2015) Mechanism of antibacterial activity of liposomal linolenic acid against *Helicobacter pylori*. PloS one 10: e0116519.

11. Obonyo M, Zhang L, Thamphiwatana S, Pornpattananangkul D, Fu V, et al. (2012) Antibacterial Activities of Liposomal Linolenic Acids against Antibiotic-Resistant *Helicobacter pylori*. Molecular Pharmaceutics 9: 2677-2685.

12. Thamphiwatana S, Gao W, Obonyo M, Zhang L (2014) *In vivo* treatment of *Helicobacter pylori* infection with liposomal linolenic acid reduces colonization and ameliorates inflammation. Proceedings of the National Academy of Sciences 111: 17600-17605.

13. Agah S, Shidfar F, Khandouzi N, Baghestani AR, Hosseini S (2015) Comparison of the Effects of Eicosapentaenoic Acid With Docosahexaenoic Acid on the Level of Serum Lipoproteins in *Helicobacter pylor*i: A Randomized Clinical Trial. Iranian Red Crescent Medical Journal 17: e17652.

14. Khandouzi N, Shidfar F, Agah S, Hosseini AF, Dehnad A (2015) Comparison of the Effects of Eicosapentaenoic Acid and Docosahexaenoic Acid on the Eradication of *Helicobacter pylor*i Infection, Serum Inflammatory Factors and Total Antioxidant Capacity. Iranian Journal of Pharmaceutical Research : IJPR 14: 149-157.

15. Dang Y, Reinhardt JD, Zhou X, Zhang G (2014) The Effect of Probiotics Supplementation on *Helicobacter pylori* Eradication Rates and Side Effects during Eradication Therapy: A Meta-Analysis. PLoS One 9: e111030.

16. Li S, Huang X-l, Sui J-z, Chen S-y, Xie Y-t, et al. (2014) Meta-analysis of randomized controlled trials on the efficacy of probiotics in *Helicobacter pylori* eradication therapy in children. European Journal of Pediatrics 173: 153-161.

17. Lorca GL, Wadstrom T, Valdez GF, Ljungh A (2001) *Lactobacillus acidophilus* autolysins inhibit *Helicobacter pylori* in vitro. Curr Microbiol 42: 39-44.

18. Johnson-Henry KC, Mitchell DJ, Avitzur Y, Galindo-Mata E, Jones NL, et al. (2004) Probiotics reduce bacterial colonization and gastric inflammation in *H. pylori*-infected mice. Dig Dis Sci 49: 1095-1102.

19. Fernandes M, Gonçalves IC, Nardecchia S, Amaral IF, Barbosa MA, et al. (2013) Modulation of stability and mucoadhesive properties of chitosan microspheres for therapeutic gastric application. International Journal of Pharmaceutics 454: 116-124.

20. Gonçalves IC, Magalhães A, Costa AMS, Oliveira JR, Henriques PC, et al. (2016) Bacteria-targeted biomaterials: Glycan-coated microspheres to bind *Helicobacter pylori*. Acta Biomaterialia 33: 40-50.

21. Gonçalves IC, Magalhães A, Fernandes M, Rodrigues IV, Reis CA, et al. (2013) Bacterial-binding chitosan microspheres for gastric infection treatment and prevention. Acta Biomaterialia 9: 9370-9378.

22. Nogueira F, Gonçalves IC, Martins MCL (2013) Effect of gastric environment on *Helicobacter pylori* adhesion to a mucoadhesive polymer. Acta Biomaterialia 9: 5208-5215.

23. Parreira P, Magalhães A, Gonçalves IC, Gomes J, Vidal R, et al. (2011) Effect of surface chemistry on bacterial adhesion, viability, and morphology. Journal of Biomedical Materials Research Part A 99A: 344-353.

24. Parreira P, Magalhães A, Reis CA, Borén T, Leckband D, et al. (2013) Bioengineered surfaces promote specific protein–glycan mediated binding of the gastric pathogen *Helicobacter pylori*. Acta Biomaterialia 9: 8885-8893.

25. Koch M, Meyer TF, Moss SF (2013) Inflammation, Immunity, Vaccines for *Helicobacter pylori* infection. Helicobacter 18: 18-23.

26. Chen J, Lin M, Li N, Lin L, She F (2012) Therapeutic vaccination with *Salmonella*-delivered codon-optimized outer inflammatory protein DNA vaccine enhances protection in *Helicobacter pylori* infected mice. Vaccine 30: 5310-5315.

27. Malfertheiner P, Schultze V, Rosenkranz B, Kaufmann SHE, Ulrichs T, et al. (2008) Safety and Immunogenicity of an Intramuscular *Helicobacter pylori* Vaccine in Noninfected Volunteers: A Phase I Study. Gastroenterology 135: 787-795.

28. Zeng M, Mao XH, Li JX, Tong WD, Wang B, et al. (2015) Efficacy, safety, and immunogenicity of an oral recombinant *Helicobacter pylori* vaccine in children in China: a randomised, double-blind, placebo-controlled, phase 3 trial. Lancet 386: 1457-1464.

29. Desbois AP (2012) Potential applications of antimicrobial fatty acids in medicine, agriculture and other industries. Recent Pat Antiinfect Drug Discov 7: 111-122.

30. Desbois AP, Smith VJ (2010) Antibacterial free fatty acids: activities, mechanisms of action and biotechnological potential. Appl Microbiol Biotechnol 85: 1629-1642.

31. Petschow BW, Batema RP, Ford LL (1996) Susceptibility of *Helicobacter pylori* to bactericidal properties of medium-chain monoglycerides and free fatty acids. Antimicrob Agents Chemother 40: 302-306.

32. Thompson L, Cockayne A, Spiller RC (1994) Inhibitory effect of polyunsaturated fatty acids on the growth of *Helicobacter pylori*: a possible explanation of the effect of diet on peptic ulceration. Gut 35: 1557-1561.

33. Khulusi S, Ahmed HA, Patel P, Mendall MA, Northfield TC (1995) The effects of unsaturated fatty acids on *Helicobacter pylori in vitro*. J Med Microbiol 42: 276-282.

34. Frieri G, Pimpo MT, Palombieri A, Melideo D, Marcheggiano A, et al. (2000) Polyunsaturated fatty acid dietary supplementation: An adjuvant approach to treatment of *Helicobacter pylori* infection. Nutrition Research 20: 907-916.

35. Correia M, Michel V, Matos AA, Carvalho P, Oliveira MJ, et al. (2012) Docosahexaenoic acid inhibits *Helicobacter pylori* growth in vitro and mice gastric mucosa colonization. PLoS One 7: e35072.

36. Correia M, Michel V, Osorio H, El Ghachi M, Bonis M, et al. (2013) Crosstalk between *Helicobacter pylori* and gastric epithelial cells is impaired by docosahexaenoic acid. PLoS One 8: e60657.

37. Seabra CL, Nunes C, Gomez-Lazaro M, Correia M, Machado JC, et al. (2017) Docosahexaenoic acid loaded lipid nanoparticles with bactericidal activity against *Helicobacter pylori*. International Journal of Pharmaceutics 519: 128-137.

38. Loh B, Grant C, Hancock RE (1984) Use of the fluorescent probe 1-N-phenylnaphthylamine to study the interactions of aminoglycoside antibiotics with the outer membrane of Pseudomonas aeruginosa. Antimicrobial Agents and Chemotherapy 26: 546-551.

39. Alakomi HL, Paananen A, Suihko ML, Helander IM, Saarela M (2006) Weakening Effect of Cell Permeabilizers on Gram-Negative Bacteria Causing Biodeterioration. Applied and Environmental Microbiology 72: 4695-4703.

40. Parsons JB, Yao J, Frank MW, Jackson P, Rock CO (2012) Membrane Disruption by Antimicrobial Fatty Acids Releases Low-Molecular-Weight Proteins from Staphylococcus aureus. Journal of Bacteriology 194: 5294-5304.

41. Patman G (2015) Therapy: High-tech linolenic acid kills *Helicobacter pylori*. Nat Rev Gastroenterol Hepatol 12: 5-5.

42. Chu Y-T, Wang Y-H, Wu J-J, Lei H-Y (2010) Invasion and Multiplication of *Helicobacter pylori* in Gastric Epithelial Cells and Implications for Antibiotic Resistance. Infection and Immunity 78: 4157-4165.

43. Rogers AB, Dintzis RZ (2012) Liver and Gallbladder. In: Treuting PM, Dintzis SM, editors. Comparative Anatomy and Histology. San Diego: Academic Press. pp. 193-201.

44. Treuting PM, Valasek MA, Dintzis SM (2012) Upper Gastrointestinal Tract. In: Treuting PM, Dintzis SM, editors. Comparative Anatomy and Histology. San Diego: Academic Press. pp. 155-175.

45. Kelley DS, Siegel D, Vemuri M, Mackey BE (2007) Docosahexaenoic acid supplementation improves fasting and postprandial lipid profiles in hypertriglyceridemic men. Am J Clin Nutr 86: 324-333.

46. Taylor NS, Fox JG (2012) Animal Models of *Helicobacter*-Induced Disease: Methods to Successfully Infect the Mouse. Methods in molecular biology (Clifton, NJ) 921: 131-142.

47. Moyat M, Velin D (2014) Immune responses to *Helicobacter pylori* infection. World Journal of Gastroenterology : WJG 20: 5583-5593.

48. Algood HMS, Cover TL (2006) *Helicobacter pylori* Persistence: an Overview of Interactions between *H. pylori* and Host Immune Defenses. Clinical Microbiology Reviews 19: 597-613.

CHAPTER VII

GENERAL DISCUSSION AND FUTURE PERSPECTIVES

7.1- General Discussion

Despite the wide success of antibiotics, the treatment of *H. pylori* infection still faces significant challenges, particularly through the rapid emergence of *H. pylori* strains resistant to existing antibiotics. Current treatment regimens show a fast decline of their eradication rates, being inefficient in 20% of patients [1,2]. Alternative therapeutic approaches and treatment strategies have been developed, aiming to overcome *H. pylori* resistance strains. A series of free PUFA including linolenic acid (LA), eicosapentaenoic acid (EPA), docosahexaenoic acid (DHA) have attracted much attention as they have shown antibactericidal activities a diverse range of bacteria including *H. pylori* [3]. In addition, PUFA induce lower drug resistance in *H. pylori* than conventional antibiotics [4]. Despite promising results have been reported, the use of PUFA in inhibiting *H. pylori* remains challenging. Correia *et al.* [5] demonstrated that an omega-3 PUFA, DHA, has the ability to inhibit *H. pylori* growth *in vitro*. Concentrations of 100 μM of free DHA only decreased *H. pylori* growth, whereas concentrations higher than 250 μM were bactericidal against this bacterium. However, free DHA (50μM) efficiency in the eradication of *H. pylori* from mice gastric mucosa was lower than the standard antibiotherapy and failed in 50% of infected mice [5]. This reduced DHA efficiency *in vivo* could be related to its low stability (easy oxidation and gastric degradation), its low penetration through the mucus layer, its low residence time in the stomach and its low bioavailability at the infection site [6,7]. Moreover, it was described that the acidic pH in the stomach decreases PUFA solubility, making these molecules ineffective [3]. Therefore, the development of a DHA local delivery system could be essential to overcome these challenges, namely to protect DHA from gastric oxidation and degradation.

The main goal of this work was the development of an antibiotic-free engineered system for the treatment of *H. pylori* gastric infection. The strategy is based on the development of lipid nanoparticles to create a DHA delivery system that after oral administration will kill *H. pylori* at the infection site.

Several types of nanoparticles, such as polymeric, inorganic, dendrimers and lipid-based colloidal carriers can be used for drug encapsulation. Taking into consideration the lipophilic character of DHA, lipid nanoparticles were chosen due to their i) ability to incorporate hydrophobic and lipophilic drugs into their lipid matrix, ii) biocompatibility and safety of lipids used for their production (FDA approval), and iii) low cytotoxicity [8-11]. The increasing interest in lipid nanoparticles has been also associated with their production in absence of organic solvents, and the low cost of their large-scale production comparing to other types of nanoparticles [8,12-16].

As a first approach, solid lipid nanoparticles (SLN) without DHA (unloaded-SLN) were produced and optimized in terms of size, polydispersion, and reproducibility (Appendix 1). During optimization of the SLN production, different reagents (solid lipids with different melting points and surfactants) and reaction conditions (ratio between lipids and surfactants, homogenization time and sonication time and intensity) were tested. The first exclusion criterion was nanoparticles size, since, according to Lin *et al.,* nanoparticles with sizes between 130 and 300 nm are able to reach *H. pylori* at the infection site, infiltrate cell-cell junctions and interact with *H. pylori* in intercellular spaces [17]. Polydispersion index values greater than 0.5 were also an exclusion criterion. Due to micelles formation when Tween®80 was used, SLN optimizations were proceeded using Tween®60.

Due to the lack of reproducibility during SLN production, another type of lipid nanoparticles, nanostructured lipid carriers (NLC), were optimized as a second approach. NLC differ from SLN by the integration of a liquid lipid that is blended to solid lipid and incorporated in the core of nanoparticle [8,9]. The major advantage of NLC over SLN is that many drugs like DHA, are more soluble in a liquid lipid than in a solid lipid, leading to a higher loading capacity and controlled release of drugs [18]. Here, the production of NLC was firstly optimized using the solid lipids that were selected during the optimization of SLN (cetyl palmitate and Precirol®ATO5). NLC production was optimized basing on Neves *et al*. study [19], using Miglyol®812 as liquid lipid and Tween®60 as surfactant. The proportion between solid and liquid lipid and surfactant were optimized until NLC, with size around 200 nm and charge around -30 mV, was obtained. Negatively charged around -30 mV is an indicator of colloidal stability maintained by electrostatic repulsion [20-22]. Comparing to SLN, NLC production was more reproducible in terms of size and charge, independently of solid lipid used.

DHA was then incorporated into NLC prepared using cetyl palmitate or Precirol®ATO5 as solid lipid (Appendix 2). NLC size and charge were dependent on the amount of DHA used during NLC production. DHA entrapment efficiency was higher than 52% for all NLC produced, independently of solid lipid used. However, NLC prepared with Precirol®ATO5 presented higher stability and higher DHA release than NLC prepared with cetyl palmitate. Moreover, in opposite

to cetyl palmitate, Precirol®ATO5 is FDA approval, have a GRAS status, and is already used in pharmaceutical products, namely Serenelfi®. Therefore, NLC prepared with Precirol®ATO5 were used in all biological studies described in this thesis.

In the subsequent part of study, DHA-loaded NLC, containing around 60% of DHA (NLC produced with 2% v/v) in its matrix, with ~302 nm of size and negative charge (~28 mV) were successfully produced and characterized using several techniques (DLS, ELS, NanoSight®, cryo-SEM, DSC). Unloaded-NLC with ~211 nm of size and negative charge (~28 mV) were also produced as a control to DHA incorporation. These NLC are suitable for oral administration, since both NLC were stable in simulated gastric fluid (pH 1.2) over 3 hours.

We demonstrated that DHA-loaded NLC were bactericidal against *H. pylori* J99 (human) and SS1 (mouse-adapted) strains. DHA loading improved bactericidal activity, since DHA-loaded NLC were bactericidal at all concentrations tested (10 to 500 μM), although free DHA was only bactericidal at concentrations higher than 100 μM. However, we also observed that unloaded-NLC, used as control of DHA encapsulation, were also bactericidal to *H. pylori* at all concentrations tested although in a slower rate than in the presence of DHA. This effect of unloaded-NLC is not associated with individual compounds used in NLC production (Precirol®ATO5, Tween®60 and Miglyol®812), because when they alone are not bactericidal at concentrations used during our *H. pylori* experiments [23-26], demonstrating that bactericidal effect may be related with nanoparticles 3D format.

NLC time-killing of *H. pylori* was dependent on NLC concentration and on the presence DHA. The bactericidal effect of 0.5% (v/v) DHA-loaded NLC (containing 10 μM DHA) against *H. pylori* J99 was observed after 6h, while for the same amount of unloaded-NLC this bactericidal effect was only observed after 18h. A faster bactericidal effect was demonstrated for higher NLC concentrations. DHA-loaded NLC at 2.5% v/v (containing 50 μM DHA) were bactericidal in 30 min, while any effect was observed for the same concentration of free DHA and unloaded-NLC. It important to notice, this concentration is not toxic to human gastric cells, and it is safe and well-tolerated by mouse gastric mucosa. Moreover, due to this shorter killing time (30 min), it is not probable that bacteria develop resistance to these nanoparticles, because *H. pylori* need to 2.5 h for its complete replication cycle [3,27].

H. pylori adopt two major morphologies, spiral and coccoid form. *H. pylori* in coccoid form can play a critical role in disease transmission (for example oral-oral or oral-fecal routes) and subsequent treatment [28,29]. The coccoid form of the bacteria was also show to contribute to the development of relapses following antimicrobial therapy in *H. pylori* infection [30]. In comparison with linolenic acid liposome [31] that bacteria adopt both morphologies, in our study, the morphology transformation of *H. pylori* from spiral form to coccoid form was not observed. *H. pylori* treated with NLC shown a bacillary form, while Correia *et al* [5] reported that *H. pylori* treated with free DHA displayed coccoid form which was associated with lower bacteria viability. These results suggest that the morphological transition of *H. pylori* from spiral to coccoid form may be prevented by the fast bactericidal effect of these NLC.

The mechanisms of action of NLC (unloaded and DHA-loaded) against *H. pylori* were also studied by us. Results showed that both NLC were able to bind to *H. pylori* membrane, increasing their permeability (outer and inner membrane), which leads to the disruption of membrane integrity and bacteria killing. This increase of membrane permeability could be related with nanoparticles integration into the bacteria membrane, as described by Jung *et al*. [32] for liposomes containing LA. Moreover, it is known that free DHA is rapidly incorporated into phospholipids of the cell membrane and mitochondria. Due to its incorporation into mitochondria, free DHA has a larger effect in bioenergetics proprieties, namely ATP production, H^+ permeability and membrane potential [33]. Free DHA concentrations higher than 100 μM have a significant impact on *H. pylori* ATP production, decreasing drastically its metabolic activity as well as in their protein profile [34]. This DHA effect can suggest that when DHA is released from NLC, beyond to increase membrane permeability, it may also be incorporated into bacteria mitochondria, which can explain the faster bactericidal effect of DHA-loaded NLC than unloaded-NLC.

All developed NLC (unloaded and DHA-loaded) are negatively charged and have on their surface the hydrophilic moiety of the non-ionic surfactant used in nanoparticle production. This non-ionic surfactant may decrease the surface tension between NLC and bacteria enabling their interaction with proteins and lipids of *H. pylori* membrane [35], allowing their adhesion and entry in bacteria membrane.

Using gold nanoparticles loaded into NLC, it was visualized by TEM that, unloaded-NLC were internalized by bacteria, being found in bacterial periplasmic space after 3h (promoting an increase of periplasmic space and separation between the outer and inner membrane) and in the cytoplasmic after 12h. At the same time, a decrease of bacteria thickness was observed by AFM. This NLC internalization associated with changes in the outer and inner bacteria membrane allows the leakage of bacterial cytoplasmic content as showed by SEM and AFM. These results suggest that NLC enter as a 3D particle in periplasmic space and, as DHA-loaded NLC is more unstable than unloaded-NLC, DHA is released over there, allowing a faster bacterial membrane disruption and consequently the leakage of cytoplasm and bacteria death. This entering of NLC on bacteria membrane may be helped by the presence of surfactant on NLC surface that may solubilize sections in the bacteria membrane, disrupting them. The faster bactericidal activity of DHA-loaded NLC could be also explained by the decrease of pH related with DHA release into bacteria. Similar to fatty acids and metronidazole mechanism, DHA may also inhibit bacterial growth by creating an acidic environment in the cytoplasm that damages pH-sensitive intracellular enzymes or amino acid transporters [36]. Such antibacterial activities are physical, broad and unspecific, which may explain a lower frequency of resistance development observed when bacteria are treated with fatty acids.

Although their bactericidal effect, NLC are not cytotoxic to human gastric adenocarcinoma cells (MKN45 cell line) at bactericidal concentrations, namely up to 2.5% v/v NLC (50 μM DHA). As expected, DHA-loaded NLC decreases metabolic activity of cells at 100 μM of DHA, as well is reported for free DHA [34,37].

Attending that the main goal of this work is the development of an antibiotic-free alternative to fight *H. pylori* gastric infection, an exploratory *in vivo* study was performed using 1.25% v/v (25 μM DHA) of DHA-loaded NLC, to evaluate nanoparticles toxicity and dosage for the treatment of *H. pylori*-infected mice. Histological sections of stomach and liver revealed no changes in gastric morphology and a normal architecture of gastric mucosa. Regarding treatment efficiency, mice treated with 1.25% v/v (25 μM DHA) of DHA-loaded NLC had a reduction of 63.8% of *H. pylori* colonization. However, this reduction was not statistically significant compared with untreated mice.

Taking these results into consideration, the same assay was performed using a higher dosage of DHA-loaded NLC (2.5% v/v [50 μM of DHA]). This concentration is within the range of concentration reachable with diet in the human stomach for any PUFA [38]. An enhance of efficiency was observed, obtaining a reduction of *H. pylori* colonization of 92.6% with treatment of DHA-loaded NLC and 82.5% with unloaded-NLC, compared with untreated mice. This reduction of *H. pylori* colonization was higher than 50% reduction reported by Correia *et al* [5]. However, at the end of treatment, four mice (in twelve) were not infected in the untreated *H. pylori*-infected group (group that only received water). This result may be related to several factors associated with *H. pylori* SS1 strain that can reduce the infection reproducibility in the laboratory. Culture viability, frequency of dosing or volume of inoculum, and excessive passage of the isolates may affect *H. pylori* SS1 strain colonization and virulence [39]. Another explanation is related to the immunity of mice to *H. pylori*. Despite C57BL/6 mice used are specific-pathogen-free, its persistent *H. pylori* infection over more than one month (one month of infection establishment plus 14 days of treatment), may result in an *H. pylori* clearance due to immunization mice that began between 8 to 16 weeks of exposure to *H. pylori* [40-42]. This reduction in bacterial load is associated with gastric inflammation that subsides over time [42]. Unloaded-NLC treatment was less efficient *in vivo* than DHA-loaded NLC, which could be related to their low efficiency *in vitro*.

The concentration of NLC (2.5% v/v) given to mice in our experiments are also within safe and well tolerated range of concentrations with no toxic effect observed maintaining a gastric mucosa without changes in the gastric morphology and normal architecture [43,44]. These results are in agreement with several clinical trials that have used DHA supplementation at higher doses with no reports of toxicological effects [45,46]

In the subsequent part of this study, the selectivity of unloaded-NLC to fight *H. pylori* was evaluated using other bacteria with different structural (Gram-positive *vs* Gram-negative) and morphological (rod *vs* spherical) features and different surface charge. Gastrointestinal bacteria, such as *Lactobacillus casei* and *Escherichia coli*, were used. NLC were also tested on pathogenic bacteria from skin and mucosae, namely *Staphylococcus epidermidis* and *Staphylococcus aureus*, trying to find a novel application of these unloaded-NLC, as a topical application. Results demonstrated that unloaded-NLC did not affect the growth of other bacteria tested, except in *S. aureus*, where unloaded-NLC at 5% (v/v) were able to decrease bacteria

growth after 6h, although without a bactericidal effect. However, this concentration was cytotoxic for human gastric adenocarcinoma cells.

One explanation for NLC selectivity to *H. pylori* could be associated to their unique and specific features, such as their LPS that have an unusual cellular composition based on fatty acid, lipid profile and molecular mimicry of Lewis antigens [47,48]. Moreover, *H. pylori* is cholesterol-dependent [49,50]. A depletion of cholesterol levels in epithelial cells, leading to a lower synthesis of cholesteryl glucosides by *H. pylori* and interfere in the bacteria survival and their ability to colonize, namely in the translocation of *H. pylori* virulence factors, such as vacuolating cytotoxin (VacA) and cytotoxin-associated gene A (CagA) [51,52].

Overall, we demonstrated that NLC can profoundly change *H. pylori* growth, survival, and morphology. The abovementioned changes decrease *H. pylori in vitro* and reduce *H. pylori* mice gastric colonization, opening new perspectives to the management of this bacterial infection. Altogether, these results highlight that NLC, unloaded and DHA-loaded, should be explored as a new alternative treatment for *H. pylori* eradication.

7.2- Future Perspectives

In the follow-up of the work described in this thesis, we will repeat the *in vivo* study, testing the same and higher concentration than the used before in comparison with standard antibiotic treatment. In parallel, it would be very interesting to study the retention time of NLC and their ability to cross mucus layer. If NLC would have low retention time, we can coat NLC using a mucoadhesive polymer, as chitosan, in order to increase their retention time in mouse stomach and/or develop a pH sensitive delivery system.

Another issue that needs further elucidation is evaluation of NLC effect against isolates of *H. pylori* strains from patients resistant to standard antibiotic therapies and to evaluate if NLC can induce bacteria resistance.

Biocompatibility of NLC using normal gastric cells instead of gastric adenocarcinoma cell line used in this study and intestinal cells should be tested, aiming to evaluate if NLC may have a side-effect to this type of cells.

Despite free DHA activity against *E. coli* (at concentration higher than 1mM), DHA-loaded NLC safety to human microbiome will be tested, using *E. coli,* and *Lactobacillus.*

Additional experimentation is needed to clarify the mechanisms of action of DHA effects on bacteria membranes as well as, mechanism of action of NLC as a 3D particle. This additional experimentation could be done by biophysics assays using membrane models that mimic the mammalian and bacterial lipid composition.

Finally, gerbils could be considered in animal experiments, since they are known for mimicking human's gastric progression of the gastric disease, allowing a more broad knowledge of NLC effects.

References

1. Patman G (2015) Therapy: High-tech linolenic acid kills *Helicobacter pylori*. Nat Rev Gastroenterol Hepatol 12: 5-5.

2. Vakil N (2006) Helicobacter pylori Treatment: A Practical Approach. Am J Gastroenterol 101: 497-499.

3. Desbois AP, Smith VJ (2010) Antibacterial free fatty acids: activities, mechanisms of action and biotechnological potential. Appl Microbiol Biotechnol 85: 1629-1642.

4. Petschow BW, Batema RP, Ford LL (1996) Susceptibility of *Helicobacter pylori* to bactericidal properties of medium-chain monoglycerides and free fatty acids. Antimicrob Agents Chemother 40: 302-306.

5. Correia M, Michel V, Matos AA, Carvalho P, Oliveira MJ, et al. (2012) Docosahexaenoic acid inhibits *Helicobacter pylori* growth in vitro and mice gastric mucosa colonization. PLoS One 7: e35072.

6. Kaushik P, Dowling K, Barrow CJ, Adhikari B (2015) Microencapsulation of omega-3 fatty acids: A review of microencapsulation and characterization methods. Journal of Functional Foods 19, Part B: 868-881.

7. Kralovec JA, Zhang S, Zhang W, Barrow CJ (2012) A review of the progress in enzymatic concentration and microencapsulation of omega-3 rich oil from fish and microbial sources. Food Chemistry 131: 639-644.

8. Martins S, Sarmento B, Ferreira DC, Souto EB (2007) Lipid-based colloidal carriers for peptide and protein delivery--liposomes versus lipid nanoparticles. Int J Nanomedicine 2: 595-607.

9. Beloqui A, Solinis MA, Rodriguez-Gascon A, Almeida AJ, Preat V (2016) Nanostructured lipid carriers: Promising drug delivery systems for future clinics. Nanomedicine 12: 143-161.

10. Battaglia L, Gallarate M (2012) Lipid nanoparticles: state of the art, new preparation methods and challenges in drug delivery. Expert Opin Drug Deliv 9: 497-508.

11. Das S, Chaudhury A (2011) Recent advances in lipid nanoparticle formulations with solid matrix for oral drug delivery. AAPS PharmSciTech 12: 62-76.

12. Carbone C, Leonardi A, Cupri S, Puglisi G, Pignatello R (2014) Pharmaceutical and biomedical applications of lipid-based nanocarriers. Pharm Pat Anal 3: 199-215.

13. Battaglia L, Gallarate M (2012) Lipid nanoparticles: state of the art, new preparation methods and challenges in drug delivery. Expert Opinion on Drug Delivery 9: 497-508.

14. Müller RH, Mäder K, Gohla S (2000) Solid lipid nanoparticles (SLN) for controlled drug delivery – a review of the state of the art. European Journal of Pharmaceutics and Biopharmaceutics 50: 161-177.

15. Beloqui A, Solinis MA, Delgado A, Evora C, Isla A, et al. (2014) Fate of nanostructured lipid carriers (NLCs) following the oral route: design, pharmacokinetics and biodistribution. J Microencapsul 31: 1-8.

16. Muller RH, Shegokar R, Keck CM (2011) 20 years of lipid nanoparticles (SLN and NLC): present state of development and industrial applications. Curr Drug Discov Technol 8: 207-227.

17. Lin Y-H, Chang C-H, Wu Y-S, Hsu Y-M, Chiou S-F, et al. (2009) Development of pH-responsive chitosan/heparin nanoparticles for stomach-specific anti-*Helicobacter pylori* therapy. Biomaterials 30: 3332-3342.

18. Tamjidi F, Shahedi M, Varshosaz J, Nasirpour A (2013) Nanostructured lipid carriers (NLC): A potential delivery system for bioactive food molecules. Innovative Food Science & Emerging Technologies 19: 29-43.

19. Neves AR, Lucio M, Martins S, Lima JL, Reis S (2013) Novel resveratrol nanodelivery systems based on lipid nanoparticles to enhance its oral bioavailability. Int J Nanomedicine 8: 177-187.

20. Cho EJ, Holback H, Liu KC, Abouelmagd SA, Park J, et al. (2013) Nanoparticle Characterization: State of the Art, Challenges, and Emerging Technologies. Molecular Pharmaceutics 10: 2093-2110.

21. Lin P-C, Lin S, Wang PC, Sridhar R (2014) Techniques for physicochemical characterization of nanomaterials. Biotechnology Advances 32: 711-726.

22. Clogston JD, Patri AK (2011) Zeta Potential Measurement. In: McNeil SE, editor. Characterization of Nanoparticles Intended for Drug Delivery. Totowa, NJ: Humana Press. pp. 63-70.

23. Cerreto F, Paolicelli P, Cesa S, Abu Amara HM, D'Auria FD, et al. (2013) Solid lipid nanoparticles as effective reservoir systems for long-term preservation of multidose formulations. AAPS PharmSciTech 14: 847-853.

24. Blackburn P (1997) Polysorbate-containing compositions and their use against *Helicobacter*. European Patent Office WO/1997/036600.

25. Santucci A, Figura N, Spreafico A, Cavallo G, Marcolongo RF (2013) Compositions for treating *Helicobacter pylori* infection. European Patent Office WO2011IT00175.

26. Seabra CL, Nunes C, Gomez-Lazaro M, Correia M, Machado JC, et al. (2017) Docosahexaenoic acid loaded lipid nanoparticles with bactericidal activity against *Helicobacter pylori*. International Journal of Pharmaceutics 519: 128-137.

27. Chu Y-T, Wang Y-H, Wu J-J, Lei H-Y (2010) Invasion and Multiplication of *Helicobacter pylori* in Gastric Epithelial Cells and Implications for Antibiotic Resistance. Infection and Immunity 78: 4157-4165.

28. Kusters JG, van Vliet AHM, Kuipers EJ (2006) Pathogenesis of *Helicobacter pylori* Infection. Clinical Microbiology Reviews 19: 449-490.

29. Andersen LP, Rasmussen L (2009) *Helicobacter pylori*– coccoid forms and biofilm formation. FEMS Immunology & Medical Microbiology 56: 112-115.

30. She F-F, Su D-H, Lin J-Y, Zhou L-Y (2001) Virulence and potential pathogenicity of coccoid *Helicobacter pylori* induced by antibiotics. World Journal of Gastroenterology 7: 254-258.

31. Obonyo M, Zhang L, Thamphiwatana S, Pornpattananangkul D, Fu V, et al. (2012) Antibacterial Activities of Liposomal Linolenic Acids against Antibiotic-Resistant *Helicobacter pylori*. Molecular Pharmaceutics 9: 2677-2685.

32. Jung SW, Thamphiwatana S, Zhang L, Obonyo M (2015) Mechanism of antibacterial activity of liposomal linolenic acid against *Helicobacter pylori*. PloS one 10: e0116519.

33. Khulusi S, Ahmed HA, Patel P, Mendall MA, Northfield TC (1995) The effects of unsaturated fatty acids on *Helicobacter pylori in vitro*. J Med Microbiol 42: 276-282.

34. Correia M, Michel V, Osorio H, El Ghachi M, Bonis M, et al. (2013) Crosstalk between *Helicobacter pylori* and gastric epithelial cells is impaired by docosahexaenoic acid. PLoS One 8: e60657.

35. Ishikawa S, Matsumura Y, Katoh-Kubo K, Tsuchido T (2002) Antibacterial activity of surfactants against *Escherichia coli* cells is influenced by carbon source and anaerobiosis. Journal of Applied Microbiology 93: 302-309.

36. Knapp HR, Melly MA (1986) Bactericidal effects of polyunsaturated fatty acids. J Infect Dis 154: 84-94.

37. Lee SE, Lim JW, Kim H (2009) Activator protein-1 mediates docosahexaenoic acid-induced apoptosis of human gastric cancer cells. Ann N Y Acad Sci 1171: 163-169.

38. Thompson L, Cockayne A, Spiller RC (1994) Inhibitory effect of polyunsaturated fatty acids on the growth of *Helicobacter pylori*: a possible explanation of the effect of diet on peptic ulceration. Gut 35: 1557-1561.

39. Taylor NS, Fox JG (2012) Animal Models of *Helicobacter*-Induced Disease: Methods to Successfully Infect the Mouse. Methods in molecular biology (Clifton, NJ) 921: 131-142.

40. Moyat M, Velin D (2014) Immune responses to *Helicobacter pylori* infection. World Journal of Gastroenterology : WJG 20: 5583-5593.

41. Algood HMS, Cover TL (2006) *Helicobacter pylori* Persistence: an Overview of Interactions between *H. pylori* and Host Immune Defenses. Clinical Microbiology Reviews 19: 597-613.

42. Garhart CA, Redline RW, Nedrud JG, Czinn SJ (2002) Clearance of *Helicobacter pylori* Infection and Resolution of Postimmunization Gastritis in a Kinetic Study of Prophylactically Immunized Mice. Infection and Immunity 70: 3529-3538.

43. Rogers AB, Dintzis RZ (2012) Liver and Gallbladder. In: Treuting PM, Dintzis SM, editors. Comparative Anatomy and Histology. San Diego: Academic Press. pp. 193-201.

44. Treuting PM, Valasek MA, Dintzis SM (2012) Upper Gastrointestinal Tract. In: Treuting PM, Dintzis SM, editors. Comparative Anatomy and Histology. San Diego: Academic Press. pp. 155-175.

45. Kelley DS, Siegel D, Vemuri M, Mackey BE (2007) Docosahexaenoic acid supplementation improves fasting and postprandial lipid profiles in hypertriglyceridemic men. Am J Clin Nutr 86: 324-333.

46. Duggan AE, Atherton JC, Cockayne A, Balsitis M, Evison S, et al. (1997) Clarification of the link between polyunsaturated fatty acids and *Helicobacter pylori*-associated duodenal ulcer disease: a dietary intervention study. Br J Nutr 78: 515-522.

47. Morales-Guerrero SE, Mucito-Varela E, Aguilar-Gutiérrez GR, Lopez-Vidal Y, Castillo-Rojas G (2013) The Role of CagA Protein Signaling in Gastric Carcinogenesis — CagA Signaling in Gastric Carcinogenesis.

48. O'Toole PW, Clyne M (2001) Cell Envelope.

49. McGee DJ, George AE, Trainor EA, Horton KE, Hildebrandt E, et al. (2011) Cholesterol enhances *Helicobacter pylori* resistance to antibiotics and LL-37. Antimicrob Agents Chemother 55: 2897-2904.

50. Correia M, Casal S, Vinagre J, Seruca R, Figueiredo C, et al. (2014) *Helicobacter pylori*'s cholesterol uptake impacts resistance to docosahexaenoic acid. Int J Med Microbiol 304: 314-320.

51. Lai C-H, Chang Y-C, Du S-Y, Wang H-J, Kuo C-H, et al. (2008) Cholesterol Depletion Reduces *Helicobacter pylori* CagA Translocation and CagA-Induced Responses in AGS Cells. Infection and Immunity 76: 3293-3303.

52. Patel HK, Willhite DC, Patel RM, Ye D, Williams CL, et al. (2002) Plasma Membrane Cholesterol Modulates Cellular Vacuolation Induced by the *Helicobacter pylori* Vacuolating Cytotoxin. Infection and Immunity 70: 4112-4123.

APPENDIX

APPENDIX 1

1. Lipid nanoparticles optimization

Lipid nanoparticles production and DHA loading were optimized in terms of size, charge, and entrapment. During the optimization process, several parameters were tested, including different solid lipid with a different melting point, different surfactants (Tween®80 and Tween®60), ratios of lipids and surfactant, time of sonication, and intensity (or amplitude) of sonication.

Table 1 summarizes the different solid lipid tested and respective melting point measured.

Table 1- Different solid lipid and respective melting point tested for lipid nanoparticles production

Solid Lipid	Melting point (ºC)
Witepsol® S51	30
Witepsol® S58	33
Witepsol® E76	37
Witepsol® E85	42
Cetyl palmitate	50
Precirol® ATO 5	56
Compritol®E ATO	70

The first choice of lipid nanoparticles was solid lipid nanoparticles (SLN), produced by hot homogenization and ultrasonication, using 4.2 mL of ultrapure water (type 1) and testing different amounts of solid lipid and surfactant (Tween®80). SLN production was firstly optimized

without DHA, using Witepsol® as solid lipid due to its melting point around 30 to 37ºC. However, SLN aggregated after cooling and two different populations: ~30 nm and higher than 300 nm to 8000 nm were identified (Table 2), probably due to the presence of micelles of surfactant.

Table 2- Production of SLN of using Witepsol® S51, S58, H32, E76 as a solid lipid, testing different mass of solid lipid and surfactant and time of sonication. Time of homogenization was the same for all SLN produced (30 s of ultra-turrax at 1200 rpm).

Parameters tested		**Solid lipid (mg)**	100	200	200
		Tween®80(mg)	20	60	80
		Sonication (min) at 80% of amplitude	2	3	3
Results of size (nm) by DLS	**Witepsol®**	**S51**	No results (aggregates)	30-300	24-825
		S58		157.5-1000	16-6439
		H32		300-1300	21-7456
		E76		60-501	21-8635

Due to persistent small sizes of SLN produced with Witepsol® solid lipid S51, S58, H32 and E76, and the high amount of micelles of Tween®80, this surfactant was substituted by Tween®60 and other solids lipids, namely Witepsol®E85, cetyl palmitate, Precirol®ATO5 and Compritol®E ATO were tested. The time of sonication was decreased to 30s in order to increase of size of SLN (Table 3).

Table 3- Characterization of SLN using Witepsol®E85, cetyl palmitate, Precirol®ATO5 and Compritol®E ATO as solid lipid, in terms of size and polydispersion index (PDI).

Parameters tested	**Solid lipid (mg)**	200	200	200
	Tween®60 (mg)	100	100	100
	Sonication (30 s) at amplitude (%)	80	70	60
Results of size (nm)[PDI] by DLS	**Witepsol®E85**	41 [0.10]	30.9 [0.33	NT
	Cetyl palmitate	85 [0.18]	139 [0.32]	245 [0.23]
	Precirol®ATO5	41 [0.36]	100 [0.18]	358 [0.20]
	Compritol®E ATO	577 [0.18]	816 [0.03]	718 [0.06]

Abbreviations: NT- non-tested; PDI- polydispersion index

Taking in consideration that nanoparticles with 130-300 nm of size are able to adhere to and infiltrate cell-cell junctions and interact locally with *H. pylori* infection in intercellular spaces [1], we selected the SLN with 245 to 718 nm of size. These SLN was produced by hot homogenization (30 s of ultra-turrax) and sonication (30s at 60% of amplitude), using 200 mg of solid lipid, 100 mg of surfactant (Tween®60) and 4.2 mL of ultrapure water. Afterward, we proceeded to DHA-loaded SLN production, using 1% v/v of DHA, and their characterization in

terms of size, polydispersion, and zeta potential. Two independent assays were performed in order to evaluate the reproducibility of DHA-loaded SLN. Table 4 summarizes two independent productions of unloaded and DHA-loaded SLN using three different solid lipids.

Table 4- Characterization in terms of size, polydispersion index (PDI) and charge of unloaded and DHA-loaded SLN of cetyl palmitate, Precirol®ATO5, and Compritol®E ATO.

			SLN		
		Assay	**Size (nm)**	**PDI**	**Zeta potential (mV)**
unloaded	**Cetyl palmitate**	1	26	0.24	-1.72
		2	40	0.26	+10.87
	Precirol®ATO5	1	727	0.08	-7.10
		2	550	0.36	-14.76
	Compritol®E ATO	1	580	0.085	-12.80
		2	1040	0.23	+10.87
DHA-loaded	**Cetyl palmitate**	1	55	0.27	+11.58
		2	186	0.15	+13.20
	Precirol®ATO5	1	814	0.05	-1.62
		2	337	0.39	-18.08
	Compritol®E ATO	1	742	0.10	-2.70
		2	337	0.39	-18.08

Due to the lack of reproducibility during the production of SLN, with and without DHA, nanostructured lipid carriers (NLC) were produced. It is known that NLC differ from SLN by the inclusion of a liquid lipid that is incorporated into their solid structure. Liquid lipid confers to the nanoparticle a less ordered crystalline structure, greater physical stability and avoids drug expulsion during storage [2,3]. The conditions of NLC production was optimized basing on Neves *et al* study [4] and the previous results obtained during SLN optimization. Thus, NLC were produced using cetyl palmitate or Precirol®ATO5 as solid lipid, Miglyol®812 as liquid lipid and Tween®60 as surfactant. Nevertheless, Compritol®E ATO was not used as solid lipid for NLC production due to its high melting point that would avoid DHA released at 37ºC.

NLC were produced using 200 mg of solid lipid, 90 mg of liquid lipid and 60 mg of Tween®60. Figure 1 demonstrated that NLC can be produced with higher reproducibility in terms of size and charge than SLN (Figure 1).

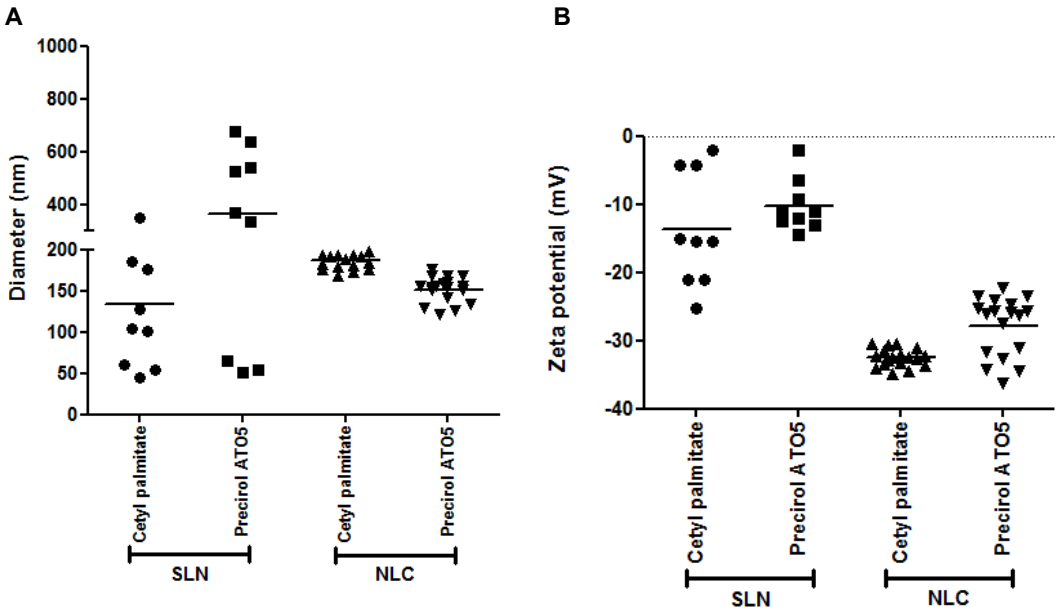

Figure 1- Characterization of unloaded-SLN and NLC of cetyl palmitate and Precirol® ATO5 in terms of size and charge.

After NLC optimization, DHA loading was performed using cetyl palmitate and Precirol®ATO5 as a solid lipid as described in Appendix 2 and Chapter IV, respectively.

References

1. Lin Y-H, Chang C-H, Wu Y-S, Hsu Y-M, Chiou S-F, et al. (2009) Development of pH-responsive chitosan/heparin nanoparticles for stomach-specific anti-*Helicobacter pylori* therapy. Biomaterials 30: 3332-3342.

2. Martins S, Sarmento B, Ferreira DC, Souto EB (2007) Lipid-based colloidal carriers for peptide and protein delivery--liposomes versus lipid nanoparticles. Int J Nanomedicine 2: 595-607.

3. Beloqui A, Solinis MA, Rodriguez-Gascon A, Almeida AJ, Preat V (2016) Nanostructured lipid carriers: Promising drug delivery systems for future clinics. Nanomedicine 12: 143-161.

4. Neves AR, Lucio M, Martins S, Lima JL, Reis S (2013) Novel resveratrol nanodelivery systems based on lipid nanoparticles to enhance its oral bioavailability. Int J Nanomedicine 8: 177-187.

APPENDIX 2

2. Bactericidal effect of nanostructured lipid carriers composed of cetyl palmitate solid lipid

During this work the production and characterization of NLC, with and without DHA, were firstly optimized using cetyl palmitate as solid lipid, and Miglyol®812 as liquid lipid and Tween®60 as surfactant. The bacterial activity and biocompatibility were also evaluated as described in Chapter IV.

This appendix shows a comparison between NLC prepared with cetyl palmitate (NLC_CP) and Precirol®ATO5 NLC (NLC_P).

In terms of characterization, the size and charge of NLC_CP change with the incorporation of different DHA concentrations (Figure 2A). However, a similar DHA loading and entrapment was observed independently of solid lipids used on NLC production. A higher DHA entrapment efficiency was obtained when NLC was produced with 2% v/v of DHA (Figure 2B).

NLC stability was followed by measuring the change of NLC size and charge after their storage in aqueous solution up to 8 weeks (2 months) at 4ºC and 20ºC. As shown in Figure 3, NLC_CP were not stable, since it was observed alterations in their size after 1 week of storage, independently of the temperature. However, the surface zeta potential of DHA-loaded NLC_CP was only maintained during 1 week, independently of the temperature. These results suggest that Precirol®ATO5 confer more stability to NLC than cetyl palmitate.

Concerning the DHA release profile, studies were performed in bacteria liquid medium (BB + 10% FBS medium), which is the medium used during NLC bactericidal evaluation. Figure 4 shows that DHA was released in slow rate from DHA-loaded NLC_CP (22%) than DHA-loaded NLC_P (40%) after 3h.

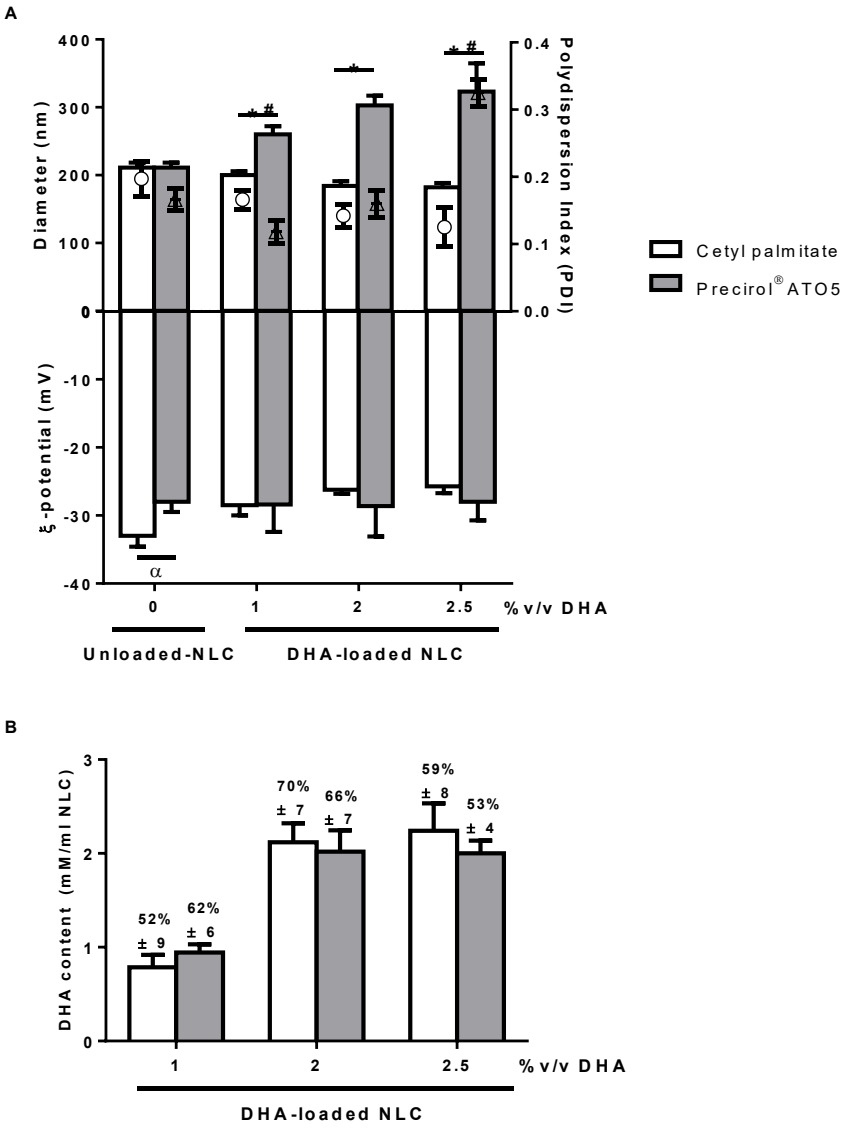

Figure 2- (**A**) NLC were characterized in terms of diameter (bars), polydispersion index (dots) and charge surface (zeta potential) (bars) performed using dynamic light scattering at 37ºC. $^{*, \#, \alpha}$ $p < 0.05$; statically significant differences of NLC of cetyl palmitate and Precirol®ATO5, in terms of diameter, PDI and zeta potential, respectively (Kruskal-Wallis test). (**B**) NLC characterization in terms of DHA content (bars) and entrapment efficiency (values in percentage). No statically differences were observed (Kruskal-Wallis test). All data is reported as the mean ± standard deviation (n = 3).

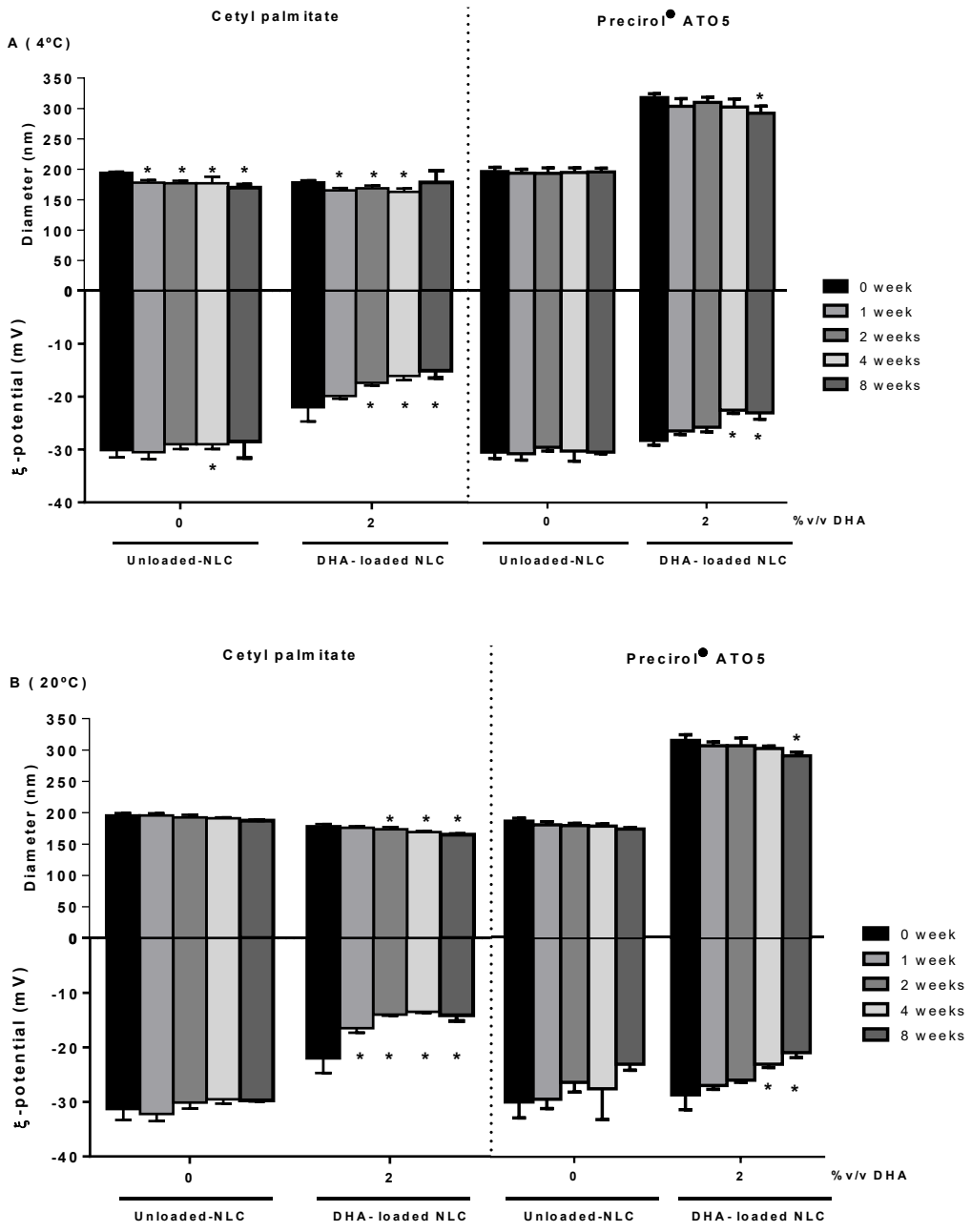

Figure 3- Storage time effect regarding diameter and charge on unloaded-NLC and 2% DHA-loaded NLC produced with cetyl palmitate and Precirol®ATO5 in water at (**A**) 4ºC and (**B**) 20ºC. Data is reported as the mean ± standard deviation (n = 3). *Statistically significance different from the same NLC at day 0 ($p < 0.05$; Kruskal-Wallis test).

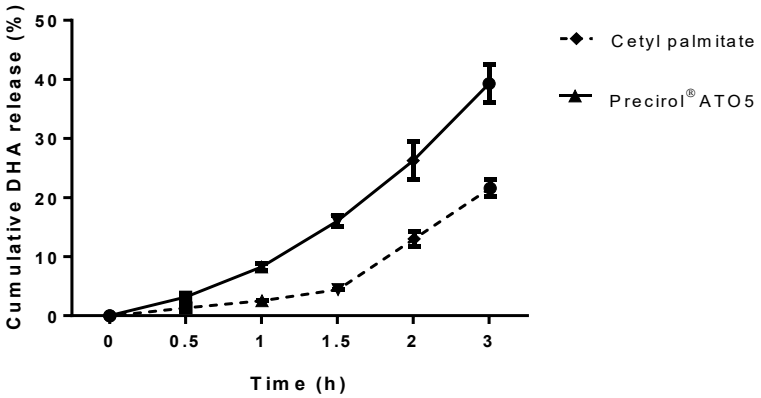

Figure 4- *In vitro* release curve of DHA from 2% DHA-loaded NLC produced with cetyl palmitate and Precirol®ATO5 in bacteria medium (Brucella-broth + 10% FBS medium) during 3 h.

Figure 5 shows the effect of NLC_CP (unloaded and DHA-loaded) on *H. pylori* J99 growth. Both NLC_CP were bactericidal against *H. pylori,* however DHA-loaded NLC_CP (Figure 5A) had a faster bactericidal activity than unloaded-NLC_CP (Figure 5A). Figure 5B also demonstrated that DHA-loaded NLC_CP had a similar bactericidal profile against *H. pylori J99* strain than DHA-loaded NLC_P, in all concentrations tested since they were able to kill 99.9% (>3 logs) bacteria in 24 h of incubation.

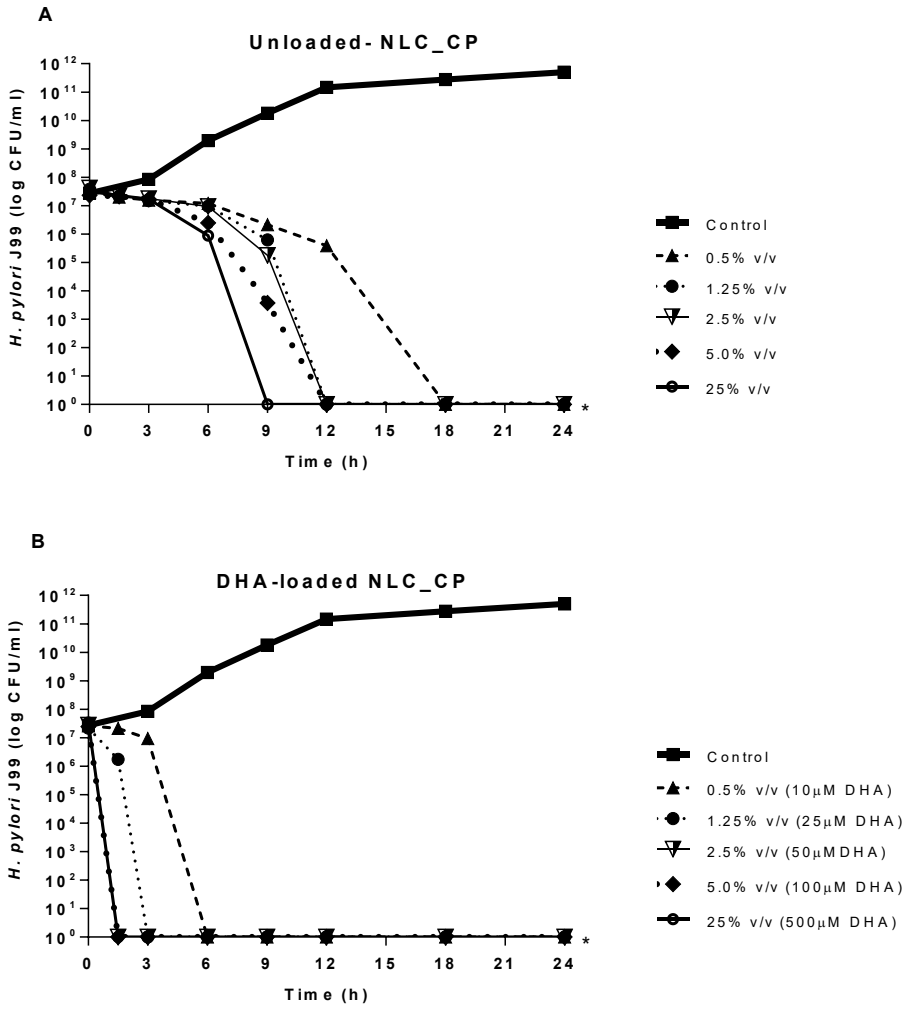

Figure 5- *H. pylori* J99 growth over 24 h in the presence of increasing concentrations of (**A**) unloaded-NLC_CP (cetyl palmitate NLC) and (**B**) 2% v/v DHA-loaded NLC_CP. Data is expressed as mean ± standard deviation (n = 3). * $p < 0.05$, refers to significant differences in *H. pylori* growth between control (bacteria untreated) and unloaded or DHA-loaded NLC (Kruskal-Wallis test).

The effect of NLC_CP on human gastric adenocarcinoma cells viability and lysis determined by MTT (Figure 6A) and LDH (Figure 6B) assays, respectively was determined as previously described in Chapter IV. Figure 6A demonstrated that NLC_CP had a higher reduction in cell viability than NLC_P, independently of concentration used. A well as observed with NLC_P, a severe reduction in cell viability was observed when MKN45 cells were exposed to the highest concentration of DHA-loaded NLC tested (5.0% corresponding to 100 mM DHA). In relation to the effect of NLC on gastric cell lysis (Figure 6B), a lower damage on the cell was observed for NLC_CP comparing to NLC_P. No toxicity was observed for NLC concentration up to 2.5% (DHA-loaded NLC). High toxicity was observed for 5.0% of DHA-loaded NLC (100 μM DHA). These results suggest that NLC_CP decrease the cell viability on human gastric cells, but they does not damage to cells.

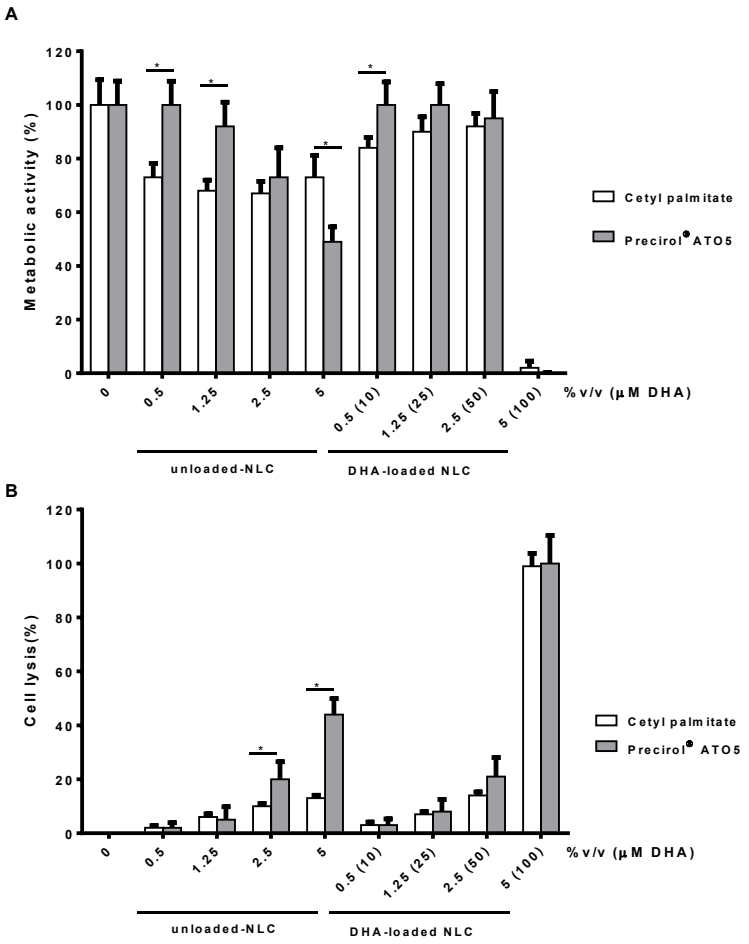

Figure 6- MKN45 gastric carcinoma cell line (**A**) viability and (**B**) cytotoxicity were assessed by the MTT and LDH assays, respectively, after 24 h of exposure to different concentrations of unloaded and DHA-loaded NLC produced with cetyl palmitate and Precirol®ATO5. Data is reported as mean ± standard deviation (n = 3). * Statically significant differences of MKN45 gastric cells treated with cetyl palmitate NLC between Precirol®ATO5 NLC ($p < 0.05$; Kruskal-Wallis test).

APPENDIX 3

3. Patent: Specific bactericidal activity of unloaded-nanostructured lipid carriers against *Helicobacter pylori*

Attending to unexpected effect of unloaded-NLC and their specificity to fight *H. pylori* growth *in vitro*, without affecting human microbiota, we submitted a national patent, opening a new perspective for the development of an antibiotic-free treatment against *H. pylori* gastric infection.

inpi instituto nacional da propriedade industrial

Campo das Cebolas - 1149-035 Lisboa - Portugal
Tel: +351 218818100 / Linha Azul: 808 200689 / Fax: +351 218875308 / Fax: +351 218860066 / E-mail: atm@inpi.pt / www.inpi.pt

Nº	CÓDIGO	DATA E HORA DE RECEÇÃO	MODALIDADE	PROCESSO RELACIONADO
20161000042469	0198	2016/06/28-19:44:57	PAT	

PEDIDO DE PATENTE, MODELO DE UTILIDADE OU
DE TOPOGRAFIA DE PRODUTOS SEMICONDUTORES

1 REQUERENTES

Código **Nacionalidade** PORTUGUESA
Nome INEB - INSTITUTO NACIONAL DE ENGENHARIA BIOMÉDICA
Endereço RUA ALFREDO ALLEN, 208
Localidade PORTO **Código Postal** 4200-135
Telefone 220408800 **Telemóvel** 220408800 **Fax**
E-mail INFO@INEB.UP.PT
Atividade (CAE)
NIF 502312220

Código 340787 **Nacionalidade** PORTUGUESA
Nome UNIVERSIDADE DO PORTO
Endereço PRAÇA GOMES TEIXEIRA, S/N, 4º, S. 463
Localidade PORTO **Código Postal** 4099-002
Telefone 220 408 077 **Telemóvel** **Fax** 220 408 378
E-mail UPIN@REIT.UP.PT
Atividade (CAE)
NIF

Tipo de Representação Representante legal da entidade
Nome FERNANDO JORGE MONTEIRO **Código**
Endereço RUA ALFREDO ALLEN, 208
Localidade PORTO **Código Postal** 4200-135
Telefone 220408800 **Telemóvel** 220408800 **Fax**
E-mail fjmont@ineb.up.pt

FIELD OF THE INVENTION

This invention discloses the bactericidal activity of nanostructured lipid carriers (NLCs) or lipid nanoparticle shells, without carrying pharmacological agents, the characterization of said antibacterial NLCs, and their use as an agent to kill *Helicobacter pylori*. These NLCs do not affect other bacteria, such *Lactobacillus casei*, *Staphylococcus epidermidis and Escherichia coli*. Moreover, these NLCs are not cytotoxic to gastric cells at bactericidal concentrations. This invention opens new perspectives for the development of an antibiotic-free treatment against *H. pylori* gastric infection.

BACKGROUND OF INVENTATION

Helicobacter pylori is a Gram-negative bacteria that infect one-half of the World population. This bacterium is the major etiological factor in chronic active gastritis, gastric ulcers, and gastric cancer [1-3].

The currently recommended treatment includes a combination of two antibiotics, commonly clarithromycin plus amoxicillin or metronidazole, and a proton-pump inhibitor [4]. However, this therapy fails in 20% of patients for several reasons, but principally due to poor patient compliance and bacteria resistance to the antibiotics used [5]. More complex regimens, including the use of non-bismuth or bismuth-containing quadruple therapies, were also recommended as a second-line option [4], but their complexity potentiates patient non-compliance and bacterial resistance, leading to treatment failure. The exacerbated increase of antibiotic resistance has generated alarming impact and new antibiotic-free strategies are necessary.

The application of nanotechnology, especially, the use of nanoparticles as drug nanocarriers has generated a significant impact in medicine. The increasing interest by lipid nanocarriers is associated with their higher biocompatibility and lower toxicity compared to polymeric nanoparticles, as well as lower production cost and scalability [6-9]. Nanostructured lipid carriers (NLCs) are lipid nanoparticles specifically designed and patented as delivery systems for pharmaceutical, cosmetic and/or alimentary active ingredients [10]. They are characterized by a solid lipid core consisting of a mixture of solid and liquid lipids. The resulting particles matrix displays a melting depression when compared with the original solid lipid but is still solid at body temperature [6, 7]. NLCs can be prepared using a wide variety of lipids including fatty acids, glyceride mixtures or waxes, stabilized with selected biocompatible surfactants (non-ionic or ionic). Moreover, most of NLCs ingredients are safe and under the Generally Recognized as Safe (GRAS) status issued by the Food and Drug Administration (FDA) [11, 12]. Using spatially different lipids induces many imperfections in the crystal and if a proper amount of liquid lipid is

mixed with the solid lipid, a phase separation and the formation of oily nanocompartments within the solid lipid matrix can occur [13].

This invention describes the specific bactericidal activity of NLCs without any active ingredient (unloaded-NLC), prepared using glyceryl palmitostearate as solid lipid, caprylic/capric triglyceride as liquid lipid and polysorbate 60 as a surfactant against *Helicobacter pylori*. This effect was not observed against other bacteria, such as the Gram-positive *Staphylococcus epidermidis* and *Lactobacillus casei* and the Gram-negative *Escherichia coli*. The behavior of unloaded-NLCs against *H. pylori* was not expected, since results described in the literature, that only uses unloaded-NLCs as controls of the drug-loaded NLCs, always demonstrated their null or very low activity against other bacteria [14, 15]. Moreover, the utilization of NLCs, with and without drugs, for the treatment of *H. pylori* gastric infection was not previously reported.

DESCRIPTION OF THE INVENTION

This invention describes the unexpected specific bactericidal effect of unloaded-NLCs (Nanostructured Lipid Carriers) on *H. pylori* without affecting other bacteria, such as the Gram-positive *Staphylococcus epidermidis* and *Lactobacillus casei*, and the Gram-negative *Escherichia coli*. NLCs were developed to be used in the preparation of pharmaceutical, cosmetics and/or alimentary compositions as delivery systems for an active ingredient. Therefore, their bactericidal effect per sees (without any active ingredient/drug) was not expected and was not previously described.

EXPERIMENTAL SECTION

Nanostructured lipid carriers preparation

Nanostructured Lipid Carriers (NLCs) were produced using 200 mg of glyceryl palmitostearate (Gattefosé) as solid lipid, 90 mg of Caprylic/Capric Triglyceride (Acofarma) as liquid lipid and 60 mg of polysorbate 60 (Merck) as a surfactant. NLCs were produced using hot homogenization and ultrasonication technique. Briefly, lipids (solid and liquid) and surfactant were weighted together and heated at a temperature above the solid lipid melting point to promote their mixture. A nanoemulsion was obtained after adding to the lipid mixture, Milli-Q water preheated above the solid lipid melting point under high speed stirring (12000 rpm, 20s) using an ultra-turrax T25 (Janke and Kunkel IKA-Labortechnik). This microemulsion was homogenized using a sonicator (Vibra-Cell model VCX 130 equipped with a VC 18 probe, Sonics and Materials Inc., Newtown), with tip diameter ¼" (6 mm), at 60% amplitude for 5 minutes. Nanoemulsion was cooled to room temperature under gentle magnetic stirring allowing the inner phase of NLCs to solidify forming nanoparticles dispersed in the aqueous phase without aggregates.

Nanostructured lipid carriers size and zeta potential determination

The hydrodynamic size distribution and surface charge (ξ-potential) of NLCs were characterized by dynamic light scattering (DLS) using the Malvern Zetasizer Nano ZS. Clear disposable folded capillary cells (DTS1070) from Malvern were used for all samples. Samples were diluted (1:50) with Milli-Q water conducted at a backscattering angle of 173º at 37ºC. All measurements were performed in triplicate.

Nanostructured lipid carriers morphology determination

The morphology of NLC was observed by Cryo-Scanning Electron Microscopy (CryoSEM) using a JEOL JSM-6301F, an Oxford Instruments INCA Energy 350 and a Gatan Alto 2500. A drop of nanoparticles was placed on a grid, rapidly cooled in a liquid nitrogen slush (-210ºC), and transferred under vacuum to the cold stage of the preparation chamber. The sample was fractured, sublimated for 120 seconds min at -90ºC to reveal greater detail, and coated with a gold-palladium alloy by sputtering for 40 seconds. Finally, the sample was then transferred under vacuum into the CryoSEM chamber where they were observed at -150ºC.

Storage stability of nanostructured lipid carriers

NLCs were storage in Milli-Q water during 2 months at two different temperatures: 4ºC and 20ºC. Nanoparticles stability was evaluated by periodic measurements of their size and surface charge using the Malvern Zetasizer Nano ZS, as described above. All measurements were performed in triplicate.

Microorganisms and growth conditions

Microorganisms used in this study were the following: *Helicobacter pylori* J99 (*H. pylori*; obtained from the Department of Medical Biochemistry and Biophysics, Umea University, Sweden [16]), mouse-adapted *H. pylori* strain SS1 (obtained from Unité de Pathogenèse de *Helicobacter*, Institute Pasteur, France), *Lactobacillus casei-01* (Chr. Hansen, Hørsholm Denmark) (*L. casei*), *Staphylococcus epidermis* ATCC 35984 (*S. epidermidis)*, *Staphylococcus aureus* ATCC 33591 (methicillin resistant) (*S. aureus* MRSA) and *Escherichia coli* ATCC 25922 (*E. coli)*. Each bacterium was grown on specific solid medium plates and overnight on a liquid medium, as described in Table 1.

Table 1- Specific solid and liquid medium of each bacteria used in this study.

Microorganism	Solid medium	Liquid medium
H. pylori J99 and *H. pylori* SS1	Blood agar base 2 (Oxoid) plates supplemented with 10% defibrinated horse blood (Probiológica) and with an antibiotics-cocktail of 0.155g/L Polymixine B (Sigma-Aldrich), 6.25 g/L Vancomycin (Sigma-Aldrich), 1.25g/L Amphotericin B (Sigma-Aldrich) and 3.125g/L Trimethroprim (Sigma-Aldrich)	Brucella Broth (BB, Oxoid) supplemented with 10% of Fetal Bovine Serum (FBS, Gibco)
L. casei 01	De Man-Rogosa and Sharpe agar (MRS agar, Biokar)	De Man-Rogosa and Sharpe broth (MRS broth, Biokar)
S. epidermidis ATCC 35984 *S. aureus* ATCC 33591 *E. coli* ATCC 25922	Tryptic Soy Agar (TSA, Merck Millipore)	Tryptic Soy Broth (TSB, Merck Millipore)

Antibacterial activity of nanostructured lipid carriers

Bacteria were pre-cultured on specific liquid medium (Table1) overnight at 37ºC and 150 rpm. After washing with phosphate buffered saline (PBS 1x, pH 7.4), bacteria were adjusted to approximately 1×10^7 CFU/mL in Müeller-Hinton broth (MHB, Merck Millipore) supplemented with 10% of FBS. *H. pylori* was also tested in BB+10% FBS.

Different NLC concentrations (0%, 1.25%, 2.5% and 5% v/v) were added to bacteria culture and they're incubated during 24h, at 37ºC, 150 rpm, and in the case of *H. pylori* under microaerophilic conditions. At different time-points (0, 3, 6, 9,12, 15, 24h), a 200 µL sample of each bacterial culture was isolated, serially diluted, plated on solid medium plates (Table 1) and incubated at 37ºC for 5 days for *H. pylori*, 2 days for *L. casei* and 24h for the other bacteria. The number of viable bacteria per mL was determined by colonies forming unit (CFU) counting.

Scanning Electron Microscopy (SEM) analysis

Morphological changes of *H. pylori* J99 were studied by SEM, analyzing the effect of unloaded-NLCs on bacteria. Bacteria were incubated with unloaded-NLC (1.25% v/v) for 3 and 12h as previously described using BB medium supplemented with 10%FBS. After incubation, samples were washed in phosphate buffered saline (PBS 1x, pH 7.4) and fixed in 2.5% glutaraldehyde (Merck) in 0.14M sodium cacodylate buffer (Merck) for 30 min at room temperature. Fixed bacteria adhered on glass coverslips in a 24-well suspension plate during 2h at room temperature. Then samples were dehydrated with an increasing ethanol/water gradient (50% v/v to 99% v/v) and subjected to critical point drying (CPD 7501, Poloran). Finally, the samples were sputter-coated with gold/palladium film over 30s. *H. pylori* samples were observed by scanning electron microscopy (SEM; JEOL JSM-6310F), at magnification 30000 and 60000x, at the CEMUP (*Centro de Materiais da Universidade do Porto*).

Transmission Electron Microscopy (TEM) analysis

The effect of unloaded-NLCs on the structure of *H. pylori* J99 was also analyzed by TEM. Incubation time and concentrations were similar as described for SEM analysis. After incubation, bacteria suspension was centrifuged (3000g, 5min) and the supernatant removed. The bacterial pellet was fixed by resuspending in a mixture of 4% w/v of paraformaldehyde (Merck) with 2.5% v/v glutaraldehyde (Electron Microscopy Sciences) in 0.14M sodium cacodylate buffer (Merck) (pH 7.4). Samples were then washed with sodium cacodylate buffer, centrifuged and bacterial pellet post-fixed in 2% osmium tetroxide (Electron Microscopy Sciences) in sodium cacodylate buffer was embedded in a HistoGel (Thermo Scientific) and processed in Epon resin (Electron Microscopy Sciences). Ultrathin sections of 50 nm thickness were performed on a Ultramicrotome (RMC PowerTome PC model), by using diamond knives (Diatome). Sections were mounted on formvar-coated nickel grids, stained with uranyl acetate and lead citrate (Delta Microscopies) and examined using TEM (JEOL JEM 1400 transmission electron microscope) equipped with a CCD digital camera Orious 1100W at i3S *(Instituto de Investigação e Inovação em Saúde da Universidade do Porto*).

Effect of nanostructured lipid carriers on gastric cells line

Gastric carcinoma cell line MKN45 was grown in RPMI 1640 with Glutamax and HEPES (Gibco) supplemented with 10% inactivated FBS (Gibco) and 1% penicillin-streptomycin (Gibco) at 37ºC under 5% CO_2 in humidified air. The medium was changed every two days. For subculturing, cells were trypsinized and counted in a Neubauer chamber diluted (1:10) in a Trypan Blue solution (0.4% w/v) (Sigma-Aldrich). Cells were expanded in 75 cm^2 T-flasks with appropriate aliquots of the cell suspension with a sub-cultivation ratio of 1:3. NLC effect on MKN45 gastric cells was evaluated using direct contact assay. MKN45 cells were seeded in a 12-well plate (5×10^5 cell per well) in RPMI 1640 with Glutamax and HEPES supplemented with 10% inactivated FBS and 1% PenStrep, at 37ºC and under 5% CO_2 in humidified air, during 48h. Then, the culture medium was changed and NLCs were added with different concentrations (0, 0.5%, 1.25%, 2.5%, 5.0% v/v). Well-plate was incubated at 37ºC and under 5% CO_2 in humidified air, during 24h. Cells in Triton™ X-100 (2% w/v) (Sigma-Aldrich) and cells in fresh culture medium were used as a control, in order to normalize the results. After 24h, the supernatant was removed (transferred to 12-well plates and stored for cytotoxicity assay) and 1 mL of 5 mg/mL of Thiazolyl Blue Tetrazolium Bromide (MTT, 98%, Sigma-Aldrich) in PBS solution was added to the cultures, diluted to a final concentration of 0.5 mg/L in culture medium and incubated for 3h at 37ºC in the dark. Then, MTT solution was discarded and 1 mL of DMSO was added, to solubilize the formazan crystals formed by MTT reaction. The plate was shaken for 5 min, at room temperature, under light protection and then, the optical density was measured at 590 nm and 630 nm using a microplate reader (Synergy™ H Multi-mode Microplate Reader, BioTek Instruments). MTT assay evaluates the activity of cellular

oxidoreductase enzymes inside mitochondria by converting the MTT tetrazolium dye into its insoluble formazan (purple) that is directly proportional to the number of viable cells. The percentage of cell viability was calculated according to the following equation:

$$\text{Cell viability (\%)} = \frac{\text{Experimental value- Triton control}}{\text{Medium control-Triton control}} \times 100$$

Lactate dehydrogenase (LDH) is released to the cell culture medium when the cytoplasmic membrane is damaged. Consequently, its quantification allows having an assessment of cell death. Hence, the 12-well plates containing the cell culture supernatant collected for the MTT assay was centrifuged (250g, 10min at room temperature). Carefully, without disturbing the pellet, 100µl of the sample were transferred to the 96-well plate and 100 µl of the LDH Cytotoxicity Detection Kit (Takara Bio Inc) were added. After 5 min of incubation, at room temperature and protected from light, the absorbance was measured at 490 and 630 nm using the microplate reader. The percentage of cytotoxicity was calculated according to the following equation:

$$\text{Cytotoxicity (\%)} = \frac{\text{Experimental value- Medium control}}{\text{Triton control-Medium control}} \times 100$$

Statistical analysis

Data are reported as means ± standard deviation. Data from different groups were compared statistically using non-parametric Kruskal-Wallis test. Analyses were performed with a significance level of 0.05 using Graph Pad Prism 5.0 (Graph-Pad Software).

RESULTS AND DISCUSSION

NLCs were synthesized using a modified hot homogenization technique with no use of organic solvents [17]. Results obtained by DLS demonstrated that NLCs have a homogenous size distribution with a mean diameter of 211 ± 8 nm (Figure 1A). Polydispersion index was around 0.2 suggesting low size variability (monodisperse distribution) and no visible aggregation that was confirmed by Cryo-SEM. However, when observed by Cryo-SEM (Figure 1B), NLCs are slightly smaller, which could be related to the sublimation process used in this technique to remove the surface water that can also remove the water present in the nanoparticle matrix causing particle shrinkage. NLCs size can be important for *H. pylori* treatment since it was described that particles with sizes between 130 and 300 nm are able to infiltrate gastric cell-cell junctions and interact locally with *H. pylori* infection sites in intercellular spaces [18].

ξ-potential is a very important factor in the analysis of colloidal dispersions stability. Figure 1A also shows that NLCs have a ξ-potential around -28mV. According to literature, colloidal dispersions are stable when they are strongly charged (|30 mV|) (i.e., aggregation is avoided) [19], whereas ξ-potential values in the range of -10<0<+10mV are considered neutral [20]. Since ξ-potential is near -30mV, these NLCs can be considered physically stable.

NLCs are stable during storage in aqueous suspension for at least 1 moth at 4º and 20ºC in terms of size and charge (Figure 1C). However, at 20ºC and after 1 month of storage, there is a slight increase of the ξ-potential from -27 to -23 mV. Nevertheless, these negative charges are enough to maintain their physical stability and avoid nanoparticles aggregation.

NLC bactericidal activity was evaluated following bacteria growth during 24h in the presence of different NLC concentrations (Figure 2) using Müller-Hinton Broth (MHB), which is the recommended medium for the determination of the minimal inhibitory concentration according to the guidelines proposed by two recognized organizations: CLSI (Clinical & Laboratory Standards Institute) and EUCAST (European Society of Clinical Microbiology and Infectious Diseases) [21]. However, since *H. pylori* is a fastidious microorganism and requires a complex nutrient-rich growth media, MHB had to be supplemented with 10% of fetal bovine serum (FBS). This supplement may act as an additional source of nutrient and also protect against the toxic effects of long-chain fatty acids [22]. Nevertheless, for comparison and to demonstrate the specific bactericidal activity of NLCs to *H. pylori*, this FBS-supplemented medium was also used for bactericidal assays performed with other bacteria.

Minimal bactericidal concentration (MBC) was defined as the minimal drug concentration to kill 99.9% (>3 logs) bacteria in 24h of incubation. Figure 2A shows that NLCs are bactericidal against *H. pylori* at all concentrations used, since after 24h in the presence of NLCs, there are no live bacteria. For the highest concentration tested (5% v/v), *H. pylori* was killed after 15h of incubation time. Nonetheless, an inhibitory effect of 50% (> 1log) was detected after 9h of incubation with this NLC concentration.

NLC bactericidal effect was not detected on *Lactobacillus casei-01* (Figure 2B), Gram-positive rod-shaped and nonpathogenic bacteria found on the human gut microbiota. This bacterium has an importance for gut microbiota which enhances the integrity of the intestinal barrier, decrease translocation of bacteria across the intestinal mucosa and disease phenotypes such as gastrointestinal infections [23, 24]. This specific bactericidal activity of unloaded-NLCs against *H. pylori* (without affecting *L. casei*) opens new routes for the treatment of *H. pylori* infection without affecting gut microbiota.

NLCs were also tested on other Gram-positive cocci bacteria, *Staphylococcus epidermidis* (Figure 2C) and methicillin-resistant *Staphylococcus aureus* (MRSA) (Figure 2D). No bactericidal effect was observed for both bacteria on the concentrations used. However, the higher NLCs concentration (5% v/v) had an inhibitory effect on MRSA growth. Other bacterium tested was *Escherichia coli*, a Gram-negative rod-shaped bacterium, is the most prevalent

commensal inhabitant of the human intestinal tract and lives in a mutually beneficial association with hosts [25, 26]. *E. coli* is not usually pathogenic. NLC bactericidal effect was not detected on *E. coli* (Figure 2E); therefore, unloaded-NLCs can be used without to affect the normal flora of the gut.

The NLC bactericidal effect against *H. pylori* was also tested using a growth medium (BB) indicated for *H. pylori* growth [27]. Figure 3 shows that all bacteria are killed after 12h of incubation with NLCs for all the concentrations used. The bactericidal effect of NLC on *H. pylori* was faster when bacteria were growing in this medium than in MHB medium.

In order to understand the interaction of NLCs with *H. pylori*, their morphology after growing in the presence and absence of NLCs was evaluated by SEM and TEM. Samples were prepared after 3 and 12h of incubation with 1.25% of NLCs, since after 3h mostly of the bacteria are alive and after 12h all bacteria are dead.

SEM images of *H. pylori* grown during 3h (Figure 4A) and 12h (Figure 4C) in the absence of NLCs (control) show their characteristic bacillus shape with 2-4μm of length and 0.5-1μm wide [4-6]. When bacteria were incubated with NLCs for 3h (Figure 4B) their morphology was similar to the controls, demonstrating the integrity of its membrane. However, after 12h incubation with NLCs (Figure 4D), although high morphological changes were not observed using this technique, it was possible to visualize the leakage of their cytoplasmic contents. These results suggest that NLCs can interact with *H. pylori* by disrupting its cell membrane.

TEM images (Figure 5) corroborate with SEM images, showing *H. pylori* with the intact cell membrane and dense cytoplasm in controls (Figure 5A and 5C) and after 3 hours growing with NLCs (Figure 5B). After 12h of incubation with NLCs, TEM images revealed a disseverance of outer membrane and plasma membrane with parts of bacteria without cytoplasmic contents (Figure 5D).

NLCs cytotoxicity was evaluated against a gastric carcinoma cell line (MKN45) using thiazolyl blue tetrazolium bromide (MTT) and lactate dehydrogenase (LDH) assays (Figure 6A and 6B, respectively). Figure 6A shows that for NLC concentrations up to 2.5%v/v, the reduction of MKN45 cell viability was lower than 30%. Figure 6B demonstrated that despite its strong bactericidal activity against *H. pylori*, NLCs are not cytotoxic against MKN45 cells at concentrations up to 2.5%v/v (~20% cell lysis). These results also demonstrated that NLCs at bactericidal concentrations (1.25% v/v) have a negligible lactate dehydrogenase release and did not induce apoptosis and mitochondrial dysfunction after 24h of incubation. These NLCs, at bactericidal concentrations, are biocompatible according to ISO 10993-5 [12] since the decrease of cell metabolic activity and increase of cell lysis due to the presence of NLCs in comparison with control were lower than 30%.

References

1. Correa, P. and J. Houghton, *Carcinogenesis of Helicobacter pylori.* Gastroenterology, 2007. **133**(2): p. 659-672.
2. Amieva, M. and R.M. Peek Jr, *Pathobiology of Helicobacter pylori–Induced Gastric Cancer.* Gastroenterology, 2016. **150**(1): p. 64-78.
3. Matysiak-Budnik, T. and F. Mégraud, *Helicobacter pylori infection and gastric cancer.* European Journal of Cancer, 2006. **42**(6): p. 708-716.
4. Malfertheiner, P., et al., *Management of Helicobacter pylori infection—the Maastricht IV/ Florence Consensus Report.* Gut, 2012. **61**(5): p. 646-664.
5. Vakil, N., *Helicobacter pylori treatment: a practical approach.* Am J Gastroenterol, 2006. **101**(3): p. 497-9.
6. Carbone, C., et al., *Pharmaceutical and biomedical applications of lipid-based nanocarriers.* Pharm Pat Anal, 2014. **3**(2): p. 199-215.
7. Battaglia, L. and M. Gallarate, *Lipid nanoparticles: state of the art, new preparation methods and challenges in drug delivery.* Expert Opinion on Drug Delivery, 2012. **9**(5): p. 497-508.
8. Martins, S., et al., *Lipid-based colloidal carriers for peptide and protein delivery--liposomes versus lipid nanoparticles.* Int J Nanomedicine, 2007. **2**(4): p. 595-607.
9. Müller, R.H., K. Mäder, and S. Gohla, *Solid lipid nanoparticles (SLN) for controlled drug delivery – a review of the state of the art.* European Journal of Pharmaceutics and Biopharmaceutics, 2000. **50**(1): p. 161-177.
10. Viladot Petit, J.L.L., G.R. Delgado, and B.A. Fernández, *Lipid nanoparticle capsules*, in *US 2013/0017239 A1*. 2011, LIPOTEC S.A.: Spain.
11. Mehnert, W. and K. Mäder, *Solid lipid nanoparticles: Production, characterization and applications.* Advanced Drug Delivery Reviews, 2001. **47**(2–3): p. 165-196.
12. Svilenov, H.T., Christo *Solid lipid nanoparticles – a promising drug delivery system*, in *Nanomedicine*, A.M. Seifalian, Achala de Kalaskar, Deepak M., Editor. 2014, One Central Press (OCP): London.
13. Muchow, M., P. Maincent, and R.H. Müller, *Lipid Nanoparticles with a Solid Matrix (SLN®, NLC®, LDC®) for Oral Drug Delivery.* Drug Development and Industrial Pharmacy, 2008. **34**(12): p. 1394-1405.
14. da Silva, P.B., et al., *A Nanostructured Lipid System as a Strategy to Improve the in Vitro Antibacterial Activity of Copper(II) Complexes.* Molecules, 2015. **20**(12): p. 22534-45.
15. Manea, A.-M., B.S. Vasile, and A. Meghea, *Antioxidant and antimicrobial activities of green tea extract loaded into nanostructured lipid carriers.* Comptes Rendus Chimie, 2014. **17**(4): p. 331-341.
16. Mahdavi, J., et al., *Helicobacter pylori SabA adhesin in persistent infection and chronic inflammation.* Science, 2002. **297**(5581): p. 573-8.
17. Neves, A.R., et al., *Novel resveratrol nanodelivery systems based on lipid nanoparticles to enhance its oral bioavailability.* Int J Nanomedicine, 2013. **8**: p. 177-87.
18. Lin, Y.H., et al., *Development of pH-responsive chitosan/heparin nanoparticles for stomach-specific anti-Helicobacter pylori therapy.* Biomaterials, 2009. **30**(19): p. 3332-42.

19. Fonte, P., et al., *Chapter fifteen - Chitosan-Coated Solid Lipid Nanoparticles for Insulin Delivery*, in *Methods in Enzymology*, D. Nejat, Editor. 2012, Academic Press. p. 295-314.

20. Clogston, J. and A. Patri, *Zeta Potential Measurement*, in *Characterization of Nanoparticles Intended for Drug Delivery*, S.E. McNeil, Editor. 2011, Humana Press. p. 63-70.

21. Matuschek, E., D.F.J. Brown, and G. Kahlmeter, *Development of the EUCAST disk diffusion antimicrobial susceptibility testing method and its implementation in routine microbiology laboratories.* Clinical Microbiology and Infection, 2014. **20**: p. O255–O266.

22. Kusters, J.G., A.H.M. van Vliet, and E.J. Kuipers, *Pathogenesis of Helicobacter pylori Infection.* Clinical Microbiology Reviews, 2006. **19**(3): p. 449-490.

23. Hemarajata, P. and J. Versalovic, *Effects of probiotics on gut microbiota: mechanisms of intestinal immunomodulation and neuromodulation.* Therap Adv Gastroenterol, 2013. **6**(1): p. 39-51.

24. Okuro, P.K., et al., *Co- encapsulation of Lactobacillus acidophilus with inulin or polydextrose in solid lipid microparticles provides protection and improves stability.* Food Research International, 2013. **53**(1): p. 96-103.

25. Allocati, N., et al., *Escherichia coli in Europe: an overview.* Int J Environ Res Public Health, 2013. **10**(12): p. 6235-54.

26. Reshes, G., et al., *Cell shape dynamics in Escherichia coli.* Biophys J, 2008. **94**(1): p. 251-64.

27. Blanchard, T.G. and J.G. Nedrud, *Laboratory Maintenance of Helicobacter Species.* Current Protocols in Microbiology, 2006. **CHAPTER**: p. Unit8B.1-Unit8B.1.

FIGURES

Figure 1. NLCs characterization in terms of (A) diameter (bars), polydispersion index and charge surface (ξ-potential) performed using dynamic light scattering at 37ºC, (B) morphology evaluated by cryo-scanning electron microscopy (Cryo-SEM) (scale bar 500nm, 50000x magnification) and (C) effect of time of storage in water at 4ºC and 20ºC on diameter and charge (ξ-potential) of unloaded-NLC produced. Data is reported as the mean ± standard deviation (n=3). *p<0.05 compared to different time-points on day 0 (Kruskal-Wallis test).

A

Diameter (nm)	211 ± 8
Polydispersion index	0.2±0.02
ξ-potential (mV)	-28 ± 3

B

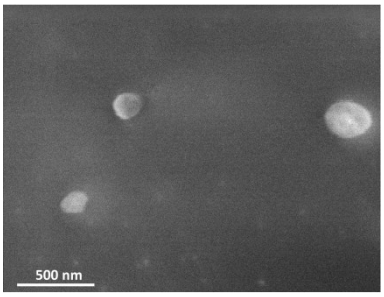

C

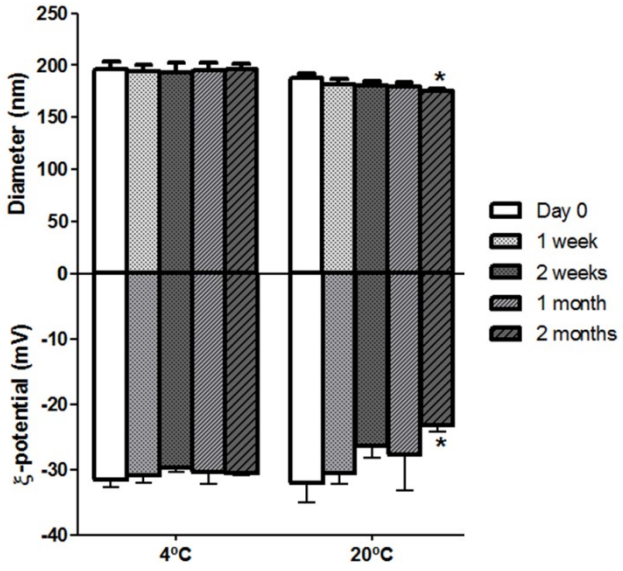

Figure 2. The growth of bacteria in increasing concentrations of unloaded-NLC in Müller-Hinton Broth medium supplemented with 10% FBS: (A) *H. pylori* J99, (B) *Lactobacillus casei-01*, (C) *Staphylococcus epidermidis* ATCC35984, (D) *Staphylococcus aureus* ATCC 33591 (methicillin resistant) and *Escherichia coli* ATCC 25922. Numerical data is reported as mean ± standard deviation (n=3). All concentrations tested with unloaded-NLCs were significantly different compared to each bacteria growth treated with unloaded-NLCs and bacteria untreated (control) ($p<0.05$, Kruskal-Wallis test).

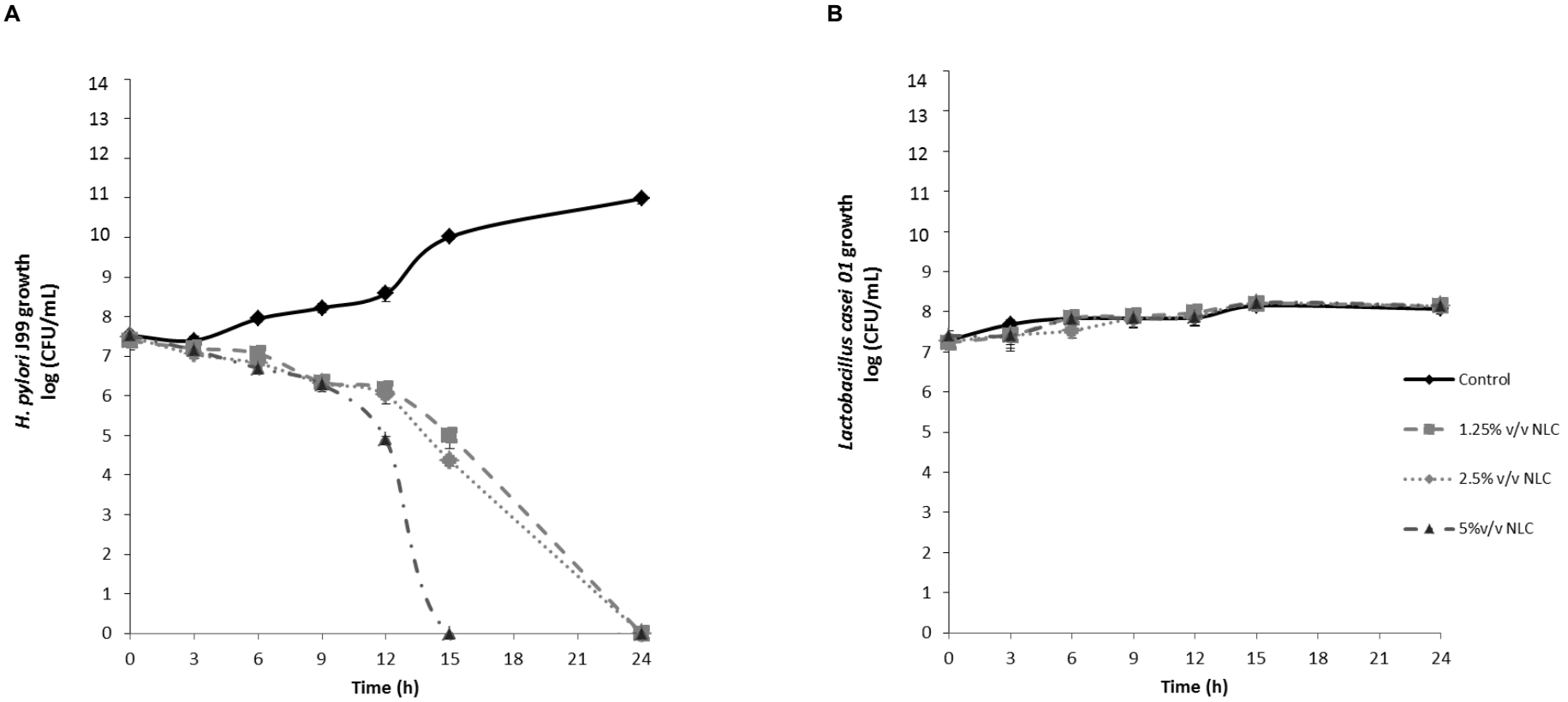

C

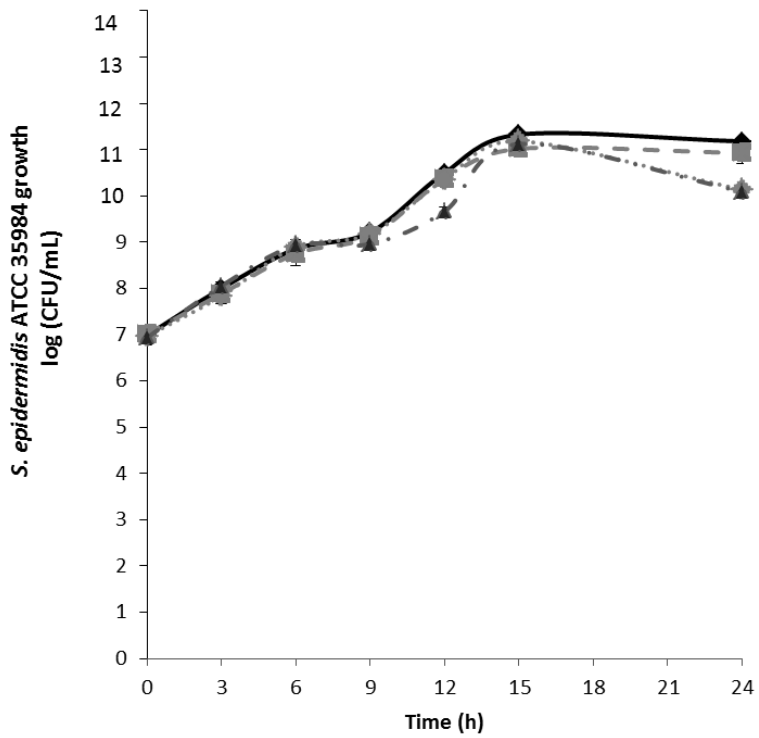
S. epidermidis ATCC 35984 growth
log (CFU/mL)
0
1
2
3
4
5
6
7
8
9
10
11
12
13
14
0
3
6
9
12
15
18
21
24
Time (h)

D

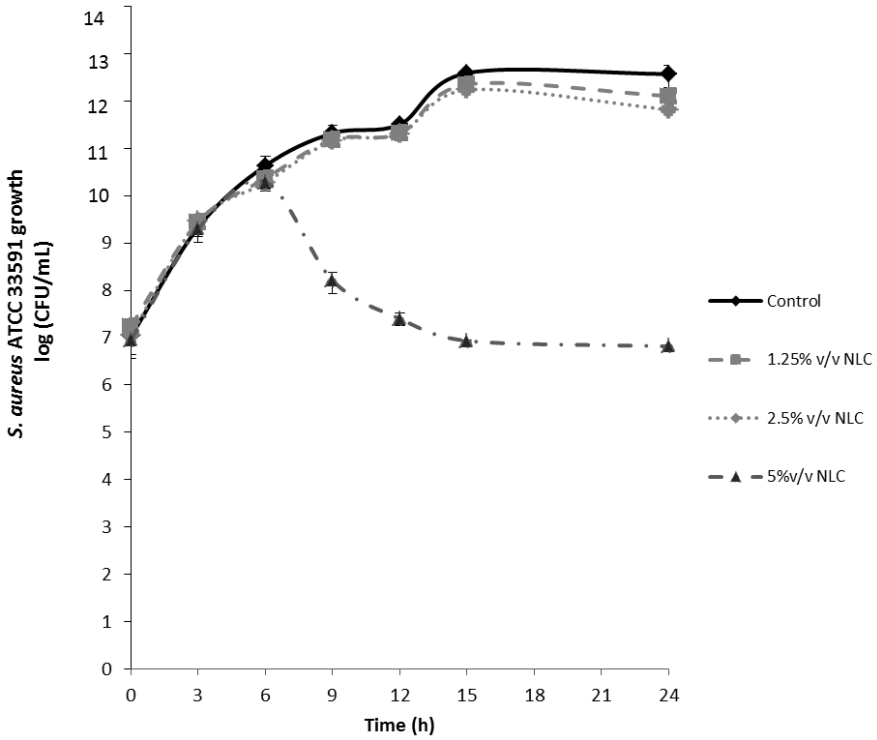
S. aureus ATCC 33591 growth
log (CFU/mL)
0
1
2
3
4
5
6
7
8
9
10
11
12
13
14
0
3
6
9
12
15
18
21
24
Time (h)
Control
1.25% v/v NLC
2.5% v/v NLC
5%v/v NLC

E

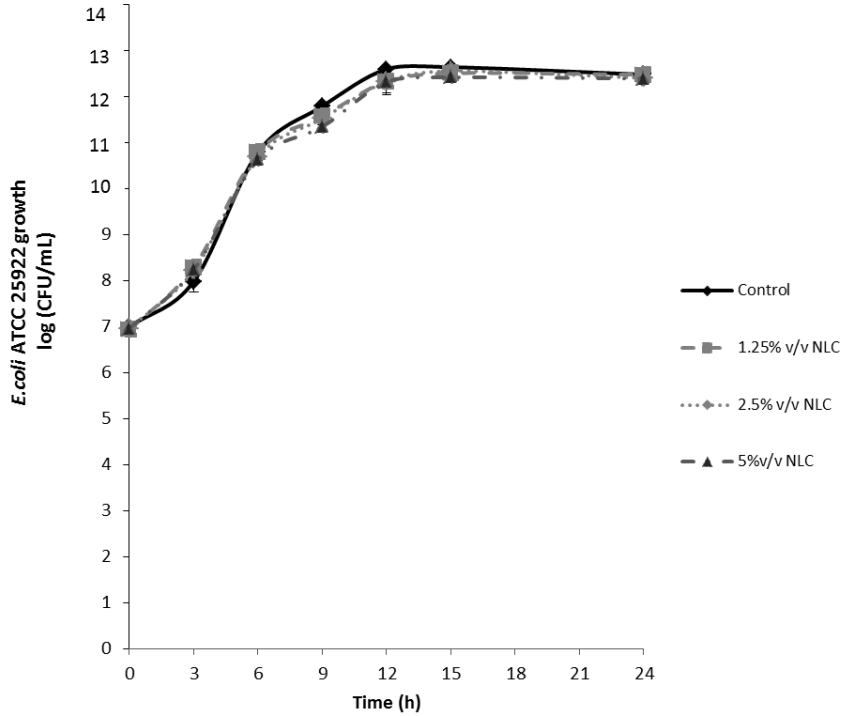
E.coli ATCC 25922 growth log (CFU/mL)
14
13
12
11
10
9
8
7
6
5
4
3
2
1
0
0
3
6
9
12
15
18
21
24
Time (h)
Control
1.25% v/v NLC
2.5% v/v NLC
5%v/v NLC

Figure 3. The growth of (A) *H. pylori* J99 and (B) *H. pylori* SS1 in increasing concentrations of unloaded-NLC in Brucella Broth medium supplemented with 10% FBS. Numerical data is reported as mean ± standard deviation (n=3). All concentrations tested with unloaded-NLCs were significantly different compared to each bacteria growth treated with unloaded-NLCs and bacteria untreated (control) ($p<0.05$, Kruskal-Wallis test).

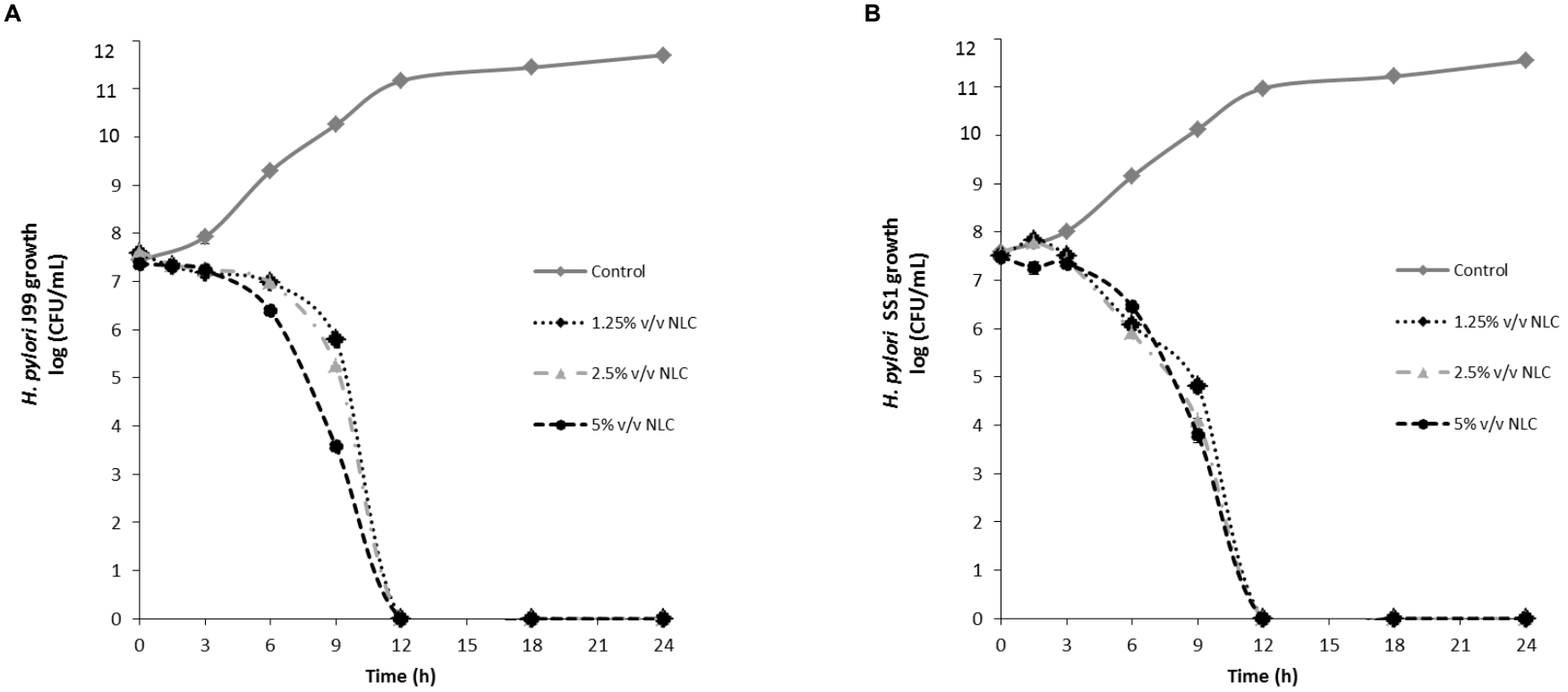

Figure 4. Scanning Electron micrographs of *H. pylori* J99 incubated during 3h (A to B) and 12h (C to D) with unloaded-NLC. In A and C, SEM images of *H. pylori* J99 was not treated (control); in B and D, *H. pylori* J99 was treated with 1.25 %v/v of unloaded-NLC. The scale bar in the SEM image represents 1 µm, 60 000 x magnifications.

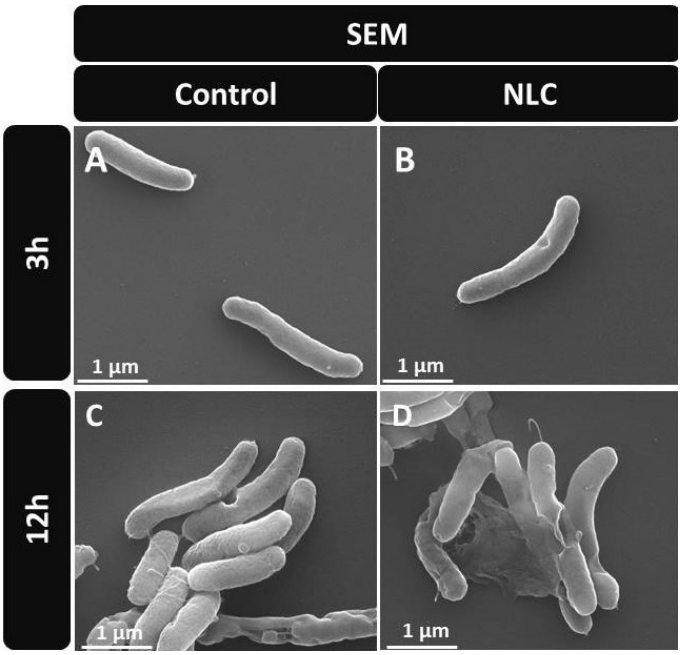

Figure 5. Transmission Electron micrographs of *H. pylori* J99 incubated during 3h (A to B) and 12h (C to D) with unloaded-NLC. In A and C, TEM images of *H. pylori* J99 was not treated (control); in B and D, *H. pylori* J99 was treated with 1.25%v/v of unloaded-NLC. The scale bar in the TEM image represents 200 nm, 50 000 x magnifications.

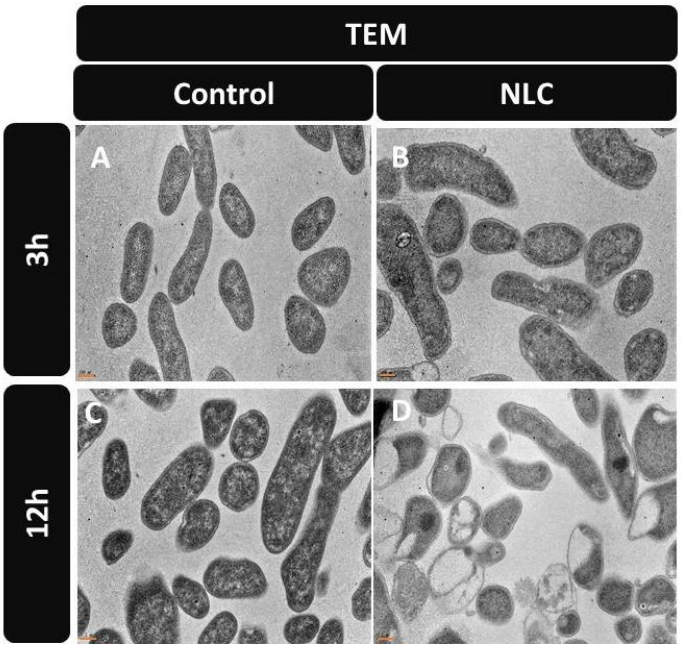

Figure 6. Effect of unloaded-NLCs of gastric carcinoma cell line in increasing amounts. MKN45 gastric carcinoma (A) cell line viability and (B) cytotoxicity assessed by the MTT and LDH assay, respectively, after 24h exposure to different amounts of NLCs. Data is reported as mean ± standard deviation (n=3). * p<0.05, refers to significant differences of MKN45 gastric cells treated cells with unloaded-NLC and cells untreated (control) (Kruskal-Wallis test).

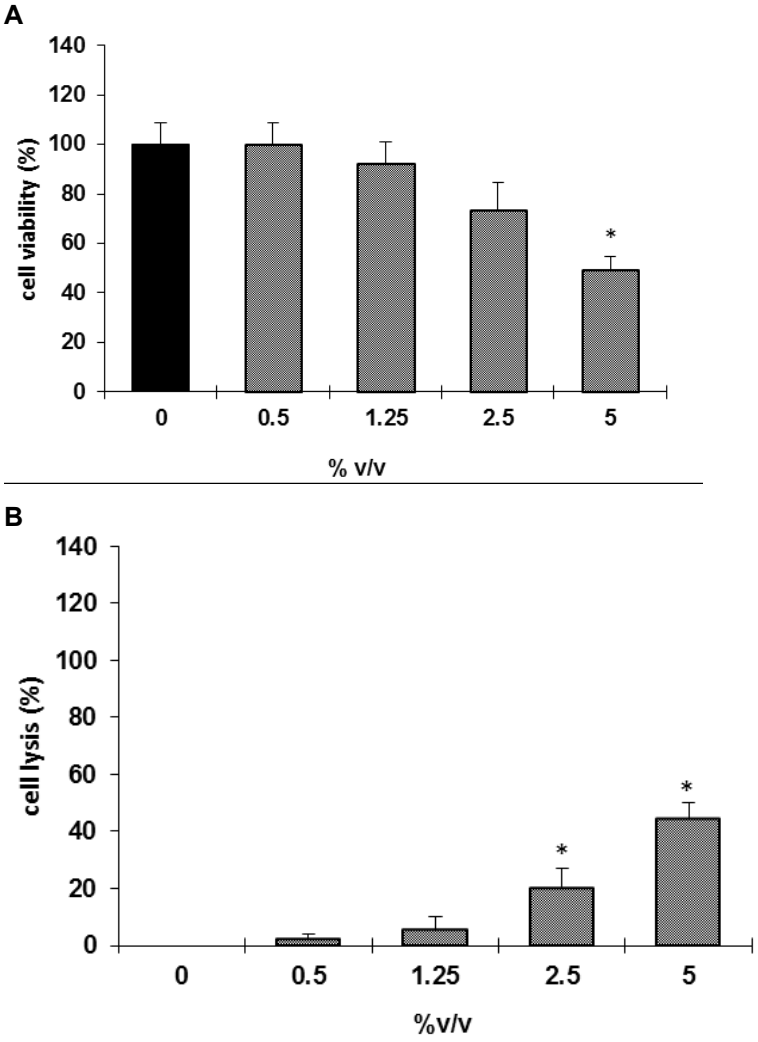

CLAIMS

1. A nanostructured lipid particle comprising particles in the form of a shell, hollow nanoparticles or lipid vesicles, and wherein said nanoparticles are capable of killing *Helicobacter pylori.*

2. A nanostructured lipid particle according to claim 1, wherein the particles can be produced by mixture of several lipids forming a nanoemulsion, using techniques that may include the use of hot homogenization and ultrasonication,

3. A nanostructured lipid particle according to claim 1, wherein the particles present with diameters between 50 and 400 nanometers, preferably between 150 and 250 nanometers, as determined by their hydrodynamic size using dynamic light scattering, at 37ºC.

4. A nanostructured lipid particle according to claim 1, wherein the particle is formed by mixtures of different lipids, selected from solid and liquid lipids and mixed with a surfactant to produce a nanoemulsion. The lipids are preferably glyceryl palmitostearate, cetyl palmitate and Caprylic/Capric Triglyceride and the surfactant polysorbate 60.

5. Nanostructured lipid particle produced according to the previous claims, wherein the therapeutically effective amount of Helicobacter pylori infection is administrated orally.

6. Nanostructured lipid particles produced according to the previous claims that can be stored during 1 month, in aqueous suspension at 4º and 20ºC.

7. Nanostructured lipid particles produced according to the previous claims, wherein the therapeutically effective amount against Helicobacter pylori does not affect other bacteria, particularly *Lactobacillus casei*, *Staphylococcus epidermidis and Escherichia coli*.

8. An oral formulation containing the nanostructured lipid particles produced according to the previous claims, in combination with one or more therapeutically active substance(s) selected from the group of gastrointestinal protectants (particularly proton pump inhibitors) and antibiotics (particularly amoxicillin, clarithromycin, metronidazole, tetracycline) used in the treatment of Helicobacter pylori infection.

9. An oral formulation containing the nanostructured lipid particles produced according to the previous claims, wherein the dosage form can be administrated in any formulation adapted for stomach delivery, particularly incorporated/combined with gastric retentive polymers such as chitosan or other pharmaceutical compounds able to release the particles in the stomach.

APPENDIX 4

4. Review: The potential utility of chitosan micro/nanoparticles in the treatment of gastric infection

During this work, a brief description of the use of chitosan in *H. pylori* treatment was reviewed. This review was used in the introduction of this thesis.

EXPERT REVIEWS

The potential utility of chitosan micro/nanoparticles in the treatment of gastric infection

Expert Rev. Anti Infect. Ther. 12(8), 981–992 (2014)

Inês C Gonçalves[1,3], Patrícia C Henriques[1,3], Catarina L Seabra[1,2,4] and M Cristina L Martins*[1,4]

[1]*INEB – Instituto de Engenharia Biomédica, Universidade do Porto, Rua do Campo Alegre, 823, 4150-180 Porto, Portugal*
[2]*IPATIMUP – Institute of Molecular Pathology and Immunology of the University of Porto, Rua Dr. Roberto Frias, 4200-465 Porto, Portugal*
[3]*Universidade do Porto, Faculdade de Engenharia, Porto, Portugal*
[4]*Universidade do Porto, Instituto de Ciências Biomédicas Abel Salazar, Porto, Portugal*
**Author for correspondence: Tel.: +351 226 074 982 cmartins@ineb.up.pt*

Gastric infections are mainly caused by *Helicobacter pylori* (*H. pylori*), a bacterium that colonizes the gastric mucosa of over 50% of the world's population. Chronic *H. pylori* infection has been associated with gastric diseases such as chronic gastritis, peptic ulcer and gastric adenocarcinoma. Current eradication treatment relies on antibiotic-based therapies that are unsuccessful in approximately 20% of the patients. Chitosan, a natural and cationic polysaccharide has been investigated in the treatment of *H. pylori* infection. Due to its mucoadhesive properties, it has been used in the form of micro/nanoparticles, polyelectrolyte complexes or coatings as antibiotic encapsulation systems for gastric delivery, but alternative molecules may also be incorporated. It has been recently proposed that chitosan can also be used for *H. pylori* binding and scavenging from the host stomach due to its antimicrobial/binding properties. In this manuscript, a brief description of the use of chitosan in *H. pylori* treatment is reviewed.

KEYWORDS: biomaterials • chitosan • crosslinking • drug delivery • gastric cancer • *Helicobacter pylori* • microspheres • mucoadhesion • nanoparticles • polyelectrolytes

Helicobacter pylori gastric infection

Helicobacter pylori (*H. pylori*), a spiral-shaped gram-negative bacterium, is one of the most common infectious agents in the world, colonizing the gastric mucosa of over 50% of the human population [1]. Although most of the infected individuals show no or few symptoms, this infection is the strongest known risk factor for gastroduodenal ulcer progression (60–80% of the cases), being also related to the development of gastric adenocarcinoma (1–3% of the cases) [1], the second leading cause of cancer-related deaths worldwide [2]. *H. pylori* was classified as a type I carcinogen by the International Agency for Research on Cancer [3], and it was recognized that its elimination is the most promising strategy to reduce the incidence of gastric cancer [4].

Due to its flagellar motility, *H. pylori* is able to escape the acidic pH of the stomach (pH 1.2–2.5) crossing the mucus layer that covers and protects the gastric cells, reaching the gastric epithelium where the pH is more neutral (pH ~7.4). In a healthy human stomach, the median thickness of the adherent mucus is 180 μm with 67% polymeric mucin, but in patients with gastric carcinoma there is an increase of thickness to 240 μm despite becoming a structurally very weak gel with only 23% polymeric mucin [5]. Furthermore, *H. pylori* can secrete urease, which converts endogenous urea into ammonia and carbon dioxide, thereby buffering gastric acid in the immediate vicinity of the organism [6].

Although most of *H. pylori* can be found free-swimming in the mucus layer, bacteria is also found adherent to the mucus layer and to the surface of gastric epithelial cells, in the intercellular spaces and even, as suggested in a few studies, inside the gastric cells [7].

Nonadherent *H. pylori* can produce and release a vacuolating cytotoxin, VacA, which induces multiple structural and functional alterations in cells, such as the formation of large intracellular vacuoles and the increase in membrane permeability [1].

 10.1586/14787210.2014.930663 ISSN 1478-7210

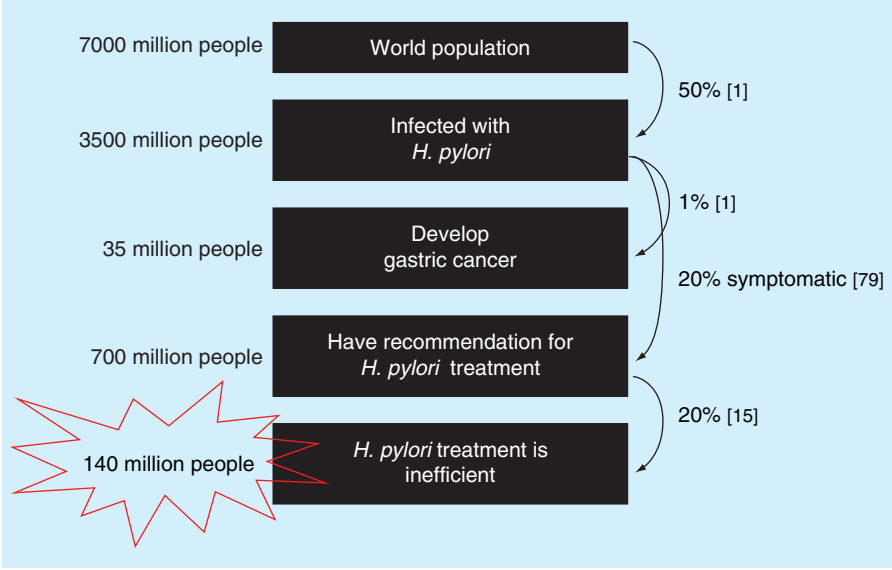

Figure 1. *Helicobacter pylori* infection and treatment figures.

H. pylori adhesion to gastric mucosa protects the bacteria from displacement by forces such as those generated by peristalsis and gastric emptying. Adhesion to the host is mediated by lectins, bacterial surface-bound adhesins, which recognize glycans expressed on the gastric mucosa [8]. *H. pylori* can express several different adhesins that are not only responsible for adhesion but for the communication system that enables *H. pylori* response to the gastric environment [9]. The best characterized adhesin–glycan interactions are the blood group antigen-binding adhesin (BabA) that recognizes the Lewis blood group antigens, such as Lewis b (Le^b) and H-type 1, and sialic acid-binding adhesin (SabA) that mediates the adherence of *H. pylori* to inflamed gastric mucosa by binding sialylated carbohydrate structures such as sialyl Lewis a (sLe^a) and sialyl Lewis a [10]. However, neutrophil activating protein was also identified as responsible for *H. pylori* binding to sulfated mucins, such as sulfo-Le^a, sulfo-Gal and sulfo-GalNAc [11]. The two adherence-associated lipoprotein A and B [12] as well as the outer inflammatory protein A [13], expressed in all bacteria strains, are also important in *H. pylori* adhesion to gastric mucosa, although their host receptors are not well known. It was also described that *H. pylori* can bind damaged tissue, where the basement membrane is exposed, through the extracellular matrix proteins, such as laminin, type IV collagen, vitronectin and heparan sulfate proteoglycan. This could be important for *H. pylori* adherence to host intercellular junctions [9].

After adhering to epithelial cells, *H. pylori* is able to assemble a type IV secretion system, encoded by the cag pathogenicity island, which translocates the cytotoxin-associated gene protein into gastric epithelial cells, conducing to numerous cellular alterations and inducing strong gastric inflammation [14].

Current treatments

Current available treatments to *H. pylori* infection rely on a triple treatment, which includes the combination of two antibiotics, such as clarithromycin and amoxicillin or metronidazole and a proton pump inhibitor (PPI) such as omeprazole. The administration of the three antibiotics together with a PPI (nonbismuth quadruple therapy) has also been considered as well as the bismuth-containing quadruple therapy (bismuth salts, tetracycline, metronidazole and a PPI) [4].

Current antibiotic eradication therapy is unsuccessful in nearly one in five patients (Figure 1) [15]. This low rate of success is mainly related to *H. pylori* resistance to the antibiotics and poor patient compliance. Furthermore, antibiotic degradation in the acidic environment of the gastric lumen or poor penetration of the antibiotic through the viscoelastic mucosal gel could lead to sub-bactericidal concentration of antibiotics in the infection site and therefore incomplete eradication of *H. pylori*, which could also induce bacterial resistance.

Alternative treatments

Several alternative treatments are being investigated in order to overcome the abovementioned problems related to antibiotic therapies. A vaccination strategy would be a valuable option to fight *H. pylori* infection [16]. However, despite several attempts to develop an *H. pylori* vaccine for humans, progress has been slow. Special attention has been given to compounds obtained from natural sources, including polyunsaturated fatty acids, terpenes and terpenoids, polyphenols and antimicrobial peptides [17,18]. The use of polyunsaturated fatty acids as co-adjuvant of the current available therapies was suggested as a promising approach [19].

Encapsulation of conventional antibiotics, for a local and controlled delivery at the infection site, has been thoroughly investigated to improve the effect of antibiotics against *H. pylori* [20,21]. These systems protect the drug from rapid degradation or clearance, extending its half-life and solubility, which may lead to lower administration frequency and hence better patient compliance [20–22]. A different strategy has been recently proposed by our group, based on the use of *H. pylori* binding systems that, after oral administration, will attract/bind bacteria and remove them from the host stomach, through the intestinal tract, after gastric mucus turnover [23].

Chitosan is a nontoxic, biodegradable and biocompatible natural polymer that has been quite investigated in the treatment of *H. pylori* infection, namely, for drug encapsulation due to its mucoadhesive properties and for *H. pylori* binding due to its antimicrobial/binding properties. Nevertheless, chitosan has also been described as adjuvant for an *H. pylori* vaccine [24]. In this manuscript, a brief description of the use of chitosan micro/nanoparticles in *H. pylori* treatment is reviewed.

Chitosan in the treatment of *H. pylori* infection

Properties of chitosan

Chitosan (Figure 2), a naturally occurring polysaccharide composed of D-glucosamine and *N*-acetyl-D-glucosamine units [25], is obtained by alkaline deacetylation of chitin, which is the second most abundant polysaccharide after cellulose and the major component of the exoskeleton of crustaceans, squid pen and cell walls of some fungi [26]. Chitosan molecular weight (MW) and degree of deacetylation (DD), which is the proportion of D-glucosamine units with respect to the total number of units, are the main factors that affect its chemical and biological properties [25]. The increase of chitosan DD will increase the number of free amine groups ($-NH_2$) that confer chitosan its almost unique properties of being positively charged and easily chemically modified.

Chitosan is stable in neutral conditions due to the strong inter- and intramolecular hydrogen bonds formed between its amine and hydroxyl groups [27]. Still, chitosan is soluble in acidic conditions, namely, below its pKa value (~6.5), due to the protonation of the free amine groups from the glucosamine residues [28].

Mucoadhesive properties of chitosan

The mucoadhesive properties of chitosan are related with the strong electrostatic interactions established between its protonated glucosamine residues and glycoproteins from gastric mucosa that, due to their sialic acids and ester sulfates [29], are negatively charged at the acidic stomach pH. These interactions are then followed by mechanical interlocking of the polymer chains, van der Waal's forces and hydrogen bonding.

Antimicrobial properties of chitosan

Chitosan antimicrobial properties are also consequence of the electrostatic interactions between chitosan cationic amine groups and the anionic groups on the bacterial wall, which leads to the inhibition of bacterial proliferation [30].

The antimicrobial activity of chitosan and its derivatives was able to inhibit the growth of fungi, parasites and several bacteria, including *H. pylori* strains NCTC 11639, NCTC 11637 and SS1 [31]. Luo *et al.* [31] have shown *in vitro* that chitosan with a DD of 95% presents higher antimicrobial activity against *H. pylori* than chitosan with a DD of 88.5%, indicating that the higher the deacetylation of chitosan the better its antimicrobial action. Furthermore, the *in vivo* administration of chitosan as solution and as nanoparticles (both DD 95%) to *H. pylori* infected BALB/c mice eradicated the bacteria in 55 and 75% of the animals, respectively.

Chitosan as drug encapsulation system

Several antibiotics have been encapsulated to treat *H. pylori* infection, although amoxicillin and clarithromycin are the most common ones. The encapsulation of two antibiotics and a PPI (omeprazole) has also been described [32].

The selection of the encapsulation technique is primarily determined by the solubility of the drug and the polymer in the solvents, and by the particle size requirements [33,34].

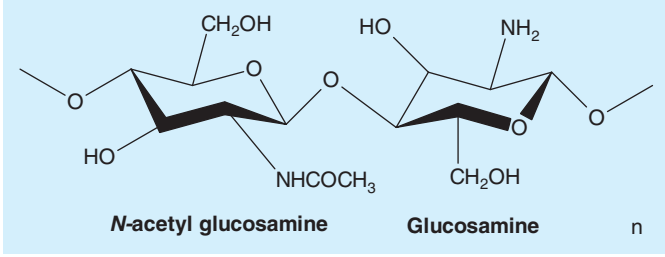

Figure 2. Chemical structure of chitosan.

Chitosan micro/nanoparticles

Chitosan micro and nanoparticles have been used for gastric drug delivery in the treatment of *H. pylori* due to its mucoadhesive properties. Besides protecting the drugs from enzymatic and acidic degradation, by adhering to gastric mucus barrier, particles residence time in the stomach will be higher prolonging drug delivery and allowing drug diffusion through the mucus barrier to the infection site [21,35].

The size and charge of chitosan particles will affect their mucoadhesion and mucopenetration and thus their retention time in the stomach. Microparticles have more difficulty to penetrate through viscoelastic mucus layer than nanoparticles. However, nanoparticles smaller than 200 nm could be internalized by gastric epithelial cells [36]. Furthermore, for an efficient mucoadhesion, particles must be positively charged, which is usually obtained by increasing chitosan MW and DD [37]. Nevertheless, an elevated number of positive charges could make the particles too mucoadhesive avoiding their penetration through the mucus layer [21], making them more prone to be washed out upon mucus turnover.

Several methods and approaches that have been proposed for the preparation of chitosan particles are summarized in Table 1 and schematized in a review from *Agnihotri et al.* [38].

Drug loading into chitosan particles is commonly performed by mixing it in the chitosan solution prior to particles formation and crosslinking [39], but incubation of previously formed particles with the drug can also be performed [40]. Hejazi and Amiji [40] demonstrated that the encapsulation of tetracycline onto chitosan microspheres was higher (69% w/w) when drug was incubated for up to 48 h with previously formed microspheres than when mixed in chitosan solution (8% w/w).

Due to the high solubility of chitosan in acidic conditions, uncrosslinked chitosan particles cannot maintain their three-dimensional structure in gastric fluids [28,41]. The rapid dissolution of chitosan particles or an extensive swelling of the particles induces a fast release of the drug, which might not be desirable. In order to overcome this restriction, ionic crosslinking of chitosan particles using tripolyphosphate (TPP) [42] or covalent crosslinking using glutaraldehyde [43] or genipin [41] can be performed. Genipin is a naturally occurring crosslinking agent described as being 10000 times less toxic than glutaraldehyde [44].

It should be considered that crosslinking after drug loading could induce chemical reactions with the active drug, which is

Table 1. Examples of methods for preparation of chitosan micro/nanoparticles.

Particle production method	Particle size	Advantages (+)/disadvantages (-)
Ionic gelation Drop wise addition of chitosan solution (positively charged) under constant stirring into a polyanionic solution (negatively charged, generally TPP). Complexation between oppositely charged species results in chitosan to precipitate as spherical particles.	Nanoparticles (nm) 20–200 [37] 550–900 [32] 152–376 [42] Microspheres (μm) ~170 [41] 100–400 [64]	+ Processing under mild conditions + Organic solvent free + Low-toxicity impact of reagents + No changes in drug chemistry - Difficult entrapment of high molecular weight drugs - Poor stability in acidic conditions
Precipitation/coacervation • Addition of a solute (generally a salt) to chitosan solution, forming micro/nanoparticles due to a decrease in chitosan solubility • Chitosan solution might also be blown into an alkali solution using a compressed air nozzle to form coacervate droplets	Nanoparticles (nm) 100–250 [65] Microspheres (μm) 1.5–2.5 [66]	+ No complex apparatus needed + Few purification steps required + Organic solvent free + High loading capacity combined with a sustained drug release - Poor stability in acidic conditions
Spray drying Preparation of chitosan solution where a suitable crosslinking agent could be added (if desired). This solution or dispersion is then atomized in a stream of hot air. Atomization leads to the formation of small droplets, from which solvent evaporates instantly leading to the formation of free flowing particles. Temperature and humidity might be regulated.	Microspheres (μm) 3–12 [67] 140–281 [68]	+ Simple, reproducible and easy to scale up + Low-cost process + Fast solvent removal + Good sphericity + Narrow size distribution + Low dependency of the solubility of the drug and polymer - High temperatures required - Size influenced by several parameters - Possible difficulty in spraying fluid of high viscosity
Supercritical antisolvent precipitation Spraying of the chitosan solution into a precipitation chamber with supercritical CO_2 (antisolvent), causing rapid contact between the two media. A higher super-saturation ratio of the solution is generated, resulting in fast nucleation and growth.	Microparticles (μm) 1.0–2.5 [47]	+ Processing under mild conditions + Complete antisolvent removal + Nontoxic reagents + Narrow size distribution + No changes in drug chemistry
Emulsion crosslinking Chitosan aqueous solution is extruded into an oil phase, generally liquid paraffin (under intensive stirring), forming and water-in-oil (w/o) emulsion. Aqueous droplets are stabilized by adding a surfactant. The stable emulsion is crosslinked by using an appropriate crosslinking agent such as glutaraldehyde.	Microspheres (μm) 60–100 [39] 100–330 [69] 350–690 [70]	+ Control of particle size + Good sphericity - Slow process - Chemical crosslinking agents used, possibly inducing chemical reactions with the drug - Difficult removal of the unreacted crosslinking agent
Solvent Evaporation Aqueous chitosan solution is added to an organic phase with vigorous stirring to form the primary water in oil emulsion (w/o). The latter is then added to a large volume of water containing a surfactant, forming a multiple emulsion (w/o/w). The double emulsion is then subjected to stirring until most of the organic solvent evaporates, leaving solid microspheres.	Microspheres (μm) 100–200 [71]	+ Processing under mild conditions + Favorable for encapsulation of thermally sensitive drugs + Indicated for delivery of small molecule drugs + Good sphericity - Organic solvents usage - Low drug encapsulation efficiency
Reverse micellar method The surfactant is dissolved in an organic solvent followed by the addition of chitosan, drug and crosslinking agent, under constant vortexing overnight. The organic solvent is evaporated, obtaining a transparent dry mass. The latter is dispersed in water and then a suitable salt is added to precipitate the surfactant out.	Nanoparticles (nm) ~100 [72]	+ Narrow size distribution - Organic solvent usage

not desirable. Also, crosslinking is performed through chitosan amine groups, reducing the number of free primary amines able to be protonated. As such, increasing the crosslinking decreases the mucoadhesion, size and swelling ability of chitosan particles in acidic conditions [41,45], affecting drug release profile. Zhu *et al.* [46] observed that chitosan microspheres ionically crosslinked with TPP present good mucoadhesive properties but allow a fast release of a hydrophilic drug (Berberine). On the other hand, chemically crosslinked chitosan microspheres enable a sustained drug release profile but show inferior mucoadhesiveness. In order to solve this inconsistency between mucoadhesiveness and release rate of chitosan microspheres, they proposed an approach where Eudragit L100 cores are encapsulated within the chitosan microsphere using an emulsification/coagulation procedure (size: 380 μm; entrapment efficiency: 71%), allowing ionic crosslinked microspheres with low crosslinking density to be used for the controlled release of hydrophilic antibiotics [46].

Regarding *H. pylori* treatment, amoxicillin-loaded chitosan microspheres (50–100 μm) were produced by Patel and Patel [39] using the emulsification crosslinking method. The improved effect of encapsulating amoxicillin to treat *H. pylori* was demonstrated *in vivo* using Wistar rats. In a single-dose administration test, the inhibition was markedly observed when dose was increased from 4 to 15 mg/kg. A similar *in vivo* study was performed by Patel and Patil [47] using smaller amoxicillin-chitosan microspheres (1.0–2.5 μm) produced using the supercritical antisolvent precipitation method, revealing that *H. pylori* inhibition was not influenced by particle size.

To improve *H. pylori* treatment, chitosan-based micro/nanoparticles can be specifically directed to the infection site by covalently binding, on the surface of the particles, ligands with affinity toward gastric mucosa or bacteria.

Lectins can specifically bind to carbohydrate moieties of glycoproteins located in gastric mucosa. Lectin can be coupled to chitosan particles improving the absorption of drugs [21] while presenting a good resistance to digestion within gastric environment [20]. The conjugation of the lectin (Con-A) on clarithromycin-loaded chitosan microspheres increased microspheres adhesion to the stomach mucosa of albino rats from 12 to 85% [48]. Retention time was also enhanced from 3 h to over 6 h in New Zealand albino rabbits for Con-A conjugated microspheres.

Fucose can be used to target lectin-type receptors on the surface of *H. pylori*. Fucose-conjugated nanoparticles containing a triple therapy (amoxicillin/clarithromycin/omeprazole) were produced by ionotropic gelation chitosan-glutamic acid conjugates and TPP as crosslinker [32]. These functionalized nanoparticles demonstrated *in vitro* an *H. pylori* eradication rate of 97% against 91% of nonconjugated chitosan nanoparticles and 81% of plain triple therapy. *In vivo* studies using *H. pylori*-infected Swiss albino mice demonstrated that fucose-conjugated nanoparticles containing the triple therapy treatment (53.57 mg/kg amoxicillin/17.8 mg/kg clarithromycin and 1.42 mg/kg omeprazole) were able to completely eradicate *H. pylori* infection. Nonfunctionalized nanoparticles and plain triple therapy were only able to eradicate 50 and 33% of the mice, respectively [32].

Chitosan-based pH-responsive micro/nanoparticles

Chitosan-based polyelectrolyte complexes can be prepared by mixing protonated chitosan with anionic polymers from natural (e.g., alginate [49,50], heparin [36], poly-y-glutamic acid [51,52], etc.) (Table 2) or synthetic (e.g., poly(acrylic acid), etc.) origin [53–55].

The advantage of using these systems for gastric applications is that they can be pH-sensitive, that is, polyelectrolyte complexes can be prepared in a way that electrostatic interactions between polymers are strong enough at acidic pH, but unstable at physiological pH to release the drug near *H. pylori* local of infection. Furthermore, these strong but reversible interactions between oppositely charged polyelectrolytes avoid the need of covalent crosslinkers and their associated disadvantages. Chitosan-based polyelectrolytes can be applied for drugs that, due to their hydrophobicity, negative charge or high MW, cannot be released from chitosan crosslinked particles. The size, charge and stability of the polyelectrolyte complexes depend on the individual properties of each polymer (charge, MW), the ratio between polymers, the ionic strength and pH of the solution, the mixing order as well as speed and diameter of the dispersing element [55].

Many different polyelectrolyte complexes, in the form of micro- or nanoparticles, have been developed for encapsulation of antibiotics for *H. pylori* treatment, and some examples are briefly summarized in Table 3.

As previously described with chitosan micro/nanoparticles, polyelectrolyte complexes can also be functionalized to target *H. pylori*. Fucose-chitosan/heparin nanoparticles loaded with amoxicillin are mentioned in Table 3.

Chitosan can also be used as coating for anionic particles. A chitosan-coated pH-responsive liposome system containing doxycycline (as a model antibiotic drug) for the treatment of *H. pylori* infection was developed [56]. Liposomes are spherical vesicles composed of one or more phospholipid bilayers that have been studied as drug delivery systems for both hydrophilic and hydrophobic compounds. Furthermore, liposomes also mimic cell membranes, allowing an effective penetration of encapsulated drug into intracellular spaces. However, the applications of liposomes, particularly those with sizes below 100 nm, are often limited due to their spontaneous fusion [56]. Chitosan-modified gold (AuCh) nanoparticles (size ~10 nm) strongly bound to the surface of anionic phospholipid liposomes (size ~75 nm) at acidic pH, inhibit liposome fusion and detached from the liposomes at physiological pH, enable free liposomes to fuse with target bacterial membrane and release the therapeutic drug. Antimicrobial studies demonstrated higher *H. pylori* antibacterial effect of the doxycycline-loaded AuCh-liposome nanoparticles when compared with the same concentration of doxycycline in solution.

Amoxicillin-loaded alginate/carboxymethyl cellulose microbeads (size 745–889 μm/entrapment efficiency 52–92%) were coated with chitosan to achieve a controlled release of the

Table 2. Anionic polymers commonly used for preparation of chitosan-based polyelectrolyte complexes.

Polymer chemical structure	Polymer characteristics
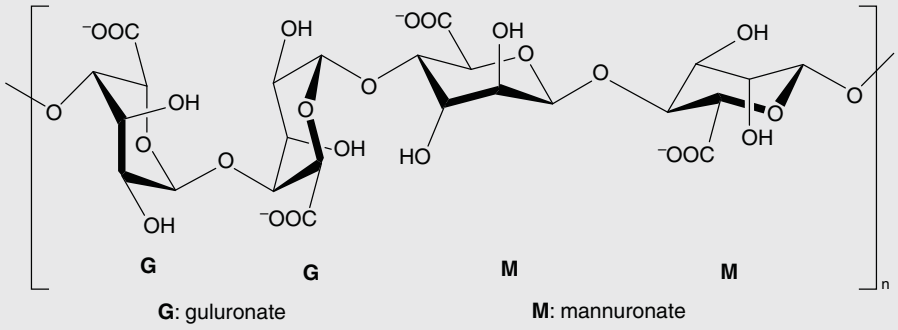	**Alginate:** • Natural anionic and hydrophilic polysaccharide typically obtained from brown seaweed or bacteria • Composed of alternating blocks of (1-4) linked α-L-guluronic (G) and β-D-mannuronic acid (M) monomers • Widely explored for biomedical applications, namely as matrix for the entrapment and/or delivery of a variety of proteins, peptides, drugs and cells, due to its excellent biocompatibility, low toxicity, biodegradability and mild gelation conditions by addition of divalent cations such as Ca^{2+}
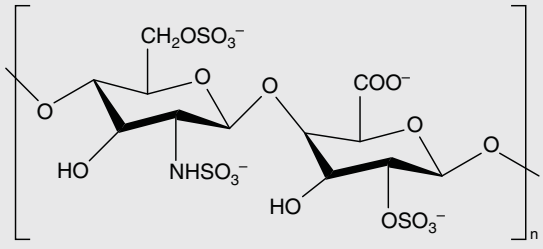	**Heparin:** • Natural anionic and highly sulfated glycosaminoglycan • Composed of repeating disaccharide units of D-glucosamine and uronic acid linked by 1-4 interglycosidic bonds • It is well known for its anticoagulant properties, but also by its ability to bind to cell receptors and accelerate gastric ulcer healing, which is associated with mucosal regeneration, proliferation and angiogenesis
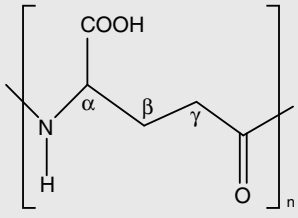	**Poly-γ-glutamic acid (γ-PGA):** • Natural, hydrophilic, nontoxic, poly-amino acid, which is biodegradable and relatively nonimmunogenic • Can be used as carriers for active substances and can be easily modulated in order to control the delivery of drugs, proteins, etc.

antibiotic in stomach environment [57]. It was demonstrated that chitosan coating induced mucoadhesive properties to the microbeads and delayed amoxicillin delivery to up to 8 h, releasing 41% of amoxicillin.

Chitosan as binding agent

The adhesion of *H. pylori* to chitosan in a pH range that simulates gastric conditions (2.6, 4.0 and 6.0) was first demonstrated using chitosan as thin films crosslinked with genipin [58]. Furthermore, the percentage of dead adherent bacteria ranged from 76% at pH 6 to 93% at pH 2.6. As such, rather than being used as a gastric drug delivery vehicle, chitosan microspheres have been designed and applied as an *H. pylori*-binding system [23,41]. It is expected that after oral administration, these microspheres will adhere *H. pylori* in the stomach and remove them through the gastrointestinal tract (upon gastric mucus turnover). Chitosan microspheres with approximately 170 μm were produced by ionotropic gelation with TPP [41] followed by the minimal genipin crosslinking necessary to avoid microspheres dissolution in acidic pH without losing their mucoadhesiveness. *In vivo* studies using C57BL/6 mice demonstrated that these chitosan microspheres have a gastric retention of 2 h [41]. *H. pylori* adhesion to these microspheres was evaluated in a range of acidic pHs, confirming that several *H. pylori* strains bind to the microspheres (Figure 3). Furthermore, these microspheres are not cytotoxic and revealed able to both partially remove and prevent *H. pylori* adhesion to a gastric cell line [23].

This system was further improved by directing the microspheres toward *H. pylori*. Immobilization of carbohydrates, namely, Le^b and sLe^x, that specifically bind to *H. pylori* adhesins was first screened using model surfaces [59] and afterwards transposed to chitosan microspheres [60]. It was found that glycan-targeted materials were able to bind specifically to *H. pylori* strains that express the corresponding adhesin, meaning that Le^b-modified materials adhere favorably to BabA-positive strains and sLe^x-modified materials adhere

Table 3. Examples of chitosan-based polyelectrolyte complexes used as drug delivery systems in *Helicobacter pylori* infection treatment.

Complex	Drug	Production method	Particle characteristics	Main conclusions	Ref.
Alginate/chitosan	Amoxicillin	**Ionic gelation:** Chitosan, amoxicillin and pluronic are mixed. To the previous mixture, alginate solution is sprayed with continuous stirring. • Alginate: 0.1% w/v (pH 5.5) • Chitosan: 0.06% w/v (pH 5.0) • Amoxicillin: 0.01% w/v • Pluronic F127 (surfactant): 0.019% w/v	Size: 651 nm ζ-Potential: ≅ +60 mV Entrapment efficiency: 91%	*In vitro* • Antibiotic protection from simulated gastric conditions for at least 6 h; • Lower mucoadhesive capacity (~76%) than plain chitosan nanoparticles crosslinked with TPP (~86%) suggesting that decreasing of the surface charge of the nanoparticles will improve their mucopenetration *In vivo* (Wistar rats) • Excellent mucopenetration into deep mucosal region	[73]
		Ionic gelation: Amoxicillin is mixed with alginate solution in ddH_2O containing DOSS using vigorous stirring. Mixture is sprayed into a $CaCl_2$ solution containing chitosan. • Alginate: 2% w/v (pH 5.5) • Chitosan: 0.75% w/v (pH 5.0) • Amoxicillin: 2-9% w/v • DOSS (surfactant): 0.075% w/v • $CaCl_2$: 1.0% w/v	Size: 840 µm Entrapment efficiency: 84%	*In vitro* • Antibiotic protection from simulated gastric acidic conditions for at least 8 h; • Highly mucoadhesive (*in vitro* gastric retention up to 8 h); • The increase of chitosan concentration enlarges particle size but reduces drug encapsulation	[74]
Heparin/chitosan	Amoxicillin	**Water-in-oil emulsification:** Nanoemulsion particles are prepared using laboratory-type rotating blade homogenizer (40 ml aqueous phase + 80 ml paraffin). Surfactant is added to liquid paraffin under continuous mixing and heparin aqueous solution is added and homogenized. Chitosan solution is dropped into the resultant heparin emulsion and homogenized. Nanoemulsion particles are collected by centrifugation. • Chitosan: 0.6 mg/ml (pH 6.0) • Heparin: 0.2 mg/ml (pH 7.4) • Amoxicillin: 0.6 mg/mL (pH 7.4) • Surfactant: Span20/Tween20 (75:25): 1.2 ml	Size: 296 nm ζ-Potential: ≅ +30 mV Entrapment efficiency: ≅ 54%	*In vitro* • Positively charged particles and stable in acidic gastric conditions; • Amoxicillin release at pH 7. Low release at pH 6 • Can be internalized by human gastric adenocarcinoma cells (AGS cell line) and be localized in intercellular spaces *In vivo* (*H. pylori* infected C57BL/6J mice) • Higher clearance in *H. pylori* infection when compared with amoxicillin in solution	[75]

H. pylori: *Helicobacter pylori*; TPP: Tripolyphosphate.

Table 3. Examples of chitosan-based polyelectrolyte complexes used as drug delivery systems in *Helicobacter pylori* infection treatment (cont.).

Complex	Drug	Production method	Particle characteristics	Main conclusions	Ref.
Heparin/ chitosan-fucose	Amoxicillin	**Ionotropic gelation + crosslinking (with genipin):** Fucose-conjugated chitosan is synthesized by addition of fucose and sodium cyanoborohydride into chitosan solution. Aqueous heparin (with amoxicillin) is added by flush mixing with a pipette tip. Nanoparticles are collected by centrifugation. Heparin/chitosan-fucose nanoparticles are mixed into a genipin solution and gently stirred. • Fucose-Chit: 1.2 mg/ml (pH 6) • Heparin: 2.0 mg/ml (pH 7.4) • Amoxicillin: 4.0 mg/ml • Genipin: 0.375 mg/ml	Size: ≅ 250 nm ζ-Potential: ≅ +27 mV Entrapment efficiency: ≅ 49%	*In vitro* • Amoxicillin protection from acidic conditions • Crosslinking delays amoxicillin delivery in acidic conditions • Adhesion and infiltration in the mucus layer • Amoxicillin release near the gastric epithelium • Particles size increase at physiological pH *In vivo* (C57BL/6J mice) • Higher reduction of *H. pylori* infection when compared with amoxicillin in solution	[76]
Heparin/chitosan	Berberine	**Ionic gelation:** Berberine/heparin nanoparticles are prepared by combining aqueous berberine with aqueous heparin by flush mixing with a pipette tip. Berberine/heparin solution is added to aqueous chitosan solution. • Berberine: 0.25 mg/ml • Berberine/heparin/Chitosan ratio (w/w/w): 3.0:6.0:4.8 (pH 6.0)	Size: ≅ 256 nm Entrapment efficiency: ≅ 54%	*In vitro* • Nanoparticles become unstable at physiological pH, allowing a rapid release of berberine; • Berberine nanoparticles act locally in the site of *H. pylori* infection and inhibit the bacterium growth	[77]
γ-PGA/chitosan	Amoxicillin	**Ionic gelation:** Chitosan/γ-PGA nanoparticles are prepared by flush mixing γ-PGA solution with a pipette tip into aqueous chitosan containing amoxicillin. Nanoparticles are collected by centrifugation. Nanoparticles are then incorporated into beads of pH-sensitive alginate-gelatin gel that are prepared by dropping aqueous alginate-gelatin into a $CaCl_2$ solution. • Amoxicillin: 2.0 mg/ml • γ-PGA: 2.0 mg/ml • Chitosan: 0.06 mg/ml • Hydrogel: Alginate 0.2% w/v and Gelatin 0.10% w/v into $CaCl_2$ 0.6 m	Size: 120–150 nm (nanoparticles) ζ-Potential: ≅ +19 mV Entrapment efficiency: ≅ 23%	*In vitro* • Alginate-gelatin hydrogel prevents nanoparticles destruction and amoxicillin release from nanoparticles in acidic pH; • Confocal laser scanning microscopy revealed that nanoparticles can infiltrate cell-cell junctions and interact with *H. pylori*	[78]

H. pylori: *Helicobacter pylori*; TPP: Tripolyphosphate.

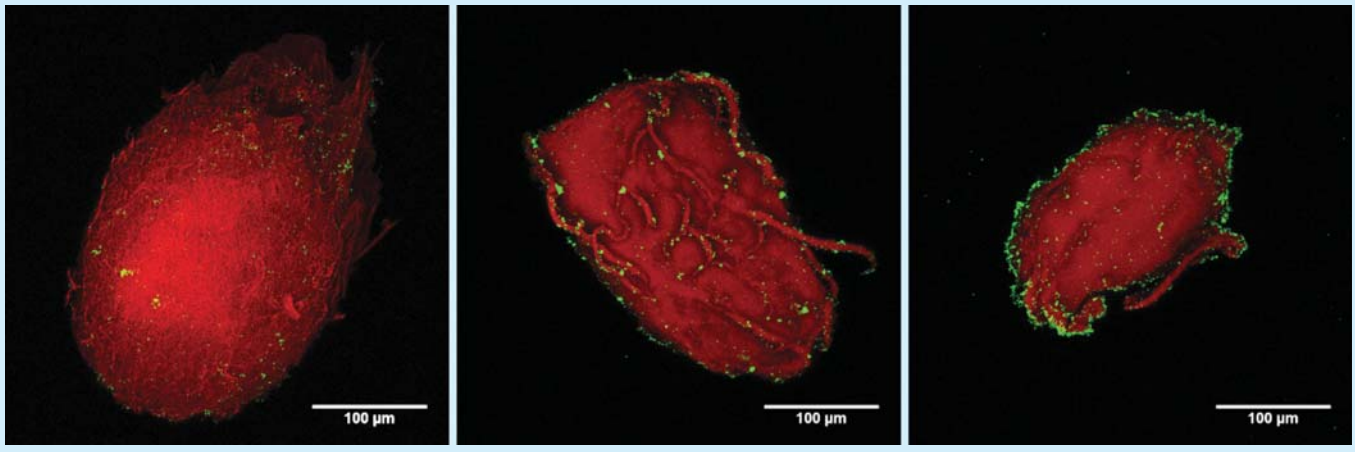

Figure 3. Confocal microscopy images of chitosan microspheres (in red) with adherent FITC-labeled *Helicobacter pylori* strain J99 (in green) under pH 2.6, pH 4.0 and pH 6.0 (from left to right).

preferentially to SabA-positive strains. This strategy is extremely promising, particularly given the present shift of focus onto a more personalized medicine. The immobilization of other carbohydrates into microspheres for administration depending on the strain of *H. pylori* that is infecting the patient, or the administration of cocktails of microspheres with different carbohydrates are interesting possibilities for future treatments.

Expert commentary & five-year view

The currently available antibiotic-based treatments for *H. pylori* gastric infection have been unsuccessful in several patients, mostly due to bacterial resistance and poor patient compliance. It is expected that the amount of antibiotic-resistant *H. pylori* will increase in a near future due to the bad use (abuse) of antibiotics, leading to an increased number of patients that need an alternative treatment. Furthermore, multiple *H. pylori* infection and even multiple-antibiotic-resistant *H. pylori* infection have been observed, which also compromises the current therapeutic efficacy.

Antibiotics encapsulation into gastric retentive polymers, namely, chitosan, has improved their biological effects, by protecting them from the acidic gastric fluids and increasing their availability at the infection site. However, although this strategy could improve patients' compliance, it will not solve the problem of antibiotic resistance.

A promising alternative to the conventional antibiotic therapy is the use of antimicrobial compounds obtained from natural sources [18,59] that have different bacteria target/pathways than most antibiotics (the ribosome–clarithromycin; the cell wall synthesis–amoxicillin and bacterial DNA replication–metronidazole [61]). Nevertheless, due to their low solubility, sensitivity and instability in gastric conditions, most of these natural-based compounds also need to be encapsulated for their *in situ* delivery. As such, we predict that chitosan micro/nanoparticles will continue to have a major role in *H. pylori* therapies, mainly due to chitosan's biocompatibility, biodegradability, mucoadhesiveness, ease of handling and facility to be chemically modified.

In all the strategies previously described, it was demonstrated that the incorporation of target molecules toward *H. pylori* such as fucose or carbohydrates (namely, Le^b or sLe^x) improved the efficiency of the systems. It is our belief that targeted treatments using chitosan micro/nanoparticles specific to *H. pylori* are highly promising since they will avoid the destruction of the normal gut microbiome of the patients [62]. This strategy may include particles chemically modified with targeting compounds that bind *H. pylori* urease, flagella, adhesins, etc., in order to inhibit, kill or remove the bacteria.

A recent investigation performed by our group takes advantage of chitosan bioadhesive and antimicrobial properties, and uses chitosan microspheres to bind and remove *H. pylori* from the stomach of infected hosts, through the normal gastrointestinal tract. Although this therapy may not be enough to remove all bacteria that infect the patient, especially the ones that are in the intercellular spaces or inside gastric cells, it is expected that they can remove most of *H. pylori* and have a synergistic effect when combined with other drugs. Since these chitosan particles will not induce bacteria resistance and can be used without damage to the patient, they can also be used to prevent reinfection.

Despite the great potential of using chitosan and chitosan derivatives in pharmaceutical and biomedical applications, none of the described chitosan systems are currently in the market. Chitosan is only US FDA approved for use in wound dressings. Nevertheless, chitosan was approved for dietary applications in Japan, Italy and Finland [63]. This difficulty in being FDA approved is mainly related with the fact that its physicochemical characteristics can change drastically with its source, MW and associated polydispersity index, DD, size and formulation. Furthermore, since chitosan is a natural compound, it is always difficult to maintain the reproducibility between batches. Nevertheless, the current growing interest in using chitosan in medical (pharmaceutical) applications improved the industrial capacity to produce more pure, cost–effective and uniform

chitosan, representing important progress for its pharmaceutical industrialization in a near future.

Financial & competing interests disclosure

This paper has been financed by FEDER funds through Programa Operacional Factores de Competitividade – COMPETE and by Portuguese funds through FCT – Fundação para a Ciência e a Tecnologia, in the framework of the projects PEst-C/SAU/LA0002/2013, NORTE-07-0124-FEDER-000005, FCOMP-01-0124-FEDER-020073 (PTDC/CTM-BPC/121149/2010) and FCOMP-01-0124-FEDER-041276 (EXPL/CTM-BIO/0762/2013) and grant SFRH/BD/89001/2012. The authors have no other relevant affiliations or financial involvement with any organization or entity with a financial interest in or financial conflict with the subject matter or materials discussed in the manuscript apart from those disclosed.

No writing assistance was utilized in the production of this manuscript.

Key issues

- *Helicobacter pylori* (*H. pylori*) infects about half of the world's population and its persistent infection is associated with a strong risk for the development of gastric adenocarcinoma.
- The failure of the current available antibiotic-based therapy (~1 in each 5 patients) demonstrated the need of alternative treatments.
- Chitosan is a natural biocompatible polymer with great potential in *H. pylori* treatment, mainly due to its gastric retentive and antimicrobial properties, but also because it can easily be chemically modified.
- Chitosan properties are mainly related with its primary amine groups that are directly related with its degree of deacetylation.
- In *H. pylori* infection treatment, chitosan is mostly used as gastric drug delivery system, whether as crosslinked particles, as polyelectrolyte complexes with anionic polymers or as coatings. Nevertheless, it has recently been proposed as an *H. pylori* binding system.
- In order to prevent premature release of the encapsulated drug, chitosan particles must be crosslinked to avoid its fast dissolution in gastric acidic conditions.
- Polyelectrolyte complex-based chitosan particles can be pH-responsive, that is, particles are stable in acidic pH (drug preservation) and unstable at physiological pH to release the drug near *H. pylori* infection site (near gastric epithelial cells).
- Chitosan microspheres crosslinked with genipin have great potential as *H. pylori*-binding systems for the clearance of this bacterium from infected host through normal gastrointestinal tract since they can bind *H. pylori*, are noncytotoxic and are stable during all the digestive process.
- In order to increase their residence time in the stomach, chitosan particles can be conjugated with lectins to target the gastric mucosa through lectin-carbohydrate recognition.
- In order to be directed toward *H. pylori*, chitosan particles can be conjugated with fucose or glycans (Le^b, sLe^x, …) to target *H. pylori* adhesins.

References

Papers of special note have been highlighted as:
• of interest
•• of considerable interest

1. Wroblewski LE, Peek RM Jr, Wilson KT. Helicobacter pylori and gastric cancer: factors that modulate disease risk. Clin Microbiol Rev 2010;23(4):713-39

• **Describes *Helicobacter pylori* (*H. pylori*) mechanisms of infection and pathogenesis of *H. pylori*-induced gastric adenocarcinoma.**

2. Ferlay J, Parkin DM, Steliarova-Foucher E. Estimates of cancer incidence and mortality in Europe in. 2008;Eur J Cancer 2010; 46(4):765-81
3. Stewart BW, Kleihues P. World cancer report. International Agency for Research on Cancer; Lyon, France: 2003. p. 351
4. Malfertheiner P, Megraud F, O'Morain CA, et al. Management of Helicobacter pylori infectio- the Maastricht IV/Florence Consensus Report. Gut 2012;61:646-64

• **Summarizes the current therapies and provides guidelines for *H. pylori* infection eradication.**

5. Allen A, Cunliffe WJ, Pearson JP, Venables CW. The adherent gastric mucus gel barrier in man and changes in peptic ulceration. J Intern Med Suppl 1990;732: 83-90
6. Celli JP, Turner BS, Afdhal NH, et al. Helicobacter pylori moves through mucus by reducing mucin viscoelasticity. Proc Natl Acad Sci USA 2009;106(34):14321-6
7. Dubois A, Boren T. Helicobacter pylori is invasive and it may be a facultative intracellular organism. Cell Microbiol 2007; 9(5):1108-16
8. Kobayashi M, Lee H, Nakayama J, Fukuda M. Carbohydrate-dependent defense mechanisms against Helicobacter pylori infection. Curr Drug Metab 2009;10(1): 29-40
9. Evans DJ Jr, Evans DG. Helicobacter pylori adhesins: review and perspectives. Helicobacter 2000;5(4):183-95
10. Aspholm M, Kalia A, Ruhl S, et al. Helicobacter pylori adhesion to carbohydrates. Methods Enzymol 2006;417: 293-339
11. Namavar F, Sparrius M, Veerman EC, et al. Neutrophil-activating protein mediates adhesion of Helicobacter pylori to sulfated carbohydrates on high-molecular-weight salivary mucin. Infect Immun 1998;66(2): 444-7
12. Odenbreit S, Faller G, Haas R. Role of the alpAB proteins and lipopolysaccharide in adhesion of Helicobacter pylori to human gastric tissue. Int J Med Microbiol 2002; 292(3-4):247-56
13. Dossumbekova A, Prinz C, Mages J, et al. Helicobacter pylori HopH (OipA) and

bacterial pathogenicity: genetic and functional genomic analysis of hopH gene polymorphisms. J Infect Dis 2006;194(10):1346-55

14. Kwok T, Zabler D, Urman S, et al. Helicobacter exploits integrin for type IV secretion and kinase activation. Nature 2007;449(7164):862-6
15. Vakil N. Helicobacter pylori treatment: a practical approach. Am J Gastroenterol 2006;101(3):497-9
16. Del Giudice G, Malfertheiner P, Rappuoli R. Development of vaccines against Helicobacter pylori. Expert Rev Vaccines 2009;8(8):1037-49
17. Parreira P, Fátima Duarte M, Reis CA, Martins MC. Helicobacter pylori infection: a brief overview on alternative natural treatments to conventional therapy. Crit Rev Microbiol 2014. [Epub ahead of print]
18. Makobongo MO, Gilbreath JJ, Merrell DS. Nontraditional therapies to treat Helicobacter pylori infection. J microbiol 2014;52(4):259-72
19. Correia M, Michel V, Matos AA, et al. Docosahexaenoic acid inhibits Helicobacter pylori growth in vitro and mice gastric mucosa colonization. PLoS One 2012;7(4):e35072
20. Adebisi A, Conway BR. Gastroretentive microparticles for drug delivery applications. J Microencapsul 2011;28(8):689-708

•• **Summarizes the role of gastric retentive microparticles on drug delivery for *H. pylori* treatment.**

21. Arora S, Bisen G, Budhiraja RD. Mucoadhesive and muco-penetrating delivery systems for eradication of Helicobacter pylori. Asian J Pharm 2012;6:18-30

•• **Summarizes the gastric drug delivery systems that have been recently developed to release antibiotics for *H. pylori* eradication.**

22. Petros RA, DeSimone JM. Strategies in the design of nanoparticles for therapeutic applications. Nat Rev Drug Discov 2010;9(8):615-27
23. Gonçalves IC, Magalhaes A, Fernandes M, et al. Bacterial-binding chitosan microspheres for gastric infection treatment and prevention. Acta Biomater 2013;9(12):9370-8

•• **Describes the ability of chitosan microspheres (crosslinked with genipin) to bind *H. pylori* and prevent/remove its adhesion to gastric cells.**

24. Xie Y, Zhou NJ, Gong YF, et al. Th immune response induced by H. pylori vaccine with chitosan as adjuvant and its relation to immune protection. World J Gastroenterol 2007;13(10):1547-53
25. Dash M, Chiellini F, Ottenbrite RM, Chiellini E. Chitosan – A versatile semi-synthetic polymer in biomedical applications. Prog Polym Sci 2011;36(8):981-1014
26. Kato Y, Onishi H, Machida Y. Application of chitin and chitosan derivatives in the pharmaceutical field. Curr Pharm Biotechnol 2003;4(5):303-9
27. Mi FL, Sung HW, Shyu SS, et al. Synthesis and characterization of biodegradable TPP/genipin co-crosslinked chitosan gel beads. Polymer (Guildf) 2003;44(21):6521-30
28. Mi FL, Sung HW, Shyu SS. Synthesis and characterization of a novel chitosan-based network prepared using naturally occurring crosslinker. J Polym Sci 2000;38(15):2804-14
29. Sogias IA, Williams AC, Khutoryanskiy VV. Why is chitosan mucoadhesive? Biomacromolecules 2008;9(7):1837-42
30. Strand SP, Vandvik MS, Varum KM, Ostgaard K. Screening of chitosans and conditions for bacterial flocculation. Biomacromolecules 2001;2(1):126-33
31. Luo D, Guo J, Wang F, et al. Preparation and evaluation of anti-Helicobacter pylori efficacy of chitosan nanoparticles in vitro and in vivo. J Biomater Sci Polym Ed 2009;20(11):1587-96
32. Ramteke S, Ganesh N, Bhattacharya S, Jain NK. Amoxicillin, clarithromycin, and omeprazole based targeted nanoparticles for the treatment of H. pylori. J Drug Target 2009;17(3):225-34

•• **Describes the *in vitro* and *in vivo* efficacy studies of fucose-conjugated chitosan nanoparticles containing a triple therapy (amoxicillin/clarithromycin/omeprazole).**

33. Crini G, Badot PM. Application of chitosan, a natural aminopolysaccharide, for dye removal from aqueous solutions by adsorption processes using batch studies: a review of recent literature. Prog Polym Sci 2008;33(4):399-447
34. Soppimath KS, Aminabhavi TM, Kulkarni AR, Rudzinski WE. Biodegradable polymeric nanoparticles as drug delivery devices. J Control Release 2001;70(1-2):1-20
35. Conway BR. Drug delivery strategies for the treatment of Helicobacter pylori infections. Curr Pharm Des 2005;11(6):775-90
36. Lin YH, Chang CH, Wu YS, et al. Development of pH-responsive chitosan/heparin nanoparticles for stomach-specific anti-Helicobacter pylori therapy. Biomaterials 2009;30(19):3332-42
37. Huang YC, Chiang CH, Yeh MK. Optimizing formulation factors in preparing chitosan microparticles by spray-drying method. J Microencapsul 2003;20(2):247-60
38. Agnihotri SA, Mallikarjuna NN, Aminabhavi TM. Recent advances on chitosan-based micro- and nanoparticles in drug delivery. J Control Release 2004;100(1):5-28
39. Patel JK, Patel MM. Stomach Specific Anti-Helicobacter pylori Therapy: Preparation and Evaluation of Amoxicillin-Loaded Chitosan Mucoadhesive Microspheres. Curr Drug Deliv 2007;4(1):41-50
40. Hejazi R, Amiji M. Stomach-specific anti-H. pylori therapy. I: preparation and characterization of tetracyline-loaded chitosan microspheres. Int J Pharm 2002;235(1-2):87-94
41. Fernandes M, Goncalves IC, Nardecchia S, et al. Modulation of stability and mucoadhesive properties of chitosan microspheres for therapeutic gastric application. Int J Pharm 2013;454(1):116-24

• **Describes the preparation and characterization of chitosan microspheres, crosslinked with genipin in terms of mucoadhesion, stability in acidic conditions and *in vivo* gastric retention time.**

42. Dong Y, Ng WK, Shen S, et al. Scalable ionic gelation synthesis of chitosan nanoparticles for drug delivery in static mixers. Carbohydr Polym 2013;94(2):940-5
43. Sung HW, Huang RN, Huang LL, et al. Feasibility study of a natural crosslinking reagent for biological tissue fixation. J Biomed Mater Res 1998;42(4):560-7
44. Mi FL, Sung HW, Shyu SS. Release of indomethacin from a novel chitosan microsphere prepared by a naturally occurring crosslinker: examination of crosslinking and polycation–anionic drug interaction. J Appl Polym Sci 2001;81(7):1700-11
45. Mi FL, Shyu SS, Peng CK. Characterization of ring-opening polymerization of genipin and pH-dependent cross-linking reactions between chitosan and genipin. J Polym Sci 2005;43(10):1985-2000

46. Zhu X, Zhou D, Guan S, et al. Preparation and characterization of novel multi-core chitosan microspheres for stomach-specific delivery of hydrophilic antibiotics. J Mater Sci Mater Med 2012;23(4):983-90

47. Patel J, Patil P. Preparation and characterization of amoxicillin mucoadhesive microparticles using solution-enhanced dispersion by supercritical CO2. J Microencapsul 2012;29(4):398-408

48. Jain SK, Jangdey MS. Lectin conjugated gastroretentive multiparticulate delivery system of clarithromycin for the effective treatment of Helicobacter pylori. Mol Pharm 2009;6(1):295-304

49. Bhattarai R, Dhandapani N, Shrestha A. Drug delivery using alginate and chitosan beads: an overview. Chron Young Sci 2011; 2(4):192-6

50. Lee KY, Mooney DJ. Alginate: properties and biomedical applications. Prog Polym Sci 2012;37(1):106-26

51. Antunes JC, Pereira CL, Molinos M, et al. Layer-by-layer self-assembly of chitosan and poly(gamma-glutamic acid) into polyelectrolyte complexes. Biomacromolecules 2011;12(12):4183-95

52. Gonçalves RM, Antunes JC, Barbosa MA. Mesenchymal stem cell recruitment by stromal derived factor-1-delivery systems based on chitosan/poly(gamma-glutamic acid) polyelectrolyte complexes. Eur Cell Mater 2012;23:249-60.discussion 260-241

53. Berger J, Reist M, Mayer JM, et al. Structure and interactions in chitosan hydrogels formed by complexation or aggregation for biomedical applications. Eur J Pharm Biopharm 2004;57(1):35-52

54. Bhattarai N, Gunn J, Zhang M. Chitosan-based hydrogels for controlled, localized drug delivery. Adv Drug Deliv Rev 2010;62(1):83-99

55. Hamman JH. Chitosan based polyelectrolyte complexes as potential carrier materials in drug delivery systems. Mar Drugs 2010;8(4):1305-22

56. Thamphiwatana S, Fu V, Zhu J, et al. Nanoparticle-stabilized liposomes for pH-responsive gastric drug delivery. Langmuir 2013;29(39):12228-33

57. Angadi SC, Manjeshwar LS, Aminabhavi TM. Novel composite blend microbeads of sodium alginate coated with chitosan for controlled release of amoxicillin. Int J Biol Macromol 2012; 51(1-2):45-55

58. Nogueira F, Goncalves IC, Martins MC. Effect of gastric environment on Helicobacter pylori adhesion to a mucoadhesive polymer. Acta Biomater 2013;9(2):5208-15

59. Parreira P, Magalhães A, Reis CA, et al. Bioengineered surfaces promote specific protein–glycan mediated binding of the gastric pathogen Helicobacter pylori. Acta Biomaterialia 2013;9:11:8885-93

60. Martins MCL, Goncalves IC, Gomes P, et al. Microspheres. WO2013164652. 2013

61. Lewis K. Platforms for antibiotic discovery. Nat Rev Drug Dis 2013;12(5):371-87

62. Jakobsson HE, Jernberg C, Andersson AF, et al. Short-term antibiotic treatment has differing long-term impacts on the human throat and gut microbiome. Plos One 2010; 5(3):e9836

63. Sarmento B, das Neves J. Chitosan-based systems for biopharmaceuticals: delivery, targeting and polymer therapeutics. John Wiley & Sons Ltd; UK: 2012

64. Ma L, Liu C. Preparation of chitosan microspheres by ionotropic gelation under a high voltage electrostatic field for protein delivery. Colloids surf B Biointerfaces 2010; 75(2):448-53

65. Mao HQ, Roy K, Troung-Le VL, et al. Chitosan-DNA nanoparticles as gene carriers: synthesis, characterization and transfection efficiency. J Control Release 2001;70(3):399-421

66. Berthold A, Cremer K, Kreuter J. Preparation and characterization of chitosan microspheres as drug carrier for prednisolone sodium phosphate as model for anti-inflammatory drugs. J Control Release 1996;39(1):17-25

67. He P, Davis SS, Illum L. In vitro evaluation of the mucoadhesive properties of chitosan microspheres. Int J Pharm 1998;166(1): 75-88

68. Torres MA, Vieira RS, Beppu MM, et al. Production of chemically modified chitosan microspheres by a spraying and coagulation method. Mater Res 2007;10:347-52

69. Roy S, Panpalia SG, Nandy BC, et al. Effect of Method of Preparation on Chitosan Microspheres of Mefenamic Acid. Int J Pharm Sci Drug Res 2009;1(1):36-42

70. Akbuğa J, Durmaz G. Preparation and evaluation of cross-linked chitosan microspheres containing furosemide. Int J Pharm 1994;111(3):217-22

71. Mi FL, Tan YC, Liang HC, et al. In vitro evaluation of a chitosan membrane cross-linked with genipin. J Biomater Sci Polym Ed 2001;12(8):835-50

72. Mitra S, Gaur U, Ghosh PC, Maitra AN. Tumour targeted delivery of encapsulated dextran–doxorubicin conjugate using chitosan nanoparticles as carrier. J Control Release 2001;74(1–3):317-23

73. Arora S, Gupta S, Narang RK, Budhiraja RD. Amoxicillin loaded chitosan-alginate polyelectrolyte complex nanoparticles as mucopenetrating delivery system for H. pylori. Sci Pharm 2011;79(3): 673-94

74. Arora S, Budhiraja RD. Chitosan-alginate microcapsules of amoxicillin for gastric stability and mucoadhesion. J Adv Pharm Technol Res 2012;3(1):68-74

75. Lin YH, Chiou SF, Lai CH, et al. Formulation and evaluation of water-in-oil amoxicillin-loaded nanoemulsions using for Helicobacter pylori eradication. Process Biochem 2012;47(10):1469-78

76. Lin YH, Tsai SC, Lai CH, et al. Genipin-cross-linked fucose-chitosan/heparin nanoparticles for the eradication of Helicobacter pylori. Biomaterials 2013; 34(18):4466-79

• **Describes the preparation and characterization of amoxicillin-loaded fucose-chitosan/heparin nanoparticles crosslinked with genipin and its efficacy *in vivo* for the treatment of *H. pylori* infection.**

77. Chang CH, Huang WY, Lai CH, et al. Development of novel nanoparticles shelled with heparin for berberine delivery to treat Helicobacter pylori. Acta Biomater 2011; 7(2):593-603

78. Chang CH, Lin YH, Yeh CL, et al. Nanoparticles incorporated in pH-sensitive hydrogels as amoxicillin delivery for eradication of Helicobacter pylori. Biomacromolecules 2010;11(1):133-42

79. Malfertheiner P, Bazzoli F, Delchier JC, et al. Helicobacter pylori eradication with a capsule containing bismuth subcitrate potassium, metronidazole, and tetracycline given with omeprazole versus clarithromycin-based triple therapy: a randomised, open-label, non-inferiority, phase 3 trial. Lancet 2011;377(9769): 905-13